Stereoselective Syntheses of Oxygenated Polyunsaturated Fatty Acid Mediators and Investigations of Biosynthetic Pathways

Dissertation for the degree of *Philosophiae Doctor*
by
Karoline Gangestad Primdahl

Faculty of Mathematics and Natural Sciences

University of Oslo

2017

Series of dissertations submitted to the
Faculty of Mathematics and Natural Sciences, University of Oslo
No. 1911

ISSN 1501-7710

Cover: Hanne Baadsgaard Utigard.
Print production: Reprosentralen, University of Oslo.

Acknowledgements

The work presented in this thesis was undertaken in the period from August 2013 to May 2017 at the School of Pharmacy, University of Oslo, except for a one month sojourn in 2016 to Senior lecturer Dalli's group at the Barts and The London School of Medicine and Dentistry and Queen Mary College in London. My main supervisor through this period has been Associate Professor Anders Vik and my co-supervisor has been Professor Trond Vidar Hansen. The School of Pharmacy, University of Oslo is gratefully acknowledged for my Ph.D.-scholarship.

First, I would like to express my deepest gratitude to my two supervisors, Associate Professor Anders Vik and Professor Trond Vidar Hansen for giving me the opportunity to work on such an interesting and inspiring project. Associate Professor Anders Vik has been a great supporter and contributed with valuable advice and guidance throughout the process. Professor Trond Vidar Hansen's enthusiasm and inexhaustible knowledge in the field that we are working in have inspired me. He has been a devoted supporter and promotor during my time as a Ph.D student.

Dr. Marius Aursnes deserves a special mention for his contributions to this work. His knowledge of organic chemistry and impressive experimental skills have inspired me. I have cherished the time we have spent together, even though he has not always been fond of my focus to keep our shared lab clean, tidy and organized at all times. In the four years we have worked together, we have become close friends.

Additionally, I have valued the company of former and current colleagues Renate, Elvar, Alexander, Marius, Jørn, Jens, Åsmund, Eirik, Geir, Christian, Anthony, Lisa, Jannicke and past and present master students. You have all contributed to a good and social working environment. A special thank is dedicated to Dr. Jørn E. Tungen, who has been a great collaborator, Dr. Jens Nolsø for his constructive criticism on this thesis and Professor Yngve Stenstrøm for his contributions on paper I.

I sincerely thank Senior Lecturer Dalli for the collaboration and the opportunity to be a part of his research group, where I gained more knowledge in the field of biology, as well as experience with several new techniques. Further, I would also like to thank the members of his group for fruitful discussions and a positive working atmosphere during my stay.

My friends and family should be thanked for their great support, encouragement and love throughout the years. Despite not always knowing what I do for a living, I have treasured the good and fun times we have spent together.

Lastly, I would like to thank my dear partner Ole Henrik Eng Eibak for his never-ending support, patience and love, which have kept me motivated and assisted me through the last years of my doctoral degree. I would also like to express my gratitude for the time he has spent proofreading my thesis, as well as constructive feedback on the language.

Oslo, August 2017

Karoline Gangestad Primdahl

Karoline Gangestad Primdahl

Table of Contents

List of Publications

Paper I:

Synthesis of 5-(S)-HETE, 5-(S)-HEPE and (+)-zooxanthellactone: Three hydroxylated polyunsaturated fatty acid metabolites

Karoline Gangestad Primdahl, Yngve Stenstrøm, Trond Vidar Hansen, Anders Vik.

Chemistry and Physics of Lipids, **2016**, *196*, 1-4.

Paper II:

An efficient total synthesis of leukotriene B4

Karoline Gangestad Primdahl, Jørn Eivind Tungen, Marius Aursnes, Trond Vidar Hansen, Anders Vik.

Organic & Biomolecular Chemistry. **2015**, *13*, 5412-5417.

Paper III:

Stereocontrolled Synthesis and Investigation of the Biosynthetic Transformations of 16(S),17(S)-epoxy-PD$_{n\text{-}3\ DPA}$

Karoline Gangestad Primdahl, Jørn Eivind Tungen, Patricia R. Souza, Romain A. Colas, Jesmond Dalli, Trond Vidar Hansen and Anders Vik.

Organic & Biomolecular Chemistry, **2017**, DOI:10.1039/c7ob0213e

Paper IV:

Synthesis of 13(R)-Hydroxy-7Z,10Z,13R,14E,16Z,19Z Docosapentaenoic Acid (13R-HDPA) and Its Biosynthetic Conversion to the 13-Series Resolvins

Karoline G. Primdahl, Marius Aursnes, Mary E. Walker, Roman A. Colas, Charles N. Serhan, Jesmond Dalli, Trond V. Hansen, Anders Vik.

Journal of Natural Products. **2016**, *79*, 2693-2702.

Manuscript not included in the dissertation:

Paper V:

Synthesis, molecular modelling studies and biological evaluations of three oxo-polyunsaturated fatty acids

Toni Giorgino, Jana Selent, Karoline Gangestad Primdahl, Anders Vik, Yngve Stenstrøm, Trond Vidar Hansen.

Manuscript.

Abstract

The last decades have witnessed extensive efforts dedicated to gain knowledge of the inflammatory processes. This has led to the identification of several oxygenated lipid mediators derived from ω-6 and ω-3 polyunsaturated fatty acids. The oxygenated lipid mediators that have anti-inflammatory and pro-resolving properties have recently been coined specialized pro-resolving mediators. These compounds play an important role in the resolution of inflammation and return to homeostasis by halting the infiltration of neutrophils and stimulating the clearance of apoptotic cells and debris. This thesis reports on new knowledge on the chemical, biochemical and cellular events mediated by some novel specialized pro-resolving lipid mediators using stereoselective total synthesis

In the first part of this thesis, a stereoselective protocol for the asymmetric reduction of the methyl esters of 5-oxo-ETE, 5-oxo-EPE and 4-oxo-DHA has been developed, rendering short and stereoselective syntheses of the natural products 5-(*S*)-HETE, 5-(*S*)-HEPE and (+)-zooxanthellactone (the lactone derived from 4-(*S*)-HDHA). 5-(*S*)-HETE is a known mediator of neutrophil recruitment during inflammatory processes, but 5-(*S*)-HEPE and 4-(*S*)-HDHA have not been thoroughly investigated. The three hydroxylated polyunsaturated fatty acids were prepared in six steps by biomimetic synthesis from arachidonic acid, eicosapentaenoic acid and docosapentaenoic acid.

In the second part of the thesis, an efficient, convergent and stereoselective total synthesis of the potent pro-inflammatory lipid mediator LTB_4 is described. The synthesis was achieved in 5% yield over ten steps from commercial starting materials. The key steps in this synthesis were the stereocontrolled Nagao acetate-aldol reaction and the *Z*-selective Boland reduction. No HPLC purification was required in any of the steps.

Knowledge of the intricate mechanism involved in the biosynthesis of the lipid mediators and the structural elucidation of each lipid mediator is necessary in the hopes of developing new strategies for the treatment of inflammation and chronic diseases. For this reason, we were interested in investigating the biosynthetic pathways of the specialized pro-resolving mediators $PD1_{n\text{-}3\ DPA}$ and the novel 13-series resolvins.

To establish the structure and involvement of the precursors of these lipid mediators, stereoselective total syntheses of the intermediates, 13*R*-HDPA and 16(*S*),17(*S*)-epoxy-$PD_{n\text{-}3\ DPA}$, were conducted. Further, biological experiments involving matching of synthetic and authentic material and acidic aqueous trapping studies confirmed the structure of both 13*R*-HDPA and 16(*S*),17(*S*)-epoxy-$PD_{n\text{-}3\ DPA}$. Additionally, incubation studies proved that 13*R*-HDPA and 16(*S*),17(*S*)-epoxy-$PD_{n\text{-}3\ DPA}$ were converted into the potent pro-resolving 13-series resolvins and $PD1_{n\text{-}3\ DPA}$, respectively. Hence, we have provided evidence for the involvement of these two intermediates in individual biosynthesis of the mentioned specialized pro-resolving lipid mediators. In addition, we provide evidence that 16(*S*),17(*S*)-epoxy-$PD_{n\text{-}3\ DPA}$ also regulates human leukocyte responses with similar potency to $PD1_{n\text{-}3\ DPA}$.

In the last part of the thesis, initial synthetic studies towards the novel 13-series resolvin lipid mediator, RvT3, is disclosed.

Graphical Abstracts

Paper I:

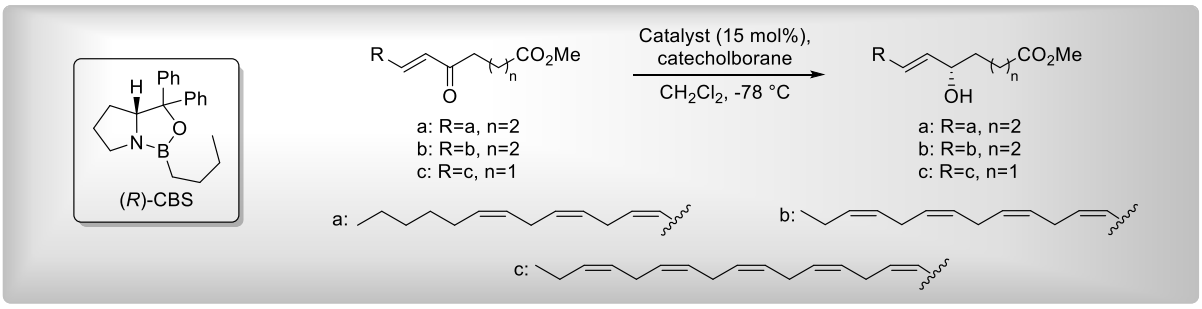

Paper II:

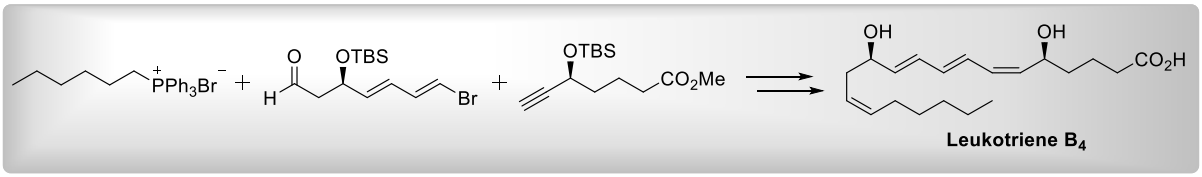

Paper III:

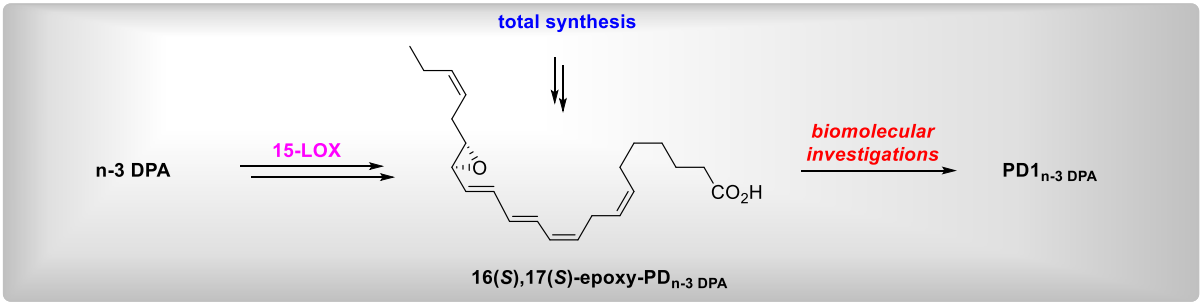

Paper IV:

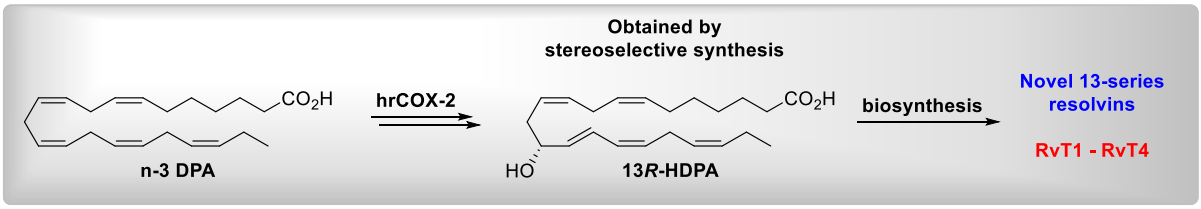

Abbreviations

9-BBN	9-Borabicyclo[3.3.1]nonane
AA	Arachidonic acid
ALA	Alpha-linoleic acid
Alpine-borane®	B-Isopinocampheyl-9-borabicyclo[3.3.1]nonane
AT	Asprin-triggered
AT-LX	Asprin-triggered lipoxin
AT-Rv	Asprin-triggered resolvin
BINAL-H	Binaphtol-modified aluminium hydride
BINAP	2,2′-*Bis*(diphenylphosphino)-1,1′-binaphthalene
BLT	B leukotriene receptor
BMS	Borane dimethyl sulfide
CAM	Cerium ammonium molybdate
CBS	Corey-Bakshi-Shibata catalyst
COX	Cyclooxygenase enzyme
CSA	Camphor sulfonic acid
CYP	Cytochrome P450
CysLT	Cysteinyl leukotriene receptor
DBU	1,8-Diazabicyclo[5.4.0]undec-7-ene
DHA	Docosahexaenoic acid
DIBAL-H	Diisobutyl aluminum hydride
DIP-chloride	B-Chlorodiisopinocampheylborane
DIPT	Diisopropyl tartrate
DMP	Dess-Martin periodinane
DMSO	Dimethyl sulfoxide
DPA	Docosapentaenoic acid
ee	Enantiomeric excess
EPA	Eicosapentaenoic acid
GGT	γ-Glutamyl transferase
GPCR	G-protein coupled receptor
HDHA	Hydroxydocosahexaenoic acid
HDPA	Hydroxydocosapentaenoic acid
HEPE	Hydroxyeicosapentaenoic acid
HETE	Hydroxyeicosatetraenoic acid
H*p*DHA	Hydroperoxydocosahexaenoic acid
H*p*DPA	Hydroperoxydocosapentaenoic acid
H*p*EPE	Hydroperoxyeicosapentaenoic acid
H*p*ETE	Hydroperoxyeicosatetraenoic acid

HUVEC	Human umbilical vein endothelial cells
HWE	Horner-Wadsworth-Emmons reaction
KHMDS	Potassium *bis*(trimethylsilyl)amide
LA	Linoleic acid
LAH	Lithium aluminum hydride
LDA	Lithium diisopropyl amide
LOX	Lipoxygenase enzyme
LT	Leukotriene
LX	Lipoxin
MaR	Maresin
m-CPBA	*meta*-Chloroperoxybenzoic acid
MCTR	Maresin conjugates in tissue regeneration
MRM	Multiple reaction monitoring
MTPA	α-Methoxy-α-trifluoromethylphenylacetic acid
NaHMDS	Sodium *bis*(trimethylsilyl)amide
PCTR	Protectin conjugates in tissue regeneration
PD1	Protectin 1
PG	Prostaglandin
PGHS	Prostaglandin synthase
PMN	Polymorphonucleat neutrophils
PPARγ	Peroxisome proliferator-activated receptor γ
p-TsOH	*p*-Toluenesulfonic acid
PUFA	Polyunsaturated fatty acid
RCAM	Ring-closing alkyne metathesis
RCM	Ring-closing metathesis
RCTR	Resolvin conjugates in tissue regeneration
Red-Al®	Sodium *bis*(2-methoxyethoxy)aluminum hydrid
RvD	Resolvin D-series
RvE	Resolvin E-series
RvT	13-Series resolvin
SPM	Specialized pro-resolving lipid mediator
TBAF	Tetrabutylammonium fluoride
TBS	*tert*-Butyldimethylsilyl
TES	Triethylsilyl
THF	Tetrahydrofuran
TMS	Trimethylsilyl

Chapter 1

1 Introduction

1.1 Inflammation and Resolution

Inflammation is the human body's immune system responding to injury or invasion of harmful pathogens. This is a protective mechanism where the ideal outcome is removal of the injurious stimuli followed by repair of damaged tissue and ultimately restoring cellular homeostasis.[1]

The signs of acute inflammation were first described by the Roman encyclopaedist of ancient times, Aulus Cornelius Celsus, and they are *tumor*, *rubor*, *calor* and *dolor* (swelling, redness, heat and pain).[2] Later, loss of function was included in the list. Resolution of acute inflammation, or its catabasis as it is also referred to,[3] involves the reduction and removal of leukocytes and debris to pre-inflammation levels and return to normalcy.[4] The absence of this process leads to a persistent immune response, eventually causing chronic inflammation. It has been recognised that uncontrolled inflammation can contribute to the pathogenesis of a variety of diseases, such as cardiovascular diseases,[5] rheumatoid arthritis,[6] periodontal diseases,[7] asthma,[8] diabetes,[9] Alzheimer's disease and cancer.[10]

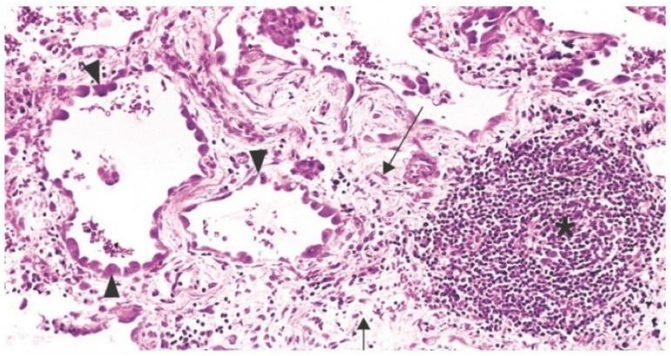

Figure 1.1 Chronic inflammation in the lung, showing all three characteristics: 1) collection of chronic inflammatory cells (asterisk), 2) normal alveoli are replaced by cuboidal epithelium (arrowheads), and 3) Fibrosis (arrows).[11]

The course of action during inflammation depends on the type of stimuli and is orchestrated by a series of highly complex biochemical events.[12] In the initiation phase, pro-inflammatory proteins, cytokines and chemokines are synthesized, which all activate the release and production of potent chemoattractants such as histamine and bradykinin, as well as the classic eicosanoids derived from arachidonic acid (AA, **1**), including the prostaglandins and the leukotrienes.[12] Polymorphonuclear neutrophils (PMNs) and other representatives of white blood cells are recruited to the inflamed site by the chemoattractants produced previously. The mobilization of PMNs is the first line of defence required for the neutralization and

removal of invading microbes by phagocytosis. However, debris from neutrophils and granule content might unintentionally leak into the extracellular milieu during incomplete phagocytosis by the neutrophils, causing tissue damage and increasing the pro-inflammatory response.[4]

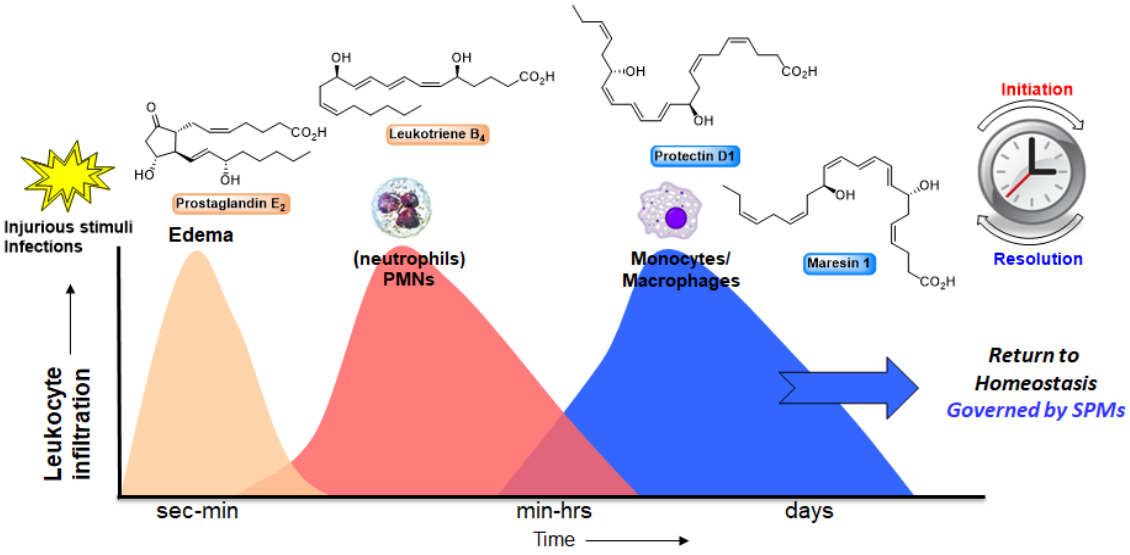

Figure 1.2 An outline of the time course of inflammation.

Resolution is the ideal outcome of inflammation, which involves the halt of neutrophil infiltration and the removal of debris and apoptotic neutrophils by macrophages, referred to as efferocytosis, ultimately leading to the return to homeostasis. Traditionally, this was thought to be a passive process where the degradation of the pro-inflammatory components was assumed to be adequate for the termination of the inflammatory response, causing the inflammation to die out with time.[13] New evidence has proven that this prosses is tightly regulated by an intricate biochemical and cellular mechanisms, confirming it beyond doubt to be an active process.[14] These mechanisms include the production of anti-inflammatory and pro-resolving oxygenated polyunsaturated fatty acids (PUFAs), such as the lipoxins, resolvins, protectins and maresins. Their actions are mediated through G-protein-coupled receptors (GPCRs) that efficiently promote the decrease in inflammatory response, tissue repair and protection of cells, as well as the complete resolution of the inflamed site.[3]

1.2 Polyunsaturated Fatty Acids and Their Oxygenated Products

The importance of dietary essential fatty acids, such as linoleic acid (LA), was first demonstrated in a study conducted by George Burr and his wife Mildred Burr in 1929. They provided evidence for the critical role of fatty acids to maintain the health of rats.[15,16] Later, several human studies have shown the beneficial effects of ω-3 fatty acids, including eicosapentaenoic acid (EPA, **2**) and docosahexaenoic acid (DHA, **3**) in cardiovascular health.[17-20] It is widely accepted that chronic inflammation may lead to several serious

diseases, such as cancer and autoimmune diseases.[10,21] The observed positive health effects are linked to the ratio between ω-3 and ω-6 PUFAs due to the formation of anti-inflammatory and pro-inflammatory lipid mediators as described below.[22]

The PUFAs predominantly exist as esters in the phospholipids of the cell membrane. Upon activation, such lipids associated PUFAs, including AA (**1**), EPA (**2**) and DHA (**3**), are released by the activation of enzymes belonging to the phospholipase family. When released, these PUFAs can be oxidized either by enzymes or via free radical mechanisms to a wide array of products. Among the biologically most interesting and active oxygenated lipids are the lipid mediators. The three main enzymatic pathways involved in the formation of these oxygenated PUFAs are catalysed by lipoxygenases (LOX), cyclooxygenases (COX) and cytochrome P450 (CYP).

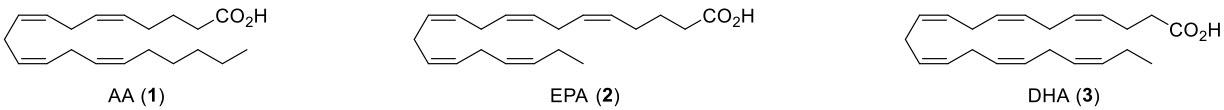

Figure 1.3 The structures of AA (**1**), EPA (**2**) and DHA (**3**).

The products resulting from enzymatic oxidation of the ω-6 fatty acid AA (**1**), namely prostaglandins of the 2-series and the leukotrienes, possess pro-inflammatory properties. On the other hand, the third class of AA-derived lipid mediators, the lipoxins, are pro-resolving.[23,24] The corresponding pathway for the ω-3 fatty acids, EPA (**2**) and DHA (**3**), primarily leads to the formation of anti-inflammatory, pro-resolving and cytoprotective lipid mediators, such as the resolvins, protectins and maresins (Figure 1.4).[25,26] The prostaglandins of the 3-series are also formed from EPA (**2**).[27]

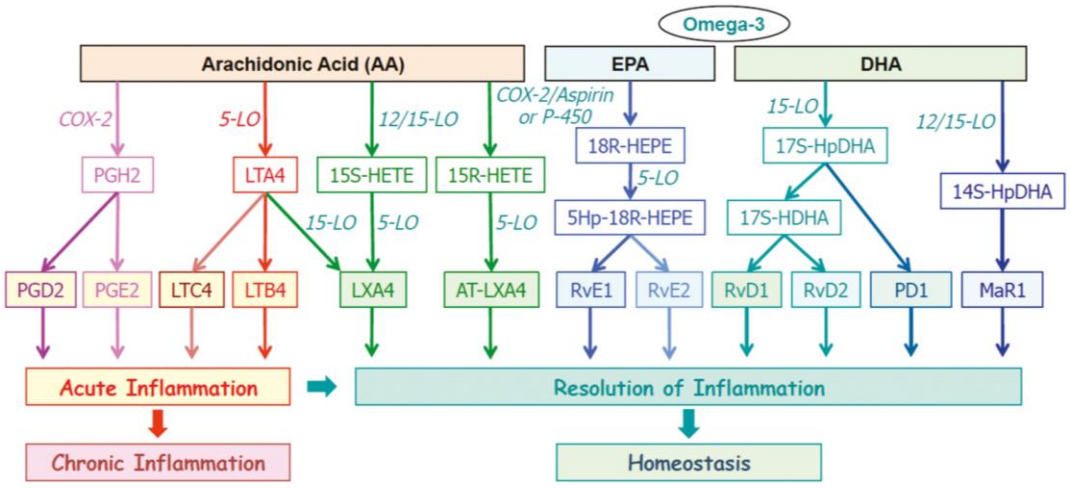

Figure 1.4 Biosynthetic cascades and actions of selected lipid mediators derived from AA (**1**), EPA (**2**) and DHA (**3**).[26]

1.2.1 Lipoxygenases

The stereoselective insertion of molecular oxygen into PUFAs containing more than one *cis*,*cis*-1,4-pentadiene component in the molecule is catalysed by a class of non-heme, iron-containing enzymes entitled lipoxygenases.[28-32] Lipoxygenases are abundant in plants, fungi and animals. In humans, five different LOXs are expressed: 5-LOX, 12-LOX, 12*R*-LOX, 12/15-LOX, and epithelial LOX. The names of the different isoforms are assigned according to which carbon in the AA fatty acid chain first subjected to dioxygenation. The lipoxygenation is initiated by the stereoselective hydrogen abstraction from a *cis*,*cis*-1,4-pentadiene moiety in the PUFA, as illustrated in Scheme 1.1. The configuration of the hydroperoxyl group formed is predominantly *S* (e.g. 5-(*S*)-H*p*ETE (**4**), 5-(*S*)-H*p*EPE (**5**), 4-(*S*)-H*p*DHA (**6**)).[33] The hydroperoxy acid products constructed by LOX enzymes are further submitted to enzymatic transformations leading to a comprehensive assembly of biologically active lipid mediators including leukotrienes, lipoxins, resolvins, protectins and maresins.[34]

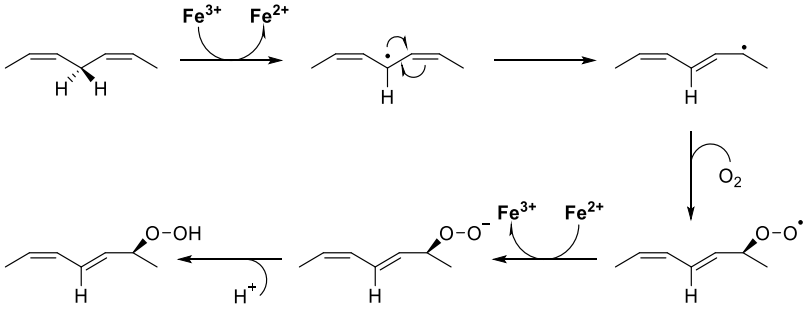

Scheme 1.1 Mechanism for lipoxygenation of a *cis*,*cis*-1,4-pentadiene system.[33]

1.2.2 Products Derived From 5-LOX Pathways and Their Biological Importance

5-LOX is predominantly expressed in cells that are involved in the immune system, including neutrophils, eosinophil, basophil, macrophages, etc. AA (**1**), EPA (**2**) and DHA (**3**) are suitable substrates for 5-LOX and molecular oxygen is stereoselectively incorporated at C5 in AA (**1**) and EPA (**2**), while DHA (**3**) can be oxygenated at either C4 or C7. The hydroperoxy species can then undergo further enzymatic conversion, either by peroxidase to the corresponding *S*-hydroxy acids, 5-(*S*)-hydroxyeicosatetraenoic acid (5-(*S*)-HETE, **7**), 5-(*S*)-hydroxyeicosapentaenoic acid (5-(*S*)-HEPE, **8**) and 4-(*S*)-hydroxydocosahexaenoic acid (4-(*S*)-HDHA, **9**)[35-38] (Scheme 1.2) or by different pathways to provide a diverse array of biologically active lipid mediators (Figure 1.4).

The biological actions of the AA derived products, 5-(*S*)-HETE (**7**) and 5-keto acid as potent chemoattractants during inflammation have been thoroughly investigated.[39-43] However, this is not the case for 5-(*S*)-HEPE (**8**) and 4-(*S*)-HDHA (**9**). These products formed from the 5-LOX oxidation of EPA (**2**) and DHA (**3**), have not been sufficiently documented.

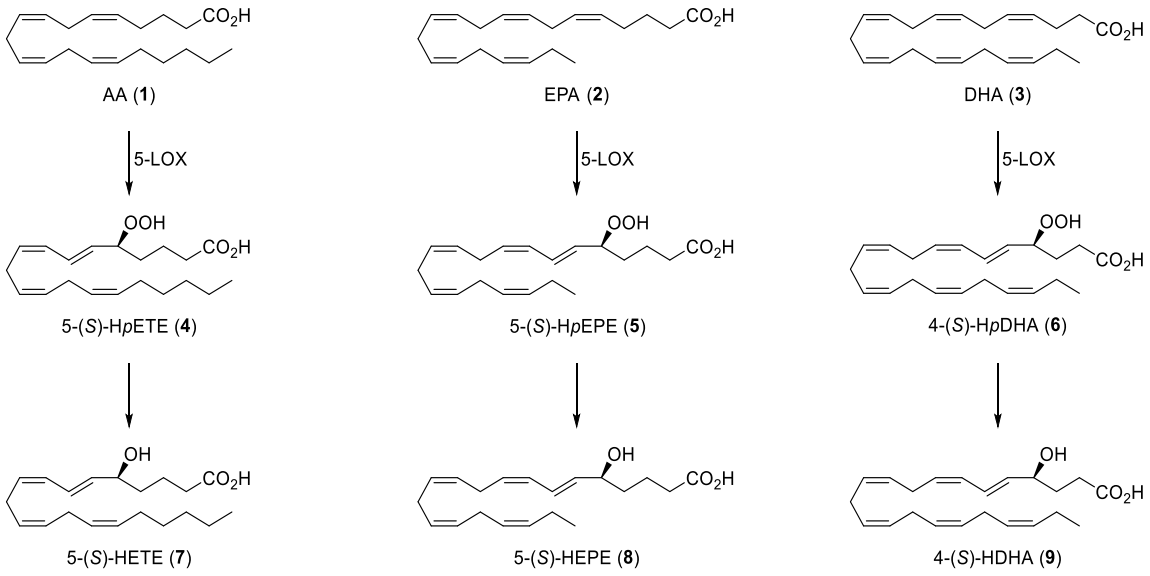

Scheme 1.2 Biogenesis of 5-(*S*)-HETE (**7**), 5-(*S*)-HEPE (**8**) and 4-(*S*)-HDHA (**9**) from AA (**1**), EPA (**2**) and DHA (**3**) respectively.

Some research has been conducted on the beneficial effects of 5-(*S*)-HEPE (**8**) and 4-(*S*)-HDHA (**9**) toward diabetes. 5-(*S*)-HEPE (**8**) was proven to be a potent agonist for the GPCR, G119, increasing glucose-dependant insulin secretion.[44] This EPA-derived metabolite also demonstrated agonistic effect towards another G-coupled receptor, G120, mediating potent insulin-sensitizing and anti-diabetic effects.[45] On the other hand, 4-(*S*)-HDHA (**9**) and its keto-analogue were identified as potent activators of the peroxisome proliferator-activated receptor γ (PPARγ) and potential anti-diabetic agents through a study conducted by Yamamoto and co-workers.[46] A further beneficial effect observed from the intake of ω-3 PUFAs was recently published by Sapieha and co-workers.[38] Their study showed that 4-(*S*)-HDHA (**9**) mediated angiogenesis, neovascularization and decreased endothelial cell proliferation through the receptor, PPARγ. 4-(*S*)-HDHA (**9**) and similar ω-3 PUFA metabolites are therefore interesting as potential therapeutics targeting vasoproliferation diseases.

1.2.3 Leukotrienes

The discovery of the leukotrienes was a result of the study on the transformation of AA (**1**) in polymorphonuclear leukocytes performed by Borgeat and Samuelsson.[47,48] The name originates from the white blood cells that biosynthesize the leukotrienes, namely the leukocytes. The latter part of its name, triene, reflects the three conjugated double bonds present in the structures. The leukotrienes are pro-inflammatory mediators of the 5-LOX pathway of AA (**1**) metabolism (Scheme 1.3). Upon activation, the enzyme phospholipase A_2 releases AA (**1**) from the membrane phospholipids. The free acid can subsequently act as a substrate for 5-LOX, which inserts molecular oxygen at C5 to produce 5-(*S*)-H*p*ETE (**4**). It is further converted to leukotriene A_4 (LTA_4, **10**) by a second catalytic activity of 5-LOX. At this stage, LTA_4 (**10**) can either undergo enzymatic hydrolysis by LTA_4 hydrolase to yield

leukotriene B_4 (LTB_4, **12**) or it can be transformed into the glutathione conjugate leukotriene C_4 (LTC_4, **11**) by leukotriene C_4 synthase (glutathione S-transferase) (Scheme 1.3).

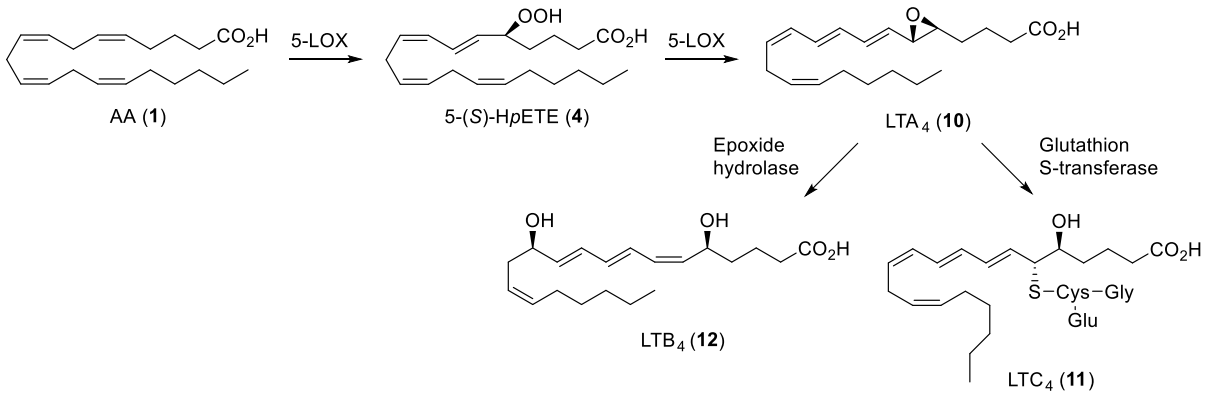

Scheme 1.3 Outline of the biosynthesis of three leukotrienes, LTA_4 (**10**), LTC_4 (**11**) and LTB_4 (**12**).

The leukotrienes are generated in the early phases of inflammation and possess pro-inflammatory properties. Their actions are mediated through GPCRs termed B leukotriene receptors (BLT_1 and BLT_2) and cysteinyl leukotriene receptors ($CysLT_1$ and $CysLT_2$), which are located on the outer plasma membrane of structural and inflammatory cells.[49,50] LTB_4 (**12**) is a potent chemoattractant causing recruitment and accumulation of neutrophils and other leukocytes at the site of inflammation.[51] The interesting biological effects of LTB_4 (**12**) have caused a demand in the market, reflected in the extensive library of published syntheses on this specific bioactive lipid mediator.[52-59] The cysteinyl-containing leukotrienes stimulate contraction of the airway through tightening of the smooth muscle as well as vascular permeability in the venous blood vessels.[60]

1.2.4 Lipoxins

The lipoxins are a class of lipid mediators consisting of a tetraene and three hydroxyl groups containing inherent pro-resolving effects. The lipoxins were isolated in 1984 as a product formed by the involvement of the enzyme 15-LOX from AA (**1**) in human leukocytes.[61,62] Lipoxins biosynthesized from EPA (**2**) by similar mechanisms have also been identified.[63] The name of these trihydroxylated lipid mediators are associated with the interaction of multiple distinct lipoxygenase pathways involved in their biogenesis.

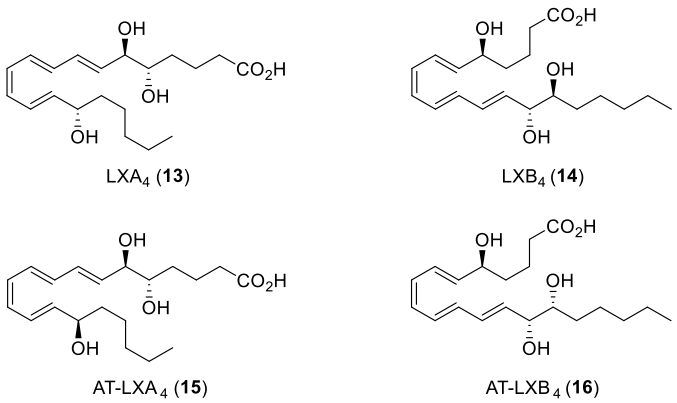

Scheme 1.4 Structures of LXA_4 (**13**), LXB_4 (**14**) and the aspirin-triggered lipoxins (AT-LXA_4 (**15**) and AT-LXB_4 (**16**)).

Lipoxin A_4 (LXA_4, **13**) and lipoxin B_4 (LXB_4, **14**) have prominent roles in the resolution of inflammation. They terminate the infiltration and accumulation of neutrophils, as well as activation of monocyte-derived macrophages to remove apoptotic PMNs by phagocytosis.[64] This is a crucial step in the resolution of inflammation. If the cell debris is not excised, the inflammatory process can become chronic and several diseases may develop. Similar biological effects are observed for the aspirin-triggered lipoxins (AT-LXA_4 (**15**) and AT-LXB_4 (**16**)), underpinning the beneficial dampening effect of aspirin on inflammation.[65] During inflammation, a switch of lipid mediator class occurs from the pro-inflammatory mediators, leukotrienes and prostaglandins to the anti-inflammatory lipoxins. This switch is initiated by prostaglandin E_2 (PGE_2, **96**) and prostaglandin D_2 (PGD_2), which induce the aforementioned change in formation of the products formed from the 5-LOX pathways to the lipoxins allocated by 15-LOX routes.[66] The lipoxins also play an essential role in the wound healing process by stimulating the nonphlogistic infiltration of monocytes.[67]

1.2.5 Cyclooxygenase

Cyclooxygenase (COX), also known as prostaglandin synthase (PGHS), is a heme-containing enzyme involved in the biosynthesis of the pro-inflammatory class of lipid mediators coined prostaglandins. Two isoforms of this enzyme have been identified, namely COX-1 and COX-2. COX-1 is expressed in most tissues and responsible for the homeostatic production of prostaglandins, while COX-2 is induced by several stimuli during inflammation.[68] Even though the two isoforms have approximately the same molecular weight, small variations in the amino acid composition might be the reason for their different courses of action.[69] There are two active sites present in each of the COX enzymes: the cyclooxygenase active site and the peroxidase active site. Aspirin and nonsteroidal anti-inflammatory drugs have the ability to inhibit COX. Several side effects, including gastrointestinal ulceration and bleeding, renal damage, and platelet dysfunction, have been associated with the incapacitation of both isoforms.[68] Selective inhibition of COX-2 is desirable because of the possible suppression of inflammatory prostaglandins. Although COX-2 is related with inflammation, recent publications show that COX-2 is involved in the biosynthesis of novel potent anti-

inflammatory and pro-resolving lipid mediators, termed 13-series resolvins (RvTs, **59-62**).[70,71]

1.2.6 Prostaglandins

The presence of vasodepressor and smooth muscle-stimulating agents in human seminal plasma and mammalian prostate glands were discovered independently by Goldblatt and von Euler in the early 1930s.[72-74] These agents are now known as the prostaglandins. The name assigned to these bioactive lipid mediators is a reflection of their prostate gland origin. Approximately 30 years after the discovery of the prostaglandins, Samuelsson and Bergström demonstrated that they were the products of AA (**1**) metabolism.[75] Shortly thereafter, the mechanism of prostaglandin biosynthesis was outlined by Hamberg and Samuelsson.[76] This mechanism is outlined in Scheme 1.5.

Prostaglandin synthesis is initiated by several different kinds of stimuli, causing the release of membrane bound AA, thus allowing AA (**1**) to act as a substrate for the cyclooxygenase enzymes. In the active site of COX-1, an oxygen-centred phenol radical on the tyrosine-385 residue may then abstract a hydrogen at the 13-position leading to the formation of a radical, which is trapped by molecular oxygen, resulting in a cyclic peroxide. Incorporation of another oxygen molecule at C15 followed by reduction of the hydroperoxyl group yields prostaglandin H_2 (PGH_2, **18**), the precursor to all the 2-series of prostaglandins and thromboxanes.[77] The inhibition of the prostaglandin biosynthesis by aspirin and NSAIDs was proven by Sir John R. Vane.[78] These drugs are now known as potent inhibitors of COX, which have a crucial role in the formation of the prostaglandins. In 1982, Sir John Vane was awarded the Nobel Prize in Physiology or Medicine together with Sune K. Bergstrøm and Bengt I. Samuelsson for their efforts concerning prostaglandins and related biologically active molecules.[79]

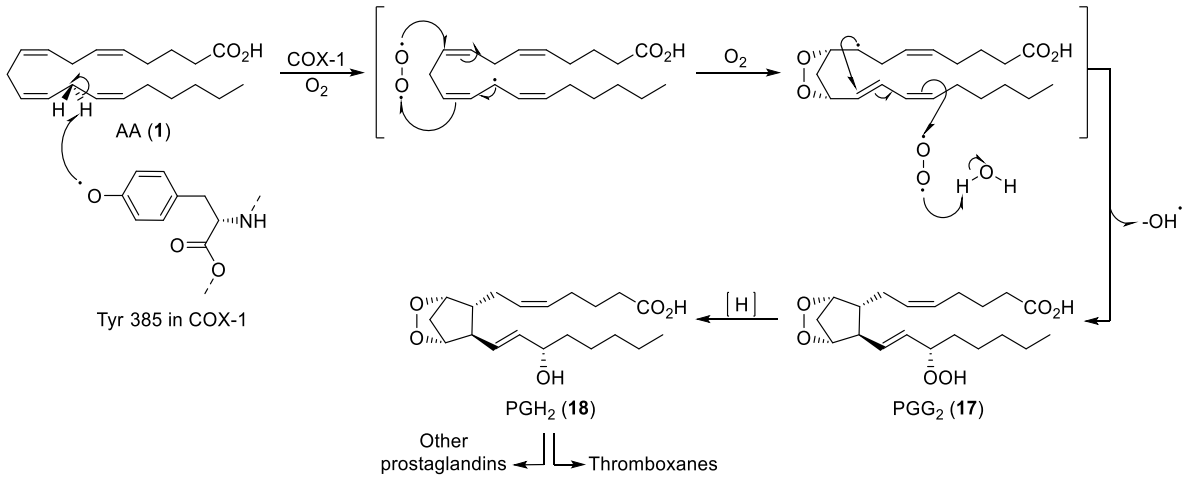

Scheme 1.5 Outline of the biosynthesis of prostaglandins and thromboxanes from AA (**1**) catalysed by COX-1.

The prostaglandins have later been found in numerous other tissues containing AA (**1**).[75] These pro-inflammatory lipid mediators are formed in the initiation phase of inflammation and they are involved in the regulation of the cardinal signs of inflammation, such as edema and redness caused by vasodilation and vasopermeability.[80,81] As previously mentioned, PGE_2 (**96**) and PGD_2 are involved in the biosynthesis of the pro-resolving mediators, lipoxins, by stimulating the transcription of the necessary enzymes for their biogenesis.[66]

1.3 Specialized Pro-Resolving Lipid Mediators (SPMs)

Several beneficial effects have been associated with the consummation of ω-3 oxygenated PUFAs, such as potential immunoregulatory and anti-inflammatory responses in arteriosclerosis, arthritis, and asthma,[82] along with antitumor and antimetastatic effects.[83] Protective effects against cardiovascular diseases have also been related with dietary supplementation of EPA (**2**) and DHA (**3**).[20] However, the underlying biomolecular mechanisms connected with the protective actions of ω-3 fatty acids have long remained unclear. In the last two decades, efforts headed by Charles N. Serhan have established resolution of inflammation to be an active process, orchestrated by several novel families of oxygenated PUFA derivatives that display both anti-inflammatory and pro-resolving effects.[34] These oxygenated PUFAs are now commonly referred to as specialized pro-resolving lipid mediators (SPMs).[84] The aforementioned compounds were discovered after Serhan and co-workers studied the fate of EPA (**2**) and DHA (**3**) in several models of inflammation by using LC-MS/MS techniques. Resolvins, protectins and maresins are families of SPMs, formed by stereoselective, enzymatic oxygenation of the essential ω-3 fatty acids, EPA (**2**) and DHA (**3**). They play an active role in the termination of inflammation by halting the infiltration of leukocytes and promoting removal of apoptotic cells, permitting the natural resolution to homeostasis.[3]

1.3.1 Resolvins of the E- and D-Series

The first SPM reported, denominated resolving E1 (RvE1, **20**), was isolated from inflamed exudates extracted from mice using the air pouch model.[85] The term resolvins is a reflection of the presence of this family of lipid mediators in the resolution phase of inflammation, as well as their potent pro-resolving abilities.[86] To confirm the absolute configuration of the stereogenic centres present in the structure of RvE1 (**20**), the biological material was compared with synthetically obtained material.[87] This method has later been used in the assignment of other lipid mediators where the absolute configuration of each compound is established. After the identification of RvE1 (**20**), two new members of the resolvin family derived from EPA (**2**) followed, namely RvE2 (**21**) and RvE3 (**22**).[88,89]

The formation of 18-(*R*)-H*p*EPE (**19**) catalysed by either aspirin acetylated COX-2 or cytochrome P450, is the first step in the biosynthesis of these three resolvins. Further, this hydroperoxide intermediate **19** can be converted in the neutrophils by the 5-LOX pathway, yielding RvE1 (**20**) and RvE2 (**21**). In the case of RvE3 (**22**) formation, 18-(*R*)-H*p*EPE (**19**)

is transformed in the eosinophils via the 12/15-LOX pathway, which leads to two equally bioactive stereoisomers with different configurations of the hydroxyl group located at C18.[89] An outline of the biosynthesis of RvE1 (**20**) - RvE3 (**22**) is shown in Scheme 1.6.

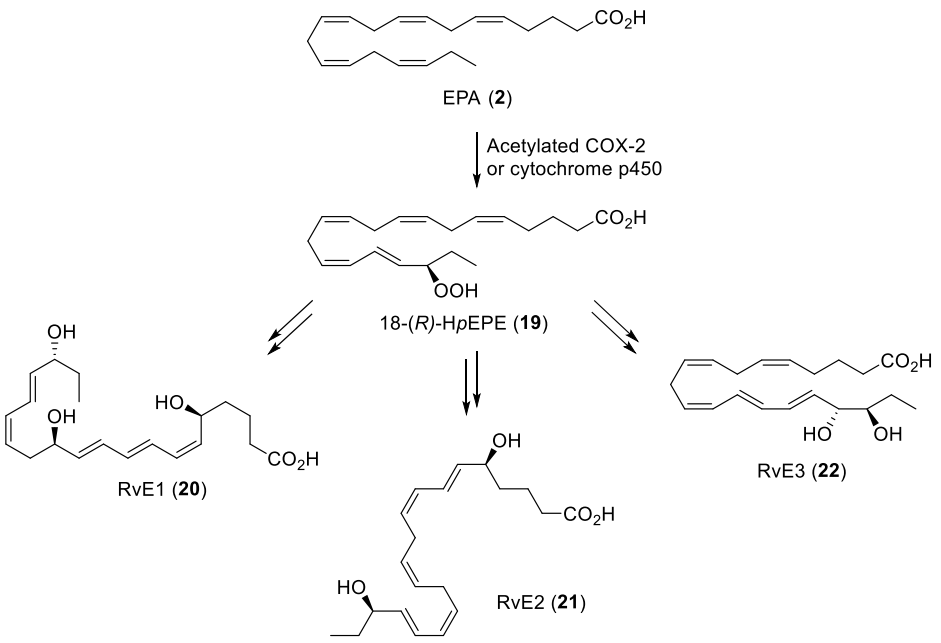

Scheme 1.6 Outline of the biosynthesis of the E-series resolvins.

A similar pathway for the DHA analogues exists and a total of six resolvins derived from DHA (**3**) (RvD1-RvD6) have been discovered (Scheme 1.7).[90,91] Depending on whether the resolvins are derived from EPA (**2**) or DHA (**3**), they are divided in two subclasses, the E- and D-series. The biosynthesis of the D-series resolvins involves the incorporation of oxygen at C17 in DHA (**3**) catalysed by 15-LOX, providing the hydroperoxy acid 17-(*S*)-H*p*DHA (**23**). Additional conversion of this intermediate **23** by lipoxygenase enzymes yields the six different DHA-originated resolvins, all carrying a hydroxyl group at carbon 17 with *S*-configuration. Aspirin can alter the biosynthesis of the D-series resolvins, where acetylated COX-2 incorporates oxygen with the opposite configuration at C17, leading to the formation of so-called aspirin-triggered resolvins (AT-Rv).[86]

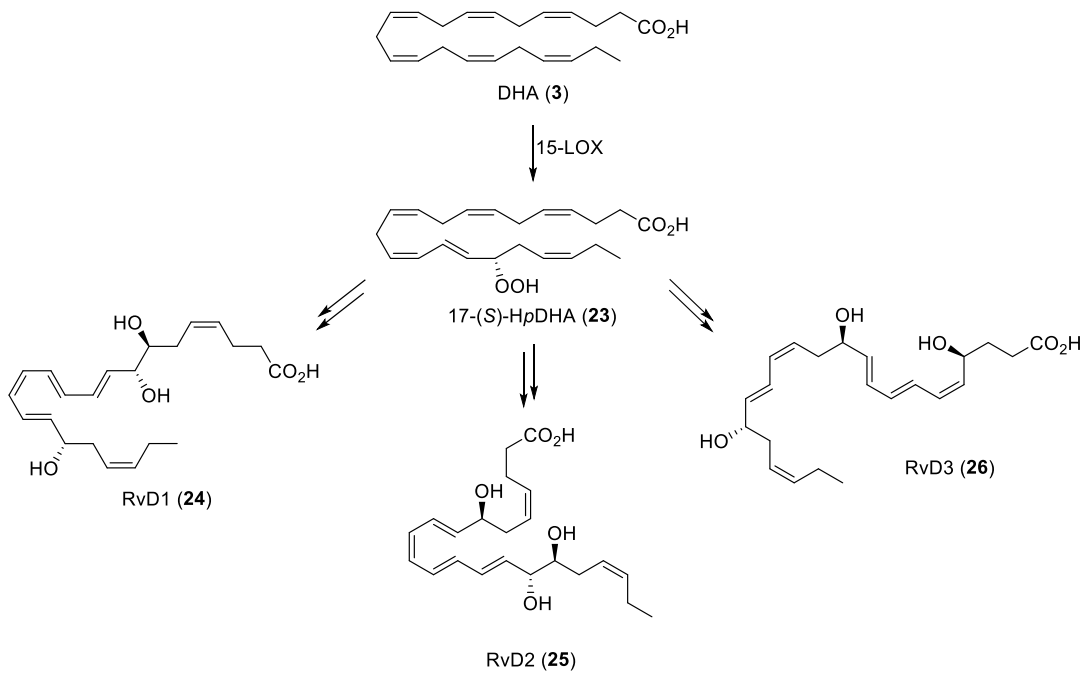

Scheme 1.7 Outline of the biosynthesis of three members of the D-series resolvins.

Anti-inflammatory and pro-resolving properties are observed for the resolvins of both the E- and D-series, also including the aspirin-triggered versions, by potently regulating the infiltration of neutrophils to the site of inflammation.[91] Additionally, RvE1 (**20**) upregulates the phagocytosis of apoptotic PMNs by macrophages[92] and the possibility of reducing pain during inflammation.[93]

1.3.2 Protectins

In 2002, Serhan and co-workers discovered a new family of the SPMs, generated from DHA (**3**) in murine inflammatory exudate and human PMNs.[86,90] The most prominent compound was a dihydroxylated fatty acid that was coined protectin D1 (PD1, **28**), reflecting its highly protective properties during the course of inflammation. This SPM is also referred to as neuroprotection D1 (NPD1) when it is biosynthesised in neural tissues. Further investigations led to the elucidation of the absolute stereochemistry of PD1 (**28**): Its configuration and structure was assigned 10*R*,17*S*-dihydroxy-docosa-4*Z*,7*Z*,11*E*,13*E*,15*Z*,19*Z*-hexaenoic acid by matching synthetically prepared material with the endogenous composed isolate. Consequently, the two carbinols were determined to be 10*R* and 17*S*, and a *E*,*E*,*Z* configuration for the conjugated triene.[94] Based on the data generated from experiments using both identification of alcohol trapping products via mass spectrometry and isotopic oxygen ($^{18}O_2$) incorporation, an epoxide intermediate **27** was proposed for the biosynthesis of PD1 (**28**).[94,95] In 2015, the structure of this epoxide intermediate **27** was established by matching of synthetic and biogenetic material.[96] Additionally, the synthetically prepared epoxide **27** was converted into PD1 (**28**), which further confirmed the involvement of an epoxide intermediate in the formation of PD1 (**28**).[96]

The biosynthesis of PD1 (**28**) commences with the formation of the 17-(*S*)-hydroperoxy intermediate **23** from DHA (**3**), catalysed by 15-LOX. Further conversion of this unstable hydroperoxide **23** by human leukocytes leads to the generation of the 16*S*,17*S*-epoxide **27**. The last step is the enzymatic hydrolysis of the previously formed epoxide **27**, providing PD1 (**28**).[94] An outline of the biosynthesis can be found in Scheme 1.8.

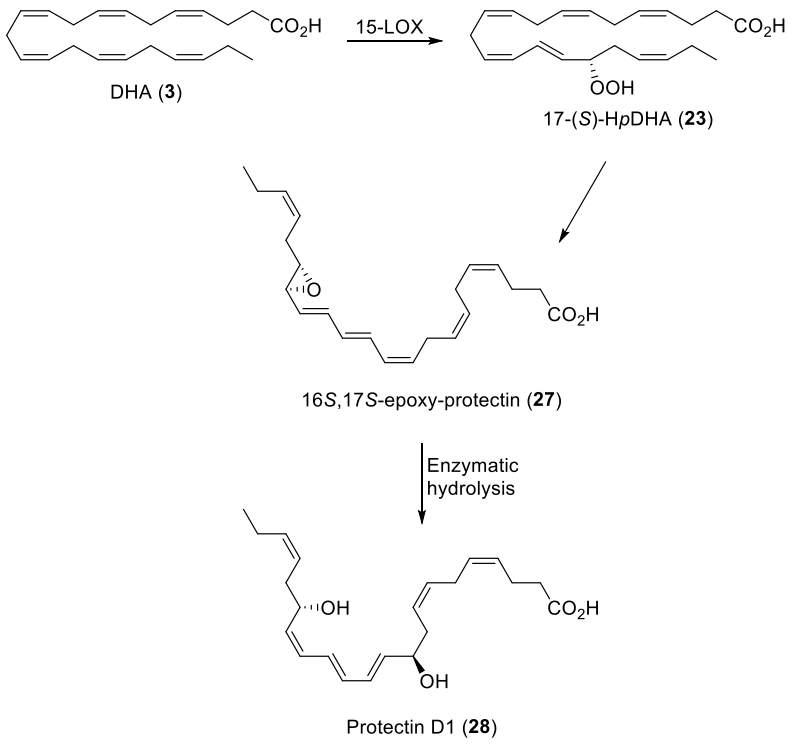

Scheme 1.8 Outline of the biosynthesis of PD1 (**28**) from DHA (**3**).

Similar to the resolvins, PD1 (**28**) in nanomolar range regulates the chemotaxis and aggregation of neutrophils, in addition to promoting the uptake of dead cell debris by macrophages at the site of inflammation.[92] During peritonitis, PD1 (**28**) has proven potently to prevent further recruitment of neutrophils,[97] modulate the production of inflammatory chemo- and cytokines,[87] promote phagocyte removal[92] and regulate T-cell migration.[98] Protective actions against damage and loss of kidney function in the case of acute kidney injury[99,100], as well as positive effects on diseases such as asthma,[101] Alzheimer's disease[102] and Parkinson's disease[103] have been indicated. PD1 (**28**) might play an important role in ocular health due to its protective properties observed in retinal injury,[104-106] neovascularization[107] (loss of sight associated with different eye diseases) and the potential of PD1 (**28**) as a therapeutic treatment of dry eye syndrome.[108]

1.3.3 Maresins

Maresin 1 (MaR1, **31**), a member of the third family of SPMs, was discovered in 2009 by Serhan and co-workers.[109] This anti-inflammatory and pro-resolving mediator derived from DHA (**3**) was first observed in self-resolving exudates by the use of lipidomics. A second member of this family, with similar mode of action as the previously mentioned MaR1 (**31**), was identified five years later and coined maresin 2 (MaR2, **32**).[110] The name maresin was established on the basis that these lipid mediators are biosynthesised by *ma*crophages in *res*olving *in*flammation.[3,109] The maresins are biosynthesized from DHA (**3**) through a 12/15-LOX pathway, generating a 14*S*-hydroperoxide **29**. Further transformation of this hydroperoxide intermediate **29** results in a 13*S*,14*S*-epoxide **30**, which upon enzymatic hydrolysis yields the maresins (**31** and **32**) (Scheme 1.9).[111] The stereochemistry of the 13*S*,14*S*-epoxy-maresin (**30**) and its role as an intermediate in the biosynthesis of the maresins were confirmed along the same line as for PD1.[111]

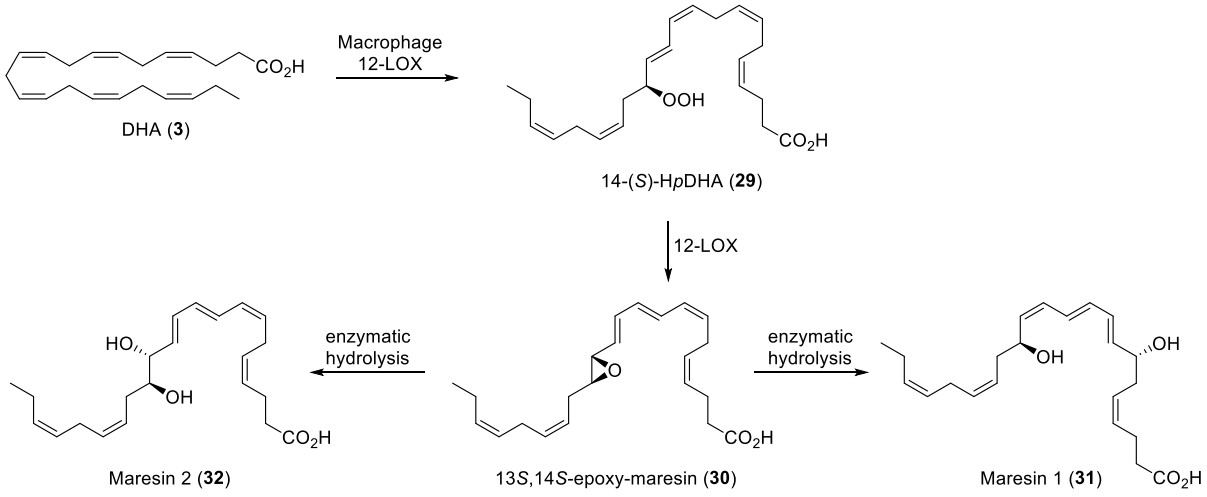

Scheme 1.9 Outline of the biosynthesis of MaR1 (**31**) and MaR2 (**32**).

The maresins display a vast array of potent bioactions resembling those observed for the other SPMs. However, MaR1 (**31**) has been proven to be more potent than RvD1 (**24**) in promoting efferocytosis by macrophages.[112] In studies where a flatworm (planarian) was decapitated, administration of MaR1 (**31**) accelerated the regeneration and reappearance of the head.[112] Additionally, relief of both inflammatory and chemotherapy-induced pain in mice and suppression of allergic lung inflammation and ILC2 function, which are involved in the pathogenesis of asthma, have been reported.[8,112]

1.3.4 The Sulfido-Conjugates of Resolvin, Protectin and Maresin

Recently, novel sulfido-conjugates of the resolvin (RCTR1-RCTR3, **34**-**36**), protectin (PCTR1-PCTR3, **37**-**39**) and maresin (MCTR1-MCTR3, **40**-**42**) were discovered by the Serhan group in *Escherichia coli* (*E.coli*) infected mice, infectious murine exudates, human spleen and human blood from sepsis patients.[113,114] These newly identified mediators originate from DHA and share a similar biosynthetic pathway with the known congeners resolvins, protectins and maresins, including the formation of a 17*S*- or 14*S*-hydroperoxide **23** and **29** by LOX enzymes, which can undergo further transformations leading to the three different epoxides **27**, **30** and **33**. Enzymatic addition of peptides to these epoxides yields PCTR1 (**37**), MCTR1 (**40**) and RCTR1 (**34**), respectively (Scheme 1.10).[114-116] γ-Glutamyl transferase (GGT) regulates the conversion of these products to PCTR2 (**38**) and PCTR3 (**39**), MCTR2 (**41**) and MCTR3 (**42**) and RCTR2 (**35**) and RCTR3 (**36**).[115] The structures of PCTR1 (**37**) and MCTR1 (**40**) were established through matching experiments of biological PCTR1 (**37**) and MCTR1 (**40**) with synthetic material obtained by ring-opening on the methyl esters of the 16*S*,17*S*-epoxy-protectin (**27**) and 13*S*,14*S*-epoxy-maresin (**30**) with glutathione. These results established the role of the epoxides **27** and **30** in the biosynthesis of these potent pro-resolving lipid mediators **37** and **40**.[115,116]

The sulfido-conjugates described above are capable of resolving *E. coli* infection by downregulating the infiltration of neutrophils and the clearance of bacteria by macrophage phagocytosis, as well as the removal of apoptotic cells.[113,114] Low concentrations of these pro-resolving mediators also accelerate tissue repair and regeneration in planarian.[113,114] The actions discussed above prove that the resolvin-, protectin- and maresin-conjugates control host responses to restrain infections, promote resolution and tissue regeneration, ultimately leading to the return to homeostasis.

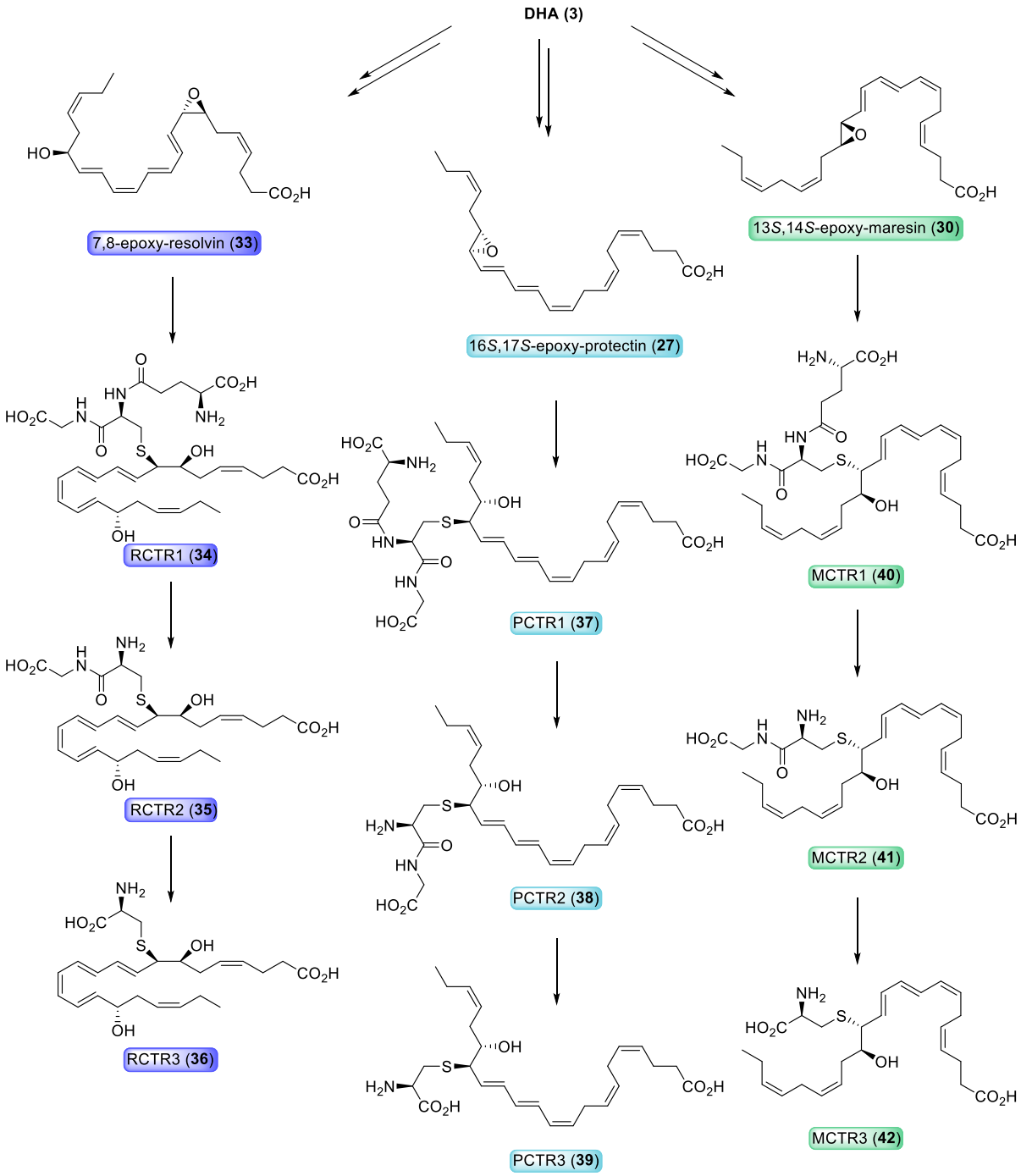

Scheme 1.10 Outline of the biosynthesis of the PCTRs (**37**-**39**) and MCTRs (**40**-**42**), as well as the proposed biosynthesis of the RTCRs (**34**-**36**).[114-116]

1.4 New SPMs Derived From n-3 Docosapentaenoic Acid

EPA (**2**) is generated from elongation and desaturation of α-linolenic acid (ALA) in mammals. This fatty acid is further converted to DHA (**3**) through the intermediate n-3 docosapentaenoic acid (n-3 DPA, **43**) (Scheme 1.11).[117-119] The only structural difference between n-3 DPA (**43**) and DHA (**3**) is the absence of the *Z*-double bond between C4 and C5, present in DHA (**3**). In 2013, Serhan and co-workers observed that n-3 DPA (**43**) is also a substrate for different LOX pathways in mice and human leukocytes, leading to the discovery of a novel family of SPMs.[120] These newly identified mediators share structural resemblance with their sister analogues of the D-series resolvins, protectins and maresins, except from the absence of the C4-C5 *Z*-double bond.[121]

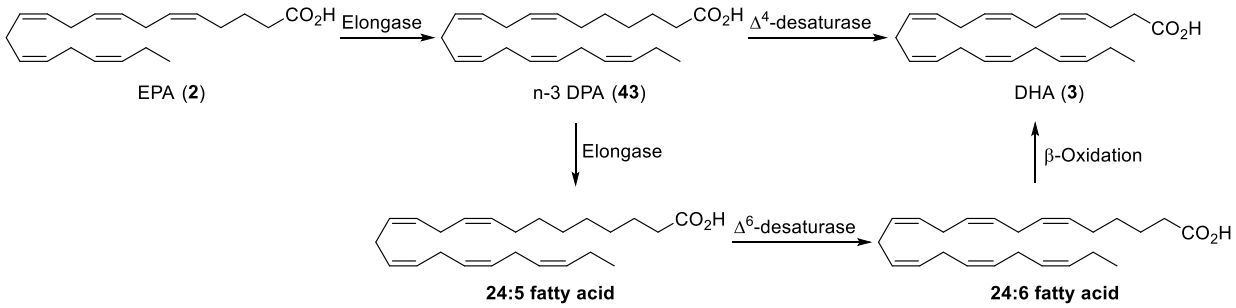

Scheme 1.11 Outline of the conversion of EPA (**2**) to DHA (**3**) through the intermediate n-3 DPA (**43**) (the longest rout occurs in mammals).

As mentioned above, these SPMs are biosynthesised by oxygen insertion, catalysed by LOX enzymes. In the formation of $PD1_{n\text{-}3\ DPA}$ (**46**), oxygen is incorporated at C17 in n-3 DPA (**43**) by 17-LOX, yielding hydroperoxide **44**, which is enzymatically converted to epoxide **45**. This transient epoxide can then undergo enzymatic hydrolysis to $PD1_{n\text{-}3\ DPA}$ (**46**). In similar fashion, n-3 DPA (**43**) may be oxidised at C14 by 12-LOX to the 14*S*-hydroperoxide **53**. Further transformation of this hydroperoxide **53** leads to the 13,14*S*-epoxide **56**, which upon enzymatic hydrolysis furnishes $MaR1_{n\text{-}3\ DPA}$ (**57**). Several other n-3 DPA-derived SPMs produced by similar pathways have been identified.[120]

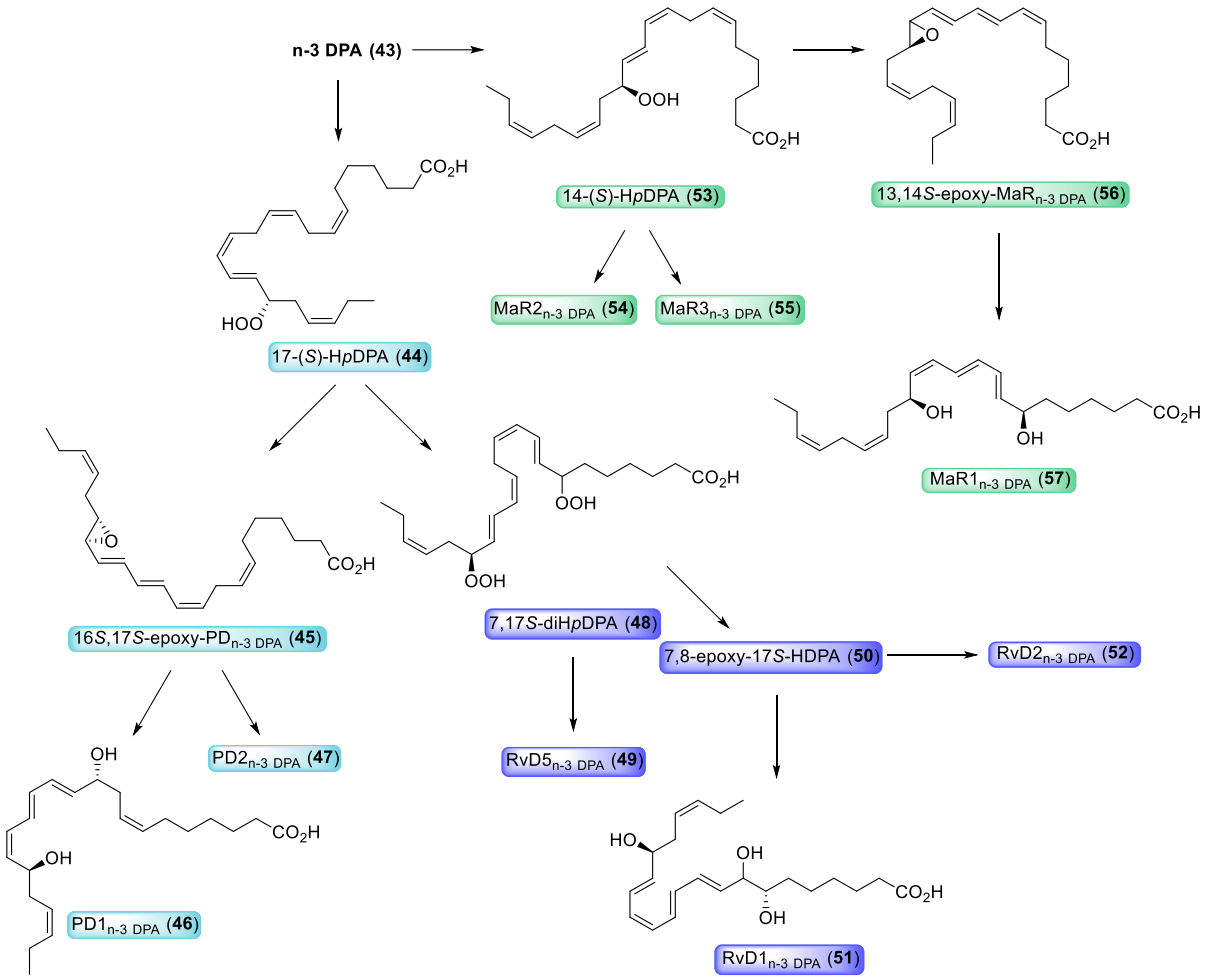

Scheme 1.12 Proposed biosynthetic scheme for novel n-3 docosapentaenoic acid derivatives.[120]

Recently, new host-protective members originating from the n-3 DPA-family of lipid mediators that are biosynthesised via a COX-2 pathway have been identified in sterile inflammation or infection in mice and humans, termed 13-series resolvins.[70] Currently, four structures have been determined, RvT1-RvT4 (**59-62**), although the complete configuration of the stereocenters present in these four molecules has as yet not been established. The RvTs increase the phagocytic removal of bacteria and regulate the production of inflammatory proteins. They have also showed potent protective actions during infection, increasing the survival rate of *E. coli*-infected mice.[70]

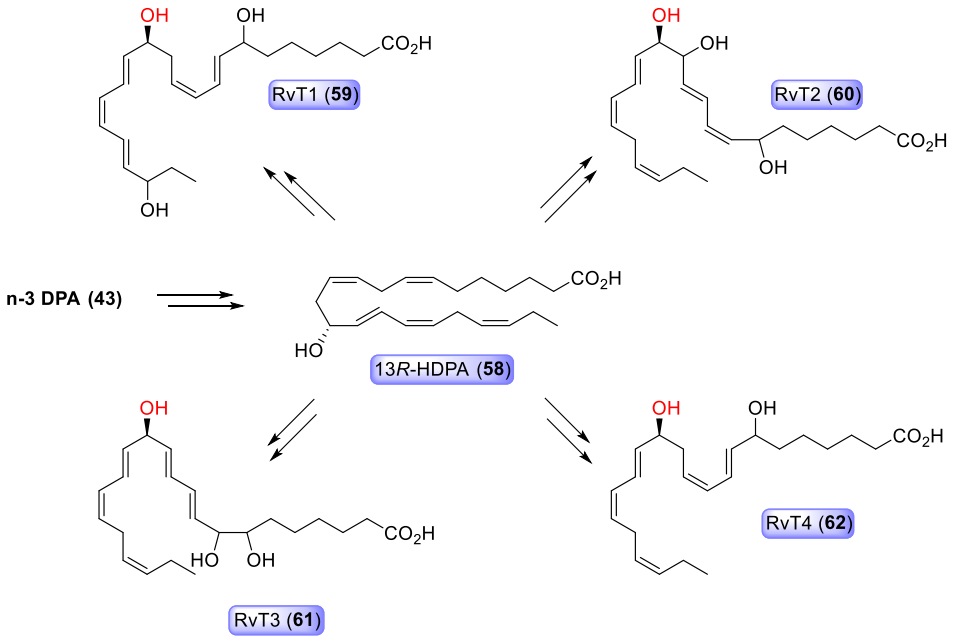

Scheme 1.13 Biosynthetic scheme for the novel RvT1-RvT4 (**59**-**62**).

The proposed biosynthesis of the RvTs (**59**-**62**) involves a two-step transcellular process that requires neutrophil-endothelial cell interaction. In the first step, n-3 DPA (**43**) is converted to the 13*R*-hydroperoxide (13-(*R*)-H*p*DPA) by endothelial COX-2. The hydroperoxyl group is then reduced to a hydroxyl group, resulting in 13*R*-hydroxydocosapentaenoic acid (13*R*-HDPA, **58**). Further, 13*R*-HDPA (**58**) is transferred to adjacent neutrophils where it is converted by 5-LOX to the four RvTs (**59**-**62**) (Scheme 1.13).[70]

1.5 Asymmetric Reduction of Ketones

The preparation of chiral secondary alcohols from the asymmetric reduction of prochiral ketones is a method of paramount importance for the construction of building blocks in the synthesis of a variety of enantiopure drugs and natural products.[122] Several methods have been developed for this purpose, including stochiometric and catalytic reactions. In this section, a selection of methods concerning the enantioselective reduction of ketones will be addressed.

One example is the binaphthol-modified aluminium hydride reagent (BINAL-H), which can be prepared *in situ* from lithium aluminium hydride (LAH), the chiral diol, 1,1'-binaphthol and an alcohol, usually ethanol.[123] BINAL-H provides highly enantioselective reduction of aromatic ketones, as well as unsaturated ketones such as alkenyl and alkynyl ketones.[124]

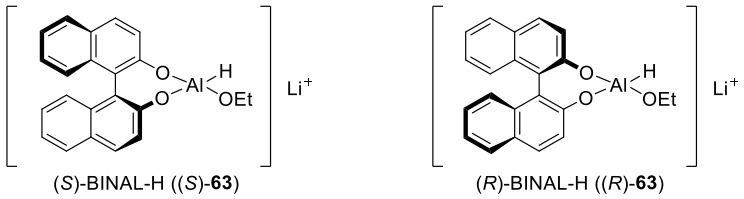

Figure 1.5 Structures of both the (*S*)-BINAL-H (**63**) and (*R*)-BINAL-H (**63**) reagents.

Predominantly, (*R*)-**63** gives the *R*-enantiomer of the alcohol, while with (*S*)-**63**, the *S*-enantiomer predominates. This can be explained by the six-membered transition state displayed in Scheme 1.14, given that the π-system has a higher priority than the alkyl chain.[124] In this transition state, the π-system present in the ketone prefers the equatorial position due to the repulsive interactions by the π-system in the ketone and the lone pair on the oxygen in BINAL-H, known as the n-π repulsion.

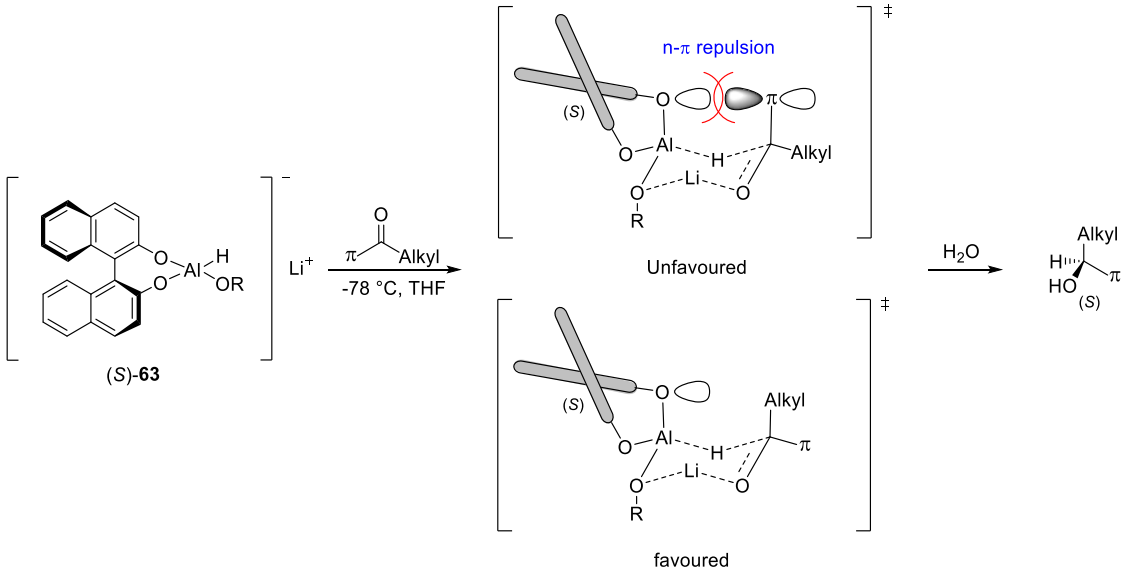

Scheme 1.14 Stereoselectivity in reduction of ketones by (*S*)-BINAL-H **63**.[124]

This method has been utilized by Noyori in the assignment of the *S*-configuration at C-15 in prostaglandin $F_{2\alpha}$ and PGE_2 (**96**) following the route published by Corey and co-workers.[125,126] In Scheme 1.15, three examples of the asymmetric reduction of α,β-unsaturated ketones, including the prostaglandin building block **69**, by BINAL-H are shown.[127] One drawback with this method is the high amount of catalyst loading.

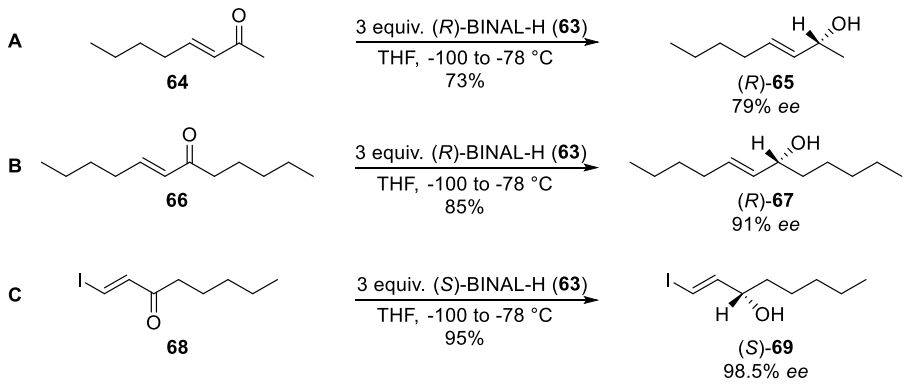

Scheme 1.15 Three examples of the asymmetric reduction of α,β-unsaturated ketones by BINAL-H.[127]

Diisopinocampheylchloroborane (Ipc_2BCl or DIP-chloride) is another reagent first used by Brown and co-workers in the asymmetric reduction of acetophenone.[128] Both enantiomers of DIP-chloride ((+)- and (-)-**72**) are commercially available, but they can also be prepared from inexpensive α-pinene. This reagent is most often used in the enantioselective reduction of aryl alkyl ketones. Nevertheless, good to excellent enantiomeric excess (*ee*) was observed in the reduction of alkynyl ketones,[129] aliphatic acylsilanes[130] and sterically hindered ketones,[131] as well as promising results for the reduction of prostaglandin intermediates **68** and **70** (Scheme 1.16).[131]

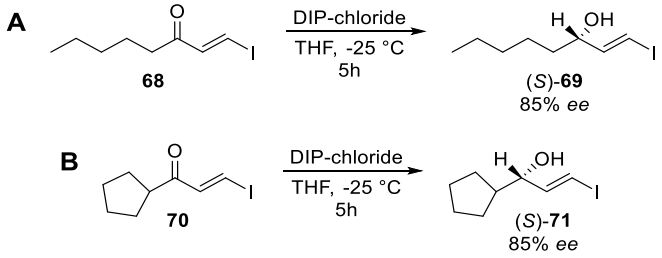

Scheme 1.16 Reduction of two prostaglandin intermediates **68** and **70** by DIP-chloride.[131]

DIP-chloride reduces prochiral ketones by the donation of the hydrogen on the tertiary carbon adjacent to the boron, also referred to as transfer hydrogenation. For this reason, the transition state involves a six-membered ring, shown in Scheme 1.17.[131] Through this transition state, it is possible to predict the conformation of the resulting chiral alcohol.

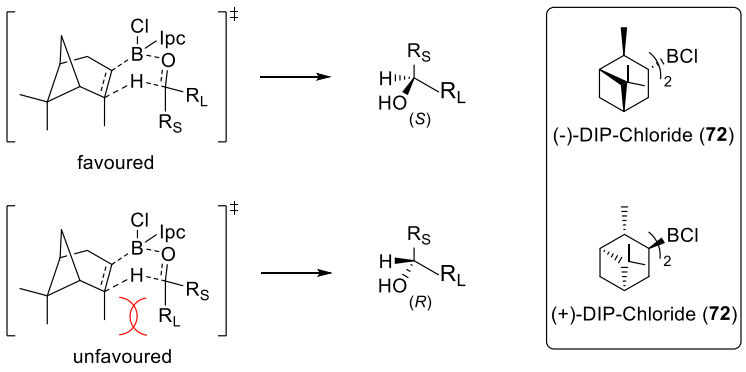

Scheme 1.17 The proposed six-membered transition state in the reduction of a ketone by DIP-chloride.[131]

B-3-pinanyl-9-borabicyclo[3.3.1]nonane (Alpine-Borane®) is an organoboron reagent which effectively reduces aldehydes and alkynic ketones.[132-137] Both the (*R*)- and (*S*)-enantiomer **75** can easily be prepared from hydroboration of either (+)- or (-)-α-pinene by 9-borabicyclo[3.3.1]nonane (9-BBN). Ketones are reduced at a much lower rate than aldehydes, and Alpine-Borane® is consequently able to selectively reduce aldehydes in the presence of a ketone.[138] One example of the chemoselective reduction of the acetylenic ketone in 2-nonyne-4,8-dione is obtained, leaving the methyl ketone untouched (Scheme 1.18).[137] The above-mentioned reagent, DIP-chloride, is considerably more efficient in the stereoselective reduction of ketones.

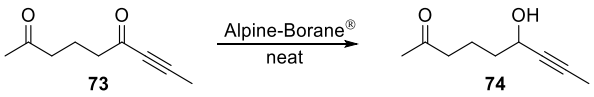

Scheme 1.18 The chemoselective reduction of 2-nonyne-4,8-dione (**73**) by Alpine-Borane®.[137]

A kinetic study confirmed that the reduction of aldehydes proceeds through a six-membered transition state (Scheme 1.19).[139] Hence, the rate of the reaction is dependent on the concentration: running the reaction neat affords the fastest rate.[140] An electron-withdrawing group in the substrate will also accelerate the rate of the reduction of aldehydes and ketones (Scheme 1.20).[139] To avoid deceleration towards the end of the reaction, an excess of Alpine-Borane® is usually exploited. A competing side reaction is the dehydroboration, which occurs under more harsh reaction condition, causing the release of 9-BBN. Free 9-BBN will then reduce carbonyl compounds to racemic products, corroding the enantiomeric purity.[141] This problem can be avoided by running the reactions at elevated pressure (Scheme 1.20).[142]

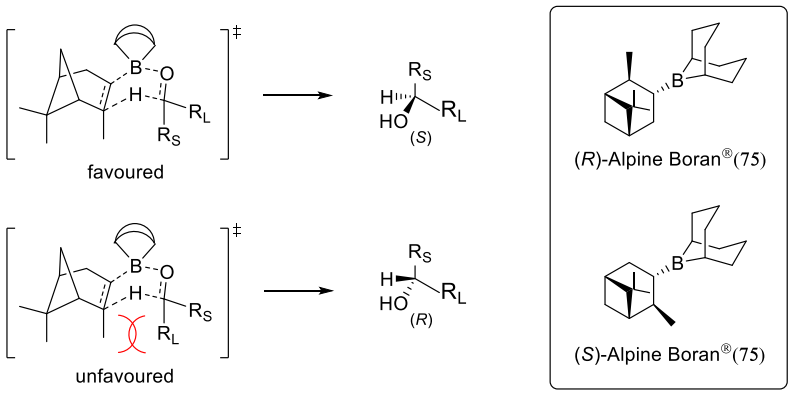

Scheme 1.19 The six-membered transition state in the Alpine-Borane® reduction.[139]

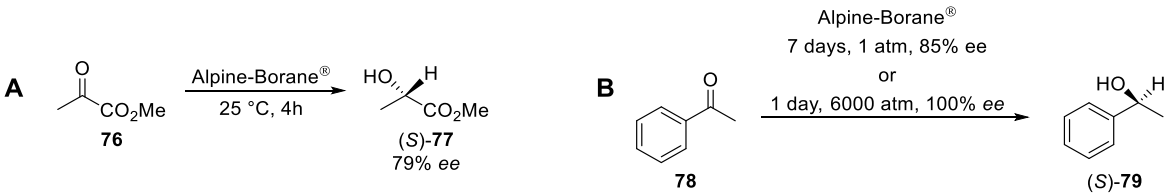

Scheme 1.20 A) Alpine-Borane reduction of a ketone with an electron-withdrawing group.[139] B) The effect observed by running the Alpine-Borane reduction at elevated pressure.[142]

A fourth alternative of a reducing agent is the enantiomers of 2,5-dimethylborolane (borolane), utilized in the stereoselective reduction of a variety of prochiral ketones.[143] The reagent system consists of 1.0 equivalent of one of the enantiomers of borolane and 0.2 equivalents of borolanyl mesylate, which can be prepared *in situ* by treating the lithium dihydridoborate **82** in pentane with methanesulfonic acid.[143] Exceptional diastereoselectivity was observed when pregnenolone (**80**) was reduced by (*R*,*R*)-borolane and (*S*,*S*)-borolane (Scheme 1.21).[143]

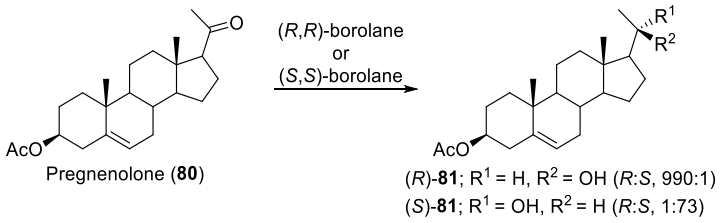

Scheme 1.21 Asymmetric reduction of pregnenolone (**80**) by (*R*,*R*)- or (*S*,*S*)-borolane.[143]

The asymmetric reduction occurs through the formation of a complex by the coordination of borolanyl mesylate **84** *syn* to the smallest alkyl group (R^1) in the ketone (Scheme 1.22).[144] Following the completion of the reaction, the chiral borolane can be recovered as a crystalline complex with 2-amino-2-methyl-1-propanol.

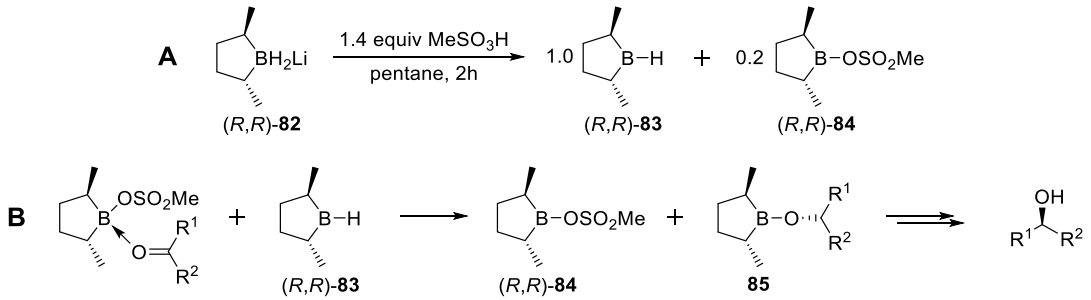

Scheme 1.22 A) Preparation of the borolane reagent system. B) The mechanism of borolane reduction.[144]

The Corey-Bakshi-Shibata (CBS) catalyst is named after its three inventors and is an efficient component in the enantioselective borane reduction of a wide array of ketones.[145-147] This proline-derived catalyst was developed based on the interesting catalytic activities observed for oxazaborolidine **87**, obtained by reacting amino alcohol **86** with borane in tetrahydrofuran (THF) and was first reported by Itsuno and his group (Scheme 1.23).[148]

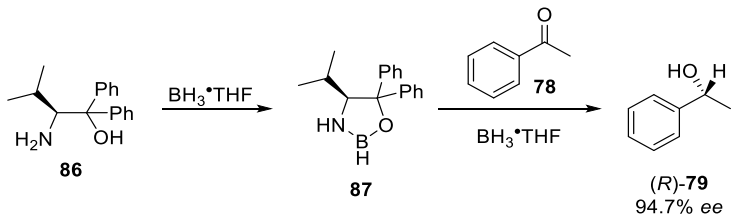

Scheme 1.23 Catalytical activity observed for oxazaborolidine **87** in the reduction of acetophenone.[148]

The proposed mechanism for the reduction of acetophenone catalysed by CBS is depicted in Scheme 1.24.[145,149] The stochiometric reductant in this case is BH_3, but catecholborane is also commonly applied. During the initial step, BH_3 coordinates to the Lewis basic nitrogen, forming a *cis*-fused complex **89**. This step activates BH_3 as a hydride donor, as well as increasing the Lewis acidity of boron. The existence of the oxazaborolidine complex **89** was confirmed by ^{11}B NMR spectroscopy[145] and single-crystal X-ray diffraction analysis.[150,151] Next, boron binds to the most sterically accessible electron lone pair on the oxygen in the ketone **78**, minimising the unfavourable interaction between the ketone and oxazaborolidine. Face-selective hydrogen transfer can then occur through a six-membered transition state, leading to the formation of intermediate **91**. Finally, the product is released either by cycloelimination or by decomposition of the six-membered BH_3-bridged species **92** formed by addition of BH_3.

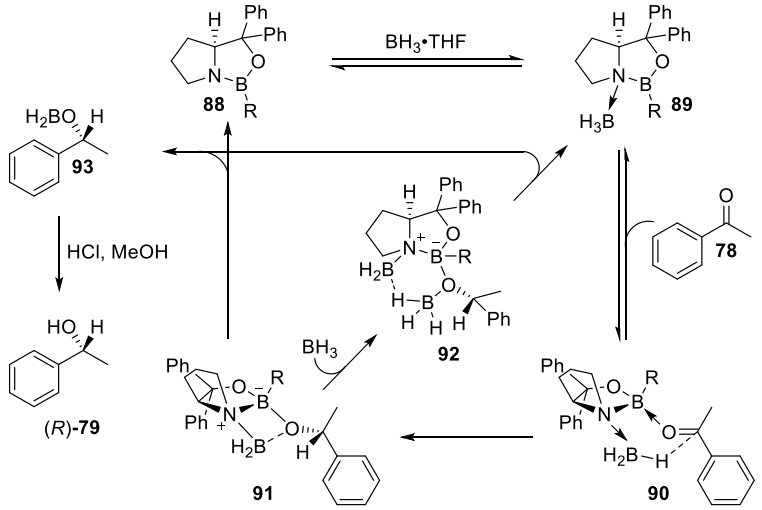

Scheme 1.24 Proposed mechanism for the CBS reduction.[147]

Considering the wide tolerability in ketones reduced by CBS with good enantioselectivity, it has been utilized in the total syntheses of several natural products. For example, the CBS reduction has been used to set the stereochemistry at C15 in the synthesis of PGE_2 (**96**)[146] and PGE_1.[152] The assignment of the stereocenter at C1 in JBIR-108 (**99**) and (**100**) was confirmed by total synthesis, where the key chiral secondary alcohol was constructed by CBS reduction of the former ketone (Scheme 1.25).[153]

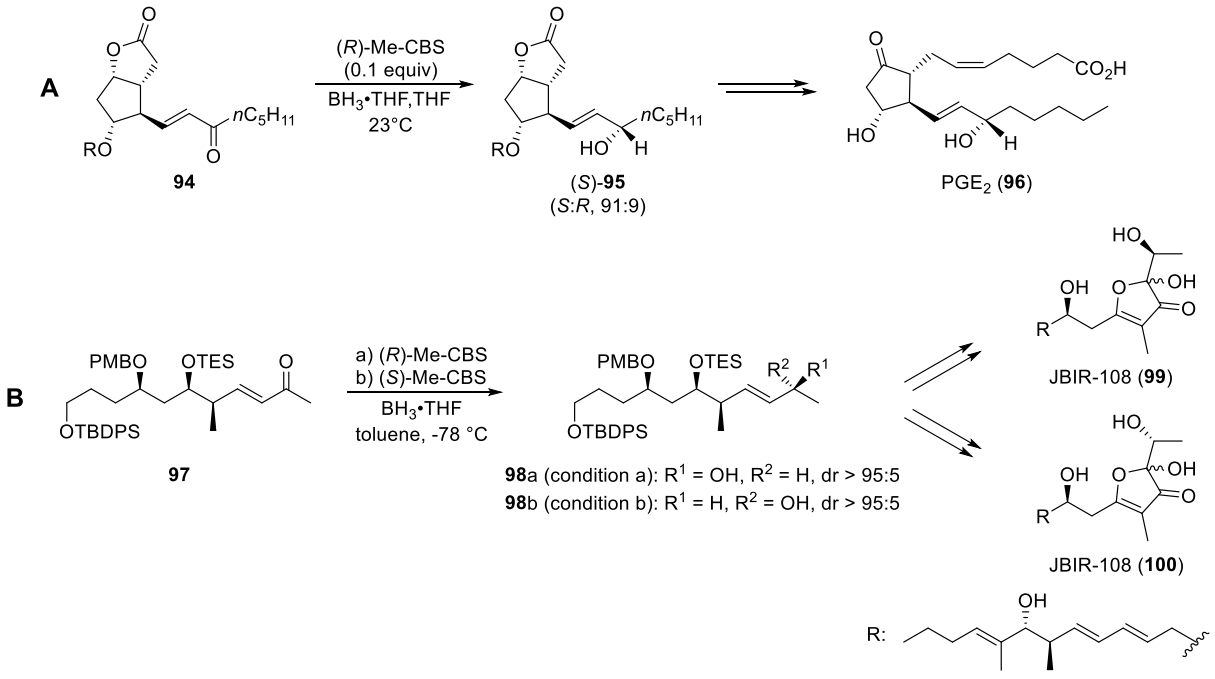

Scheme 1.25 Application of CBS reduction in the synthesis of A) PGE_2 (**96**),[146] and B) JBIR-108 (**99**) and (**100**).[153]

Noyori asymmetric hydrogenation is the asymmetric reduction of olefins and ketones catalysed by chiral ruthenium or related rhodium complexes and was introduced by Noyori

and co-workers. In 2001, Ryoji Noyori shared half of the Nobel Prize in Chemistry with William S. Knowles, "for their work on chirally catalysed hydrogenation reactions"[154]

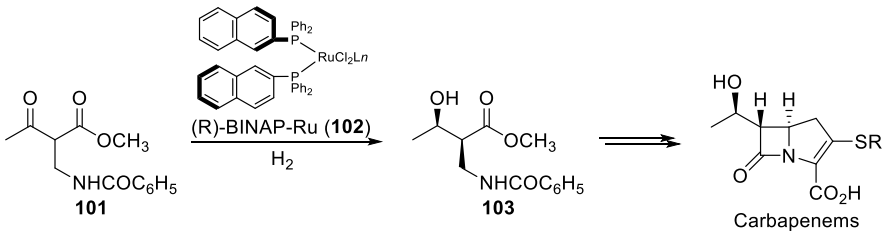

Scheme 1.26 Industrial application of BINAP-Ru catalysed hydrogenation to the asymmetric synthesis of carbapenem antibiotic.[155]

The BINAP-Ru(II) complexes efficiently hydrogenate functionalized ketones.[156,157] In Scheme 1.26, this methodology is utilized in the industrial preparation of carbapenem antibiotics. The coordination of the functional group to the catalytic centre assures stereochemical control and accelerates the reaction rate. These complexes are not able to hydrogenate simple ketones due to the lack of heteroatoms necessary for the binding to the Ru-metal core. Due to this shortcoming, an improved tertiary catalytic system **104** was developed, based on a similar catalytic system generated a few years earlier.[158] This improved complex effectively hydrogenates simple ketones in 2-propanol, such as acetophenone **78** (Scheme 1.27).[159] Another benefit with these tertiary systems are the chemoselective hydrogenation of C=O vs C=C.[160]

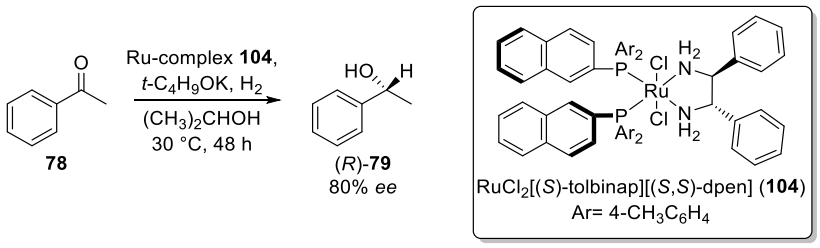

Scheme 1.27 The asymmetric hydrogenation of simple ketones in 2-propanol by Ru-complex **104**.[159]

In 1995, a new type of nonphosphin-based chiral Ru(II) pre-catalysts (Figure 1.6) was prepared. [161] These new Ru(II) complexes are more reactive than the above-mentioned phosphine-containing complexes, as they can accomplish high enantioselective reduction at room temperature and without acquiring hydrogen.[161] Instead, 2-propanol is often used as the hydrogen source in these reactions, but due to the structural similarities between the hydrogen donor and the product, both being secondary alcohols, the process is reversible and can cause a decrease in the enantiomeric purity of the product.[161] This problem can be overcome by using a mixture of formic acid and triethylamine.[162]

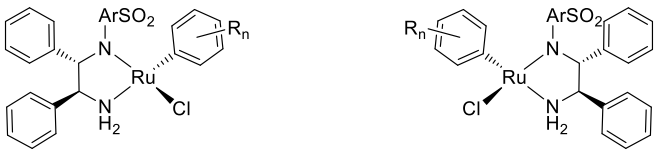

a: Ar = 4-$CH_3C_6H_4$; η^6-arene = mesitylene
b: Ar = 4-$CH_3C_6H_4$; η^6-arene = *p*-cymene
c: Ar = 4-$CH_3C_6H_4$; η^6-arene = benzene
d: Ar = 2,4,6-$(CH_3)_3C_6H_2$; η^6-arene = *p*-cymene
e: Ar = 2,4,6-$(CH_3)_3C_6H_2$; η^6-arene = benzene
f: Ar = 1-naphthyl; η^6-arene = benzene

Figure 1.6 Pre-catalysts for the asymmetric Noyori transfer hydrogenation.[161]

The proposed mechanism for the transfer hydrogenation of ketones is found in Scheme 1.29. The first asymmetric transfer hydrogenation of α,β-acetylenic ketones was achieved utilizing these chiral Ru(II) complexes and 2-propanol as the hydrogen donor (Scheme 1.28).[163] The propargylic alcohol products are of immense importance as building blocks in the synthesis of bioactive natural products and other interesting molecules.

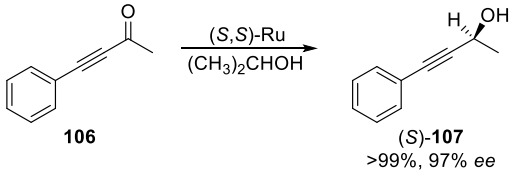

Scheme 1.28 Asymmetric Noyori transfer hydrogenation of α,β-acetylenic ketone **106**.[163]

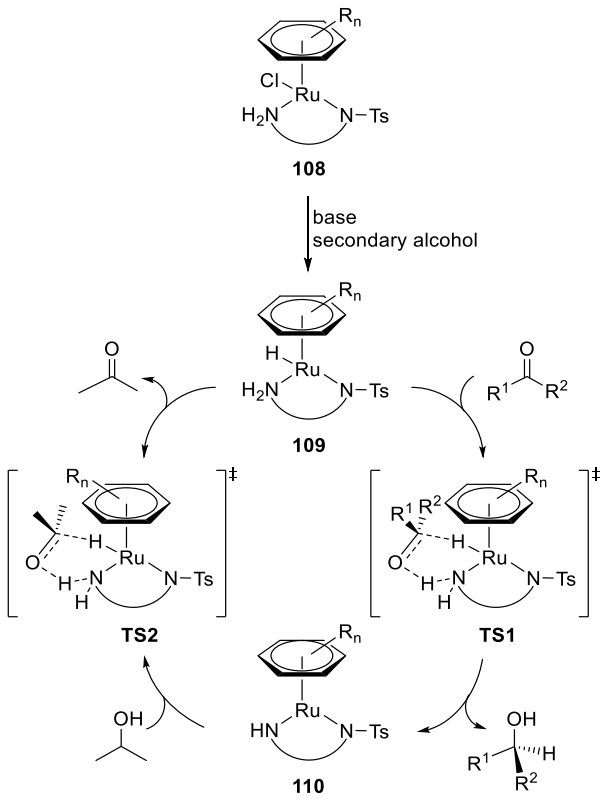

Scheme 1.29 Proposed mechanism for the asymmetric Noyori transfer hydrogenation. [164-166]

The use of biocatalysts in organic chemistry has become more prominent in the last decades, due to the fact that enzymes are able to perform reactions under mild conditions (e.g., pH and temperature) with impressive chemo-, regio- and stereoselectivity.[167] Biocatalytic reduction of achiral ketones is a green and useful tool to access enantiopure alcohols. One example is the biocatalytic reduction of ketone **111** to the key intermediate **112** in the synthesis of montelukast sodium (Singulair) (**113**) which is illustrated in Scheme 1.30.[168] This drug is a leukotriene receptor antagonist developed to control the symptoms of asthma and allergies.[169]

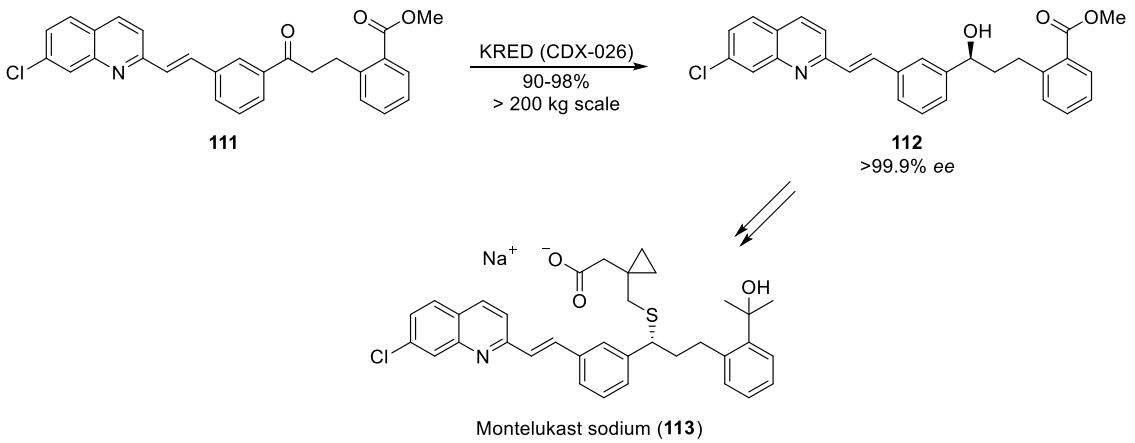

Scheme 1.30 Biocatalyst reduction of ketone **111** to the key intermediate **112** in the synthesis of montelukast sodium (**113**).[168]

1.6 Challenges and Different Strategies in the Synthesis of PUFAs

The interesting biological effects observed for the PUFAs have encouraged their preparation, considering that they are produced in minute amount from natural sources. Common structural similarities for these molecules are the presence of multiple double bonds, often as a mixture of both *E*- and *Z*-configurations, as well as skipped *Z*-olefin components and alkenes in conjugation.[170] Other familiar functional groups observed include carboxylic acids, alcohols, ketones, ethers and epoxides.[170]

In this section, a selection of the most commonly applied methods for creating *Z*-olefins and other functional groups present in the PUFAs will be highlighted.

1.6.1 Hemisynthesis of PUFAs

To construct structures containing several skipped (*Z*,*Z*)-1,4-diene moieties, an attractive and efficient alternative is to employ natural sources, where the desired skipped diene system already is incorporated in the compound, such as AA (**1**), EPA (**2**) and DHA (**3**). In the hemisynthesis of racemic 5-HETE (**7**), published by Corey and co-workers, AA (**1**) was utilized as staring material.[171] First, AA (**1**) was subjected to iodolactonization, affording iodolactone **114a**. Elimination of iodide, facilitated by DBU, provides the corresponding δ-lactone **115a**. The lactone was opened by using triethylamine and methanol, yielding the methyl ester, which after basic hydrolysis furnishes (±)-5-HETE (**7**) (Scheme 1.31). The initial iodolactonization step was later improved by Ulven and co-workers and full conversion of AA (**1**) was achieved by using γ-collidine as a base and dichloromethane as the solvent.[172] Both 4-HDHA (**9**) and 5-HEPE (**8**) were prepared by Itoh et al. by using the same approach.[173,174] The racemic lactone formed from DHA (**3**), which is a natural product in itself named (±) zooxanthellactone, was also prepared using iodolactonization followed by

elimination of iodide by Kuklev and co-workers.[175] This natural product has also been stereoselectively synthesized in our group.[176]

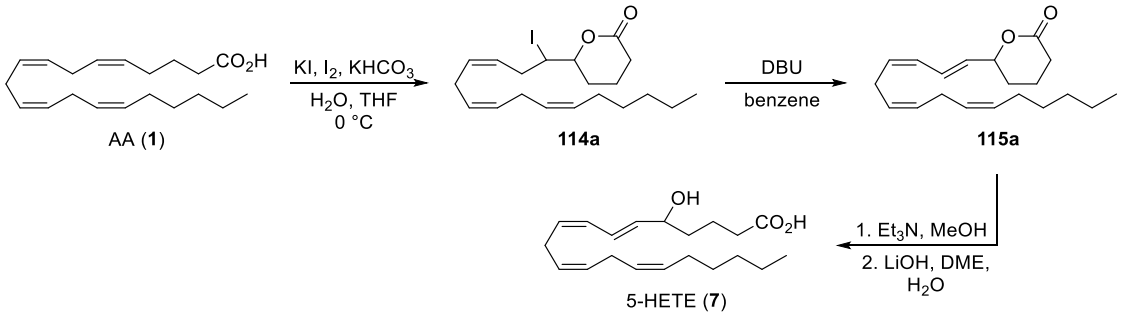

Scheme 1.31 The synthesis of racemic 5-HETE (7).[171]

Skattebøl and co-workers have utilized both EPA (**2**) and DHA (**3**) as starting materials in the syntheses of sulfur- and oxygen-containing fatty acids,[177] as well as three metabolites of EPA (**2**) and DHA (**3**).[178] In our group, hemisynthesis methodology has been used to synthesize interesting PUFAs such as,[179] juniperonic acid, eicosatetraenoic acid (ETA), stearidonic acid (SDA) and n-3 DPA (**43**).[180] The synthesis of the latter from the ethyl ester **116** is illustrated in Scheme 1.32.

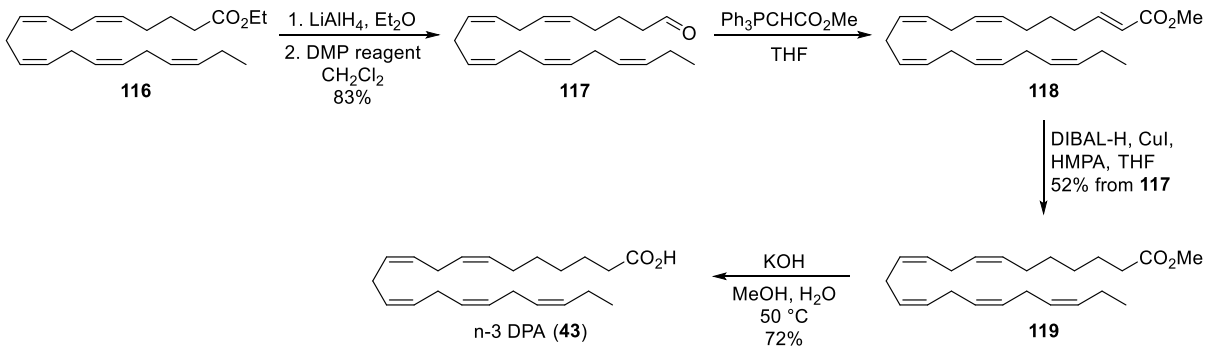

Scheme 1.32 The synthesis of n-3 DPA (**43**) from the ethyl ester **116**.[180]

Iodolactonization of PUFAs yields only the racemic product and optical resolution of the racemic mixture gives access to both enantiomers. This method was utilized to produce the *S* and *R* enantiomers of 5-HETE (**7**) and 4-HDHA (**9**).[173,181] A direct route to access enantiomeric material − without the use of time-consuming multiple step total synthesis or a maximum achievable yield of 50%, which is the case of optical resolution − is by asymmetric reduction of the ketones derived from the hydroxylated PUFAs. Itho and co-workers attempted to produce 4-(*S*)- and 4-(*R*)-HDHA (**9**) by asymmetric iodolactonization and asymmetric reduction of 4-oxo-DHA, but they reported that both asymmetric reduction of the DHA-derived ketone and the halolactonization product were obtained in poor

enantioselective excess and no reaction conditions were provided.[173] Hence, further investigation of the asymmetric reduction of keto-analogues is required.

1.6.2 *Z*-selective Wittig Reaction

The *Z*-selective Wittig reaction furnishes *Z*-alkenes from the reaction between an unstabilized ylide and an aldehyde.[182] Georg Wittig shared the Nobel Prize in Chemistry with Herbert C. Brown (mentioned in section 1.6) in 1979 "for their development of the use of boron- and phosphorus-containing compounds, respectively, into important reagents in organic synthesis", reflecting the importance of this reaction in organic chemistry.[183] The mechanism concerning the construction of these *Z*-olefins is still debated. One highly supported mechanism involves the formation of a *cis*-oxaphosphetane transition state, which ensures maximal space between the large substituents (Scheme 1.33).[184-186] The subsequent decomposition is stereospecific, where the *cis*-oxaphosphetane undergoes *syn*-elimination to give the corresponding *Z*-alkene.

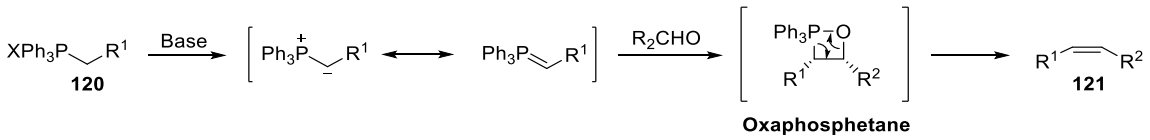

Scheme 1.33 Proposed mechanism for the Wittig reaction.

The factors that influence *Z*-selectivity can be controlled to greatly enhance the desired selectivity. These factors include the choice of ylide, running the reaction at low temperature, high dilution of the reaction mixture, and lithium-free conditions.[182] In Scheme 1.34, the construction of a (*Z*,*Z*)-1,4-diene component, in the SPM $PD1_{n\text{-}3\ DPA}$ (**46**), is established by a Wittig reaction between the ylide of Wittig salt **123**, generated by treatment of the salt **123** with NaHMDS and aldehyde **122**.[187]

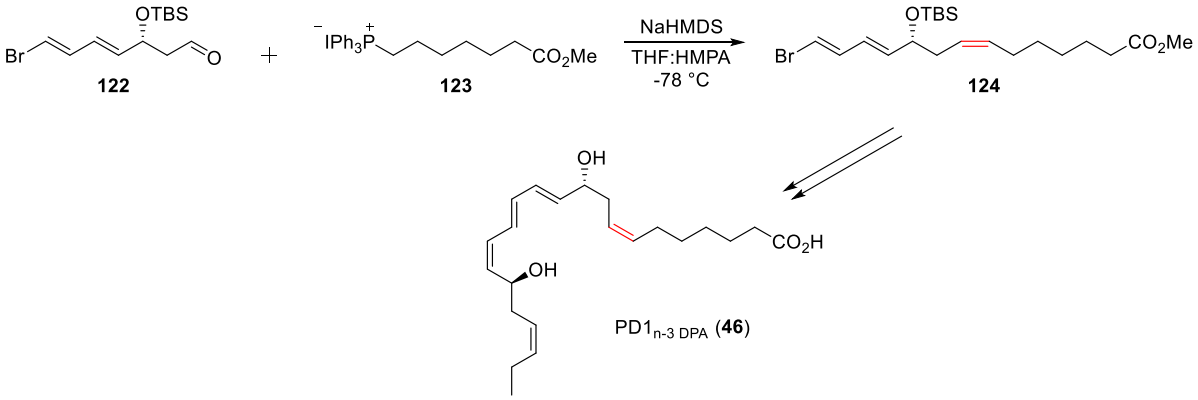

Scheme 1.34 Construction of the (*Z*,*Z*)-1,4-diene moiety by a Wittig reaction between aldehyde **122** and Wittig salt **123**.[187]

In the Horner-Wadsworth-Emmons (HWE) reaction, phosphonate-stabilized carbanions are reacted with carbonyl compounds and the double bond formed in this reaction is predominantly *E*.[188,189] The phosphonates used in the HWE reaction are more reactive. Thus, they will react with both ketones and aldehydes, assuring a wider scope for the HWE reaction, since hindered ketones are less susceptible to undergo a classic Wittig reaction.[190] Another advantage is that the phosphonates can be easily prepared, and the separation of the desired alkene and the dialkyl phosphate by-product is less complicated due to the high water-solubility of the side product.

In 1983, Still and Gennari reported a modification of the HWE reaction to generate *Z*-alkenes by reacting phosphonates with electron-withdrawing groups, such as trifluoromethyl, with aldehydes in presence of a strong base.[191] It is believed that the electron-withdrawing effect of the two trifluoroalkoxy groups on the phosphonate ester increases the nucleophile attack on phosphor by oxygen, enhancing the elimination rate of the oxaphosphetane intermediate. O'Doherty and co-workers used the Still-Gennari modification to prepare cryptocarya triacetate (**128**) (Scheme 1.35).[192]

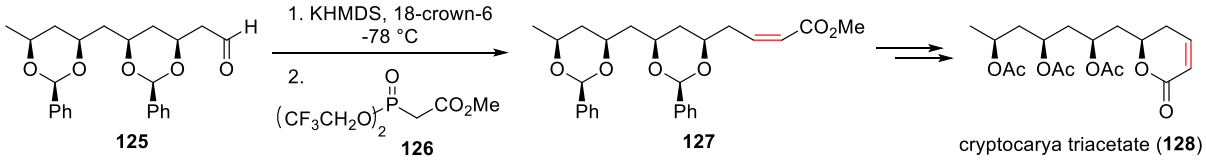

Scheme 1.35 Application of the Still-Gennari modification in the synthesis of cryptocarya triacetate (**128**).[192]

Z-alkenes can also be prepared by using the Ando method as illustrated in Scheme 1.36,[193] which is a another modification of the HWE reaction.[194]

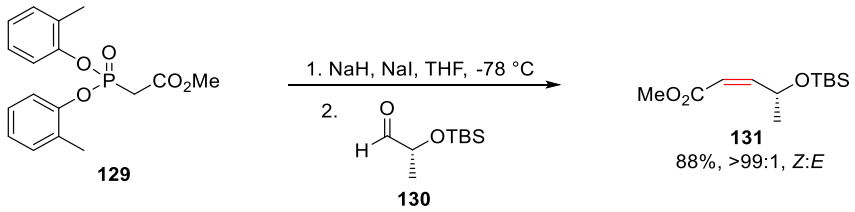

Scheme 1.36 Application of the Ando method in the generation of *Z*-alkene **131**.[193]

1.6.3 *Z*-selective Hydrogenation of Alkynes

The constructions of the carbon skeletons of PUFAs often include acetylene chemistry. Terminal alkynes are useful intermediates in organic syntheses, since they easily can be deprotonated to undergo organometallic cross-coupling reaction, metathesis and other advantageous reactions.[170] The internal alkyne present in the resulting product can then be

subjected to partial hydrogenation, providing a double bond with *Z*-geometry by numerous established methods.

The most frequently utilized reagents for *Z*-selective hydrogenations of alkynes are the palladium-based, such as the Lindlar catalyst in which palladium is deposited on $CaCO_3$ and further poisoned with lead acetate or lead oxide to decrease the reactivity of the catalyst to avoid over-reduction to the corresponding alkane.[195,196] However, over-reduction may still occur when using this method. For this reason, pyridine and 1-octene (sacrificial olefin) have been added as co-solvents in the reaction to avoid this problem.[187,197-200] The reduction of the alkyne is proposed to proceed through *syn*-addition of hydrogen, which is bound on the surface of the catalyst, generating *Z*-alkenes exclusively. Quinoline and 2,2'-(ethylenedithio) diethanol are additives that can be used to enhance the selectivity.[196] Palladium on activated charcoal is disfavoured for the partial hydrogenation due to the high risk of over-reduction. The Lindlar reduction has found extensive applications in organic chemistry since the introduction by Herbert Lindlar in 1952.[195] One example of the application of the Lindlar catalyst is in the semi-hydrogenation of intermediate **132**, furnishing the methyl ester of DHA **133** (Scheme 1.37).[201]

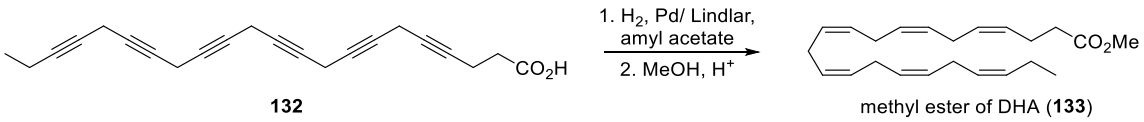

Scheme 1.37 Selective semi-hydrogenation of intermediate **132** by Lindlar's catalyst.[201]

Z-geometry by partial hydrogenation can be obtained by other methods as well, including nickel-based catalyst such as P-2 Ni[202] and Raney®-nickel,[203] and the copper (I) hydride reagent, known as Stryker's reagent.[204] Of the three, P-2 Ni, introduced by Brown, is the most commonly used. The black nickel catalyst can easily be prepared *in situ* by the reduction of nickel acetate by sodium borohydride in ethanol and the addition of ethylenediamine increases the *Z*-selectivity of the reaction.[202] A more recently published protocol for the preparation of *Z*-double bond from the corresponding internal alkyne is the platinum-catalysed hydrosilylation of internal alkynes followed by desilylation.[205,206]

The reduction of an alkene in conjugation is challenging to achieve when using the above-mentioned methods. The conjugated systems are more reactive, making them susceptible for unwanted side reactions, even though these systems are considered to be thermodynamically more stable. This problem was overcome by the development of an activated zinc complex (Zn(Cu/Ag)) by Boland and co-workers, which efficiently reduced conjugated acetylenes in MeOH and H_2O solvent systems to *Z*-alkenes.[207] One example is the reduction of the *E*,*E*-conjugated dialkyne **134** to the methyl ester of bosseopentaenoic acid **135**, which was achieved in high yield and good diastereomeric ratio (50:1 of the desired *Z*,*E*,*E*,*Z*-isomer) using the Zn(Cu/Ag)) complex, further activated by 10 equivalents of TMSCl.[208]

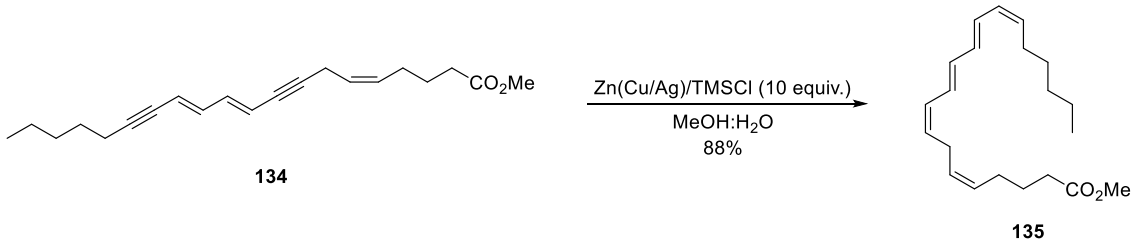

134 **135**

Scheme 1.38 Application of Boland reduction in the synthesis of the methyl ester of bosseopentaenoic acid **135**.[208]

1.6.4 Metathesis in the Construction of *Z*-Alkenes

Olefin metathesis is the transformation involving the cleaving and formation of a new carbon-carbon double bond.[209] The most commonly and versatile catalysts used in this field are the first-,[210] and the second[211] generation of the ruthenium-based catalyst developed by Grubbs and co-workers. The first[212] and second[213] generation of the Hoveyda-Grubbs catalysts, and the tungsten and molybdenum complexes developed by Schrock and co-workers[214] are also commonly employed in metathesis reactions. The ring-closing metathesis (RCM) is a widely used variant of the olefin metathesis reactions. This reaction comprises the formation of diverse sized unsaturated rings by intramolecular metathesis of two terminal alkenes. A drawback with the RCM is the lack of control of the configuration of the newly formed double bond in macrocycles, leading to the formation of a mixture of *E*- and *Z*-isomers in the product, where the thermodynamically most stable *E*-isomer often dominates in large macrocycles.[209] Even so, improvements have been made during the last decade with the development of the Ru-, Mo- and W-based catalysts mentioned above, which provide *Z*-alkenes in satisfactory selectivity. Further development might increase the utilization of this methodology in total synthesis of natural products. The value of olefin metathesis methodology was acknowledged by awarding the Nobel Prize in Chemistry in 2005 to Yves Chauvin, Robert H. Grubbs and Richard R. Schrock, “for the development of the metathesis method in organic synthesis".[215]

To address the problem with the lack of stereo-control observed in RCM, a new strategy was developed by the Fürstner group, which includes ring-closing alkyne metathesis (RCAM) followed by Lindlar reduction of the alkyne, which provides *Z*-macrocycloalkenes selectively.[216] Fürstner utilized this strategy in the synthesis of PGE_2-1,15-lactone (**138**), as illustrated in Scheme 1.39.[217]

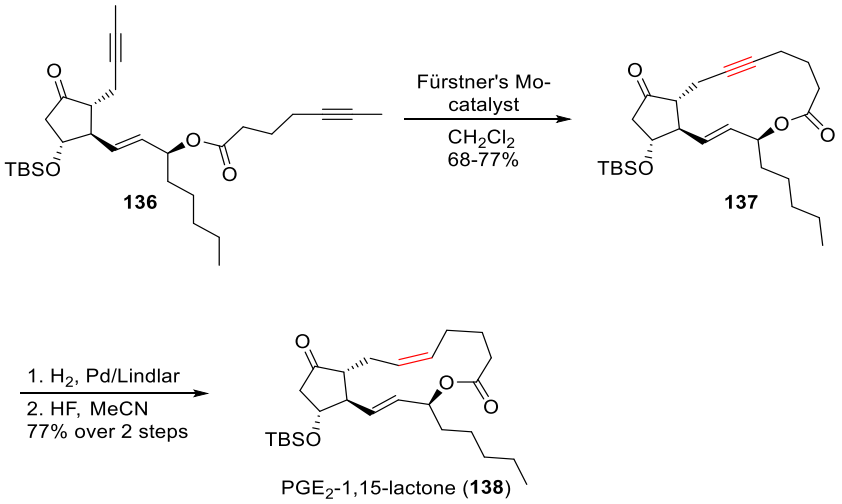

Scheme 1.39 Preparation of PGE_2-1,15-lactone (**138**) by RCAM followed by Lindlar reduction.[217]

Olefin cross-metathesis (CM) is another method to generate functionalized olefins from simple alkene precursors. This reaction predominantly produces *E*-double bonds, due to the thermodynamic control of metathesis.[218] For this reason, CM is less prominent than the above-mentioned metathesis reactions. More *Z*-selective catalysts have been developed, including the previously mentioned Ru-, Mo- and W-based catalysts, which have improved the *Z*-selectivity in CM reactions. One example of a *Z*-selective CM-reaction in the total synthesis of falcarindiol (**143**) is illustrated in Scheme 1.40.[219]

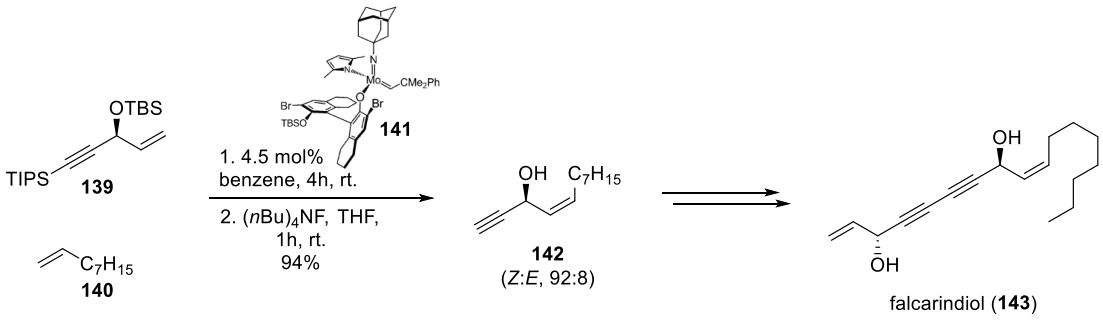

Scheme 1.40 Application of *Z*-selective cross-metathesis reaction in the total synthesis of falcarindiol (**143**).[219]

1.6.5 Cross-Coupling Reactions in the Construction of Alkenes

A powerful tool for accessing both *Z*- and *E*-olefins are the Pd- or Ni-catalyzed cross-coupling reactions, such as Heck,[220] Negishi,[221] Stille,[222] Suzuki-Miyaura[223] and the Sonogashira reactions.[224] The stereochemistry of the starting alkenyl halides or alkenylmetal species is retained through the reaction as a consequence of the cross-coupling step being mainly stereospecific. As a reflection of the importance of the cross-coupling reactions in organic chemistry, Richard F. Hech, Ei-ichi Negishi and Akira Suzuki were jointly awarded

the Nobel Prize in Chemistry in 2010 for their work on palladium-catalysed cross-coupling reactions.[225] Cross-coupling reactions are frequently utilized in the synthesis of the highly unsaturated PUFAs. One example of the application of the Sonogashira reaction in the synthesis of RvD3 (**26**) is illustrated in Scheme 1.41.[226]

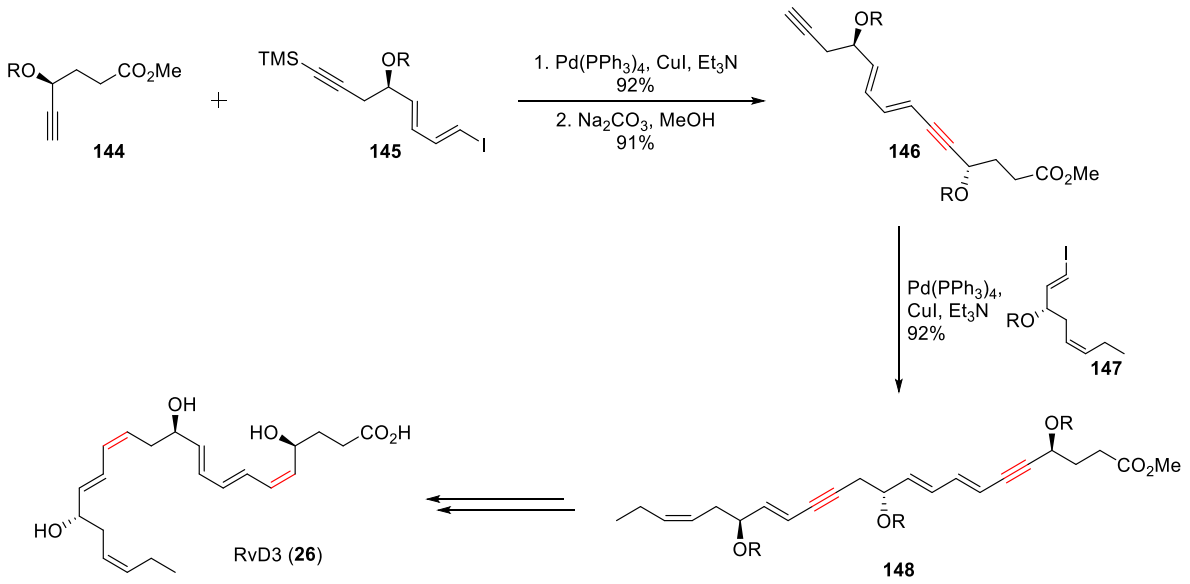

Scheme 1.41 The use of the Sonogashira reaction in the synthesis of RvD3 (**26**).[226]

1.6.6 Pyridinium Salt Derived Dienals in the Synthesis of PUFAs

Dienals can be prepared by ring-opening of quaternary pyridinium salt, rendering access to functionalized conjugated dienes. This *E*,*E*-polyene motif is often present in natural products, such as macrolides, polyketides and PUFAs, thus increasing the utilization of these conjugated dines in total synthesis of the aforementioned structures.[227] Treatment of a pyridine sulfur trioxide complex with potassium hydroxide gives rise to a glutaconaldehyde alkoxide. Subsequent interconversion provides the corresponding 5-halopenta-2,4-dienal, which is generally considered exceptionally useful in terms of synthetic application. Our group has synthesised various SPMs, including PD1 (**28**),[198] MaR1(**31**)[199] and their n-3 DPA congeners (**46** and **57**)[187,200] from (2*E*,4*E*)-5-bromopenta-2,4-dienal (**149**), as illustrated in Scheme 1.42.

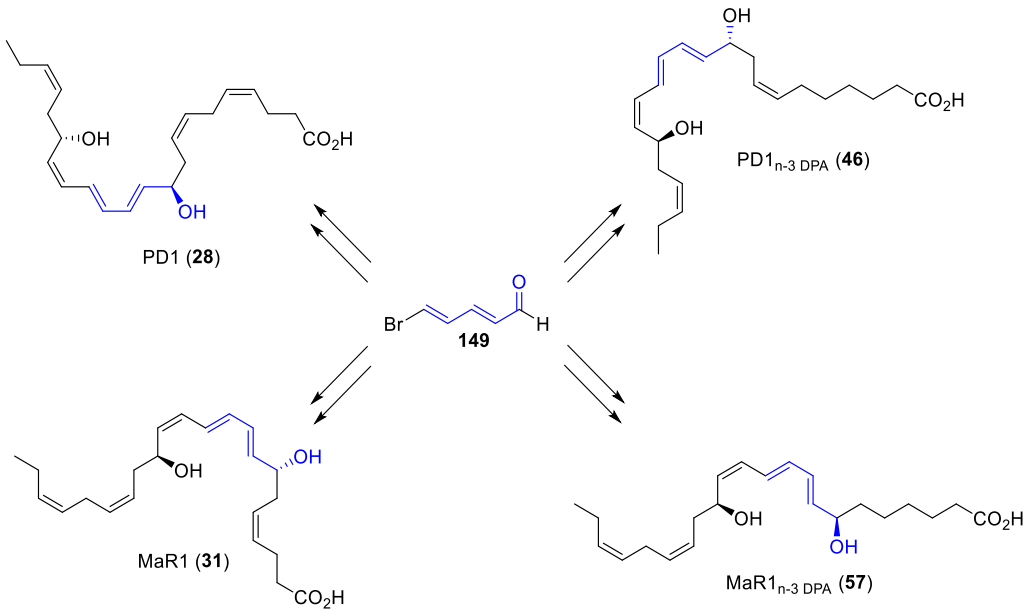

Scheme 1.42 Synthesis of several SPMs from (2*E*,4*E*)-5-bromopenta-2,4-dienal (**149**).[227]

1.6.7 The Aldol Reaction

The aldol reaction was discovered independently by Borodin[228] and Wurtz[229,230] in the 1870s. They almost concurrently observed the self-condensation of the aldehyde starting material through similar experiments, and the product obtained by Wurtz featured both an alcohol and an aldehyde. Hence, he named the term aldol. The diastereofacial selectivity in the aldol reaction can be rationalized based on the Zimmerman-Traxler model published in 1957.[231] They proposed that the metal enolates proceed through a six-membered chair-like transition state, where the *E*-enolates give rise to the *anti*-diastereomer, while the *Z*-enolates lead to the *syn*-diastereomer. The enolate imposes the orientation of the R^2-group to be either *pseudo*-equatorial or -axial in the six-membered transition state, while the R^3-group in the aldehyde orients itself in the more stable *pseudo*-equatorial position, minimizing the steric interference (Scheme 1.43).[231,232]

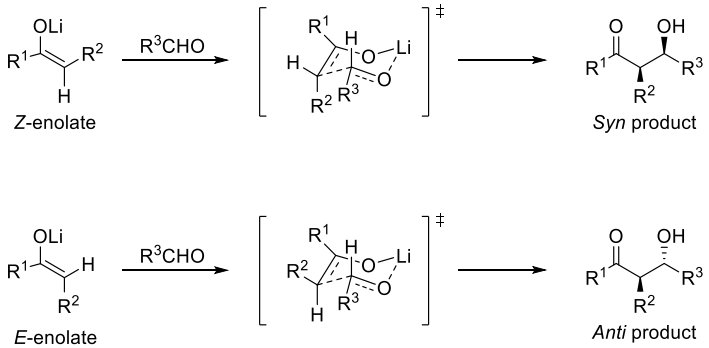

Scheme 1.43 The Zimmerman-Traxler six-membered transition state of the *Z*- and *E*-enolate.[231,232]

Particularly when the process occurs through the Zimmerman-Traxler transition state, controlling the geometry of the enolate formed in the reaction will also control the stereoselective outcome of the aldol reaction. Lithium and boron are often preferred as the metal source due to the relatively short bond between the oxygen and the previously mentioned metals. This leads to a tighter transition state, which in turn elevates the stereoselectivity.[232] Titanium[233] and silyl-based Lewis acids are also used in the generation of enolates. The aldol reaction between silyl enol ethers and an aldehyde is known as the Mukaiyama aldol reaction.[234]

1.6.8 Evans Aldol

The Evans aldol is a highly successful and broadly used version of the aldol reaction where chiral oxazolidinones are deployed in the generation of enantiopure alcohols.[232,235] Generally, both enantiomers of the chiral oxazolidinones are commercially available. To minimize the steric interactions, the geometry of the formed enolate will be *Z*, and the chirality of the auxiliary usually ensures that the nucleophile addition occurs to one face of the aldehyde, leading to *syn* products.[232,235] The Zimmerman-Traxler transition state can be used to rationalize the observed stereochemistry in the Evans aldol reaction.[231] This is illustrated in Scheme 1.44, where nBu$_2$BOTf and Et$_3$N are utilized to generate the enolate. In the favoured transition state, the dipoles of the oxygen in the enolate and the carbonyl group of the auxiliary are placed opposite of each other. In addition, the *R*-group of the aldehyde is oriented in the *pseudo*-equatorial position, consequently minimizing steric interactions.

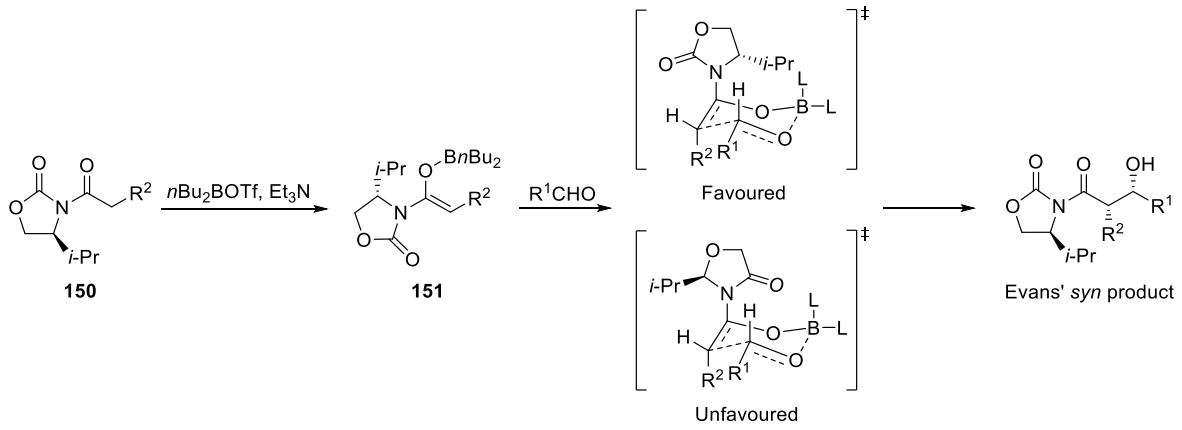

Scheme 1.44 Mechanism for the Evans aldol reaction.

1.6.9 The Nagao Acetate-Aldol Reaction

The discovery that acetylated thiazolidinethiones undergo highly stereoselective acetate-aldol reactions in the presence of Sn(OTf)$_2$ and 1-*N*-ethylpiperidine was made by Nagao and co-workers in 1986.[236] Both the oxazolidinone- and thiazolidinethione auxiliaries can be

converted into the corresponding alcohols, esters or acids. An additional advantage observed for the thiazolidinethiones is that they can be transformed into the aldehyde by DIBAL-H. The Nagao acetate aldol reaction has since its discovery been extensively utilized in natural product synthesis. One example of its application in the total synthesis of (+)-phorboxazole A (**155**) is illustrated in Scheme 1.45.[237]

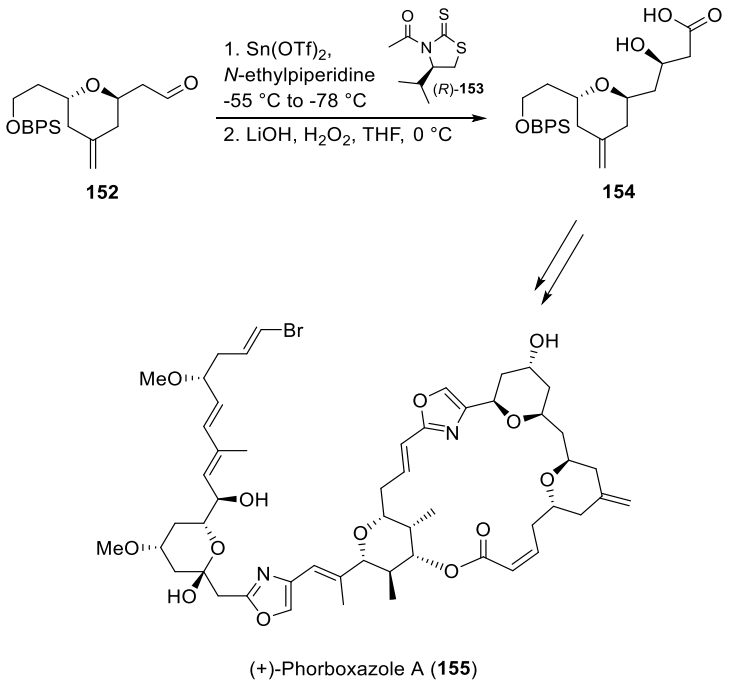

Scheme 1.45 Application of Nagao acetate-aldol reaction in the synthesis of (+)-phorboxazole A (**155**).[237]

1.7 Aims

The main aim of this study was to exploit different strategies to obtain both pro-inflammatory and anti-inflammatory lipid mediators. The partial objectives of this work are listed below:

- Develop stereoselective protocols for the synthesis of 5-(*S*)-HETE (**7**), 5-(*S*)-HEPE (**8**), 4-(*S*)-HDHA (**9**).

- Develop an efficient, stereoselective and convergent synthesis of LTB_4 (**12**).

- Develop a stereoselective synthesis of 16*S*,17*S*-epoxy $PD_{n\text{-}3\ DPA}$ (**45**), enabling investigations of its role in the biosynthesis of the specialized pro-resolving mediator $PD1_{n\text{-}3\ DPA}$ (**46**).

- Develop a stereoselective synthesis rendering 13*R*-HDPA (**58**) to assign its absolute stereochemistry and confirm the role of 13*R*-HDPA (**58**) as the key intermediate in the biogenesis of the 13-series resolvins (**59**-**62**).

- Develop a stereoselective synthesis of the novel specialized pro-resolving mediator RvT3 (**61**).

References

1. G. Majno.; I. Joris, *Cells, Tissue, and Disease: Principles of General Pathology.*, Oxford University Press, USA, 2 edn., 2004.
2. A. C. Celsus, *De Medicina*, Self published. A.D. 25.
3. C. N. Serhan, *Am. J. Pathol.*, 2010, **177**, 1576-1591.
4. C. N. Serhan.; N. Chiang.; T. E. Van Dyke, *Nat. Rev. Immunol.*, 2008, **8**, 349-361.
5. C. R. Harper.; T. A. Jacobson, *Arch. Intern. Med.*, 2001, **161**, 2185-2192.
6. L. G. Cleland.; M. J. James.; S. M. Proudman, *Drugs*, 2003, **63**, 845-853
7. T. E. Van Dyke.; C. N. Serhan, *J. Dent. Res.*, 2003, **82**, 82-90.
8. N. Krishnamoorthy.; P. R. Burkett.; J. Dalli.; R.-E. E. Abdulnour.; R. Colas.; S. Ramon.; R. P. Phipps.; N. A. Petasis.; V. K. Kuchroo.; C. N. Serhan.; B. D. Levy, *J. Immunol.*, 2015, **194**, 863-867.
9. J. A. Nettleton.; R. Katz, *J. Am. Diet. Assoc.*, 2005, **105**, 428-440.
10. S. C. Larsson.; M. Kumlin.; M. Ingelman-Sundberg.; A. Wolk, *Am. J. Clin. Nutr.*, 2004, **79**, 935-945.
11. V. Kumar.; A. K. Abbas.; J. C. Aster, *Robbins & Cotran Pathologic Basis of Disease*, Saunders Elsevier, Philadelphia, USA, 9 edn., 2014.
12. E. J. Corey.; B. Czakó.; K. László, *Molecules and medicine*, Wiley, Hoboken, New Jersey, USA., 2007.
13. R. S. Contran.; V. Kumar.; T. Collins, *Robbins Pathologic Basis of Disease.*, W.B. Saunders Co, Philadelphia, Pennsylvania, USA, 1999.
14. C. N. Serhan.; S. D. Brain.; C. D. Buckley.; D. W. Gilroy.; C. Haslett.; L. A. J. O'Neill.; M. Perretti.; A. G. Rossi.; J. L. Wallace, *FASEB J.*, 2007, **21**, 325-332.
15. G. O. Burr.; M. M. Burr, *J. Biol. Chem.*, 1929, **82**, 345-367.
16. G. O. Burr.; M. M. Burr, *J. Biol. Chem.*, 1930, **86**, 587-621.
17. H. O. Bang.; J. Dyerberg.; A. B. Nielsew, *The Lancet*, 1971, **1**, 1143-1146.
18. J. Dyerberg.; H. O. Bang.; N. Hjorne, *Am. J. Clin. Nutr.*, 1975, **28**, 958-966.
19. H. O. Bang.; J. Dyerberg.; H. M. Sinclair, *J. Am. Clin. Nutr.*, 1980, **33**, 2657-2661.
20. GISSI-Prevenzione-Investigators, *The Lancet*, 1999, **354**, 447-455.
21. A. P. Simopoulos, *J. Am. Coll. Nutr. ,* 2002, **21**, 495-505.
22. C. N. Serhan, *Mol. Aspects Med.*, 2017, http://dx.doi.org/10.1016/j.mam.2017.1003.1001.
23. B. Samuelsson, *Biosci. Rep.*, 1983, **3**, 791-813.
24. C. D. Funk, *Science* 2001, **294**, 1871-1875.
25. G. Bannenberg.; C. N. Serhan, *Biochim. Biophys. Acta*, 2010, **1801**, 1260-1273.
26. C. N. Serhan.; N. A. Petasis, *Chem. Rev. ,* 2011, **111**, 5922-5943.
27. S. Bergström.; F. Dressler.; R. Ryhage.; B. Samuelsson.; J. Sjövall, *Arkiv Kemi*, 1962, **19**, 563-567.
28. H. W.-S. Chan, *Biochim. Biophys. Acta* 1973, **327**, 32-35.
29. A. Dolev.; W. K. Rohwedder.; T. L. Mounts.; H. J. Dutton, *Lipids*, 1967, **2**, 32-35.
30. M. Hamberg.; B. Samuelsson, *J. Biol. Chem.*, 1967, **242**, 5329-5335.
31. E. K. Pistorius.; B. Axelrod, *J. Biol. Chem.*, 1974, **249**, 3183-3180.
32. M. Roza.; A. Francke, *Biochim. Biophys. Acta*, 1973, **327**, 24-31.
33. J. Z. Haeggström.; C. D. Funk, *Chem. Rev.*, 2011, **111**, 5866-5898.
34. C. N. Serhan, *Nature* 2014, **510**, 92-101.
35. P. Borgeat.; M. Hamberg.; B. Samuelsson, *J. Biol. Chem.*, 1976, **251**, 7816-7820.
36. P. S. Kulkarni.; B. D. Srinivasan, *Prostaglandins*, 1986, **31**, 1159-1164.

37. P. S. Kulkarni.; P. L. Kaufman.; B. D. Srinivasan, *J. Ocul. Pharmacol.*, 1987, **3**, 349-356.
38. P. Sapieha.; A. Stahl.; J. Chen.; M. R. Seaward.; K. L. Willett.; N. M. Krah.; R. J. Dennison.; K. M. Connor.; C. M. Aderman.; E. Liclican.; A. Carughi.; D. Perelman.; Y. Kanaoka.; J. P. San Giovanni.; K. Gronert.; L. E. H. Smith, *Sci. Transl. Med.*, 2011, **3**, 1-12.
39. J. T. O'Flaherty.; M. J. Thomas.; C. J. Lees.; C. E. McCall, *Am. J. Pathol.*, 1981, **104**, 55-62.
40. K. A. Potter.; R. W. Leid.; P. E. Kolattukudy.; K. E. Espelie, *Am. J. Pathol.*, 1985, **121**, 361-368.
41. W. Dodge.; M. Thomas, *Biochem. Biophys. Res. Commun.*, 1985, **131**, 731-735.
42. W. S. Powell.; J. Rokach, *Prog. Lipid Res.*, 2013, **52**, 651-665.
43. W. S. Powell.; J. Rokach, *Biochim. Biophys. Acta*, 2015, **1851**, 340-355.
44. R. Kogure.; K. Toyama.; S. Hiyamuta.; I. Kojima.; S. Takeda, *Biochem. Biophys. Res. Commun.*, 2011, **416**, 58-63.
45. D. Y. Oh.; S. Talukdar.; E. J. Bae.; T. Imamura.; H. Morinaga.; W.-Q. Fan.; P. Li.; W. J. Lu.; S. M. Watkins.; J. M. Olefsky, *Cell*, 2010, **142**, 687-698.
46. K. Yamamoto.; T. Itho.; D. Abe.; M. Shimizu.; T. Kanda.; T. Koyama.; M. Nishikawa.; T. Tamai.; H. Ooizumi.; S. Yamada, *Bioorg. Med. Chem. Lett.*, 2005, **15**, 517-522.
47. P. Borgeat.; B. Samuelsson, *J. Biol. Chem.*, 1979, **254**, 2643-2646.
48. P. Borgeat.; B. Samuelsson, *J. Biol. Chem.*, 1979, **254**, 7865-7869.
49. A. M. Targer.; A. D. Luster, *Prostaglandins, Leukotrienes and Essential Fatty Acids*, 2003, **69**, 123-134.
50. Y. Kanaoka.; J. A. Boyce, *J. Immunol*, 2004, **173**, 1503-1510.
51. B. Samuelsson, *J. Biol. Chem.*, 2012, **287**, 10070-10080.
52. K. C. Nicolaou.; R. E. Zipkin.; R. E. Dolle.; B. D. Harris, *J. Am. Chem. Soc.*, 1984, **106**, 3548-3551.
53. C.-Q. Han.; D. DiTullio.; Y.-F. Wang.; C. J. Sih, *J. Org. Chem.*, 1986, **51**, 1253-1258.
54. Y. Guindon.; D. Delorme.; C. K. Lau.; R. Zamboni, *J. Org. Chem.*, 1988, **53**, 267-275.
55. G. Solladie.; G. B. Stone.; C. Hamdouchi, *Tetrahedron Lett.*, 1993, **34**, 1807-1810.
56. G. Solladie.; A. Urbano.; G. B. Stone, *Tetrahedron Lett.*, 1993, **34**, 6489-6492 and references cited therein.
57. F. A. J. Kerdesky.; S. P. Schmidt.; D. W. Brooks, *J. Org. Chem.*, 1993, **58**, 3516-3520.
58. A. Rodriguez.; M. Nomen.; B. W. Spur.; J. J. Godfroid.; T. H. Lee, *Tetrahedron*, 2001, **57**, 25-37.
59. B. M. Trost.; R. C. Livingston, *J. Am. Chem. Soc.*, 2008, **130**, 11970-11978.
60. B. Samuelsson, *Science*, 1983, **220**, 568-575.
61. C. N. Serhan.; M. Hamberg.; B. Samuelsson, *Biochem. Biophys. Res. Commun*, 1984, **118**, 943-949.
62. C. N. Serhan.; M. Hamberg.; B. Samuelsson, *Proc. Natl. Acad. Sci. U. S. A.*, 1984, **81**, 5335-5339.
63. P. Y. K. Wong.; R. Hughes.; B. Lam, *Biochem. Biophys. Res. Commun.*, 1985, **126**, 763-772.
64. C. Godson.; S. Mitchell.; K. Harvey.; N. A. Petasis.; N. Hogg.; H. R. Brady, *J. Immunol.*, 2000, **164**, 1663-1667.
65. T. Takano.; C. B. Clish.; K. Gronert.; N. Petasis.; C. N. Serhan, *J. Clin. Invest.*, 1998, **101**, 819-826.

66. B. D. Levy.; C. B. Clish.; B. Schmidt.; K. Gronert.; C. N. Serhan, *Nat. Immunol.*, 2001, **2**, 612-619.
67. J. F. Maddox.; C. N. Serhan, *J. Exp. Med.*, 1996, **183**, 137-146.
68. J. R. Vane.; Y. S. Bakhle.; R. M. Botting, *Annu. Rev. Pharmacol. Toxicol.*, 1998, **38**, 97-120.
69. A. L. Zografos, *From Biosynthesis to Total Synthesis: Strategies and Tactics for Natural Products*, John Wiley & sins, Inc., Hoboken, New Jersey, 2016.
70. J. Dalli.; N. Chiang.; C. N. Serhan, *Nat. Med.*, 2015, **21**, 1071-1075.
71. K. G. Primdahl.; M. Aursnes.; M. E. Walker.; R. A. Colas.; C. N. Serhan.; J. Dalli.; T. V. Hansen.; A. Vik, *J, Nat. Prod.*, 2016, **79**, 2693-2702.
72. M. W. Goldblatt, *J. Soc. Chem. Ind.*, 1933, **52**, 1056-1057.
73. M. W. Goldblatt, *J. Physiol*, 1935, **84**, 208-218.
74. U. S. v. Euler, *Naunyn-Schmiedebergs Arch. Pharmakol.*, 1934, **175**, 78-84.
75. S. Bergström.; H. Danielsson.; B. Samuelsson, *Biochim. Biophys. Acta*, 1964, **90**, 207-210.
76. M. Hamberg.; B. Samuelsson, *J. Biol. Chem.*, 1967, **242**, 5336-5343.
77. W. L. Smith.; L. J. Marnett.; D. L. DeWitt, *Pharmac. Ther.*, 1991, **49**, 153-179.
78. J. R. Vane, *Nature*, 1971, **231**, 232-235.
79. *The Nobel Prize in Physiology or Medicine 1982*, http://www.nobelprize.org/nobel_prizes/medicine/laureates/1982/ (1904.1902.1914).
80. T. J. Williams.; M. J. Peck, *Nature* 1977, **270**, 530-532.
81. S. G. Harris.; J. Padilla.; L. Koumas.; D. Ray.; R. P. Phipps, *Trends Immunol.*, 2002, **23**, 144-150.
82. R. De Catrina.; S. Endres.; S. Kristensen.; E. Schmidt, *n-3 Fatty Acids and Vascular Disease*, Springer-Verlag, London, 1993.
83. M. Ligo.; T. Nakagawa.; C. Ishikawa.; Y. Iwahori.; M. Asamoto.; K. Yazawa.; E. Araki.; H. Tsuda, *Br. J. Cancer*, 1997, **75**, 650-655.
84. M. Shinohara.; V. Mirakaj.; C. N. Serhan, *Front Immunol*, 2012, **3**, 81.
85. C. N. Serhan.; C. B. Clish.; J. Brannon.; S. P. Colgan.; N. Chiang.; K. Gronert, *J. Exp. Med.*, 2000, **192**, 1197-1204.
86. C. N. Serhan.; S. Hong.; K. Gronert.; S. P. Colgan.; P. R. Devchand.; G. Mirick.; R.-L. Moussignac, *J. Exp. Med.*, 2002, **196**, 1025-1037.
87. M. Arita.; F. Bianchini.; J. Aliberti.; A. Sher.; N. Chiang.; S. Hong.; R. Yang.; N. A. Petasis.; C. N. Serhan, *J. Exp. Med.*, 2005, **201**, 713-722.
88. E. Tjonahen.; S. F. Oh.; J. Siegelman.; S. Elangovan.; K. Percarpio, B.; S. Hong.; M. Arita.; C. N. Serhan, *Chem. Biol.*, 2006, **13**, 1193-1202.
89. Y. Isobe.; M. Arita.; S. Matsueda.; R. Iwamoto.; T. Fujihara.; H. Nakanishi.; R. Taguchi.; K. Masuda.; K. Sasaki.; D. Urabe.; M. Inoue.; H. Arai, *J. Biol. Chem.*, 2012, **287**, 10525-10534.
90. S. Hong.; K. Gronert.; P. R. Devchand.; R.-L. Moussignac.; C. N. Serhan, *J. Biol. Chem.*, 2003, **278**, 14677-14687.
91. C. N. Serhan.; K. Gotlinger.; S. Hong.; M. Arita, *prostaglandins Other lipid mediat.*, 2004, **73**, 155-172.
92. J. M. Schwab.; N. Chiang.; M. Arita.; C. N. Serhan, *Nature*, 2007, **447**, 869-874.
93. Z.-Z. Xu.; L. Zhang.; T. Liu.; J. Y. Park.; T. Berta.; R. Yang.; C. N. Serhan.; R.-R. Ji, *Nat. Med.* , 2010, **16**, 592-597.
94. C. N. Serhan.; K. Gotlinger.; S. Hong.; Y. Lu.; J. Siegelman.; T. Baer.; R. Yang.; S. P. Colgan.; N. A. Petasis, *J. Immunol.*, 2006, **176**, 1848-1859.
95. A. Ariel.; P.-L. Li.; W. Wang.; W.-X. Tang.; G. Fredman.; S. Hong.; K. Gotlinger, H.; C. N. Serhan, *J. Biol. Chem.*, 2005, **280**, 43079-43086.

96. M. Aursnes.; J. E. Tungen.; R. A. Colas.; I. Vlasakov.; J. Dalli.; C. N. Serhan.; T. V. Hansen, *J. Nat. Prod.*, 2015, **78**, 2924-2931.
97. G. L. Bannenberg.; N. Chiang.; A. Ariel.; M. Arita.; E. Tjonahen.; K. H. Gotlinger.; S. Hong.; C. N. Serhan, *J. Immunol.*, 2005, **174**, 4345-4355.
98. A. Ariel.; P.-L. Li.; W. Wang.; W.-X. Tang.; G. Fredman.; S. Hong.; K. H. Gotlinger.; C. N. Serhan, *J. Biol. Chem.*, 2005, **280**, 43079-43086.
99. J. S. Duffield.; S. Hong.; V. S. Vaidya.; Y. Lu.; G. Fredman.; C. N. Serhan.; J. V. Bonventre, *J. Immunol*, 2006, **177**, 5902-5911.
100. I. R. Hassan.; K. Gronert, *J. Immunol.*, 2009, **182**, 3223-3232.
101. B. D. Levy.; P. Kohli.; K. Gotlinger.; O. Haworth.; S. Hong.; S. Kazani.; E. Israel.; K. J. Haley.; C. N. Serhan, *J. Immunol.*, 2006, **178**, 496-502.
102. W. J. Lukiw.; J.-G. Cui.; V. L. Marcheselli.; M. Bodker.; A. Botkjaer.; K. Gotlinger.; C. N. Serhan.; N. G. Bazan, *J. Clin. Invest.*, 2005, **115**, 2774-2783.
103. *Neuroprotectin D1 (NPD1) as a Disease-modifying Therapy for Parkinson's Disease*, https://www.michaeljfox.org/foundation/grant-detail.php?grant_id=1177 (18.05.17).
104. P. K. Mukherjee.; V. L. Marcheselli.; C. N. Serhan.; N. G. Bazan, *Proc. Natl. Acad. Sci.*, 2004, **101**, 8491-8496.
105. K. Sheets, G..; Y. Zhou.; M. K. Ertel.; E. J. Knott.; C. E. Regan Jr..; J. R. Elison.; W. C. Gordon.; P. Gjorstrup.; N. G. Bazan, *Mol. Vis.*, 2010, **16**, 320-329.
106. J. He.; H. E. P. Bazan, *Prostaglandins leukot. Essent. fatty acid*, 2010, **82**, 319-325.
107. K. M. Connor.; J. P. SanGiovanni.; C. Lofqvist.; C. M. Aderman.; J. Chen.; A. Higuchi.; S. Hong.; E. A. Pravda.; S. Majchrzak.; D. Carper.; A. Hellsrom.; J. X. Kang.; E. Y. Chew.; N. Salem Jr..; C. N. Serhan.; L. E. H. Smith, *Nat. Med.* , 2007, **13**, 868-873.
108. M. S. Cortina.; H. E. P. Bazan, *Curr. Opin. Clin. Nutr. Metab. Care*, 2011, **14**, 132-137.
109. C. N. Serhan.; R. Yang.; K. Martinod.; K. Kasuga.; P. S. Pillai.; T. F. Porter.; S. F. Oh.; M. Spite, *J. Exp. Med.*, 2009, **206**, 15-23.
110. B. Deng.; C.-W. Wang.; H. H. Arnardottir.; Y. Li.; C.-Y. C. Cheng.; J. Dalli.; C. N. Serhan, *PLoS One*, 2014, **9**, e102362/102361-e102362/102369, 102369 pp.
111. J. Dalli.; M. Zhu.; N. A. Vlasenko.; B. Deng.; J. Z. Haeggstrom.; N. A. Petasis.; C. N. Serhan, *FASEB J.*, 2013, **27**, 2573-2583.
112. C. N. Serhan.; J. Dalli.; S. Karamnov.; A. Choi.; C.-K. Park.; Z.-Z. Xu.; R.-R. Ji.; M. Zhu.; N. A. Petasis, *FASEB J.*, 2012, **26**, 1755-1765.
113. J. Dalli.; N. Chiang.; C. N. Serhan, *Proc. Natl. Acad. Sci. U. S. A.*, 2014, **111**, E4753-E4761.
114. J. Dalli.; S. Ramon.; P. C. Norris.; R. A. Colas.; C. N. Serhan, *FASEB J.*, 2015, **29**, 2120-2136.
115. J. Dalli.; I. Vlasakov.; I. R. Riley.; A. R. Rodriguez.; B. W. Spur.; N. A. Petasis.; N. Chiang.; C. N. Serhan, *Proc. Natl. Acad. Sci.*, 2016, **113**, 12232-12237.
116. S. Ramon.; J. Dalli.; J. M. Sanger.; J. W. Winkler.; M. Aursnes.; J. E. Tungen.; T. V. Hansen.; C. N. Serhan, *Am. J. Pathol.*, 2016, **186**, 962-973.
117. P. C. Calder, *Eur. J. Pharmacol.*, 2011, **668**, S50-S58.
118. R. De Caterina, *N. Engl. J. Med.*, 2011, **364**, 2439-2450.
119. R. N. Lemaitre.; T. Tanaka.; W. Tang.; A. Manichaikul.; M. Foy.; E. K. Kabagambe.; J. A. Nettleton.; I. B. King.; L.-C. Weng.; S. Bhattacharya.; S. Bandinelli.; J. C. Bis.; S. S. Rich.; D. R. Jacobs.; A. Cherubini.; B. McKnight.; S. Liang.; X. Gu.; K. Rice.; C. C. Laurie.; T. Lumley.; B. L. Browning.; B. M. Psaty.; Y.-D. I. Chen.; Y. Friedlander.; L. Djousse.; J. H. Y. Wu.; D. S. Siscovick.; A. G. Uitterlinden.; D. K.

Arnett.; L. Ferrucci.; M. Fornage.; M. Y. Tsai.; D. Mozaffarian.; L. M. Steffen, *PLoS Genet.*, 2011, **7**, e1002193.
120. J. Dalli.; R. A. Colas.; C. N. Serhan, *Sci Rep*, 2013, **3**, 1940.
121. A. Vik.; J. Dalli.; T. V. Hansen, *Bioorg. Med. Chem. Lett.*, 2017, **27**, 2259-2266.
122. S. Itsuno, in *Organic Reactions*, John Wiley & Sons, Inc, 1998, vol. 52, pp. 395-576.
123. R. Noyori.; I. Tomino.; Y. Tanimoto, *J. Am. Chem. Soc.*, 1979, **101**, 3129-3131.
124. R. Noyori.; I. Tomino.; Y. Tanimoto.; M. Nishizawa, *J. Am. Chem. Soc.*, 1984, **106**, 6709-6716.
125. E. J. Corey.; N. M. Weinshenker.; T. K. Schaaf.; W. Huber, *J. Am. Chem. Soc.*, 1969, **91**, 5675-5677.
126. R. Noyori.; I. Tomino.; M. Nishizawa, *J. Am. Chem. Soc.*, 1979, **101**, 5843-5844.
127. R. Noyori, *Pure Appl. Chem.*, 1981, **53**, 2315-2322.
128. H. C. Brown.; J. Chandrasekharan.; P. V. Ramachandran, *J. Am. Chem. Soc.*, 1988, **110**, 1539-1546.
129. P. V. Ramachandran.; A. V. Teodorovic.; M. V. Rangaishenvi.; H. C. Brown, *J. Org. Chem.*, 1992, **57**, 2379-2386.
130. J. A. Soderquist.; C. L. Anderson.; E. I. Miranda.; I. Rivera, *Tetrahedron Lett.*, 1990, **31**, 4677-4680.
131. H. C. Brown.; P. V. Ramachandran, *Acc. Chem. Res.*, 1992, **25**, 16-24.
132. M. M. Midland.; S. Greer.; A. Tramontano.; S. A. Zedric, *J. Am. Chem. Soc.*, 1979, **101**, 2352-2355.
133. M. M. Midland, *Chem. Rev.*, 1989, **89**, 1553-1561.
134. M. M. Midland.; R. S. Graham, *Org. Synth.*, 1985, **63**, 57-65.
135. M. M. Midland.; R. S. Graham, *Org. Synth. Coll. Vol*, 1990, **7**, 402-409.
136. M. M. Midland.; D. C. McDowell.; R. L. Hatch.; A. Tramontano, *J. Am. Chem. Soc.*, 1980, **102**, 867-869.
137. M. M. Midland.; A. Tramontano.; A. Kazubski.; R. S. Graham.; D. J. S. Tsai.; D. Cardin, B, *Tetrahedron*, 1984, **40**, 1371-1380.
138. M. M. Midland.; A. Tramontano, *J. Org. Chem.*, 1978, **43**, 1470-1471.
139. M. M. Midland.; S. A. Zedric, *J. Am. Chem. Soc.*, 1982, **104**, 525-528.
140. H. C. Brown.; G. G. Pai.; P. K. Jadhav, *J. Am. Chem. Soc.*, 1984, **106**, 1531-1533.
141. M. M. Midland.; J. E. Petre.; S. A. Zedric.; A. Kazubski, *J. Am. Chem. Soc.*, 1982, **104**, 528-531.
142. M. M. Midland.; J. I. McLoughlin.; J. Gabriel, *J. Org. Chem.*, 1989, **54**, 159-165.
143. T. Imai.; T. Tamura.; A. Yamamoro.; T. Sato.; T. A. Wollmann.; R. M. Kennedy.; S. Masamune, *J. Am. Chem. Soc.*, 1986, **108**, 7402-7404.
144. S. Masamune.; R. M. Kennedy.; J. S. Petersen.; K. N. Houk.; Y.-D. Wu, *J. Am. Chem. Soc.*, 1986, **108**, 7404-7405.
145. E. J. Corey.; R. K. Bakshi.; S. Shibata, *J. Am. Chem. Soc.*, 1987, **109**, 5551-5553.
146. E. J. Corey.; R. K. Bakshi.; S. Shibata.; C.-P. Chen.; V. K. Singh, *J. Am. Chem. Soc.*, 1987, **109**, 7925-7926.
147. E. J. Corey.; C. J. Helal, *Angew. Chem. Int. Ed.* , 1998, **37**, 1986-2012.
148. S. Itsuno.; K. Ito.; A. Hirao.; S. Nakahama, *J. Chem. Soc., Chem. Commun.*, 1983, 469-470.
149. E. J. Corey, *Pure Appl. Chem.*, 1990, **62**, 1209-1216.
150. E. J. Corey.; M. Azimioara.; S. Sarshar, *Tetrahedron Lett.*, 1992, **33**, 3429-3430.
151. D. J. Mathre.; A. S. Thompson.; A. W. Douglas.; K. Hoogsteen.; J. D. Carroll.; E. G. Corley.; E. J. J. Grabowski, *J. Org. Chem.*, 1993, **58**, 2880-2888.
152. A. Rodriguez.; M. Nomen.; B. W. Spur.; J.-J. Godfroid, *Eur. J. Org. Chem.*, 1999, 2655-2662.

153. K. Fujiwara.; H. Tsukamoto.; M. Izumikawa.; T. Hosoya.; N. Kagaya.; M. Takagi.; H. Yamamura.; M. Hayakawa.; K. Shin-ya.; T. Doi, *J. Org. Chem.*, 2015, **80**, 114-132.
154. *The Nobel Price in Chemistry 2001*, https://www.nobelprize.org/nobel_prizes/chemistry/laureates/2001/ (2002.2006.2017).
155. R. Noyori.; T. Ohkuma, *Angew. Chem. Int. Ed.*, 2001, **40**, 40-73.
156. R. Noyori.; T. Ohkuma.; M. Kitamura.; H. Takaya.; N. S. H. Kumobayashi.; S. Akutagawa, *J. Am. Chem. Soc.*, 1987, **109**, 5856-5858.
157. M. Kitamura.; T. Ohkuma.; S. Inoue.; N. Sayo.; H. Kumobayashi.; S. Akutagawa.; T. Ohta.; H. Takaya.; R. Noyori, *J. Am. Chem. Soc.*, 1988, **110**, 629-632.
158. T. Ohkuma.; H. Ooka.; S. Hashiguchi.; T. Ikariya.; R. Noyori, *J. Am. Chem. Soc.*, 1995, **117**, 2675-2676.
159. H. Doucet.; T. Ohkuma.; K. Murata.; T. Yokozawa.; M. Kozawa.; E. Katayama.; A. F. England.; T. Ikariya.; R. Noyori, *Angew. Chem. Int. Ed.*, 1998, **37**, 1703-1707.
160. T. Ohkuma.; H. Ooka.; T. Ikariya.; R. Noyori, *J. Am. Chem. Soc.*, 1995, **117**, 10417-10418.
161. S. Hashiguchi.; A. Fujii.; J. Takehara.; T. Ikariya.; R. Noyori, *J. Am. Chem. Soc.*, 1995, **117**, 7562-7563.
162. A. Fujii.; S. Hashiguchi.; N. Uematsu.; T. Ikariya.; R. Noyori, *J. Am. Chem. Soc.*, 1996, **118**, 2521-2522.
163. K. Matsumura.; S. Hashiguchi.; T. Ikariya.; R. Noyori, *J. Am. Chem. Soc.*, 1997, **119**, 8738-8739.
164. M. Yamakawa.; H. Ito.; R. Noyori, *J. Am. Chem. Soc.*, 2000, **122**, 1466-1478.
165. R. Noyori.; M. Yamakawa.; S. Hashiguchi, *J. Org. Chem.*, 2001, **66**, 7931-7944.
166. B. Štefane.; F. Požgan, *Asymmetric Hydrogenation and Transfer Hydrogenation of Ketones*, InTech, 2012.
167. A. Goswami.; J. D. Stewart, *Organic Synthesis Using Biocatalysis*, Elsevier Science, 2015.
168. J. Liang.; J. Lalonde.; B. Borup.; V. Mitchell.; E. Mundorff.; N. Trinh.; D. A. Kochrekar.; R. N. Cherat.; G. G. Pai, *Org. Process Res. Dev.*, 2010, **14**, 193-198.
169. A. O. King.; E. G. Corley.; R. K. Anderson.; R. D. Larsen.; T. R. Verhoeven.; P. J. Reider, *J. Org. Chem.*, 1993, **58**, 3731-3735.
170. S. Durand.; J.-L. Parrain.; M. Santelli, *J. Chem. Soc., Perkin Trans. 1*,, 2000, 253-273.
171. E. J. Corey.; J. O. Albright.; A. E. Barton.; S. Hashimoto, *J. Am. Chem. Soc.*, 1980, **102**, 1435-1436.
172. R. Tyagi.; B. Shimpukade.; S. Blättermann.; E. Kostenis.; T. Ulven, *Med. Chem. Commun*, 2012, **3**, 195-198.
173. T. Itoh.; I. Murota.; K. Yoshikai.; S. Yamada.; K. Yamamoto, *Bioorg. Med. Chem.*, 2006, **14**, 98-108.
174. T. Itho.; N. Yoshimoto.; K. Yamamoto, *Heterocycles*, 2010, **80**, 689-695.
175. D. V. Kuklev.; W. L. Smith, *Chem. Phys. Lipids*, 2004, **130**, 145-158.
176. M. G. Jakobsen.; A. Vik.; T. V. Hansen, *Tetrahedron Lett.*, 2014, **55**, 2842-2844.
177. S. Flock.; M. Lundquist.; L. Skattebøl, *Acta Chem. Scand.*, 1999, **53**, 436-445.
178. S. Flock.; L. Skattebøl, *J. Chem. Soc., Perkin Trans 1*, 2000, 3071-3076.
179. A. Vik.; T. V. Hansen.; A. K. Holmeide.; L. Skattebol, *Tetrahedron Lett.*, 2010, **51**, 2852-2854.
180. M. G. Jakobsen.; A. Vik.; T. V. Hansen, *Tetrahedron Lett.*, 2012, **53**, 5837-5839.
181. E. J. Corey.; S.-I. Hashimoto, *Tetrahedron Lett.*, 1981, **22**, 299-302.
182. G. Wittig.; U. Schöllkopf, *Chem. Ber.*, 1954, **97**, 1318-1330.

183. *The Nobel Prize in Chemistry 1979*, http://www.nobelprize.org/nobel_prizes/chemistry/laureates/1979/ (1905.1902.1915).
184. F. Ramirez.; C. P. Smith.; J. F. Pilot, *J. Am. Chem. Soc.*, 1968, **90**, 6727-6732.
185. E. Vedejs.; K. A. J. Snoble, *J. Am. Chem. Soc.*, 1973, **95**, 5778-5780.
186. E. Vedejs.; G. P. Meier.; K. A. J. Snoble, *J. Am. Chem. Soc.*, 1981, **103**, 2823-2831.
187. M. Aursnes.; J. E. Tungen.; A. Vik.; R. Colas.; C.-Y. C. Cheng.; J. Dalli.; C. N. Serhan.; T. V. Hansen, *J. Nat. Prod.*, 2014, **77**, 910-916.
188. L. Horner.; H. Hoffmann.; H. G. Wippel, *Chem. Ber.*, 1958, **91**, 61-63.
189. W. S. J. Wadsworth.; W. D. Emmons, *J. Am. Chem. Soc.*, 1961, **83**, 1733-1738.
190. L. Kurti.; B. Czako, *Strategic Applications of Named Reactions in Organic Synthesis*, Elsevier Inc., 2005.
191. W. C. Still.; C. Gennari, *Tetrahedron Lett.*, 1983, **24**, 4405-4408.
192. G. A. O'Doherty.; C. M. Smith, *Org. Lett.*, 2003, **5**, 1959-1962.
193. P. M. Pihko.; T. M. Salo, *Tetrahedron Lett.*, 2003, **44**, 4361-4364.
194. K. Ando, *J. Org. Chem.*, 1997, **62**, 1934-1939.
195. H. Lindlar, *Helv. Chim. Acta*, 1952, **35**, 446-450.
196. H. Lindlar.; R. Dubuis, *Org. Synth.*, 1966, **46**, 89.
197. S. V. Naidu.; P. Gupta.; P. Kumar, *Tetrahedron*, 2007, 7624-7633.
198. M. Aursnes.; J. E. Tungen.; A. Vik.; J. Dalli.; T. V. Hansen, *Org. Biomol. Chem*, 2014, **12**, 432-437.
199. J. E. Tungen.; M. Aursnes.; T. V. Hansen, *Tetrahedron Lett.*, 2015, **56**, 1843-1846.
200. J. E. Tungen.; M. Aursnes.; J. Dalli.; H. Arnardottir.; C. N. Serhan.; T. V. Hansen, *Chem. Eur. J.*, 2014, **20**, 14575-14578.
201. W. H. Kunau.; H. Lehmann.; R. Gross, *Physiol. Chem.*, 1971, **352**, 542-548.
202. C. A. Brown.; V. K. Ahuja, *J. Chem. Soc., Chem. Commun.*, 1973, DOI: 10.1039/c39730000553, 553-554.
203. *U.S. patent 1628190 Pat.*, US1628190, 1927.
204. J. F. Daeuble.; C. McGettigan.; J. M. Stryker, *Tetrahedron Lett.*, 1990, **31**, 2397-2400.
205. P. Yang.; M. Yao.; J. Li.; Y. Li.; A. Li, *Angew. Chem. Int. Ed.*, 2016, **55**, 6964-6968.
206. D. A. Rooke.; E. M. Ferreira, *Angew. Chem. Int. Ed.*, 2012, **51**, 3225-3230.
207. W. Boland.; N. Schroer.; C. Sieler.; M. Feigel, *Helv. Chim. Acta*, 1987, **70**, 1025-1040.
208. Y. M. A. Mohamed.; T. V. Hansen, *Tetrahedron*, 2013, **69**, 3872-3877.
209. A. Fürstner, *Angew. Chem. Int. Ed.*, 2000, **39**, 3012-3043.
210. P. Schwab.; M. B. France.; J. W. Ziller.; R. H. Grubbs, *Angew. Chem., Int. Ed.* , 1995, **34**, 2039-2041.
211. M. Scholl.; S. Ding.; C. W. Lee.; R. H. Grubbs, *Org. Lett.*, 1999, **1**, 953-956.
212. J. S. Kingsbury.; J. P. A. Harrity.; P. J. Bonitatebus, Jr..; A. H. Hoveyda, *J. Am. Chem. Soc.*, 1999, **121**, 791-799.
213. S. B. Garber.; J. S. Kingsbury.; B. L. Gray.; A. H. Hoveyda, *J. Am. Chem. Soc.*, 2000, **122**, 8168-8179.
214. R. R. Schrock, *Acc. Chem. Res.*, 1986, **19**, 342-348.
215. *The Nobel Prize in Chemistry 2005*, http://www.nobelprize.org/nobel_prizes/chemistry/laureates/2005/ (2005.2007.2017).
216. A. Fürstner.; O. Guth.; A. Rumbo.; G. Seidel, *J. Am. Chem. Soc.*, 1999, **121**, 11108-11113.
217. A. Fürstner.; K. Grela.; C. Mathes.; W. Lehmann, *J. Am. Chem. Soc.*, 2000, **122**, 11799-11805.
218. R. H. Grubs, *Handbook of Metathesis;*, 2003, Wiley-VCH: Weinheim.

219. T. J. Mann.; A. W. H. Speed.; R. R. Schrock.; A. H. Hoveyda, *Angew. Chem., Int. Ed.*, 2013, **52**, 8395-8400.
220. R. F. Heck.; J. P. Nolley, Jr., *J. Org. Chem.*, 1972, **37**, 2320-2322.
221. A. O. King.; N. Okukado.; E. Negishi, *J. Chem. Soc., Chem. Commun.*, 1977, DOI: 10.1039/c39770000683, 683-684.
222. J. K. Stille, *Angew. Chem.*, 1986, **98**, 504-519.
223. N. Miyaura.; K. Yamada.; A. Suzuki, *Tetrahedron Lett.*, 1979, 3437-3440.
224. K. Sonogashira.; Y. Tohda.; N. Hagihara, *Tetrahedron Lett.*, 1975, 4467-4470.
225. *The Nobel Prize in Chemistry 2010*, http://www.nobelprize.org/nobel_prizes/chemistry/laureates/2010/ (2010.2006.2017).
226. W. W. Winkler.; J. Uddin.; C. N. Serhan.; N. A. Petasis, *Org. Lett.*, 2013, **15**, 1424-1427.
227. J. M. J. Nolsøe.; M. Aursnes.; J. E. Tungen.; T. V. Hansen, *J. Org. Chem.*, 2015, **80**, 5377-5385.
228. D. C. Gesellschaft, *Berichte der Deutschen Chemischen Gesellschaft.*, Berlin, Verlag Chemie, 1868.
229. A. Wurtz, *Bull. Soc. Chim. Fr.* , 1872, **17**, 436-443.
230. A. Wurtz, *Chem. Ber.*, 1872, **5**, 326-327.
231. H. E. Zimmerman.; M. D. Traxler, *J. Am. Chem. Soc.*, 1957, **79**, 1920-1923.
232. D. A. Evans.; J. M. Takacs.; L. E. McGee.; M. D. Ennis.; D. J. Mathre.; J. Bartroli, *Pure Appl. Chem.*, 1981, **53**, 1109-1127.
233. I. Paterson, *Comprehensive Organic Synthesis*, Pergamon Press, New York, USA, 1991.
234. T. Mukaiyama.; K. Narasaka.; K. Banno, *Chem. Lett.*, 1973, 1011-1014.
235. D. A. Evans.; J. Bartroli.; T. L. Shih, *J. Am. Chem. Soc.*, 1981, **103**, 2127-2129.
236. Y. Nagao.; Y. Hagiwara.; T. Kumagai.; M. Ochiai.; T. Inoue.; K. Hashimoto.; E. Fujita, *J. Org. Chem.*, 1986, **51**, 2391-2393.
237. A. B. Smith.; T. M. Razler.; J. P. Ciavarri.; T. Hirose.; T. Ishikawa.; R. M. Meis, *J. Org. Chem.*, 2008, **73**, 1192-1200.

Chapter 2

2 Results and Discussion

2.1 Paper I: Synthesis of 5-(*S*)-HETE, 5-(*S*)-HEPE and (+)-Zooxanthellactone: Three Hydroxylated Polyunsaturated Fatty Acid Metabolites

The following section will give an outline of the results obtained from the investigation of the asymmetric reduction of the methyl ester of 5-oxo-eicosatetraenoic acid (5-oxo-ETE) **157a**, the methyl ester of 5-oxo-eicosatetraenoic acid (5-oxo-EPE) **157b** and the methyl ester of 4-oxo-docosahexaenoic acid (4-oxo-DHA) **157c** to the corresponding 5-(*S*)- and 4-(*S*)-hydroxylated analogues of AA (**1**), EPA (**2**) and DHA (**3**), respectively.

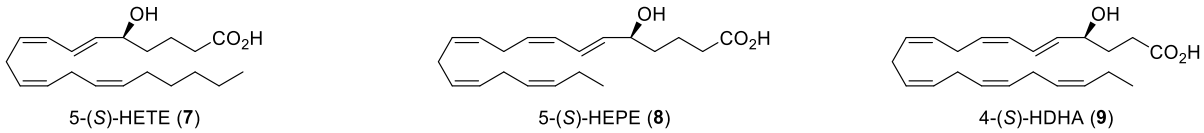

5-(*S*)-HETE (**7**) 5-(*S*)-HEPE (**8**) 4-(*S*)-HDHA (**9**)

Figure 2.1 The structure of 5-(*S*)-HETE (**7**), 5-(*S*)-HEPE (**8**) and 4-(*S*)-HDHA (**9**).

Studies have shown interesting antidiabetic effect for 5-(*S*)-HEPE (**8**)[1,2] and 4-(*S*)-HDHA (**9**).[3] Antiangiogenetic effects have also been observed for the latter.[4] Thus, further biological investigation is necessary to thoroughly understand the biological effects of 5-(*S*)-HEPE (**8**) and 4-(*S*)-HDHA (**9**). So far, both racemic and stereoselective syntheses of 5-HETE (**7**) are reported,[5-11] while for the EPA derived analogues, only racemic syntheses have been published.[12,13] 4-HDHA (**9**) has been prepared racemic and in the synthesis reported by Yamamoto and co-workers, 4-(*S*) and 4-(*R*)-HDHA (**9**) were accessed by optical resolution.[3,12,14] Hence, the need for efficient stereoselective synthesis of these oxygenated PUFAs is of interest. In this context, we wanted to investigate if stereoselective reductions of the corresponding oxo-compounds of 5-HETE (**7**), 5-HEPE (**8**) and 4-HDHA (**9**) could yield the target molecules with high stereoselectivity.

2.1.1 Investigation of Reaction Conditions

The three oxo compounds **157a-c** were prepared as illustrated in Scheme 2.1. Following a procedure reported by Ulven and co-workers, the free acids were converted into the iodolactones **114a-c**.[11] Further, a DBU induced elimination reaction was preformed, affording lactones **115a-c**.[15] Ring opening of the lactones **115a-c** to the corresponding hydroxy methyl esters **156a-c** was achieved using Et_3N in methanol.[15,16] The secondary alcohols **156a** and **156b** were then oxidized by Dess-Martin periodinane, furnishing the ketones **157a** and **157b**. The Swern oxidation[17] was utilized to oxidize the secondary alcohol in compound **156c** according to a procedure reported by Itho and co-workers.[14]

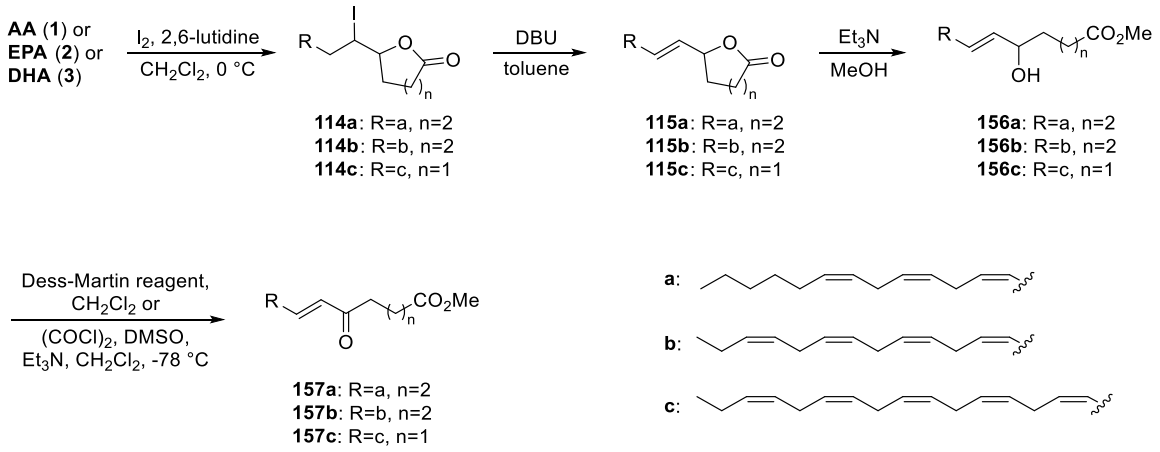

Scheme 2.1 Preparation of oxo compounds **157a-c**.

Next, various methods and protocols for the stereoselective reduction of the ketones **157a-c** were investigated. We decided to focus on the Noyori's transfer hydrogenation catalyst and Corey-Bakshi-Shibata (CBS) catalyst because they are readily available from commercial sources. Additionally, the CBS catalyst have proven to reduce α,β-unsaturated ketones to the corresponding alcohol in good yields and high %*ee*.[18-20]

Noyori's transfer hydrogenation catalyst **105a** and CBS catalyst (*R*)-**158** were tested in the stereoselective reduction of the methyl ester of 5-oxo-EPE **157b**. Employing Noyori's catalyst **105a** in the asymmetric reduction of oxo-compound **157b** afforded the desired 5-hydroxy-compound (*S*)-**156b** in moderate yield and *ee*-values in the mid 70's (Table 2.1, entries 1 and 2). It became apparent that the results were difficult to reproduce. Hence, the focus was shifted to the CBS reduction and CBS catalyst (*R*)-**158**. When borane dimethyl sulfide (BMS) was utilized as the reducing agent with 15 mol% of the catalyst (*R*)-**158** in either THF or toluene the product (*S*)-**156b** was formed in poor yields and poor *ee*-values (Table 2.1, entries 3 and 4) In entry 5, the reducing agent was switched to catecholborane, which remarkably increased both the yield and the selectivity. The selectivity was further enhanced when switching the solvent from toluene to dichloromethane (entry 6). Also important, the obtained results were reproducible. The opposite enantiomer of the catalyst (*S*)-**158**, the (*S*)-catalyst, provided the (*R*)-enantiomer of the product (*R*)-**156** in comparable yield and *ee*-value to the results obtained with the (*R*)-catalyst **158** (entry 7). Increasing the catalyst loading did not affect the yield or *ee*-value to a great extent (entry 8).

Table 2.1 Stereoselective reduction of compounds **157a-c**.

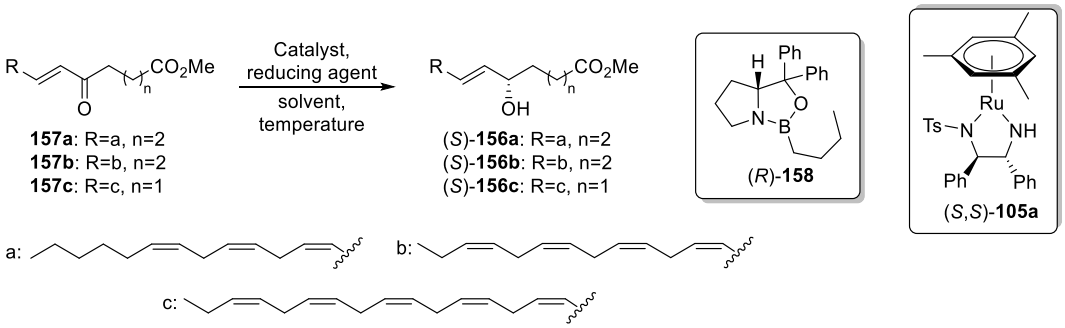

Entry	Solvent	Substrate	Catalyst	Reducing agent	Temperature (°C)	Yield (%)[a]	*ee* (%)[b]
1	*i*-PrOH	**157b**	(*S*,*S*)-**105a** (2 mol%)	−	rt	58	74
2	CH_2Cl_2	**157b**	(*S*,*S*)-**105a** (2 mol%)	−	rt	60	77
3	THF	**157b**	(*R*)-**158** (15mol%)	BMS	-50 to -10	21	42
4	Toluene	**157b**	(*R*)-**158** (15 mol%)	BMS	0	19	34
5	Toluene	**157b**	(*R*)-**158** (15 mol%)	CB	-78	80	63
6	CH_2Cl_2	**157b**	(*R*)-**158** (15 mol%)	CB	-78	85	79
7	CH_2Cl_2	**157b**	(*S*)-**158** (15 mol%)	CB	-78	81	75
8	CH_2Cl_2	**157b**	(*R*)-**158** (50 mol%)	CB	-78	83	69
9	CH_2Cl_2	**157a**	(*R*)-**158** (15 mol%)	CB	-78	84	71
10	CH_2Cl_2	**157c**	(*R*)-**158** (15 mol%)	CB	-78	63	69

[a] Isolated material

[b] Determined by HPLC analysis

Since the conditions in entry 6 gave the best results in the reduction of **157b**, the same conditions were applied for the remaining reduction of the methyl ester **157a** and the methyl ester **157c**. Similar *ee*-values were obtained for products **156a** and **156c** (entries 9 and 10). The reason for the moderate yield obtained in the reduction of **157c** was due to the formation of the γ-lactone during the reaction. The final step was the hydrolysis of the methyl esters **156a-c**. This worked well for the (*S*)-alcohols **156a** and **156b**, affording 5-(*S*)-HETE (**7**) and

5-(*S*)-HEPE (**8**) in 90% and 84% yields, respectively (Scheme 2.2). The hydrolysis of methyl ester **156c** resulted in the γ-lactone, which is a natural product called (+)-zooxanthellactone (**115c**). This is most likely due to the easily formed γ-lactone.[21,22]

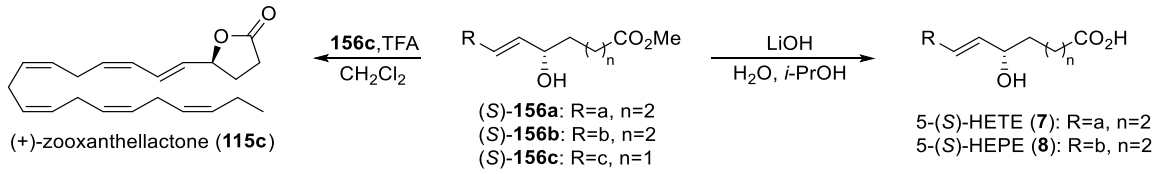

Scheme 2.2 Hydrolysis of compound **156a**, **156b** and the transformation of **156c** to (+)-zooxanthellactone (**115c**).

2.1.2 Conclusion

The three naturally occurring PUFAs, 5-(*S*)-HETE (**7**), 5-(*S*)-HEPE (**8**) and (+)-zooxanthellactone (**115c**), were obtained by short and stereoselective syntheses. By the use of the chiral CBS-catalyst **158**, *ee*-values up to 79% were achieved and the results proved to be reproducible. The preferred protocol was applied in a convenient synthesis of (+)-zooxanthellactone (**115c**). Thus, a highly stereoselective synthesis of this natural product is still elusive.

The three keto-metabolites 5-oxo-ETE, 5-oxo-EPE and 4-oxo-DHA, as well as the oxo methyl esters **157a-c** synthesized in the above-mentioned work, have been subjected to molecular modelling studies and evaluations as agonists towards the GPCR receptor oxoeicosanoid receptor 1 (OXER1). This receptor mediates the undesirable effects observed for the potent chemoattractant 5-oxo-ETE.[4] The results reported from this study indicate that the oxo-compounds likely migrates through the membrane in order to access the receptor. Further, 5-oxo-EPE proved to activate the OXER1 receptor with similar efficiency as the natural agonist 5-oxo-ETE, while the methyl ester of **157a** and **157b** proved to be less efficient. 4-oxo-DHA and the methyl ester **157c** did not activate the receptor at all. These finding spiked the interest in performing molecular modeling studies towards the OXER1 receptor and the results obtained from these molecular modeling studies will be useful in the design of novel synthetic antagonist for OXER1.

Table 2.2 Agonist effects measured in the β-arrestin assay.

Compound	EC_{50} (μM)[a]	Max Response*
5-oxo-AA Me ester (157a)	1,54±0.1	133
5-oxo-ETE	0,22±0.1	100
5-oxo-EPA Me ester (157b)	2,08	119
5-oxo-EPA	0,38	80
4-oxo-DHA Me ester (157c)	>100	64
4-oxo-DHA	>100	23

[a]Based on three experiments in triplicates.

In addition, the lactones **115b** and **115c** (both racemic and (+)-zooxanthellactone) have been subjected to preliminary evaluations in their ability to increase Ca^{2+} in endothelial cells. This study is currently ongoing and further biological experiments are needed.

2.2 Paper II: An Efficient Total Synthesis of Leukotriene B_4

LTB_4 (**12**) is a potent pro-inflammatory lipid mediator biosynthesized from AA (**1**) by the 5-LOX pathway. This powerful chemoattractant promotes recruitment and accumulation of leukocytes at the inflamed site.[23] Herein, an overview of the synthetic planning and synthesis will be given.

2.2.1 Retrosynthetic Analysis of Leukotriene B_4

The conjugated *Z*,*E*,*E*-triene present in LTB_4 (**12**) is highly labile and prone to undergo isomerization in the presence of light, oxygen and acidic conditions. The two chiral allylic alcohols flanking the triene moiety are predisposed to encounter water elimination, further increasing the instability of the labile triene. To avoid disarrangement of the geometry in the structure, the instalment of the *Z*,*E*,*E*-triene is preferred at a late stage. In our group, several SPMs containing similar triene moieties by the use of the acetate–aldol reaction using the key building block (2*E*,4*E*)-5-bromopenta-2,4-dienal (**149**) have been synthesised.[24-28] Based on the success in these syntheses, a retrosynthetic analysis, including this strategy, was designed for an efficient and convergent synthesis of LTB_4 (**12**) (Figure 2.2).

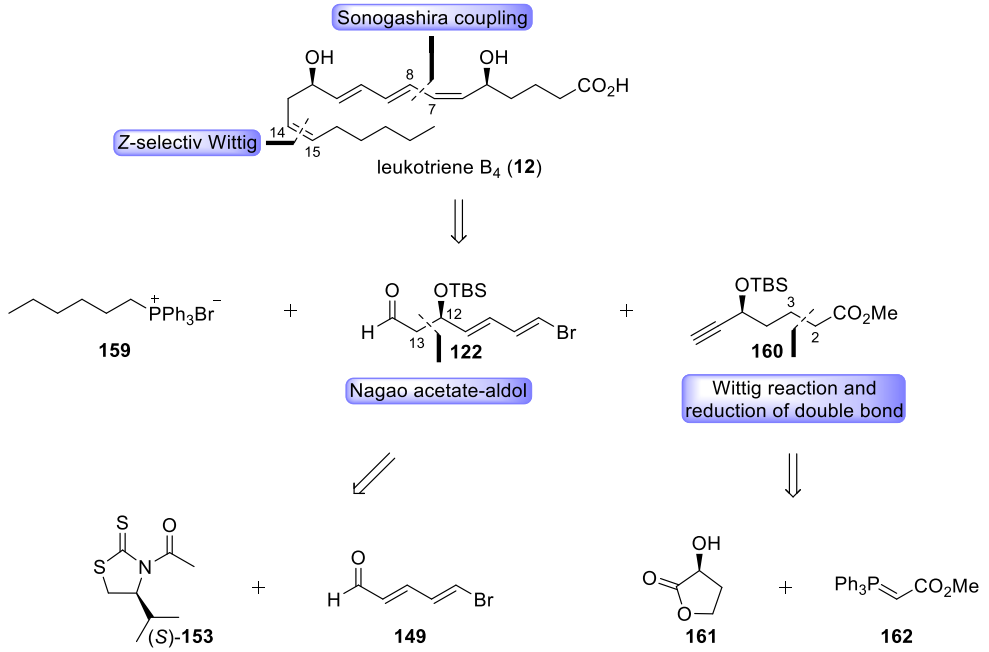

Figure 2.2 Retrosynthetic analysis of LTB_4 (**12**).

The first disconnection was done between C7 and C8, envisioning the construction of the *Z*-double bond by a Sonogashira cross-coupling reaction[29] between the terminal alkyne **160** and a suitable vinyl bromide, followed by *Z*-selective partial hydrogenation of the internal alkyne. This strategy ensures a late instalment of the labile *Z*,*E*,*E*-triene moiety. Next, the *Z*-double bond between C14 and C15 may result from a *Z*-selective Wittig reaction.[30] These two

disconnections will divide the desired molecule in three fragments of comparable size, labelled the ω-end **159**, the middle fragment **122** and the α-end **160**.

The middle fragment **122** contains a β-hydroxy carbonyl moiety that can be constructed by a Nagao acetate-aldol reaction.[31] Consequently, this fragment may be cleaved between C12 and C13, rendering the acetylated chiral auxiliary (*S*)-**153** and (2*E*,4*E*)-5-bromopenta-2,4-dienal (**149**), as illustrated in Figure 2.2. To generate the terminal alkyne, with the Colvin reaction in mind,[32] the α-end **160** can be disconnected back to the corresponding ylide **162** and an aldehyde, which in turn can be prepared from the commercially available hydroxy lactone **161**.

2.2.2 Total Synthesis of LTB_4

The synthesis towards LTB_4 (**12**) commenced with the preparation of the α-end **160**, as illustrated in Scheme 2.3. The secondary alcohol of commercially available (*S*)-(−)-α-hydroxy-γ-butyrolactone (**161**) was protected using TBS-triflate. Further, **163** was reduced to the corresponding lactole **164** by DIBAL-H and subjected to a Colvin reaction to generate the terminal alkyne **165**.[32] The Dess-Martin periodinane reagent was utilized in the oxidation of the primary alcohol **165** and the resulting aldehyde **166** was reacted with methyl (triphenylphosphoranylidene)acetate (**162**) in a Wittig reaction,[30] affording the α,β-unsaturated methyl ester **167**. The next step was the reduction of the conjugated double bond in **167**. First, based on a paper published by Tsuda,[33] DIBAL-H in the presence of CuI dissolved in a mixture of THF and HMPA was used. In our hands, however, this procedure gave low conversion of the starting material **167**. Thereafter, the Stryker reagent was used,[34] giving the desired product in a disappointing 41% yield. The best result was obtained using magnesium turnings in methanol,[35] which enhanced the yield of **160** to 60%.

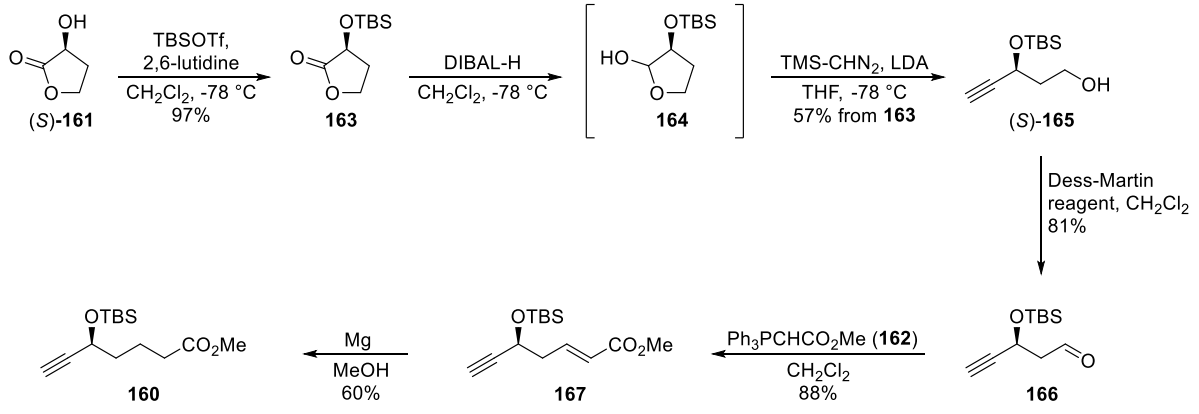

Scheme 2.3 Synthesis of the α fragment **160**.

Aldehyde **149** was prepared according to a slightly modified literature procedure from the commercially available pyridinium salt **168**.[36,37] The salt **168** was treated with aqueous

potassium hydroxide, affording the potassium salt **169**. Further, **169** was reacted with a PPh_3/Br_2 complex in dichloromethane, followed by treatment with *p*-TsOH in diethyl ether, which yielded multi-gram quantities of (2*E*,4*E*)-5-bromopenta-2,4-dienal (**149**). The chiral alcohol in the middle fragment **122** was introduced by using a Nagao acetate aldol reaction between aldehyde **149** and enantiopure *N*-acetyl thiazolidinethione (*S*)-**153**, using TiCl as the Lewis acid and Hünig's base.[38,39] This reaction gave intermediate **170** in good yield and a 15.3:1 ratio of the desired diastereomer. Next, the secondary alcohol in **170** was protected, affording TBS silyl ether **171** (Scheme 2.4).

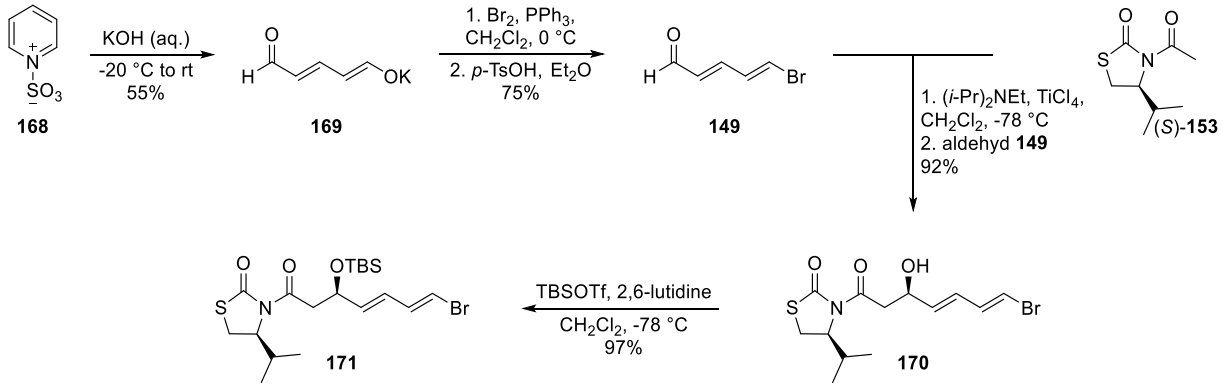

Scheme 2.4 Preparation of TBS silyl ether **171**.

The chiral auxiliary in **171** was removed by reductive cleavage using DIBAL-H, giving aldehyde **122**, which was immediately employed in a *Z*-selective Wittig reaction[30] with the ylide generated by treating the commercially available Wittig salt **159** with NaHMDS. After purification by flash chromatography, only the desired *Z*-isomer **172** was detected by ^1H and ^{13}C NMR analysis. Next, the two key fragments **172** and **160** were assembled by a Sonogashira cross-coupling reaction,[29] using $Pd(PPh_3)_4$ and CuI in Et_3N. The coupled product **173** was obtained in 84 % yield. Five equivalents of TBAF were used to efficiently remove the two TBS groups, affording diol **174** (Scheme 2.5).

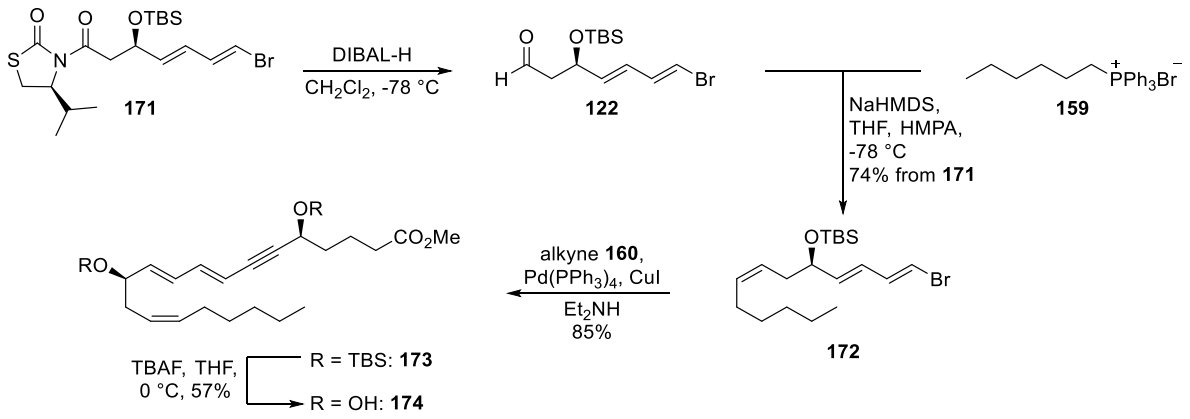

Scheme 2.5 Assembly of the middle fragment **122** and the ω-end **159**, and the preparation of **174**.

Semihydrogenation of the conjugated alkyne **174** to the corresponding *Z*-alkene **175**, using Lindlar's catalyst,[40] gave disappointing yields and an undesired by-product, which we were not able to separate from the desired product. The Boland protocol,[41] on the other hand, with freshly prepared Zn(Cu/Ag) in methanol and water, yielded the chemically pure methyl ester **175** in acceptable yields. The free hydroxyl groups promote adsorption to the surface of the metal catalyst, which in turn activates the selective reduction of the internal alkyne.[42] Finally, basic hydrolysis of the methyl ester **175** furnished LTB_4 (**12**) in 78% yield (Scheme 2.6).

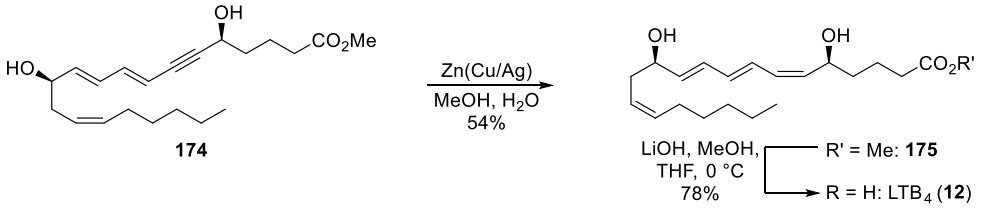

Scheme 2.6 Final steps in the total synthesis of LTB_4 (**12**).

2.2.3 Conclusion

The potent inflammatory lipid mediator leukotriene B_4 (**12**) was synthesized in ten steps (longest linear sequence) using 19 synthetic operations in an overall yield of 5%. This synthesis is one of the most efficient syntheses published and none of the steps required purification by HPLC.

2.3 Paper III: Stereocontrolled Synthesis and Investigation of the Biosynthetic Transformations of 16(*S*),17(*S*)-epoxy-PD$_{n\text{-}3\ DPA}$

The role of epoxides in the biosynthesis of oxygenated PUFAs, including SPMs originated from EPA (**2**) and DHA (**3**), has earlier been reported.[43] In 2015, the Lipchem group in collaboration with Serhan's group at Harvard Medical School, Brigham and Women's Hospital, established the biosynthesis of PD1 (**28**).[44] Recently, it was reported that n-3 DPA (**43**) is converted to n-3 products, congeners of D-series resolvins, protectins and maresins.[45,46] The configuration of PD1$_{n\text{-}3\ DPA}$ (**46**), illustrated in Scheme 2.7, was later confirmed by the matching of authentic and synthetic material.[25] Based on structural similarities with PD1 (**28**), it is highly likely that an epoxide intermediate is involved in the biosynthesis of PD1$_{n\text{-}3\ DPA}$ (**46**) as well.[45] However, to confirm the role of epoxide **45** in the biosynthesis of PD1$_{n\text{-}3\ DPA}$ (**46**) total synthesis of **45** is required, as well as subjecting the synthetic material to biological systems. Hence, we became interested in developing a stereoselective synthetic strategy for the synthesis of 16(*S*),17(*S*)-epoxy-PD$_{n\text{-}3\ DPA}$ (**45**). In this section, the planning and synthesis of 16(*S*),17(*S*)-epoxy-PD$_{n\text{-}3\ DPA}$ (**45**) will be discussed.

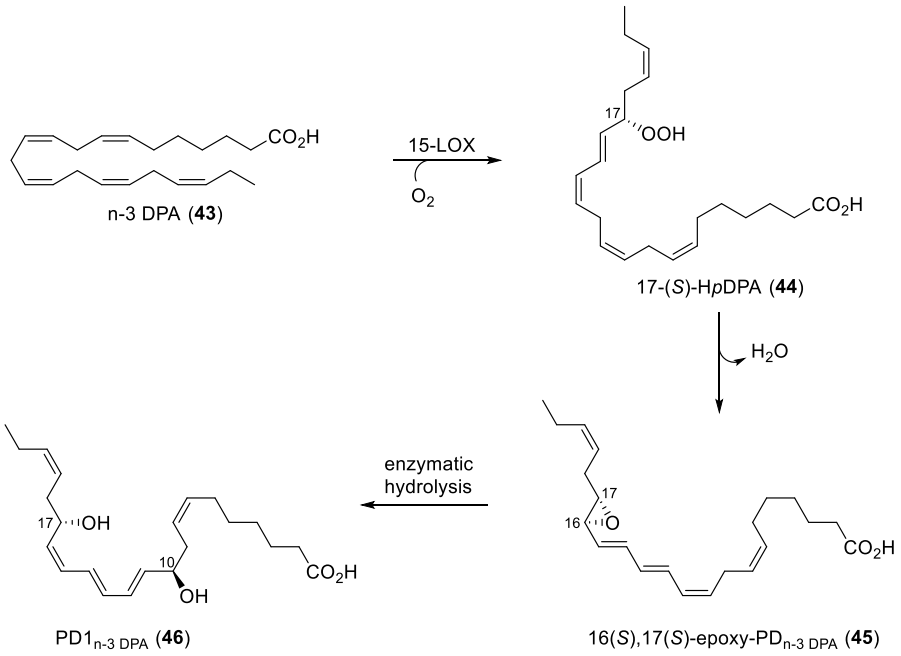

Scheme 2.7 Proposed biosynthesis of PD1$_{n\text{-}3\ DPA}$ (**46**) from n-3 DPA (**43**).

2.3.1 Retrosynthetic Analysis of 16(*S*),17(*S*)-epoxy-PD$_{n\text{-}3\ DPA}$

Using a synthetic strategy with similarities to that reported for the synthesis of 16(*S*),17(*S*)-epoxy-protectin (**27**),[44] retrosynthetic scissoring between C10 and C11 was made, which will divide the target molecule into two fragments of similar size **176** and **177**, as shown in Figure 2.3. This carbon-carbon bond may in turn be forged by a *Z*-selective Wittig reaction.[30] Recognising that the two *E*-double bonds in aldehyde **176** may be generated by a Wittig

homologation, **176** can in a forward direction consequently be prepared from the commercially available ylide, (triphenylphosphoranylidene)acetaldehyde (**179**) and aldehyde **178**, obtained from the corresponding alcohol. With a Katsuki-Sharpless epoxidation reaction[47] in mind, the epoxide moiety in **178** can be transformed back to the alkene. Making a functional group manipulation of the primary alcohol in the previously mentioned alkene back the methyl ester **181**, followed by a disconnection between C16 and C17, leads to the commercially available (*Z*)-hex-3-en-ol (**182**) and a suitable ylide as potential precursors. The Wittig salt **177** may be prepared from a *Z*-selective Wittig reaction[30] after making two functional group manipulations. Disconnection between C7 and C8 leads back to the aldehyde **180**, obtained from commercially available 3-((*tert*-butyldimethylsilyl)oxy)-propanol and Wittig salt **123**, which in turn can be prepared from cycloheptanone (**183**).

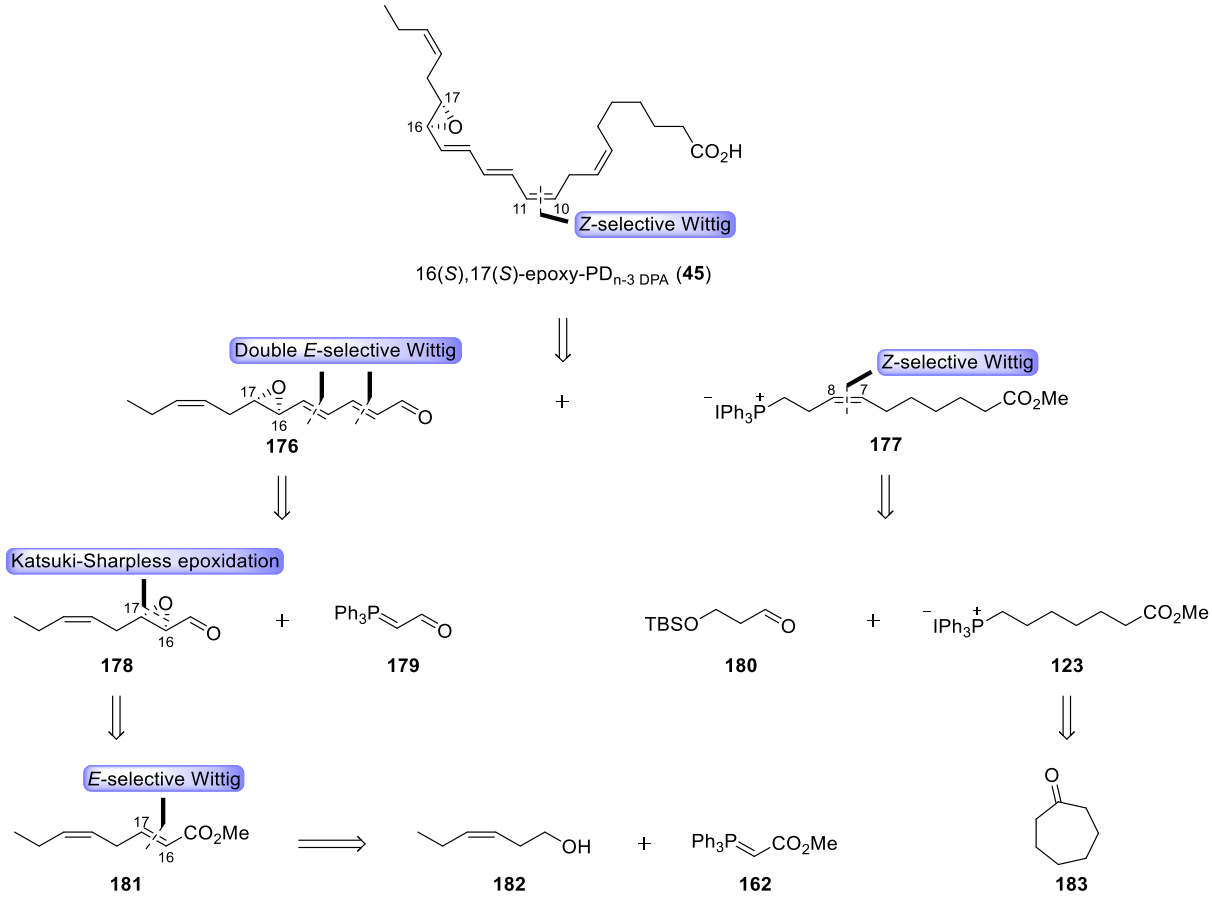

Figure 2.3 Retrosynthetic analysis of 16(*S*),17(*S*)-epoxy-PD$_{n\text{-}3\ DPA}$ (**45**).

2.3.2 Total Synthesis of the Methyl Ester of 16(*S*),17(*S*)-epoxy-PD$_{n\text{-}3\ DPA}$

First, aldehyde **176** was prepared in five steps, as previously reported,[44] from commercially available (*Z*)-hex-3-en-ol (**182**). This work commenced with the conversion of the primary alcohol in **182** to an aldehyde by the Dess-Martin reagent, which was utilized in a Wittig

olefination to obtain intermediate **181**. The methyl ester in **181** was reduced using DIBAL-H to the corresponding alcohol **184**, which was further transformed to epoxide **185** under the Sharpless condition[47] in 70% yield and 96% *ee*. The oxidation of the primary alcohol in **185** was achieved by a Swern oxidation,[17] and the resulting aldehyde was then immediately subjected in a Wittig homologation with the commercially available ylide (triphenylphosphoranylidene)-acetaldehyde (**179**), furnishing aldehyde **176** in 61% yield after purification by flash chromatography (Scheme 2.8).

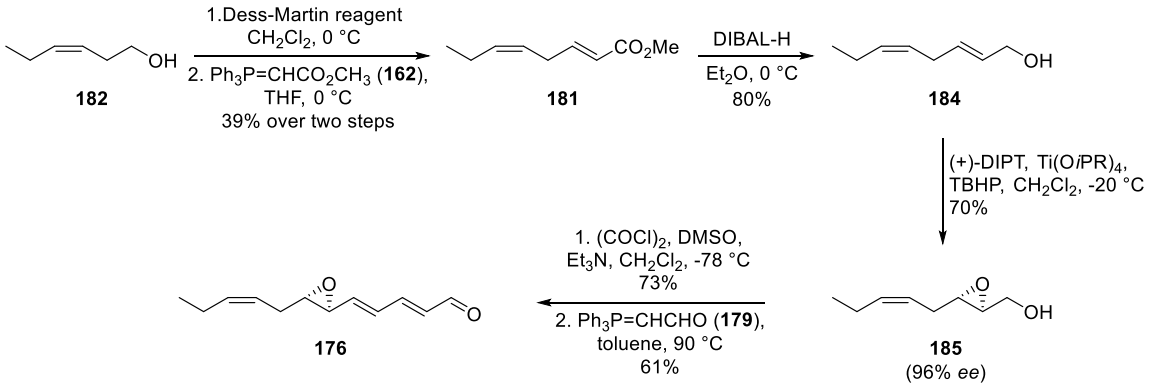

Scheme 2.8 Preparation of aldehyde **176**.

The Wittig salt **177** was obtained from cycloheptanone (**183**). The first four steps were performed as previously reported.[25] The sequence started with a Baeyer-Villager oxidation[48] of **183**. The resulting lactone was treated with catalytic amount of H_2SO_4 in methanol, affording hydroxy methyl ester **186**.[49] The primary alcohol in **186** was then converted into Wittig salt **123**, by first reacting **186** in an Apple reaction,[50] followed by addition of PPh_3 to afford **123**.[25] This Wittig salt **123** was treated with NaHMDS at -78 °C to generate the corresponding ylide and then reacted in a *Z*-selective Wittig reaction[30] with aldehyde **180**, yielding the desired product containing an internal *Z*-double bond as the single stereoisomer. The TBS-protecting group was then removed using camphorsulfonic acid (CSA) in methanol and dichloromethane, furnishing hydroxy methyl ester **187**, which was converted into the Wittig salt **177**, as outlined in Scheme 2.9.

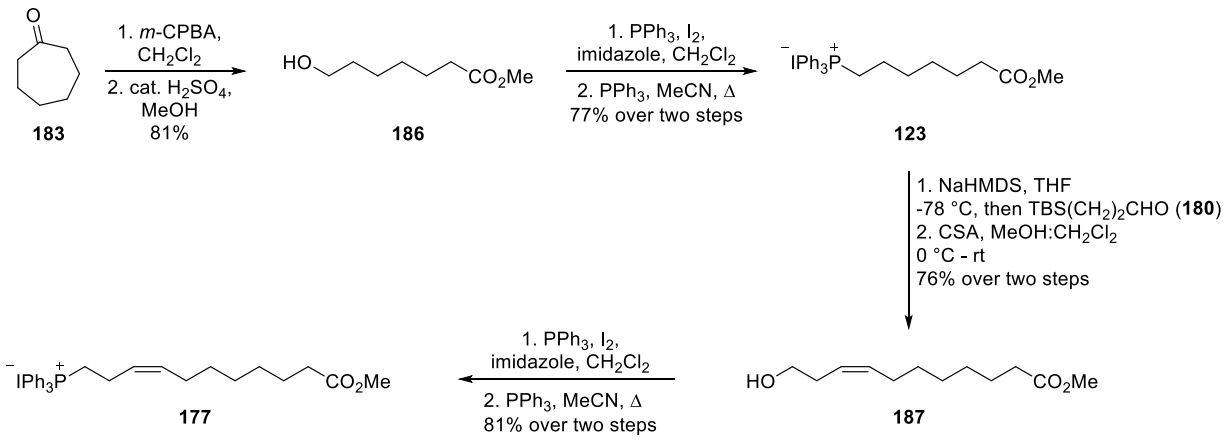

Scheme 2.9 Preparation of the second key α fragment **177**.

The aldehyde **176** and the ylide of Wittig salt **177** were assembled in a *Z*-selective Wittig reaction.[30] The desired methyl ester **188** was obtained in 58% yield (Scheme 2.10). Due to the instability of the hydrolysed product, this step was performed just prior to conducting the biological experiments, which were executed by our collaborators in Dalli's group in London. They observed full conversion of **188** to the highly labile 16(*S*),17(*S*)-epoxy-PD$_{n\text{-}3\ DPA}$ (**45**), which was confirmed by LC/MS-MS experiments, while UV-data confirmed the presence of the *E*,*E*,*Z*-triene after saponification.

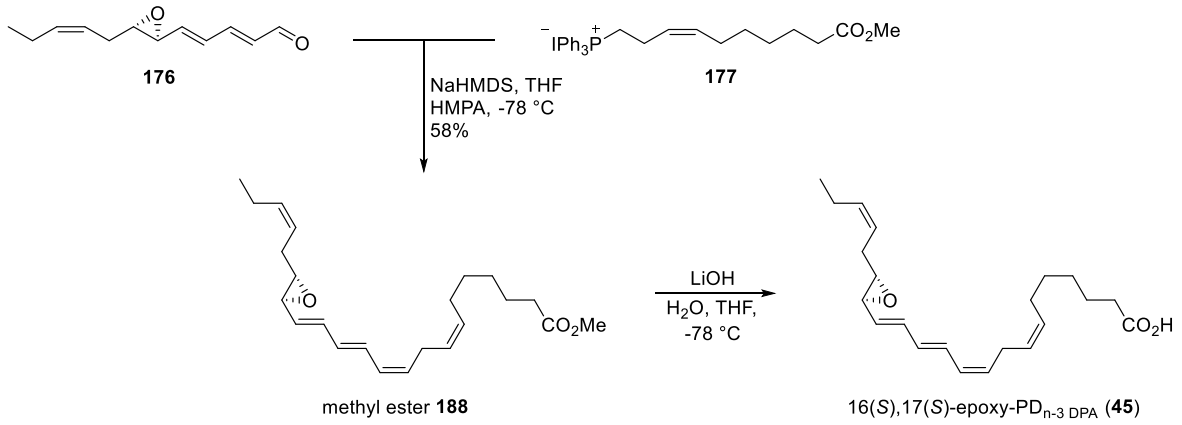

Scheme 2.10 Final step in the synthesis of 16(*S*),17(*S*)-epoxy-PD$_{n\text{-}3\ DPA}$ (**45**).

2.3.3 Biological Actions of 16(*S*),17(*S*)-epoxy-PD$_{n\text{-}3\ DPA}$

First, we wanted to investigate whether an enzyme was involved in the hydrolysis of epoxide **45** to PD1$_{n\text{-}3\ DPA}$ (**46**). Thus, acidified water (pH = 3.0) was added to the epoxide **45** and a shift in the λ_{max} (MeOH) from 280 nm to 270 nm in the UV-visible absorption spectra was observed (Figure 2.4A, B). This newly formed ultraviolet absorbance profile is consistent with the formation of a conjugated *E*,*E*,*E*-triene moiety. From the aqueous hydrolysis of **45**, four main products with a parent ion of m/z 361 were detected and characterized by LC/MS-MS metabololipidomics (Figure 2.4C). The MS-MS fragmentation of product I and II resulted in identical spectra, which were in accordance with two isomers of 10,17(*S*)-dihydroxydocosa-7*Z*,11*E*,13*E*,15*E*,19*Z*-pentaenoic acid (**189**) (Figure 2.4D). This product is the result of water added to the least sterically-hindered carbon of the putative carbocation intermediate (Scheme 2.11)

When assessing the MS-MS fragmentation spectra of product III and IV, it became evident that they were essentially identical and consistent with products containing a vicinal diol corresponding to 16,17(S)-dihydroxydocosa-7*Z*,10*Z*,12*E*,14*E*,19*Z*-pentaenoic acid (**190**) (Figure 2.4E and Scheme 2.11). PD1$_{n\text{-}3\ DPA}$ (**46**) was not detected in any of the incubations, hence, PD1$_{n\text{-}3\ DPA}$ (**46**) does not form by non-enzymatic hydrolysis of epoxide **45**.

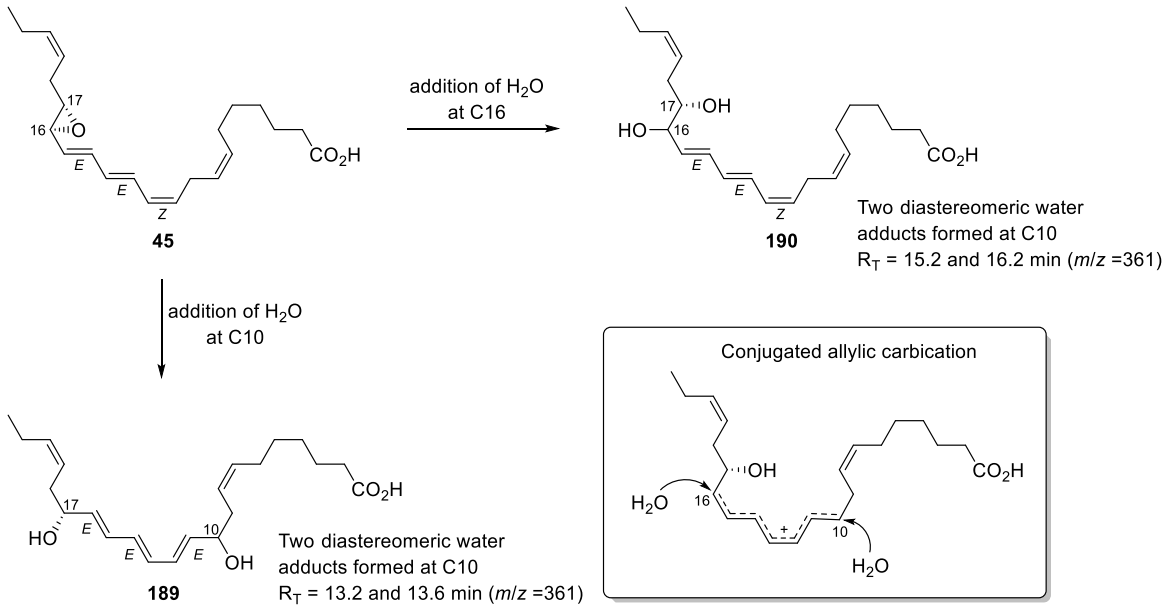

Scheme 2.11 Non-enzymatic hydrolysis of synthetic **45** at pH 3.0.

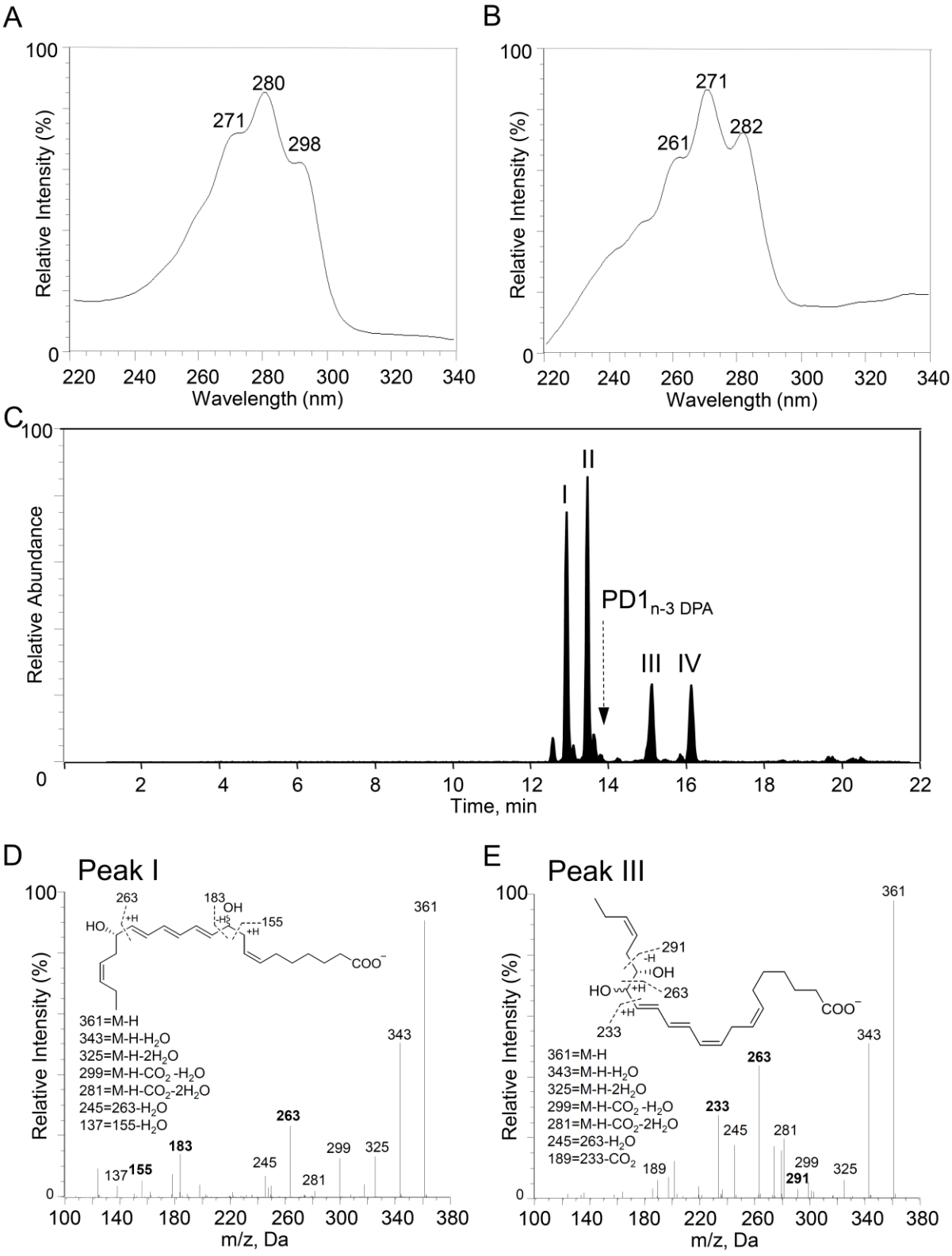

Figure 2.4 16(*S*),17(*S*)-epoxy-PD$_{n\text{-}3\ DPA}$ (**45**) is rapidly hydrolyzed in aqueous conditions. Synthetic 16(*S*),17(*S*)-epoxy-PD$_{n\text{-}3\ DPA}$ (**45**, 1 ng/1 µL) was placed in double distilled water acidified to pH = 3.0, products were extracted and profiled using lipid mediator profiling. UV chromophore of (A) 16(*S*),17(*S*)-epoxy-PD$_{n\text{-}3\ DPA}$ (**45**) and (B) 16(*S*),17(*S*)-epoxy-PD$_{n\text{-}3\ DPA}$ (**45**) non-enzymatic hydrolysis products. (C) MRM chromatogram of products *m/z* 361 > 263. Arrow denotes retention time of synthetic and authentic PD1$_{n\text{-}3\ DPA}$ (**46**). (D, E) MS-MS spectra employed for identification of products under peaks I (D) and IIII (E). Results are representative of n = 3 incubations

Next, we were interested in establishing whether 15-LOX is the enzyme involved in the biosynthesis of epoxide **45**. For this reason, n-3 DPA (**43**) was incubated with human recombinant 15-LOX type 1 and the products formed in these incubated were evaluated by LC/MS-MS based profiling.

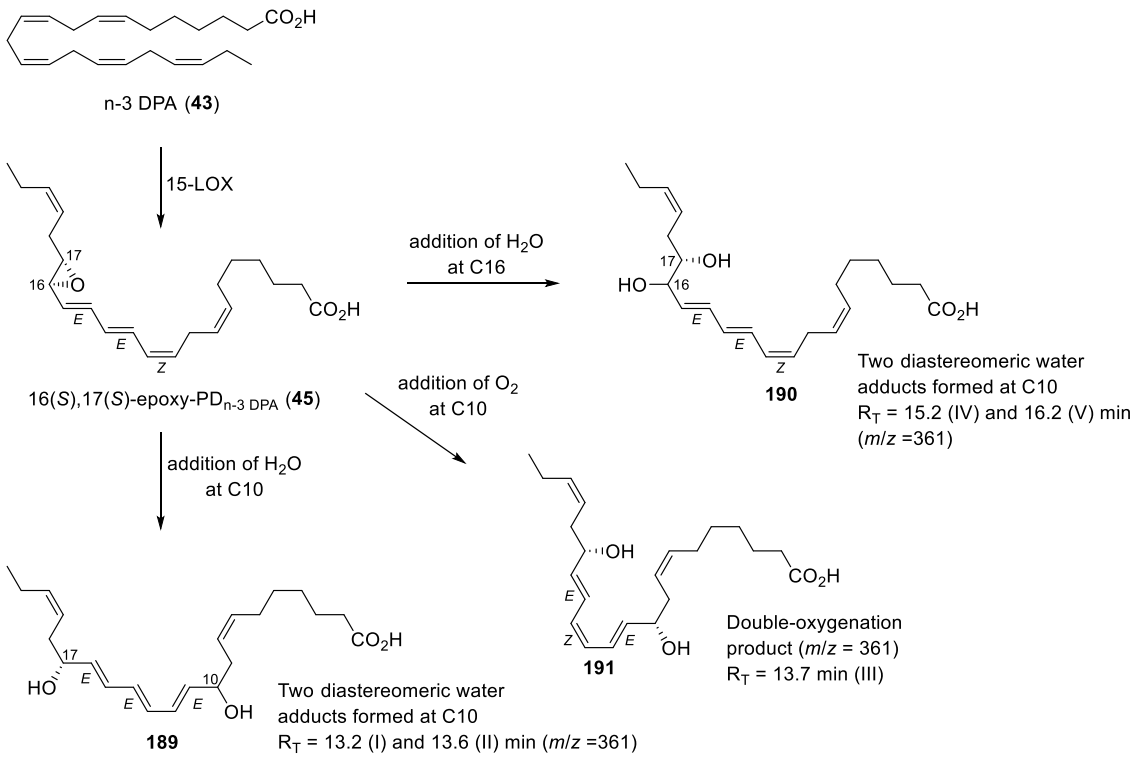

Scheme 2.12 Outline of 15-LOX mediated formation of 16(*S*),17(*S*)-epoxy-PD$_{n\text{-}3\ DPA}$ (**45**) from n-3 DPA (**43**).

Five main products were observed, where the MS-MS fragmentation patterns for the products in peak I and II (R_T = 13.2 and 13.6 min) were identical and consistent with two isomers of 10,17(*S*)-dihydroxy-7*Z*,11*E*,13*E*,15*E*,19*Z*-docosapentaenoic acid (**189**) (Figure 2.5A and B, and Scheme 2.12). The product under peak (III) (R_T =13.7 min) corresponds to the dioxygenated product, 10(*S*),17(*S*)-dihydroxy-7*Z*,11*E*,13*Z*,15*E*,19*Z*-docosapentaenoic acid (**191**) (Figure 2.5A, Scheme 2.12). The two last peaks (IV and V) gave identical MS-MS fragmentation patterns that were consistent with the two isomers formed from the aqueous hydrolysis of epoxide **45**, namely 16,17(*S*)-dihydroxy-7*Z*,10*Z*,12*E*,14*E*,19*Z*-docosapentaenoic acid (**190**) (Figure 2.5A and C, and Scheme 2.12). Hence, these results confirm that 15-LOX is involved in the biosynthesis of 16(*S*),17(*S*)-epoxy-PD$_{n\text{-}3\ DPA}$ (**45**).

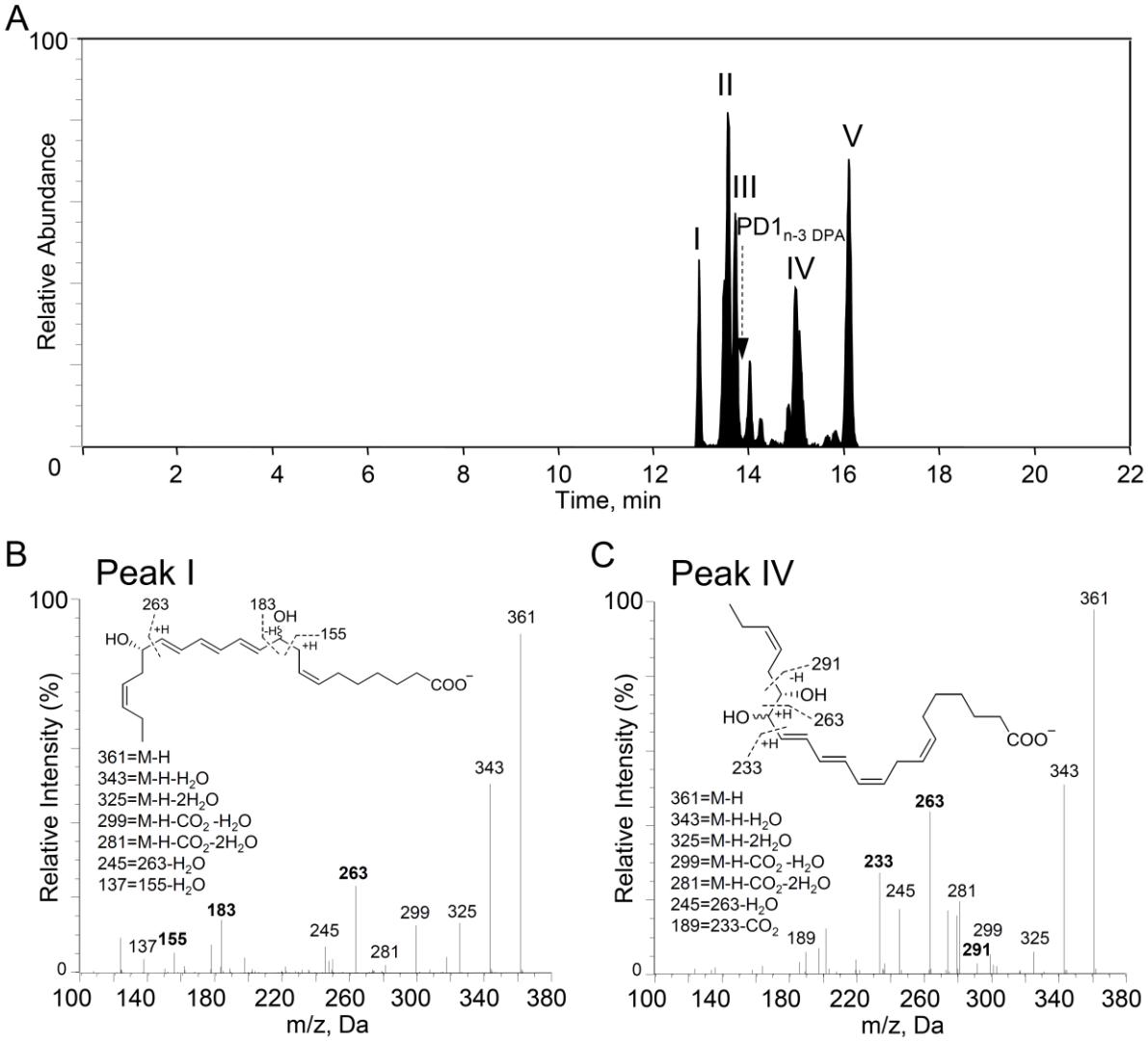

Figure 2.5 Product profile of human 15-LOX supports the formation of 16(*S*),17(*S*)-epoxy-$PD_{n\text{-}3\ DPA}$ (**45**) from n-3 DPA (**43**). Human 15-LOX was incubated with n-3 DPA (**43**) (Tris Buffer, pH = 8.0). Incubations were quenched with ice-cold methanol and products profiled using LC/MS-MS-based lipid mediator profiling. (A) MRM chromatogram of products *m/z* 361 > 263. Arrow denotes retention time of synthetic and authentic $PD1_{n\text{-}3\ DPA}$ (**46**). (B, C) MS-MS spectra employed for identification of products under peaks (B) I and (C) IV. Results are representative of n = 3 incubations.

In the next experiment, 16(*S*),17(*S*)-epoxy-$PD_{n\text{-}3\ DPA}$ (**45**) was incubated with human neutrophils to determine if the intermediate **45** is converted into $PD1_{n\text{-}3\ DPA}$ (**46**) in the presence of neutrophils. The products formed in these incubations were assessed by LC/MS-MS-based profiling. In the multiple reaction monitoring (MRM) chromatogram, one sharp peak at R_T = 13.8 min was observed (Figure 2.6A). The MS-MS fragmentation pattern of this product was consistent with data previously reported for both synthetic and endogenously produced $PD1_{n\text{-}3\ DPA}$ (**46**) (Figure 2.6B).[25,45] Of note, a significantly lower amount of $PD1_{n\text{-}3\ DPA}$ (**46**) was detected when the epoxide (**45**) was incubated with denaturated neutrophils (heated to 100 °C for 1 hour) or incubated in vehicle (Figure 2.6C and D). These results confirm that 16(*S*),17(*S*)-epoxy-$PD_{n\text{-}3\ DPA}$ (**45**) is converted to $PD1_{n\text{-}3\ DPA}$ (**46**), as well as the involvement of an epoxide hydrolase in this biosynthetic step.

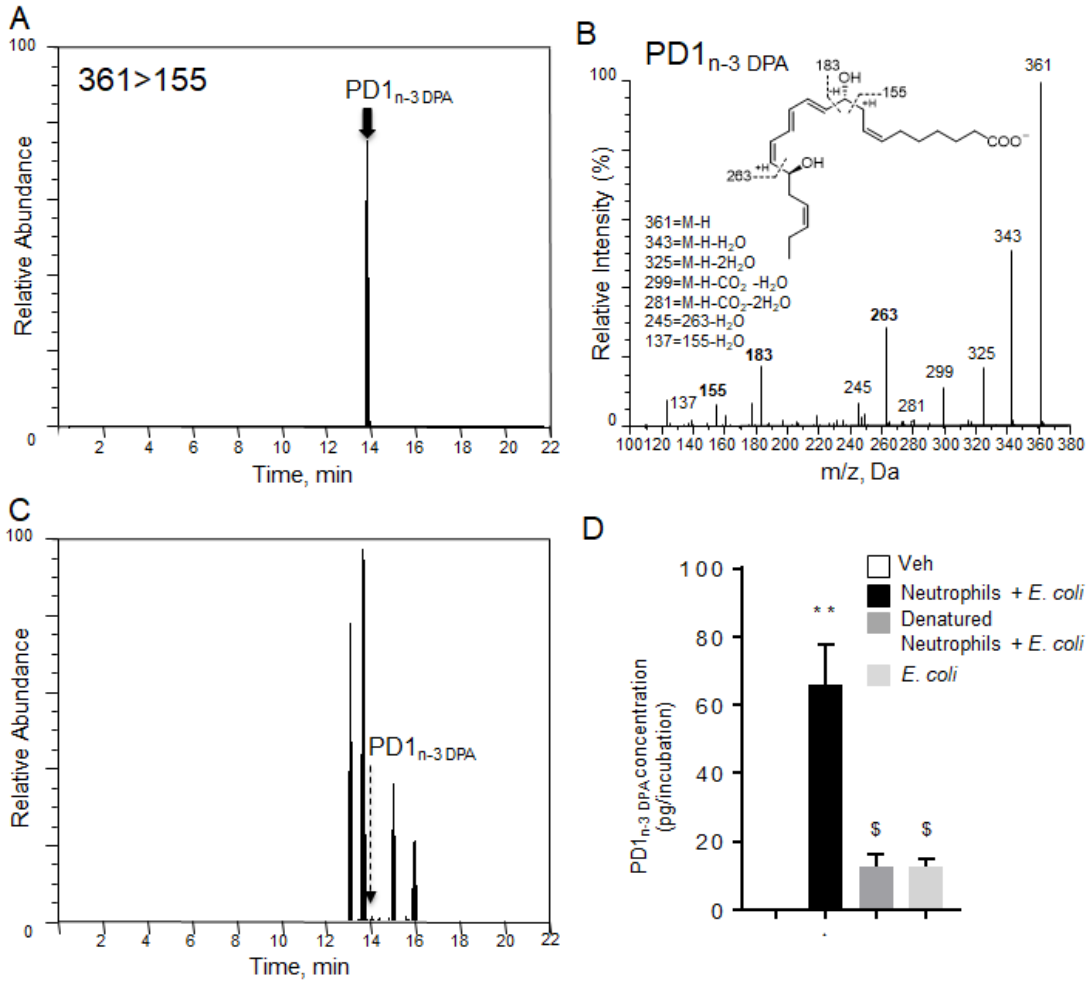

Figure 2.6 16(*S*),17(*S*)-epoxy-PD$_{n\text{-}3\ DPA}$ (**45**) is converted to PD1$_{n\text{-}3\ DPA}$ (**46**) by human neutrophils. 16(*S*),17(*S*)-epoxy-PD$_{n\text{-}3\ DPA}$ (**45**; 10 nM) was incubated with human primary neutrophils (5 x 10^6 cells), human neutrophils previously (5 x 10^6 cells) incubated at 100 °C for 1 h (denatured cells), or PBS. To these incubations, *E. coli* (2.5 x 10^8 CFU/mL) were added and cells incubated for 15 min, 37 °C. Veh denotes solution containing 0.1% EtOH in PBS (A) MRM chromatogram of PD1$_{n\text{-}3\ DPA}$ (**46**) *m/z* 361 > 155. (B) MS-MS spectrum employed for identification of PD1$_{n\text{-}3\ DPA}$ (**46**). (C) MRM chromatogram of products *m/z* 361 > 263. (D) PD1$_{n\text{-}3\ DPA}$ (**46**) concentrations in incubations. Results are representative of n = 4 incubations. ** P < 0.01 vs Veh incubations. $ < 0.05 vs neutrophils + E. coli incubations.

Allylic epoxides such as LTA$_4$ (**10**) and 13(*S*),14(*S*)-epoxy-MaR1 (**30**) have proven to regulate the activity of enzymes that are involved in the biosynthesis of lipid mediators through a suicide inactivation.[51,52] Hence, it was in our interest to examine whether 16(*S*),17(*S*)-epoxy-PD$_{n\text{-}3\ DPA}$ (**45**) shows similar biological activity. The 16(*S*),17(*S*)-PD$_{n\text{-}3\ DPA}$ epoxide's ability to regulate LTB$_4$ (**12**) biosynthesis in human neutrophils was then investigated as illustrated in Figure 2.7. Epoxide **45** dose-dependently reduces LTB$_4$ (**12**) concentrations in human peripheral blood neutrophil incubations with *E.coli*. This activity was also observed at concentrations as low as 0.1 nM. Additionally, the ability of **45** to reduce LTB$_4$ (**12**) production proved to be equivalent to that observed with equimolar concentrations of PD1$_{n\text{-}3\ DPA}$ (**46**), indicating that epoxide **45** is able to potently regulate human leukocyte responses and possesses anti-inflammatory activities.

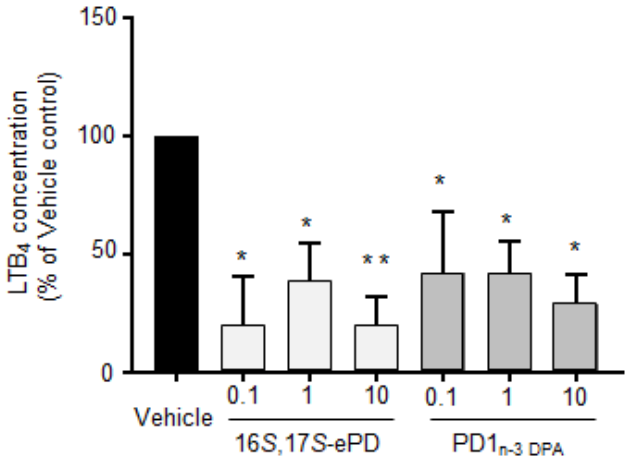

Figure 2.7 16(*S*),17(*S*)-epoxy-PD$_{n\text{-}3\ DPA}$ (**45**) and PD1$_{n\text{-}3\ DPA}$ (**46**) inhibit human neutrophil LTB$_4$ (**12**) production. Human neutrophils (5 x 10^6 cells) were incubated with either **45** or **46** at 0.1, 1 or 10 nM; 37 °C; PBS (pH = 7.45) for 5 min, then with *E. coli* (2.5 x 10^8 CFU/mL) for 30 min. Incubations were quenched and LTB$_4$ (**12**) concentrations determined using lipid mediator profiling. Results are percentage of vehicle incubations. n = 4, *p < 0.05, ** p < 0.01 vs vehicle.

2.3.4 Conclusion

Stereoselective synthesis of the methyl ester **188** was achieved in nine steps (longest linear sequence) and in an overall yield of 22% starting from cycloheptanone (**183**). The results obtained herein provide evidence for the conversion of epoxide **45** to PD1$_{n\text{-}3\ DPA}$ (**46**) by human neutrophils, confirming its role as an intermediate in the biosynthesis of this SPM. We have also established that 15-LOX is involved in the conversion of n-3 DPA (**43**) to **45**. Additionally, 16(*S*),17(*S*)-epoxy-PD$_{n\text{-}3\ DPA}$ (**45**) proved to be equally potent to PD1$_{n\text{-}3\ DPA}$ (**46**) in the regulation of the biosynthesis of the potent chemoattractant LTB$_4$ (**12**).

2.4 Paper IV: Synthesis of 13(*R*)-Hydroxy-7*Z*,10*Z*,13*R*,14*E*,16*Z*,19*Z*-Docosapentaenoic Acid (13*R*-HDPA) and Its Biosynthetic Conversion to the 13-Series Resolvins

Four novel host protective and pro-resolving lipid mediators, RvT1-4 (**59**-**62**), were recently discovered by Dalli, Chiang and Serhan.[53] These interesting SPMs all share a hydroxyl group at C13, as well as the lack of a double bond between C4 and C5. Hence, the n-3 DPA derived compound, 13(*R*)-hydroxy-7*Z*,10*Z*,13*R*,14*E*,16*Z*,19*Z* docosapentaenoic acid (13*R*-HDPA, **58**) was proposed as the intermediate in the biosynthesis of RvT1-4 (**59**-**62**). In this section, the prominent role of 13*R*-HDPA (**58**) as the key intermediate in the biosynthesis of these bioactive lipid mediators **59**-**62** will be disclosed based on results from LC/MS-MS metabololipidomics and the stereoselective synthesis of 13*R*-HDPA (**58**).

2.4.1 Retrosynthetic Analysis of 13*R*-HDPA

A disconnection between C10 and C11, with a *Z*-selective Wittig[30] in mind, will divide the target molecule into two fragments of approximately the same size, namely the ω-3 end **192** and the α-end **177**, as shown in the retrosynthetic analysis depicted in Figure 2.8. The C16-C17 *Z*-double bond in **58** may result from a *Z*-selective semihydrogenation of the corresponding internal alkyne. The resulting fragment **192** from the previous scissoring can in turn be disconnected back to the terminal alkyne **193** and vinyl iodine **194**. In the synthetic direction, this bond may be created by a Sonogashira reaction.[29] Realising that the vinyl iodide **194** may be constructed by a hydrozirconation reaction[54,55] and treatment with iodide, **194** can be taken back to the corresponding alkyne (*R*)-**165**. This alkyne is the same building block used in the synthesis of LTB_4 (**12**), except for opposite stereochemistry at the carbinol carbon, indicating that this fragment can be obtained from the hydroxy lactone (*R*)-**161**. On the other hand, mentally transforming intermediate **193** back to the corresponding alkyne enables a disconnection between C17 and C18, leading back to **195** and **196** as potential precursors.

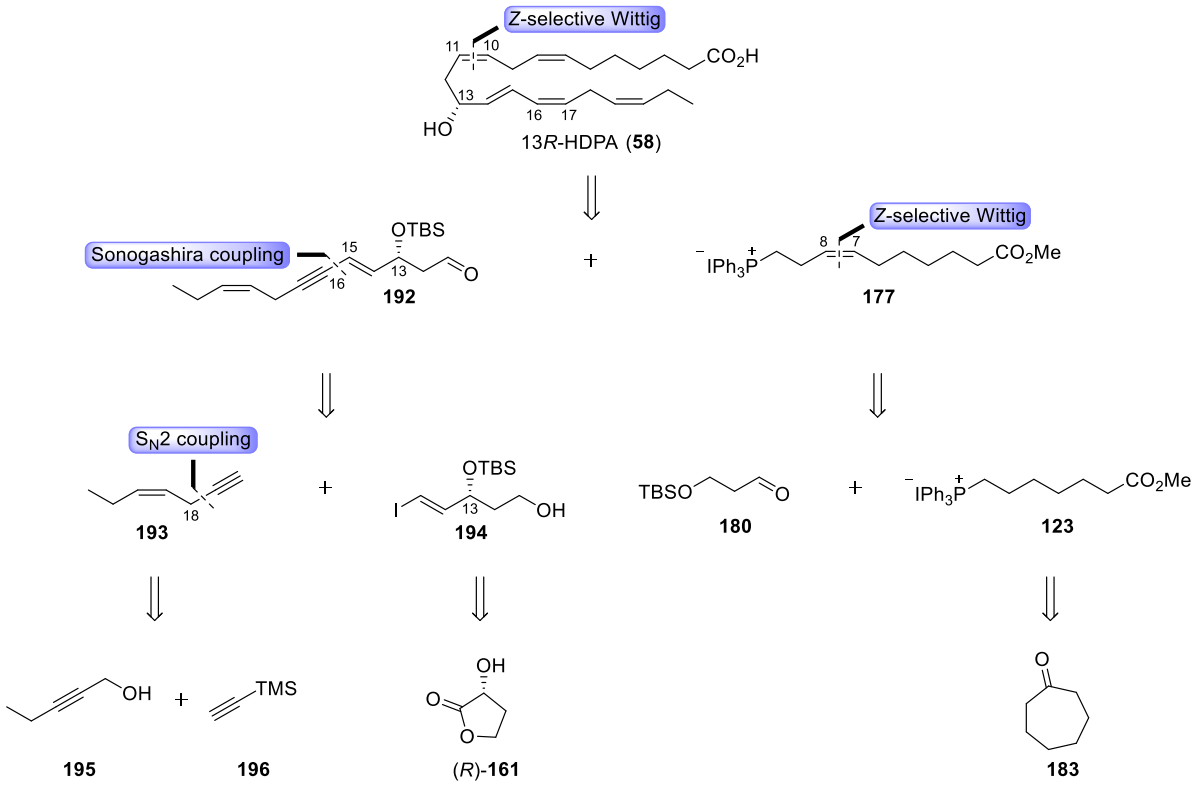

Figure 2.8 Retrosynthetic analysis of 13*R*-HDPA (**58**).

The Wittig salt **177** is the same as the one used in the synthesis of 16(*S*),17(*S*)-epoxy-$PD_{n\text{-}3\ DPA}$ (**45**), which can be prepared from commercially cycloheptanone (**183**) as illustrated in Scheme 2.9

2.4.2 Total Synthesis of 13*R*-HDPA

The synthesis of the terminal alkyne **193** started with the preparation of diyne **198** from commercially available 2-pentyn-1-ol (**195**), as illustrated in Scheme 2.13. Following a literature procedure[56], alcohol **195** was converted into the mesylate **197** and thereafter reacted with TMS-acetylene (**196**) to form diyne **198**. Furthermore, the Lindlar reduction was attempted for the reduction of the internal alkyne in **198**, but no conversion of the starting material was observed. Then, *Z*-selective reduction using P-2 nickel boride (P-2 Ni)[57] was attempted, which successfully reduced the internal alkyne in **198**, affording the desired product **199** in 80% yield. The TMS-protecting group was removed by using TBAF, buffered with acetic acid, as reported by Trost and Pinkerton.[58] Adding acetic acid was essential to avoid isomerisation of the double bond. The terminal alkyne **193** was purified by distillation. This lead to somewhat modest yield. The same fragment has been prepared previously by Trost and Pinkerton,[58] but in our hands this protocol gave a complex mixture, so we decided to abandon this strategy.

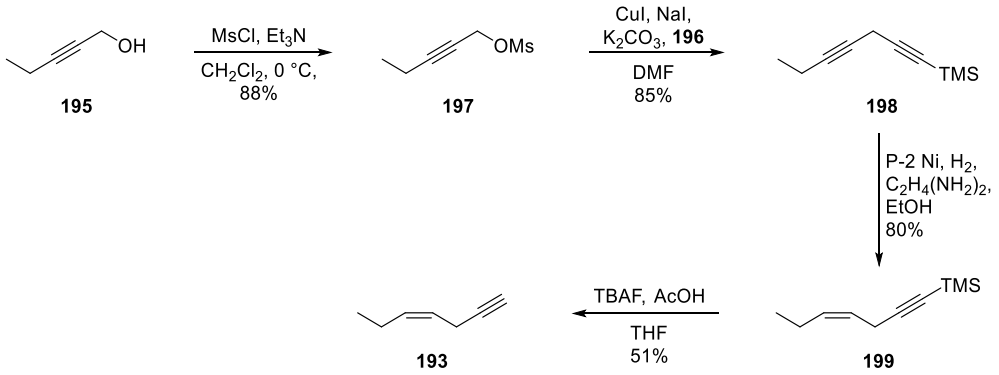

Scheme 2.13 Preparation of the terminal alkyne **193**.

Next, vinyl iodide **194** was prepared in a four-step sequence as outlined in Scheme 2.14. Through the same procedures as described for the same fragment (*S*)-**165** (opposite stereochemistry) in the synthesis of LTB_4 (**12**), alcohol (*R*)-**165** was prepared from (*R*)-α-hydroxy-γ-butyrolactone ((*R*)-**161**). Then, (*R*)-**165** was subjected to an alkyne hydrozirconation,[55,59] followed by adding iodide, which furnished the vinyl iodide **194** in 32% yield over five steps. A Sonogashira cross-coupling reaction[29] was utilized to assemble vinyl iodide **194** and terminal alkyne **193**. The coupling product **200** was obtained in 86% yield. The primary alcohol in **200** was thereafter oxidized by using Dess-Martin Periodinane to the corresponding aldehyde **192** (Scheme 2.14), which was immediately used in the next reaction.

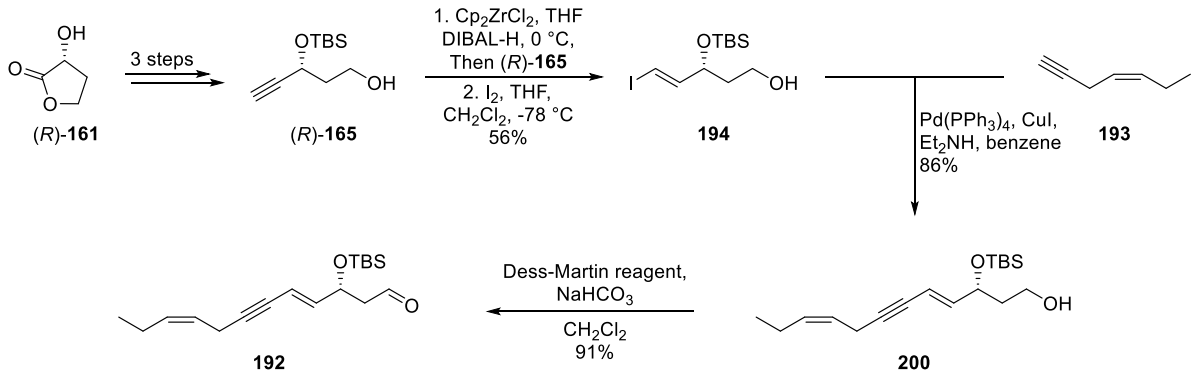

Scheme 2.14 Preparation of key ω-3 fragment **192**.

With the two key fragments in hand, a *Z*-selective Wittig reaction[30] between the ylide of **177** and freshly prepared aldehyde **192** was performed using the conditions disclosed earlier, *i.e* NaHMDS in THF and HMPA at -78 °C. The desired product **201** was obtained in 77% yield and none of the undesired *E*-isomer was detected by ^{1}H and ^{13}C NMR analysis. First, we tried to remove the TBS-protecting group with TBAF, but this gave a mixture of the desired alcohol **202** and a by-product, which we were not able to isolate. Next, *in situ*-generated HCl from AcCl in dry MeOH was attempted, which successfully removed the silyl group without

generating any by-products, affording alcohol **202** in 92% yield. The stereoselective reduction of the internal alkyne in **202** to the corresponding *E*,*Z*-diene **203** was achieved using the Boland reduction protocol[41] with freshly prepared Zn(Cu/Ag) in methanol and water. Finally, saponification of the methyl ester **203** with LiOH in methanol, water and THF at 0 °C, furnished 13*R*-HDPA (**58**) in 87% yield, as shown in Scheme 2.15.

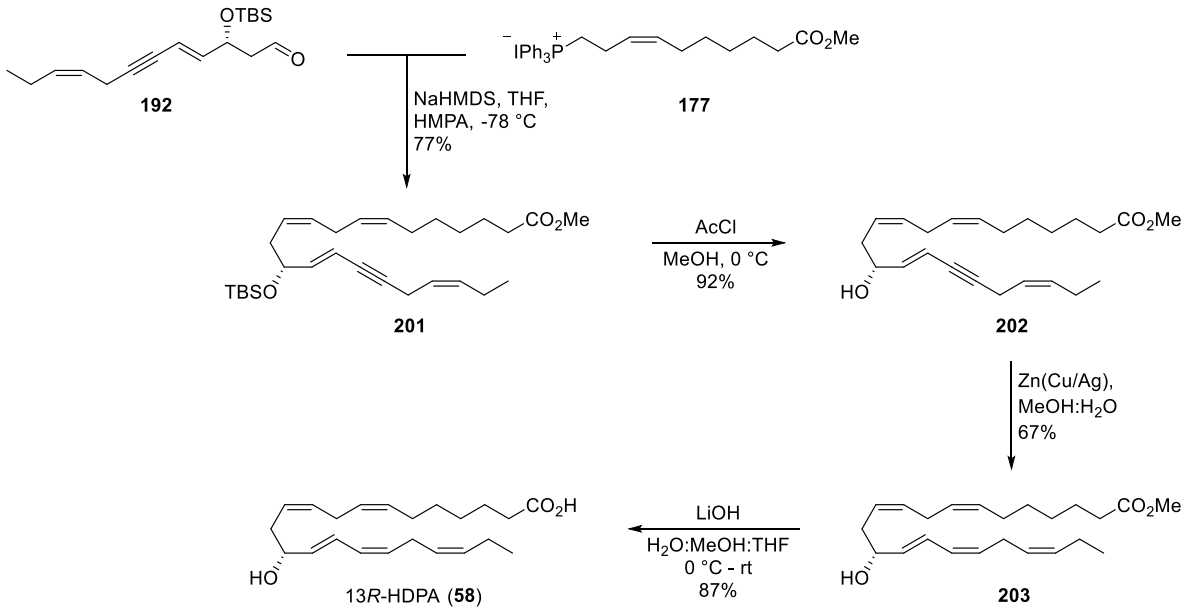

Scheme 2.15 Final steps in the total synthesis of 13*R*-HDPA (**58**).

2.4.3 Matching Experiments and Investigation of the Biosynthesis of the RvTs.

In order to confirm the absolute stereochemistry of 13-HDPA (**58**), matching experiments were conducted during my one-month sojourn in 2016 and in collaboration with Dalli's group at the William Harvey Research Institute in London. MS-MS spectra of 13-HDPA (**58**) from HUVEC incubation, infectious exudates and synthetic material of **58** were recorded to provide evidence for the matching of synthetic 13*R*-HDPA (**58**) and biogenetic material. The three spectra essentially looked identical, containing the same fragmentation pattern with *m*/*z* 327, 301, 283, 223, 205 and 195 (Figure 2.9A-C).

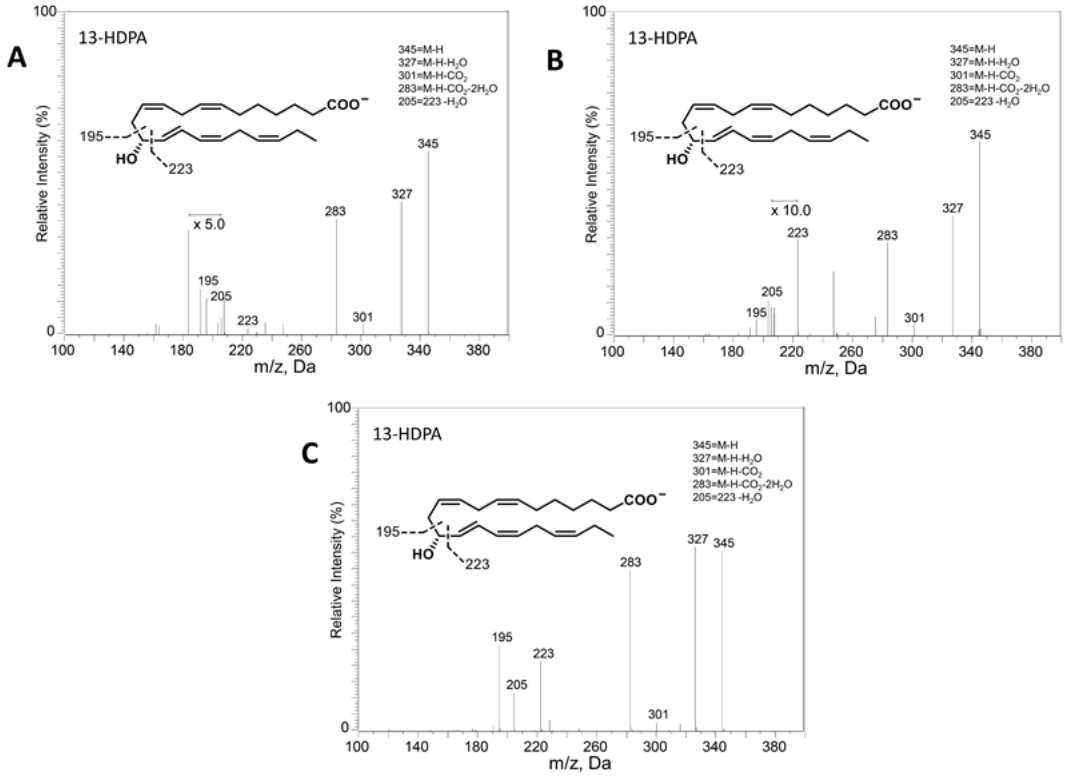

Figure 2.9 MS-MS spectra employed in the identification of 13-HDPA (**58**) from (A) endothelial cells, (B) infectious exudates, and (C) synthetic material. n = 3 endothelial cell donors, n = 3 mouse exudates, and n = 3 for synthetic material.

In Figure 2.10A-C, the peak for biologically generated 13-HDPA (**58**) is shown, and the retention time (R_T) observed is the same in all three multiple reaction monitoring (MRM) chromatograms (R_T = 17.5 min). The biological material was isolated from human umbilical endothelial cells (HUVEC), infectious exudates and human recombinant COX-2 (hrCOX-2). Synthetically prepared 13*R*-HDPA (**58**) eluted at the exact same time (R_T = 17.5 min) as the biological material, as shown in Figure 2.10D. Furthermore, one single peak with R_T at 17.5 min was observed when endogenously produced 13-HDPA (**58**) and synthetic material of **58** were co-injected (Figure 2.10E). The same results were obtained when the samples were run on a chiral HPLC-column, where both the biological and synthetic 13*R*-HDPA (**58**) eluted at 5.1 min (Figure 2.11A-E). COX-2 is not stereospecific, hence small amounts of the *S*-enantiomer were observed in the MRM chromatograms with endogenous isolated material (Figure 2.11).

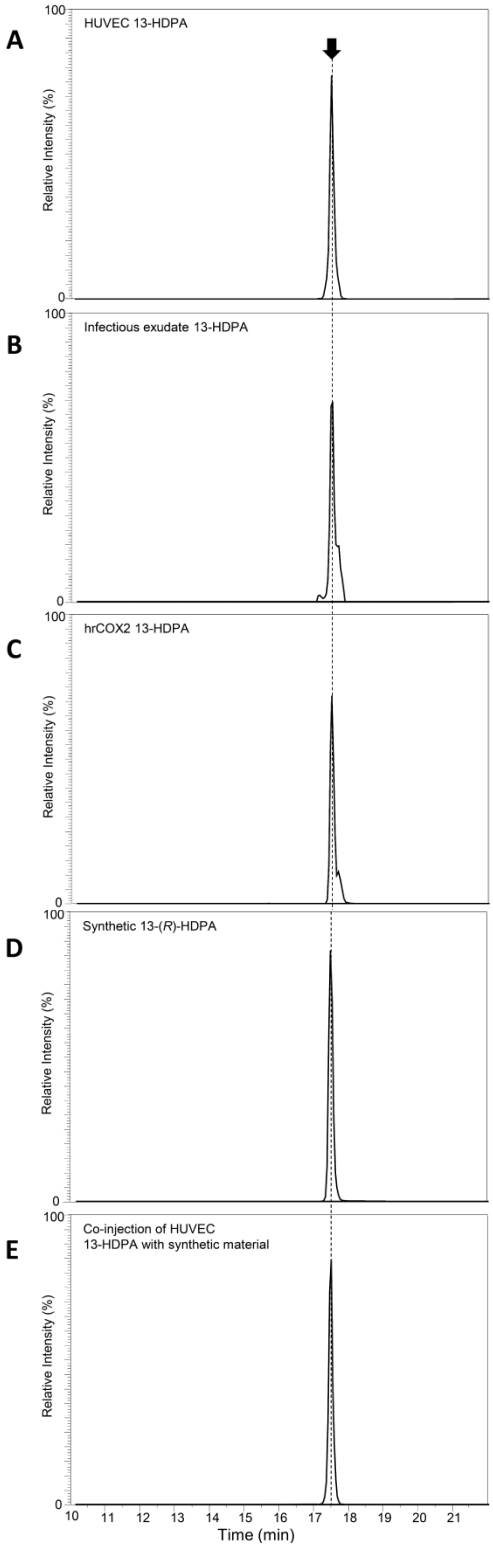

Figure 2.10 13-HDPA (**58**) MRM chromatograms from (A) endothelial cells, (B) infectious exudates, (C) hrCOX-2, and (D) synthetic material of **58**. (E) Co-injection of endothelial and synthetic **58**.

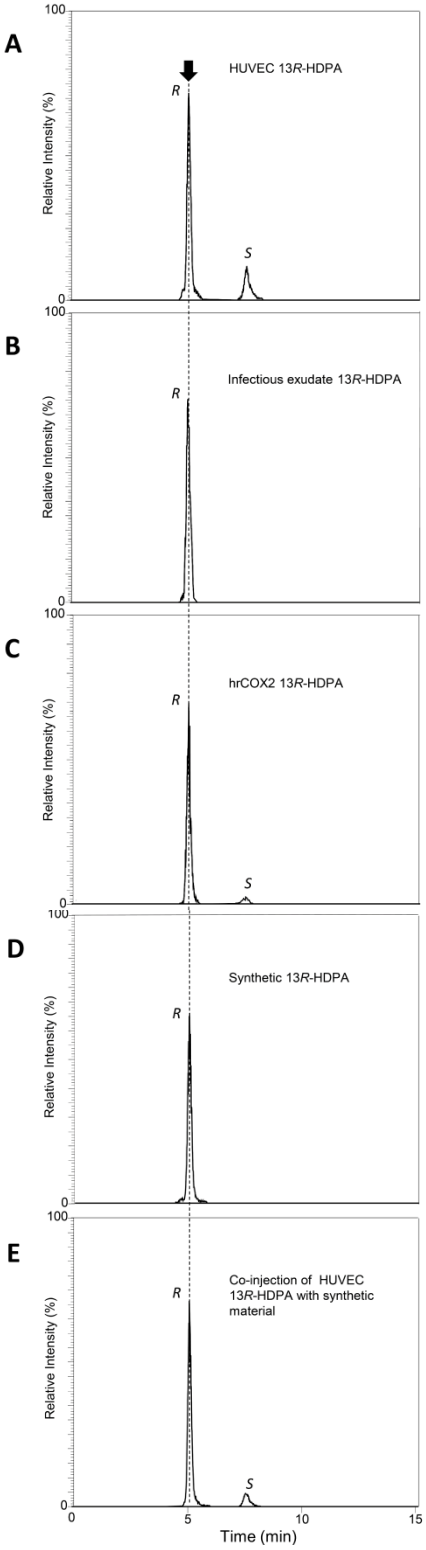

Figure 2.11 13*R*-HDPA (**58**) chiral LC-MS-MS derived from (A) endothelial cells, (B) infectious exudates, (C) hrCOX-2, and (D) synthetic material. (E) Co-injection of endothelial and synthetic 13*R*-HDPA (**58**).

Next, we wanted to investigate whether 13*R*-HDPA (**58**) acts as an intermediate in the biosynthesis of RvT1-4 (**59**-**62**). In this experiment, human neutrophils were isolated from peripheral blood of healthy donors and incubated with synthetic 13*R*-HDPA (**58**) or without. The products formed during this incubation were then profiled using lipid mediator metabololipidomics. In the MRM chromatograms shown in Figure 2.12A, the peaks represent the relative abundance of each of the RvTs (**59**-**62**) from the two incubations. Noteworthy is that the levels of RvT1-4 (**59**-**62**) detected when the neutrophils were incubated without 13*R*-HDPA (**58**) were >75% lower than when 13*R*-HDPA (**58**) was added to the incubation. In Figure 2.12B, the MS-MS spectra employed in the identification of RvT1-4 (**59**-**62**) are shown.

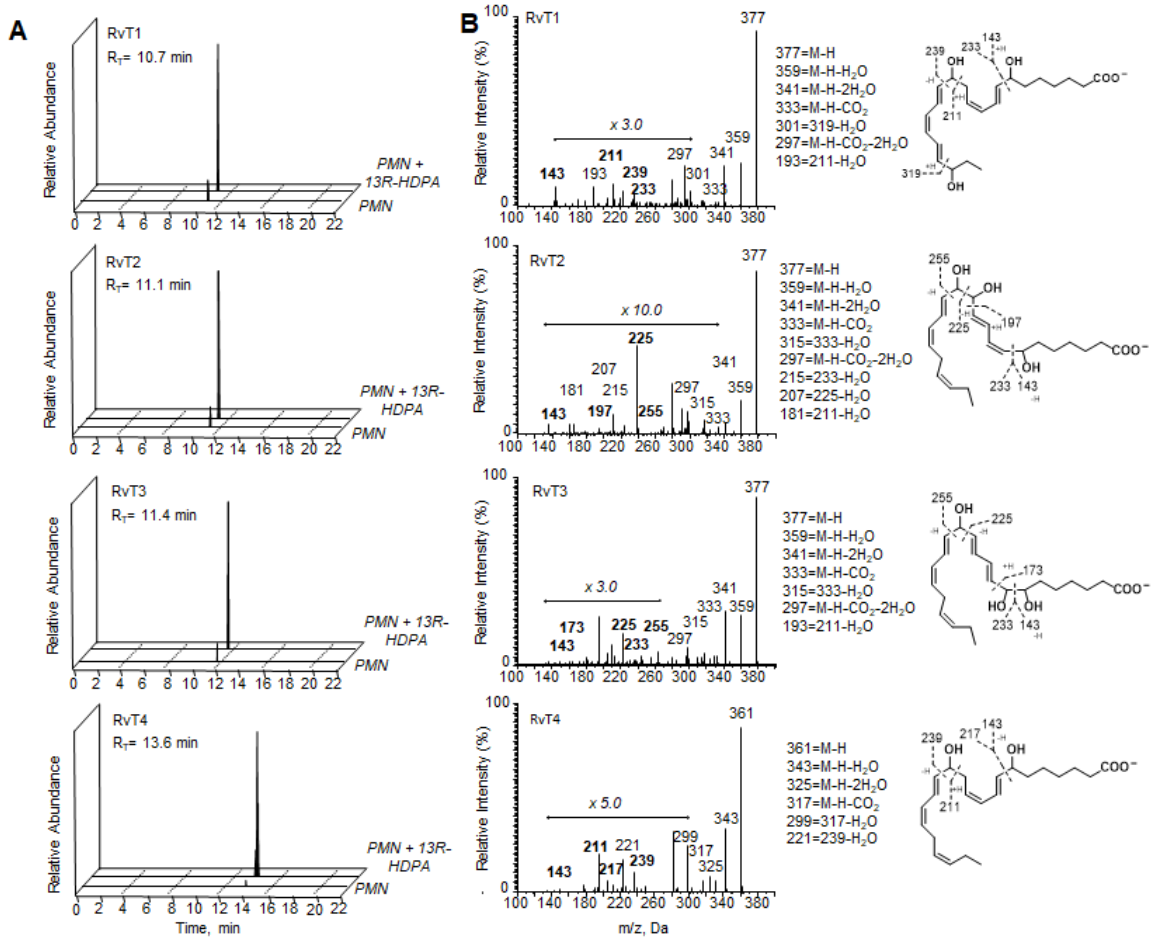

Figure 2.12 Human neutrophils convert 13*R*-HDPA (**58**) to RvT1−4 (**59**-**62**). (A) MRM chromatograms for each of the RvTs with relative abundances to their levels in each of the incubations. (B) MS-MS spectra employed in the identification of RvT1 (**59**), RvT2 (**60**), RvT3 (**61**) and RvT4 (**62**). Results are representative of n = 3 healthy volunteers.

2.4.4 Conclusion

13*R*-HDPA (**58**) was prepared in 16 steps (longest linear sequence), starting from commercially available cycloheptanone (**183**) in 16% overall yield. Synthetic material matched the biological material, confirming the structure of this intermediate. Herein, we also demonstrate that 13*R*-HDPA (**58**) is converted by human neutrophils to the four RvTs (**59-62**), confirming the role of 13*R*-HDPA (**58**) as a key intermediate in the biosynthesis of these novel SPMs, as well as the involvement of COX-2 in the biosynthesis of 13*R*-HDPA (**58**).

2.5 Synthetic Studies Towards RvT3

Four novel lipid mediators produced during the resolution phase of acute inflammation were recently reported.[53] These pro-resolving SPMs were coined 13-series resolvins, namely RvT1 (**59**), RvT2 (**60**), RvT3 (**61**) and RvT4 (**62**). Due to the low amount produced *in vivo*, total synthesis is necessary to prepare sufficient amounts of these bioactive lipid mediators to conduct further biological studies and for the assignment of the absolute configuration of RvT1-4 (**59**-**62**). No synthesis of any of the RvTs have been published so far. This section includes a discussion of the retrosynthetic analysis and the synthetic work towards RvT3 (**61**).

2.5.1 Retrosynthetic Analysis of RvT3

With a Nozaki-Hiyama-Kishi reaction in mind[60-62], a disconnection between C8 and C9 will lead to the two fragments aldehyde **205** and vinyl bromide **204**. With a chiral heteroatom α to the aldehyde, the NHK reaction generally affords the Felkin-Anh product in moderate to good stereoselectivity.[63] In order to ascertain the 1,2-anti relationship depicted in the synthetic material **61**, a two-step approach based on both theoretical and experimental data was chosen. First, density functional theory-calculations performed by Dr. Giacomo Saielli showed that the ^{3}J-coupling **H**-C(OH)-C(OSiEt$_3$)-**H** was 1.0 Hz for the *syn* conformer and 3.7 Hz for the *anti*, thus allowing us to effectively differentiate between the two diastereomers. Furthermore, the absolute configuration on the newly formed carbinol carbon was planned to be confirmed with the reliable Mosher ester analysis.

E-selective reduction of the internal alkyne may construct the double bond between C14 and C15 in **204**. The C13-C14 carbon-carbon bond may in turn be forged by an enantioselective addition of terminal acetylene **206** to aldehyde **149** mediated by Zn(OTf)$_2$ and (-)-*N*-methyl ephedrine.[64] The terminal alkyne **206** can be disconnected back to aldehyde **208** and a suitable Wittig salt, obtained for the commercially available (*Z*)-hex-3-en-ol (**182**). This *Z*-double bond may in a forward direction be created by a *Z*-selective Wittig reaction.[30]

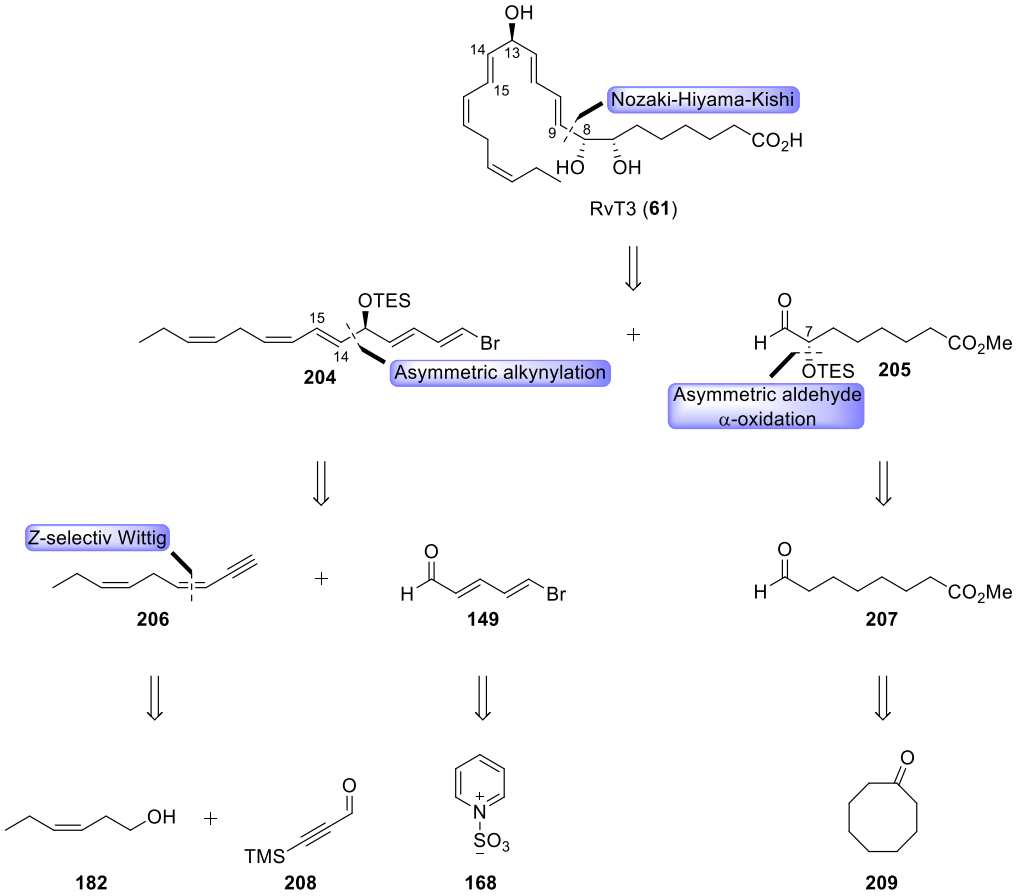

Figure 2.13 Retrosynthetic analysis of RvT3 (**61**).

Identifying that the secondary hydroxyl group in **205** can be generated by an asymmetric α-carbonyl oxidation[65-67] will consequently take **205** back to aldehyde **207**. This aldehyde can be prepared from methyl 8-hydroxyoctanoate (**224**) after one functional group manipulation. Internal cyclisation of ester **224** leads to the corresponding 9-membered lactone, which can be obtained from a Baeyer-Villiger oxidation[48] of commercially available cyclooctanone (**209**).

2.5.2 Synthesis Towards RvT3

The synthetic studies towards RvT3 (**61**) commenced with the preparation of terminal alkyne **206**, as illustrated in Scheme 2.16. First, (*Z*)-hex-3-en-ol (**182**) was converted into Wittig salt **210**, by using the previously disclosed conditions. Wittig salt **210** was then subjected to a Wittig reaction.[30] The conditions used in previous syntheses, utilizing NaHMDS in THF and HMPA, gave a 7:3 ratio of the *Z* and *E* product. We then explored a variety of conditions, listed in Table 2.3. Surprisingly, the best result was obtained using *n*-BuLi at 0 °C (entry 5). At room temperature, the same ratio of the products was observed, but at this temperature, additional by-products were also detected (entry 6). Pure *Z*-product **211** was obtained by column chromatography on silica (pentane).

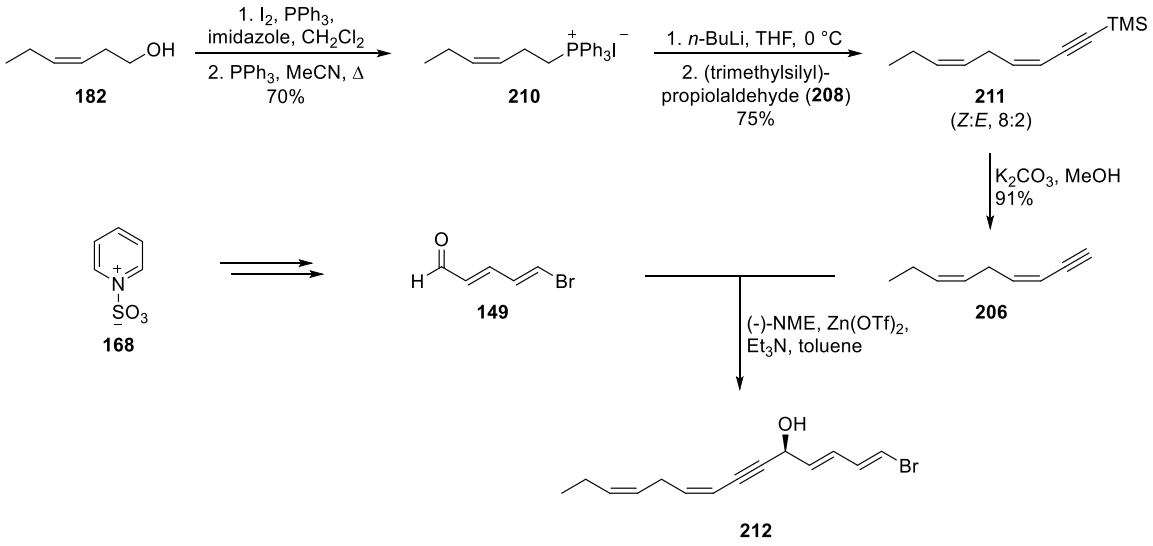

Scheme 2.16 Synthesis of fragment **212**.

Table 2.3 Reaction condition explored the Wittig reaction.

Entry	Reagent	Solvent	Temperature (°C)	Ratio (*Z*:*E*)
1	NaHMDS	THF, HMPA	-78	7:3
2	KHMDS, TMEDA	THF	-78	7:3
3	NaHMDS, 18-crown-6	THF	-78	NA
4	KHMDS, 18-crown-6	THF	-78	NA
5	*n*-BuLi	THF	0	8:2
6	*n*-BuLi	THF	rt.	8:2

Next, removal of the TMS-protecting group was achieved by K_2CO_3 in MeOH, affording **206** in good yield. This terminal acetylene **206** was then asymmetrically added to aldehyde **149**, using the chiral ligand (-)-NME, $Zn(OTf)_2$ and Et_3N, yielding fragment **212**. The first time this reaction was performed on a relatively small scale, the yield was fairly good (60%), but when the same reaction was scaled up, the yield declined drastically to around 20-30%. This problem made it difficult to obtain larger quantities of the product **212**. In addition, this fragment was highly labile and could not be stored for a great extent of time.

Thus, it was important to find suitable conditions for the swift transformation of the internal acetylene in **212** into the corresponding *E*-alkene **221**. In general, olefins of the desired geometrical configuration are available from internal alkynes. A divide does exist, however, as an excess of reliable protocols have been developed for the generation of the corresponding *Z*-isomer (*syn*-addition of hydrogen using heterogeneous and homogeneous metal catalysts,[57,68-70] diimide reduction,[71,72] frustrated-Lewis-pair catalyzed reduction,[73]

activated metals such as Zn(Cu/Ag),[41] et cetera), whereas surprisingly few methods are available for the fundamental transformation of an alkyne to an *E*-alkene.

Dissolving method reduction of alkynes, employing what is often referred to as the Birch reduction conditions,[74] represents a *tried-and-tested* protocol for the production of *E*-olefins from acetylenes. Unfortunately, the reactions conditions are often not suitable for delicate and labile compounds and this effectively limits the scope of application. Several variations involving ruthenium-catalyzed hydrosilylation, followed by proto-desilylation of the resulting vinylsilane, have been developed by the groups of Trost and Fürstner,[75,76] and these methods have also been used in the context of complex natural product synthesis. An example on the use of this methodology is illustrated in Scheme 2.17.[77]

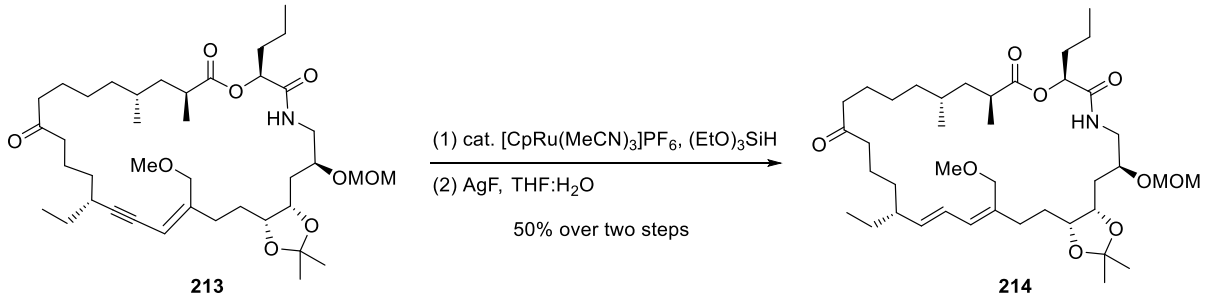

Scheme 2.17 The formation of the *E,E*-diene in **214** by ruthenium-catalysed hydrosilylation and proto-desilylation of the resulting vinylsilane.[77]

A third, and perhaps the most extensively applied method, uses lithium aluminium hydride ($LiAlH_4$) or sodium *bis*(2-methoxyethoxy)aluminumhydride (Red-Al®),[78] and is available for substrates having a suitable functional group (in practice often alcohols or ethers) situated in close proximity to the alkyne. Mechanistically, this works by complexation of aluminium to a heteroatom, intramolecular delivery of a hydride followed by the formation of an alkenylaluminium compound and finally hydrolysis during aqueous workup.

Different protocols involving the ruthenium-catalyzed hydrosilylation followed by proto-desilylation methodology were first attempted. Unfortunately, they all led to elimination of the labile propargylic and allylic hydroxyl group and furnished complex product mixtures in our hands. Following this setback, we contemplated the above-mentioned methods using $LiAlH_4$ or Red-Al®. However, we were wary at the outset given the labile vinyl bromide functionality and the few successful cases of similar transformations are documented in the literature (Scheme 2.18). In the first documented occurrence, a more robust vinyl chloride **215** is present,[79] and in the second example, the alkyne **217** is more electrophilic and reactive due to conjugation with an ester functionality.[80]

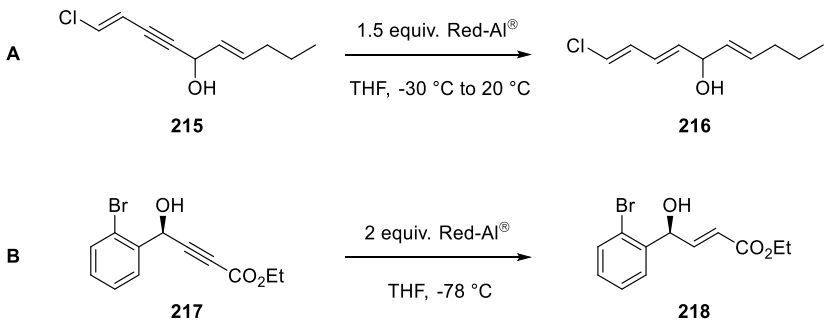

Scheme 2.18 The *E*-selective reduction of internal alkyne in A) vinyl chloride **215** and B) aryl bromide **217**.[79,80]

Indeed, after we had performed a staggering amount of experimentation, our doubt and apprehension were proved right, as considerable amounts of reductive debromination were observed to occur in all cases – even with careful variation and control of stoichiometry, temperature of -78 °C and also addition of sacrificial bromobenzene.

On a more positive note, we did observe reduction of the internal alkyne **212** to the *E*-olefin **221** in the above-mentioned reactions, and after considering the generally accepted mechanism, we realized that the problem occurred from the fact that both reductive reagents, $LiAlH_4$ and Red-Al®, are in the form of activated *ate* complexes. Whereas we needed an aluminium hydride species which only becomes activated *after* it has formed a complex with the hydroxyl moiety. This way, no *ate* complex capable of reducing the vinylbromide should be in close proximity to the labile functionality.

As we were thinking along these lines, DIBAL-H invoked our interest, as it is an *electrophilic* reducing agent which is only activated when forming the mentioned *ate* complex, *after* coordination to a hetereoatom – for example oxygen as in a typical ester reduction. The reagent only has one hydride, however, and complexation with the hydroxyl group followed by the release of hydrogen gas would obviously not be conducive to achieving the desired transformation. It dawned on us immediately that the solution was simply to deprotonate the alcohol moiety prior to the addition of DIBAL-H. In this manner, the reducing agent ought to efficiently bind to the alkoxide, form the activated *ate* complex **219** and thereafter reduce the alkyne in an intramolecular fashion (Figure 2.14).

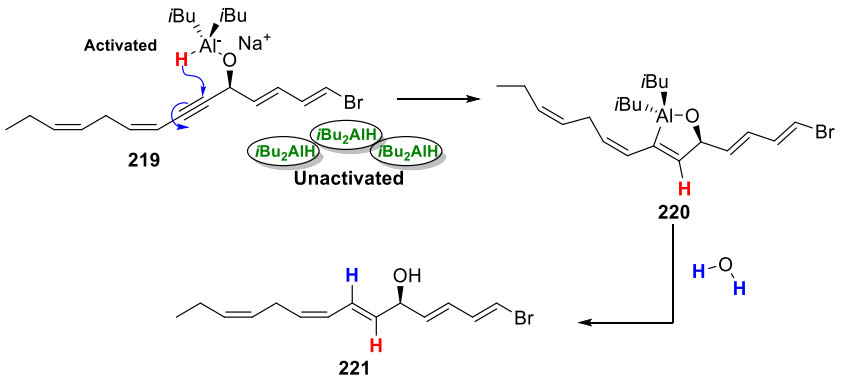

Figure 2.14 Mechanism for the reduction of the internal alkyne in **212** by DIBAL-H.

These predictions did in fact bear out when we attempted this experimentally in the laboratory and the crucial chemoselectivity between the acetylene and vinyl bromide functionality was as planned and hoped (Scheme 2.19).

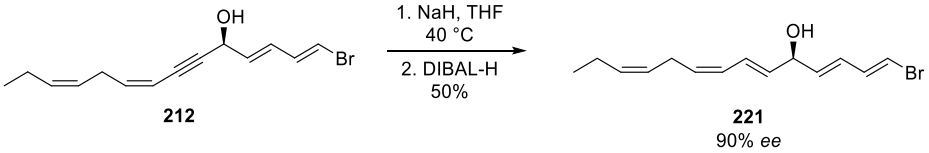

Scheme 2.19 The *E*-selective reduction of the internal alkyne in **212** by DIBAL-H.

The isolated yield for the transformation illustrated above was 50%, and examination of the crude product mixture revealed unreacted starting material as well as decomposed material, presumably due to the instability of the propargylic alcohol. To confirm the *S*-configuration of the newly constructed carbinol Mosher ester analysis was carried out. From these results, we also determined the %*ee* to be 90%. Indeed, when applying this protocol on more robust compounds such as **222**, high yields were observed (Scheme 2.20).

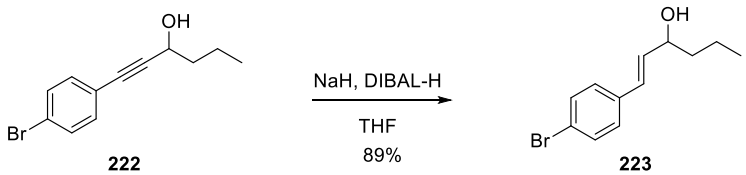

Scheme 2.20 The *E*-selective reduction of the internal alkyne in **222** by DIBAL-H.

A literature search was performed in order to check the novelty of the developed procedure, and while numerous examples of hydroalumination of alkynes are reported, only one example was found using DIBAL-H for the reduction of internal alkynes to the

corresponding *E*-alkene. In this procedure 10 equivalents of DIBAL-H was used and the reaction mixture was refluxing in THF for 15 hours, resulting in a yield of only 38%.[81] In addition, several examples were found where DIBAL-H was premixed with n-butyllithium, forming an *ate* complex reagent which presumably functions in a similar manner as $LiAlH_4$. None of the identified substrates contained a vinyl halide moiety.[82,83]

After we found a suitable method for the reduction of the internal alkyne in fragment **212**, the secondary alcohol in **221** was protected with a TES-group, affording **204** in 85% yield.

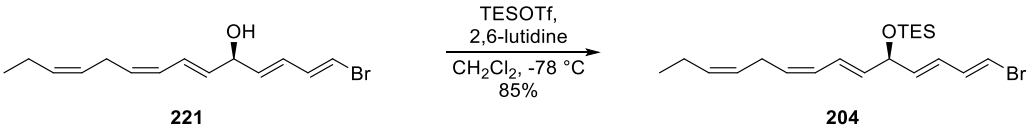

221 **204**

Scheme 2.21 Preparation of vinyl bromide **204**.

Next, we began investigations towards the synthesis of aldehyde **207**, needed for the synthesis of the key α-hydroxy-aldehyde **205** intended for the Nozaki-Hiyama-Kishi reaction (Scheme 2.22).[60-62] Aldehyde **207** was prepared by the following sequence: cyclooctanone (**209**) was converted to the lactone in a Baeyer-Villiger reaction,[48] followed by ring-opening of the lactone, catalysed by H_2SO_4 in methanol, affording hydroxy methyl ester **224**. The primary alcohol in **224** was subsequently oxidized to the corresponding aldehyde **207** by Dess-Martin periodinane. When this work started, a literature search of aldehyde **207** revealed that this aldehyde can be prepared in a more step-efficient and higher yielding way by ozonolysis of *cis*-cyclooctene **227** (Scheme 2.23),[84,85] but we were not able to use this protocol due to the lack of a ozonolysis apparatus.

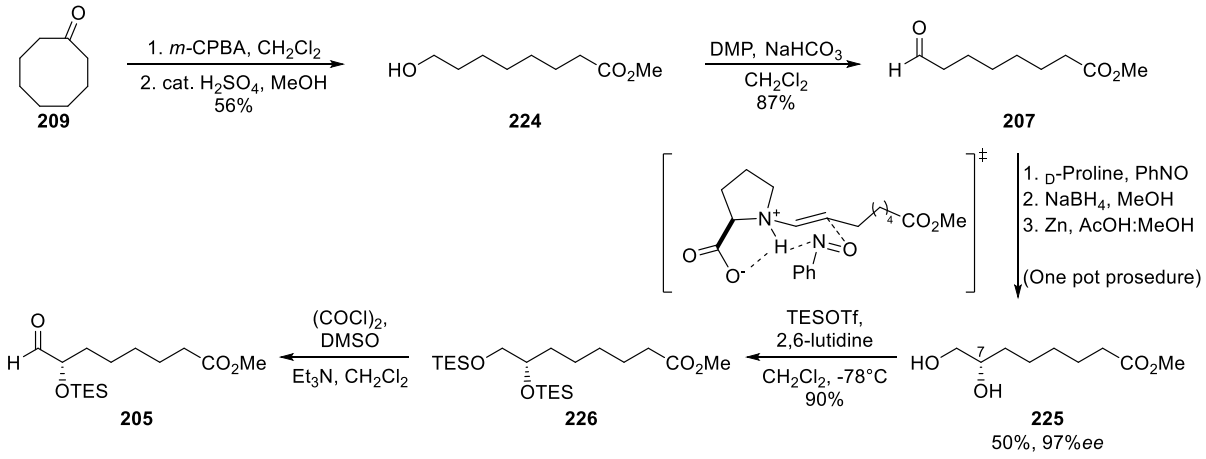

209 **224** **207**

205 **226** **225**
50%, 97%*ee*

Scheme 2.22 preparation of aldehyde **205**.

The asymmetric α-aminoxylation of aldehyde **207** was accomplished by using chiral D-proline and nitrosobenzene. The aldehyde in the resulting product was reduced by adding $NaBH_4$, followed by N-O cleavage, which gave diol **225** in 50% and 97% *ee*, as illustrated in Scheme 2.22. The measured optical rotation was very close to the literature value,[86] confirming the conformation of C7 to be *S*. Since our work on the enantioselective organocatalytic α-oxidation, a recent investigation has found that the corresponding potassium and tetrabutylammonium prolinate salts are more efficient catalysts, thus enabling shorter reaction time, lower catalyst loading, as well as affording both higher yields and %*ee*.[87]

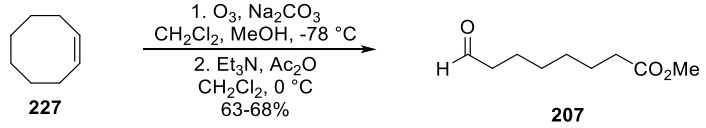

Scheme 2.23 An alternative way to prepare aldehyde **207**.[84,85]

Both hydroxyl groups were then protected with TES-groups, knowing that selective oxidation of the primary hydroxy group can be achieved under the Swern conditions.[17,88] This worked well the first time, but unexpectedly, we were not able to reproduce these results at a later stage. We observed the desired product, but in all the later attempts, an inseparable by-product was present as well.

Before time ran out, we were able to do one test-reaction with the Nosaki-Hiyama-Kishi reaction.[60-62] Since we could not prepare large amounts of vinyl bromide **204**, we decided to use a more stable and easily prepared vinyl bromide such as **228** in the first attempt. This lead to 58% yield of a 2:1 mixture of the two diastereomers **229** and **230**, show in Scheme 2.24.

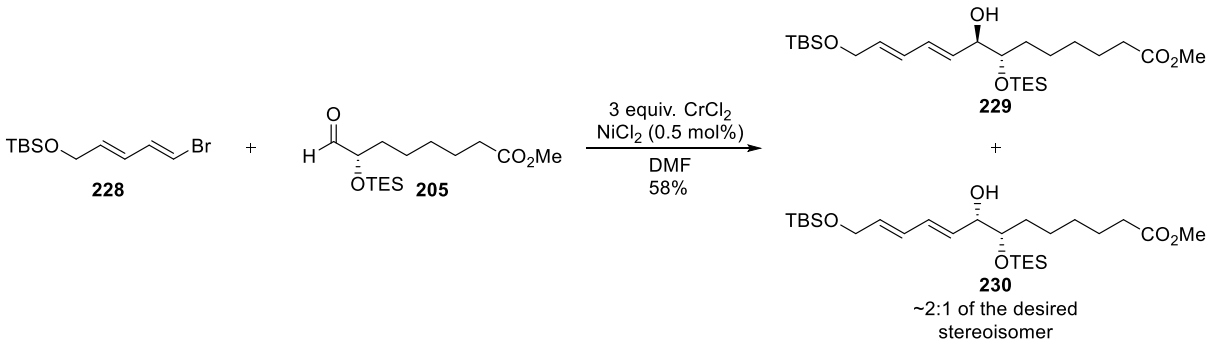

Scheme 2.24 Test-reaction of the Nozaki-Hiyama-Kishi reaction.

Chapter 3

3 Summary and Future Perspectives

This thesis contains efforts concerning the synthesis of the pro-inflammatory lipid mediator LTB_4 (**12**). This lipid mediator was synthesized in ten steps in an overall yield of 5% and no HPLC purification was needed.

Protocols for the asymmetric reduction of oxo methyl esters **157a-c** to the corresponding 5-(*S*)-HETE (**7**), 5-(*S*)-HEPE (**8**) and (+)-zooxanthellactone (**115c**) was developed. The products of the latter were obtained in up to 79% *ee* by the use of CBS catalyst **158**.

We were also interested in investigating the biosynthetic pathway of both the novel identified RvTs (**59**-**62**) and the n-3 DPA-derived SPM, $PD1_{n\text{-}3\ DPA}$ (**46**). Hence, the proposed intermediates in these biosynthetic pathways were synthesised, namely the 13*R*-HDPA (**58**) and 16(*S*),17(*S*)-epoxy-$PD_{n\text{-}3\ DPA}$ (**45**). Matching and biological experiments were undertaken by our collaborators in the Dalli group and in the experiments regarding 13*R*-HDPA (**58**), I had the honour to participate in the execution of the experiments as a visitor in his group.

Additionally, the synthetic work towards the potent pro-inflammatory lipid mediator, RvT3 (**61**), has been initiated, and the progression hitherto is described herein. At this point, we have encountered a few obstacles in the strategy chosen towards the target molecule **61**, which has halted the progress. Luckily, in synthetic organic chemistry, there is rarely only one route to the target molecule. As we were not able to reproduce the Swern oxidation of the diTES fragment **226**, the diol **225** can be protected with other silyl groups, *i.e.* TBS, which would allow selective deprotection of the primary TBS group followed by oxidation of the resulting primary alcohol in **232**,[89,90] as illustrated in Scheme 3.1.

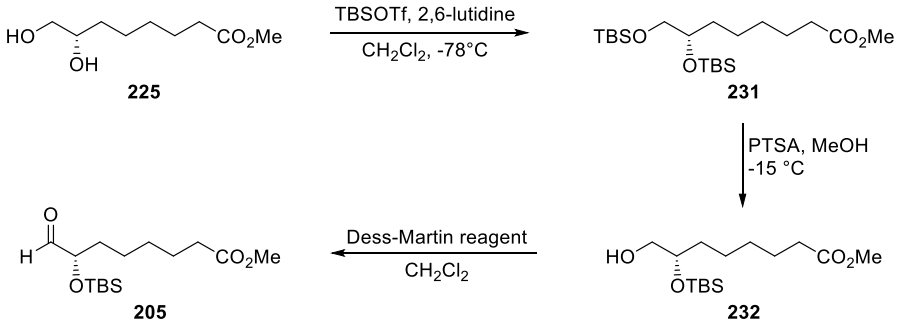

Scheme 3.1 Alternative preparation of aldehyde **205**.

A possible solution to the problem concerning the low yield observed for vinyl bromide **212** is to prepare the fragment by racemic alkynylation, which hopefully will proceed in better yield and then either do an oxidation of the secondary alcohol followed by asymmetric reduction to the desired product or to perform a racemate resolution (Scheme 3.2). In this case the Noyori asymmetric hydrogenation should be the first choice, as this protocol usually reduces propargylic ketones with high stereoselectivity.[91]

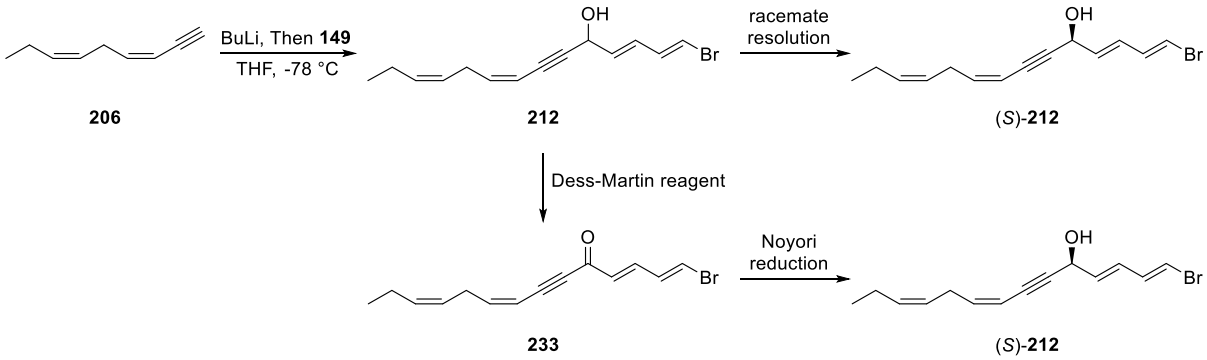

Scheme 3.2 Two alternative preparations of vinyl bromide **212**.

Furthermore, to confirm the structure and stereochemistry of the remaining RvTs (**59**, **60** and **62**), total synthesis and matching experiments are necessary. For example, making the mentioned disconnections between C9 and C10, as well as C16 and C17 of RvT2 (**60**), will lead back to the following fragments: the ω-end **234**, the α-end **235** and aldehyde **238**, which can be obtained from commercially available D-threono-1,4-lactone (**242**) and ylide **179**. The α-end **235** may in turn be prepared from cycloheptanaone (**183**) and terminal acetylene **240** (Figure 3.1).

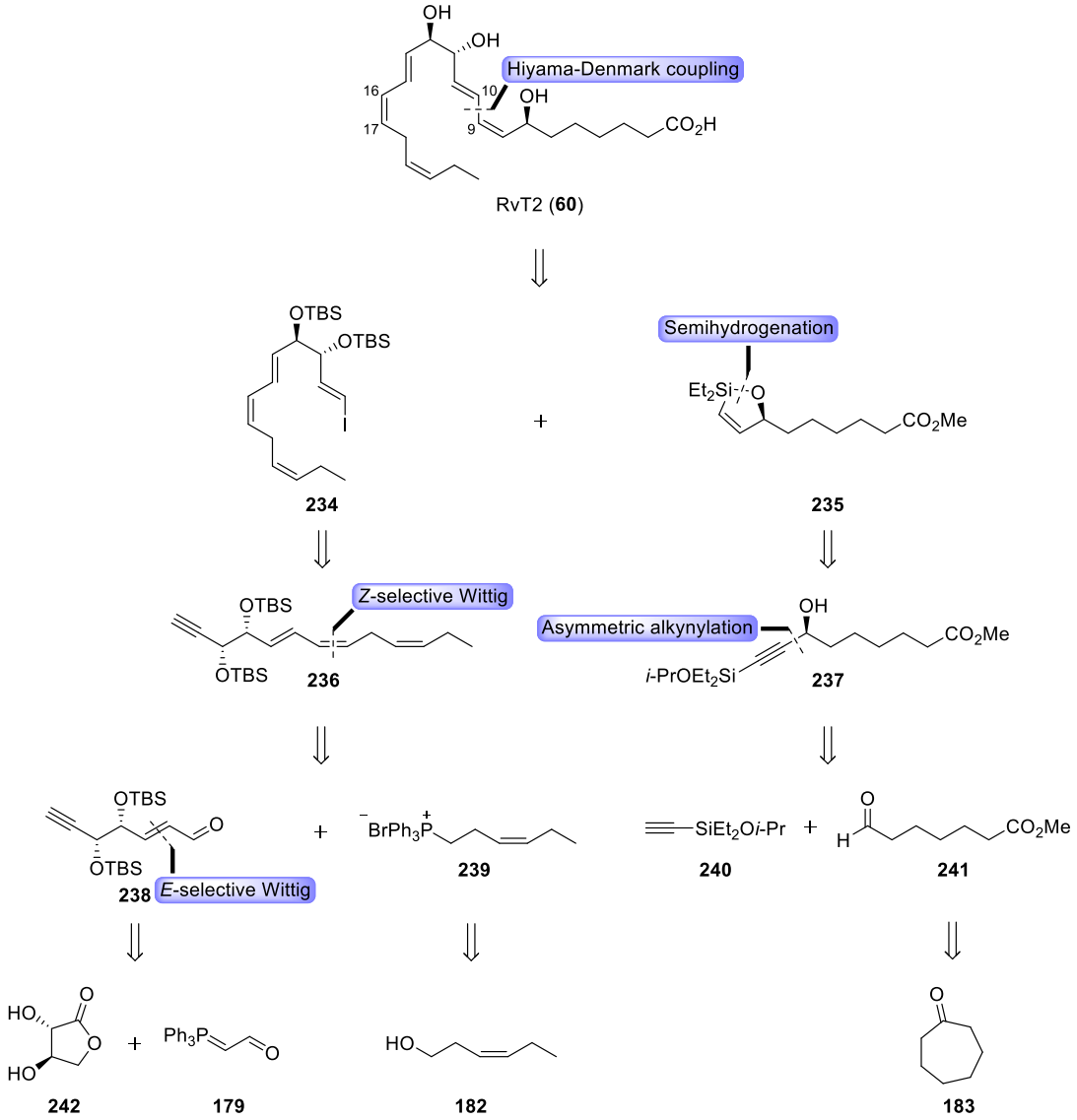

Figure 3.1 Retrosynthetic analysis of RvT2 (**60**)

Considering that the epoxide precursors of protectins and maresins are converted to potent pro-resolving and tissue-protecting sulfido-conjugated mediators,[92,93] it is highly likely that also the 16(*S*),17(*S*)-epoxy-$PD_{n\text{-}3\ DPA}$ (**45**) can be subjected to the same transformation, as illustrated in Scheme 3.3. Thus, it should be possible to convert this epoxide **45** to the corresponding sulfido-conjugates **243-245** by previously established methods[94] to provide material for biological evaluation and the identification of new pro-resolving agents.

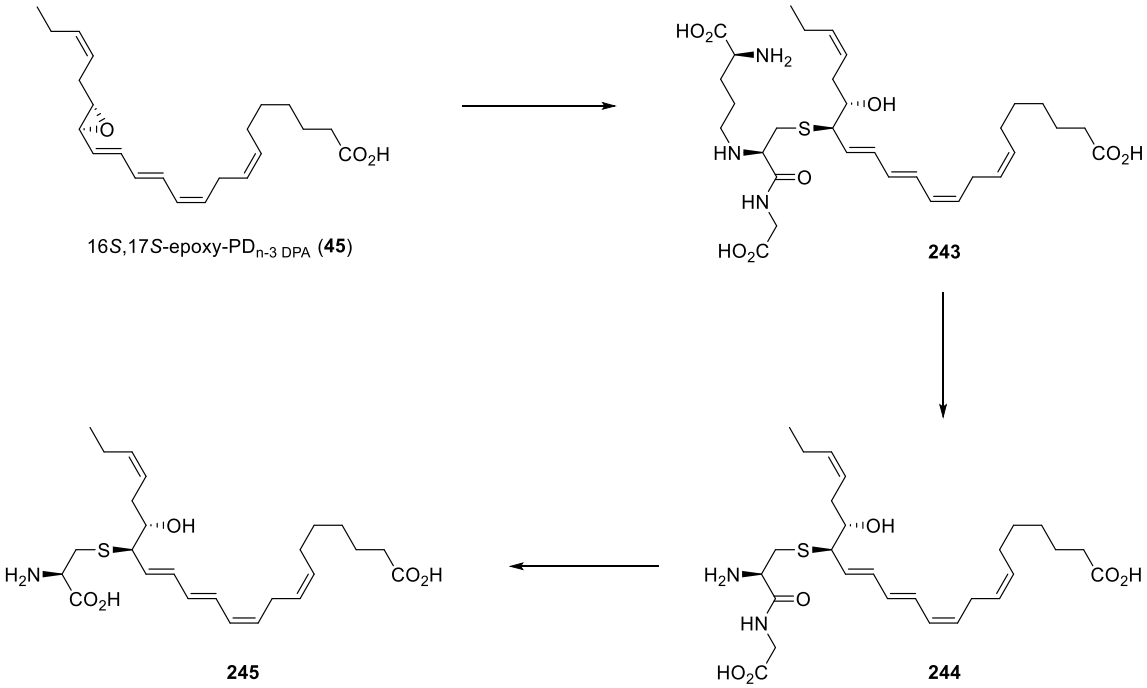

Scheme 3.3 Proposed biosynthesis of the 16(*S*),17(*S*)-epoxy-$PD_{n\text{-}3\ DPA}$ derived CTRs (**243**-**245**).

Chapter 4

4 Conclusion

Since the discovery of the classic eicosanoids, prostaglandins, leukotrienes and lipoxins during the 20th century, immense efforts have been dedicated to understand the course of inflammation where these lipid mediators participate. Through the pioneering work in this field, headed by Charles N. Serhan, several novel anti-inflammatory SPMs derived from EPA (**2**), DHA (**3**), n-3 DPA (**43**) have been identified, as well as an extensive understanding of the inflammatory process. This new class of lipid mediators provide the basis for medicinal chemistry programs towards the development of novel anti-inflammatory drugs using immunoresolvents as biotemplates. If successful, these efforts may result in the development of new strategies for treating infections and chronic inflammatory diseases. However, such efforts will only be successful if the detailed biosynthetic pathways of the SPMs are determined, as well as performing structural assignment for each individual SPM.

In this thesis, the total synthesis of the pro-inflammatory lipid mediator LTB_4 (**12**) is reported. An asymmetric protocol was developed for the preparation of 5-(*S*)-HETE (**7**), 5-(*S*)-HEPE (**8**) and (+)-zooxanthellactone (**115c**). In addition, our efforts towards the synthesis the potent pro-resolving SPM, RvT3 (**61**) are reported herein.

Furthermore, as mentioned above, it is of considerable interest to investigate the biosynthetic pathways of the SPMs. Hence, the work concerning the preparation of the intermediates **45** and **58** in the biogenesis of $PD1_{n\text{-}3\ DPA}$ (**46**) and RvTs (**59**-**62**) is presented herein.

References

1. R. Kogure.; K. Toyama.; S. Hiyamuta.; I. Kojima.; S. Takeda, *Biochem. Biophys. Res. Commun.*, 2011, **416**, 58-63.
2. D. Y. Oh.; S. Talukdar.; E. J. Bae.; T. Imamura.; H. Morinaga.; W.-Q. Fan.; P. Li.; W. J. Lu.; S. M. Watkins.; J. M. Olefsky, *Cell*, 2010, **142**, 687-698.
3. K. Yamamoto.; T. Itho.; D. Abe.; M. Shimizu.; T. Kanda.; T. Koyama.; M. Nishikawa.; T. Tamai.; H. Ooizumi.; S. Yamada, *Bioorg. Med. Chem. Lett.*, 2005, **15**, 517-522.
4. P. Sapieha.; A. Stahl.; J. Chen.; M. R. Seaward.; K. L. Willett.; N. M. Krah.; R. J. Dennison.; K. M. Connor.; C. M. Aderman.; E. Liclican.; A. Carughi.; D. Perelman.; Y. Kanaoka.; J. P. San Giovanni.; K. Gronert.; L. E. H. Smith, *Sci. Transl. Med.*, 2011, **3**, 1-12.
5. E. J. Corey.; J. O. Albright.; A. E. Barton.; S. Hashimoto, *J. Am. Chem. Soc.*, 1980, **102**, 1435-1436.
6. E. J. Corey.; S.-I. Hashimoto, *Tetrahedron Lett.*, 1981, **22**, 299-302.
7. R. Zamboni.; J. Rokach, *Tetrahedron Lett.*, 1983, **24**, 999-1002.
8. K. C. Nicolaou.; T. Ladduwahetty.; I. M. Taffer.; R. E. Zipkin, *Synthesis*, 1986, **4**, 344-347.
9. T. Shimazaki.; Y. Kobayashi.; F. Sato, *Chem. Lett.*, 1988, 1785-1788.
10. S. Gueugnot.; M. Alami.; G. Linstrumelle.; L. Mambu.; Y. Petit.; M. Larchevêque, *Tetrahedron*, 1996, **52**, 6635-6646.
11. R. Tyagi.; B. Shimpukade.; S. Blättermann.; E. Kostenis.; T. Ulven, *Med. Chem. Commun*, 2012, **3**, 195-198.
12. D. V. Kuklev.; W. L. Smith, *Chem. Phys. Lipids*, 2004, **130**, 145-158.
13. T. Itho.; N. Yoshimoto.; K. Yamamoto, *Heterocycles*, 2010, **80**, 689-695.
14. T. Itoh.; I. Murota.; K. Yoshikai.; S. Yamada.; K. Yamamoto, *Bioorg. Med. Chem.*, 2006, **14**, 98-108.
15. A. K. Holmeide.; L. Skattebøl.; M. Sydnes, *J. Chem. Soc., Perkin Trans. 1*, 2001, 1942-1946.
16. E. J. Corey.; J. O. Albright.; A. E. Barton.; S. Hashimoto, *J. Am. Chem. Soc.*, 1980, **102**, 1435-1436.
17. K. Omura.; D. Swern, *Tetrahedron*, 1978, **34**, 1651-1660.
18. E. J. Corey.; C. J. Helal, *Angew. Chem. Int. Ed.* , 1998, **37**, 1986-2012.
19. A. Rodriguez.; M. Nomen.; B. W. Spur.; J.-J. Godfroid, *Eur. J. Org. Chem.*, 1999, 2655-2662.
20. K. Fujiwara.; H. Tsukamoto.; M. Izumikawa.; T. Hosoya.; N. Kagaya.; M. Takagi.; H. Yamamura.; M. Hayakawa.; K. Shin-ya.; T. Doi, *J. Org. Chem.*, 2015, **80**, 114-132.
21. J. E. Baldwin, *J. Chem. Soc., Chem. Commun.*, 1976, DOI: 10.1039/c39760000734, 734-736.
22. M. G. Jakobsen.; A. Vik.; T. V. Hansen, *Tetrahedron Lett.*, 2014, **55**, 2842-2844.
23. B. Samuelsson, *J. Biol. Chem.*, 2012, **287**, 10070-10080.
24. M. Aursnes.; J. E. Tungen.; A. Vik.; J. Dalli.; T. V. Hansen, *Org. Biomol. Chem*, 2014, **12**, 432-437.
25. M. Aursnes.; J. E. Tungen.; A. Vik.; R. Colas.; C.-Y. C. Cheng.; J. Dalli.; C. N. Serhan.; T. V. Hansen, *J. Nat. Prod.*, 2014, **77**, 910-916.
26. J. E. Tungen.; M. Aursnes.; J. Dalli.; H. Arnardottir.; C. N. Serhan.; T. V. Hansen, *Chem. Eur. J.*, 2014, **20**, 14575-14578.
27. J. E. Tungen.; M. Aursnes.; T. V. Hansen, *Tetrahedron Lett.*, 2015, **56**, 1843-1846.

28. M. Aursnes.; J. E. Tungen.; A. Vik.; S. Ramon.; R. A. Colas.; J. Dalli.; C. N. Serhan.; T. V. Hansen, *J. Nat. Prod.*, 2014, **77**, 2241-2247.
29. K. Sonogashira.; Y. Tohda.; N. Hagihara, *Tetrahedron Lett.*, 1975, 4467-4470.
30. G. Wittig.; U. Schöllkopf, *Chem. Ber.*, 1954, **97**, 1318-1330.
31. Y. Nagao.; Y. Hagiwara.; T. Kumagai.; M. Ochiai.; T. Inoue.; K. Hashimoto.; E. Fujita, *J. Org. Chem.*, 1986, **51**, 2391-2393.
32. E. W. Colvin.; B. J. Hamill, *J. Chem. Soc., Chem. Commun.*, 1973, DOI: 10.1039/c39730000151, 151-152.
33. T. Tsuda.; T. Hayashi.; H. Satomi.; T. Kawamoto.; T. Saegusa, *J. Org. Chem.*, 1986, **51**, 537-540.
34. W. S. Mahoney.; D. M. Brestensky.; J. M. Stryker, *J. Am. Chem. Soc.*, 1988, **110**, 291-293.
35. T. Hudlicky.; G. Sinai-Zingde.; M. G. Natchus, *Tetrahedron Lett.*, 1987, **28**, 5287-5290.
36. J. Becher, *Org. Synth.*, 1979, **59**, 79-84.
37. D. Soullez.; G. Ple.; L. Duhamel, *J. Chem. Soc., Perkin Trans. 1*, 1997, 1639-1645.
38. M. Romero-Ortega.; D. A. Colby.; H. F. Olivo, *Tetrahedron Lett.*, 2002, **43**, 6439-6441.
39. R. Tello-Aburto.; A. Ochoa-Teran.; H. F. Olivo, *Tetrahedron Lett.*, 2006, **47**, 5915-5917.
40. S. V. Naidu.; P. Gupta.; P. Kumar, *Tetrahedron*, 2007, 7624-7633.
41. W. Boland.; N. Schroer.; C. Sieler.; M. Feigel, *Helv. Chim. Acta*, 1987, **70**, 1025-1040.
42. W. Boland.; S. Pantke, *J. Prakt. Chem.*, 1994, **336**, 714-715.
43. C. N. Serhan.; N. A. Petasis, *Chem. Rev.* , 2011, **111**, 5922-5943.
44. M. Aursnes.; J. E. Tungen.; R. A. Colas.; I. Vlasakov.; J. Dalli.; C. N. Serhan.; T. V. Hansen, *J. Nat. Prod.*, 2015, **78**, 2924-2931.
45. J. Dalli.; R. A. Colas.; C. N. Serhan, *Sci Rep*, 2013, **3**, 1940.
46. A. Vik.; J. Dalli.; T. V. Hansen, *Bioorg. Med. Chem. Lett.*, 2017, **27**, 2259-2266.
47. T. Katsuki.; K. B. Sharpless, *J. Am. Chem. Soc.*, 1980, **102**, 5974-5976.
48. A. Baeyer.; V. Villiger, *Ber. Dtsch. chem. Ges.*, 1899, **32**, 3625-3633.
49. K. Kai.; J. Takeuchi.; T. Kataoka.; M. Yokoyama.; N. Watanabe, *Tetrahedron*, 2008, **64**, 6760-6769.
50. R. Appel, *Angew. Chem.*, 1975, **87**, 863-874.
51. B. Caliskan.; E. Banoglu, *Expert Opin. Drug Discovery*, 2013, **8**, 49-63.
52. J. Dalli.; M. Zhu.; N. A. Vlasenko.; B. Deng.; J. Z. Haeggstrom.; N. A. Petasis.; C. N. Serhan, *FASEB J.*, 2013, **27**, 2573-2583.
53. J. Dalli.; N. Chiang.; C. N. Serhan, *Nat. Med.*, 2015, **21**, 1071-1075.
54. D. W. Hart.; J. Schwartz, *J. Am. Chem. Soc.*, 1974, **96**, 8115-8116.
55. P. C. Wailes.; H. Weigold.; A. P. Bell, *J. Organomet. Chem*, 1971, **27**, 373-378.
56. J. Mowat.; J. Senior.; B. Kang.; R. Britton, *Can. J. Chem*, 2013, **91**, 235-239.
57. C. A. Brown.; V. K. Ahuja, *J. Chem. Soc., Chem. Commun.*, 1973, DOI: 10.1039/c39730000553, 553-554.
58. B. M. Trost.; A. B. Pinkerton, *Org. Lett.*, 2000, **2**, 1601-1603.
59. D. W. Hart.; T. F. Blackburn.; J. Schwartz, *J. Am. Chem. Soc.*, 1975, **97**, 679-680.
60. Y. Okude.; S. Hirano.; T. Hiyama.; H. Nozaki, *J. Am. Chem. Soc.*, 1977, **99**, 3179-3181.
61. K. Takai.; K. Kimura.; T. Kuroda.; T. Hiyama.; H. Nozaki, *Tetrahedron Lett.*, 1983, **24**, 5281-5284.

62. H. Jin.; J.-I. Uenishi.; W. J. Christ.; Y. Kishi, *J. Am. Chem. Soc.*, 1986, **108**, 5644-5646.
63. A. Fürstner, *Chem. Rev.*, 1999, **99**, 991-1045.
64. D. Boyall.; D. E. Frantz.; E. M. Carreira, *Org. Lett.*, 2002, **4**, 2605-2606.
65. S. P. Brown.; M. P. Brochu.; C. J. Sinz.; D. W. C. MacMillan, *J. Am. Chem. Soc.*, 2003, **125**, 10808-10809.
66. Y. Hayashi.; J. Yamaguchi.; K. Hibino.; M. Shoji, *tetrahedron Lett.*, 2003, **44**, 8293-8296.
67. G. Zhong, *Angew. Chem. Int. Ed.*, 2003, **42**, 4247-4250.
68. H. Lindlar, *Helv. Chim. Acta*, 1952, **35**, 446-450.
69. *U.S. patent 1628190 Pat.*, US1628190, 1927.
70. J. F. Daeuble.; C. McGettigan.; J. M. Stryker, *Tetrahedron Lett.*, 1990, **31**, 2397-2400.
71. C. E. Miller, *J. Chem. Educ.*, 1965, **42**, 254-259.
72. D. J. Pasto, *Organic Reactions*, John Wiley & Sons, New York, 1991.
73. K. Chernichenko.; Á. Madarász.; I. Pápai.; M. Nieger.; M. Leskelä.; T. Repo, *Nat. Chem.*, 2013, 718-723.
74. A. J. Birch, *Pure Appl. Chem.*, 1996, **68**, 553-556.
75. B. M. Trost.; Z. T. Ball.; T. Jöge, *J. Am. Chem. Soc.*, 2002, **124**, 7922-7923.
76. S. M. Rummelt.; A. Fürstner, *Angew. Chem. Int. Ed.*, 2014, **53**, 3626-3630 and references cited therein.
77. A. Fürstner.; M. Bonnekessel.; J. T. Blank.; K. Radkowski.; G. Seidel.; F. Lacombe.; B. Gabor.; R. Mynott, *Chem. Eur. J.*, 2007, **13**, 8762-8783.
78. A. R. Katritzky.; S. M. Roberts.; O. Meth-Cohn.; C. W. Rees, *Comprehensive Organic Functional Group Transformations*, Elsevier, New York, 1995.
79. B. Crousse.; M. Mladenova.; P. Ducept.; M. Alami.; G. Linstrumelle, *Tetrahedron*, 1999, **55**, 4353-4368.
80. N. Kojima.; S. Nishijima.; K. Tsuge.; T. Tanaka, *Org. Biomol. Chem*, 2011, **9**, 4425-4428.
81. U. Wannagat.; R. Münstedt.; U. Harder, *Liebigs. Ann. Chem*, 1985, 950-958.
82. J. A. Miller.; G. Zweifel, *J. Am. Chem. Soc.*, 1983, **105**, 1383-1384.
83. R. E. Doolittle, *Synthesis*, 1984, **9**, 730-732.
84. G.-Y. Li.; C.-M. Che, *Org. Lett.*, 2004, **6**, 1621-1623.
85. M. P. Doyle.; W. Hu.; I. M. Phillips, *Org. Lett.*, 2000, **2**, 1777-1779.
86. W. J. Lees.; G. M. Whitesides, *J. Org. Chem.*, 1993, **58**, 1887-1894.
87. Y. Hayashi.; N. Umekubo.; T. Hirama, *Org. Lett.*, 2017, DOI: 10.1021/acs.orglett.1027b01433.
88. A. Rodriguez.; M. Nomen.; B. W. Spur.; J. J. Godfroid, *Tetrahedron Lett.*, 1999, **40**, 5161-5164.
89. U. Ramulu.; D. Ramesh.; S. P. Reddy.; S. Rajaram.; K. S. Babu, *Tetrahedron: Asymmetry*, 2014, **25**, 1409-1417.
90. J. S. Clark.; C. Xu, *Angew. Chem. Int. Ed.*, 2016, **55**, 4332-4335.
91. K. Matsumura.; S. Hashiguchi.; T. Ikariya.; R. Noyori, *J. Am. Chem. Soc.*, 1997, **119**, 8738-8739.
92. J. Dalli.; I. Vlasakov.; I. R. Riley.; A. R. Rodriguez.; B. W. Spur.; N. A. Petasis.; N. Chiang.; C. N. Serhan, *Proc. Natl. Acad. Sci.*, 2016, **113**, 12232-12237.
93. S. Ramon.; J. Dalli.; J. M. Sanger.; J. W. Winkler.; M. Aursnes.; J. E. Tungen.; T. V. Hansen.; C. N. Serhan, *Am. J. Pathol.*, 2016, **186**, 962-973.
94. A. Rodriguez.; B. W. Spur, *Tetrahedron Lett.*, 2015, **56**, 3936-3940.

Chapter 5

5 Experimental

This section contains the experimental protocols for the unpublished work concerning the synthesis of RvT3 (**61**), as well as the characterization data for the products prepared for this synthesis.

General Information

Unless stated otherwise, all commercially available reagents and solvents were used in the form they were supplied without any further purification. The stated yields are based on isolated material. All reactions were performed under an argon atmosphere using Schlenk techniques. Reaction flasks were covered with aluminium foil during reactions and stored to minimize exposure to light. Thin layer chromatography was performed on silica gel 60 F_{254} aluminum-backed plates fabricated by Merck. Flash column chromatography was performed on silica gel 60 (40-63 µm) produced by Merck. NMR spectra were recorded on a Bruker AVI600, Bruker AVII400 or a Bruker DPX300 spectrometer at 600 MHz, 400 MHz or 300 MHz respectively for ^{1}H NMR and at 150 MHz, 100 MHz or 75 MHz respectively for ^{13}C NMR. Coupling constants (*J*) are reported in hertz and chemical shifts are reported in parts per million (δ) relative to the central residual protium solvent resonance in ^{1}H NMR ($CDCl_3$ = δ 7.26, DMSO-d_6 = δ 2.50 and MeOD-d_4 = δ 3.31) and the central carbon solvent resonance in ^{13}C NMR ($CDCl_3$ = δ 77.00 ppm, DMSO-d_6 = δ 39.43 and MeOD-d_4 = δ 49.00). Mass spectra were recorded at 70 eV on Micromass Prospec Q or Micromas QTOF 2W spectrometer using EI, ES or CI as the methods of ionization. High resolution mass spectra were recorded on a Micromass Prospec Q or Micromas QTOF 2Wspectrometer using EI or ES as the methods of ionization. Optical rotations were measured using a 0.7 mL cell with a 1.0 dm path length on an Anton Paar MCP 100 polarimeter. HPLC analyses were performed on an Agilent Technologies 1200 Series instrument with diode array detector set at 254 nm and equipped with a chiral stationary phase (Chiralpak AD-H, 4.6 x 250 mm, particle size 5 µm, from DAICEL CHEMICAL IND. LTD).

Methyl 8-hydroxyoctanoate (224).

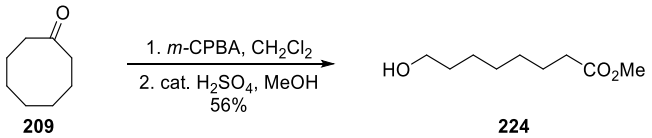

209 **224**

m-CPBA (28.4 g, 127 mmol, 2.00 equiv.) was dissolved in CH_2Cl_2 (205 mL) and cooled to 0 °C. Cyclooctanone (**209**) (8.00 g, 63.4 mmol, 1.00 equiv.) was then added, and the reaction was refluxed (40 °C) for 5 days. The reaction mixture was then cooled to 0 °C before

filtrated. The filtrate was washed with sat. aq. $NaHCO_3$ (43.0 mL) and water, dried (Na_2SO_4) and concentrated *in vacuo*. The crude product was dissolved in dry MeOH (128 mL) and a few drops of concentrated H_2SO_4 was added. The reaction mixture was refluxed overnight, cooled, and then sat. aq. $NaHCO_3$ (13.0 mL) was added before the mixture was concentrated *in vacuo*. More $NaHCO_3$ (43.0 mL) was added and the aq. phase was extracted with Et_2O (4 x 85.0 mL). The organic phases were combined, dried (Na_2SO_4), filtrated and concentrated *in vacuo*. The crude product was purified by column chromatography on silica (hexane/EtOAc 4:1) to afford the titled compound **224** as a clear oil. All spectroscopic and physical data were in full agreement with those reported in the literature.[1] Yield: 6.2 g (56%); ^{1}H NMR (400 MHz, $CDCl_3$) δ 3.66 (s, 3H), 3.63 (t, *J* = 6.6 Hz, 2H), 2.30 (t, *J* = 7.5 Hz, 2H), 1.70 – 1.50 (m, 4H), 1.43 (bs, 1H), 1.41 – 1.30 (m, 6H). ^{13}C NMR (101 MHz, $CDCl_3$) δ 174.4, 62.7, 51.5, 34.1, 32.7, 29.1, 29.0, 25.6, 24.9. TLC (hexane/EtOAc 7:3, $KMnO_4$ stain) R_f = 0.21.

Methyl 8-oxooctanoate (207).

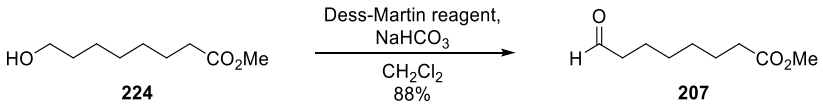

Alcohol **224** (3.00 g, 17.2 mmol, 1.00 equiv) was dissolved in CH_2Cl_2 (510 mL) before $NaHCO_3$ (8.24 g, 98.2 mmol, 5.70 equiv) and Dess−Martin periodinane (9.00 g, 21.2 mmol, 1.23 equiv) were added. The reaction mixture was stirred at room temperature for 5 hours before sat. aq. $Na_2S_2O_3$ (100 mL) was added to quench the reaction. The aq. phase was extracted with CH_2Cl_2 (3 × 70.0 mL), and the combined organic layers were dried and concentrated *in vacuo*. The crude product was purified by column chromatography on silica gel (hexane/EtOAc 4:1) to afford aldehyde **207** as a pale-yellow oil. All spectroscopic and physical data were in full agreement with those reported in the literature.[2,3] Yield: 2.6 g (88%); ^{1}H NMR (400 MHz, $CDCl_3$) δ 9.75 (t, *J* = 1.8 Hz, 1H), 3.65 (s, 3H), 2.41 (td, *J* = 7.3, 1.8 Hz, 2H), 2.29 (t, *J* = 7.5 Hz, 2H), 1.67 – 1.57 (m, 4H), 1.37-1.28 (m, 4H). ^{13}C NMR (101 MHz, $CDCl_3$) δ 202.7, 174.2, 51.6, 43.9, 34.1, 29.0, 28.9, 24.8, 22.0; TLC (hexane/EtOAc 4:1, $KMnO_4$ stain) R_f = 0.30.

Methyl (*S*)-7,8-dihydroxyoctanoate (225).

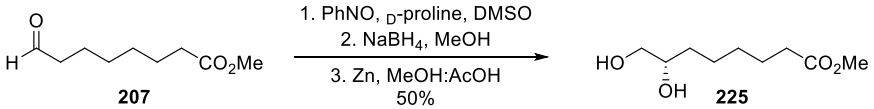

Aldehyde **207** (2.61, 15.2 mmol, 1.00 equiv) and nitrosobenzene (1.62 g, 15.2 mmol, 1.00 equiv.) were dissolved in DMSO (25 mL). D-proline (350 g, 2.53 mmol, 20.0 mol%) was added in one portion. The green reaction mixture was stirred for ~45 min, resulting in a gradual colour change from green to orange. The reaction mixture was then *carefully* pipetted

(copious effervescence) into a solution of $NaBH_4$ (2.11 g, 55.8 mmol, 3.67 equiv.) in MeOH at 0 °C. After complete addition, the cooling bath was removed and the reaction mixture was stirred at ambient temperature for 1 hour. The aq. phase was extracted with Et_2O (4 x 40.0 mL) and the combined organic phase was dried (Na_2SO_4), filtrated and concentrated *in vacuo*. The resulting brown oil was dissolved in 3:1 MeOH:AcOH (62.7 mL) and zinc powder (2.62 g, 40.1 mmol, 2.64 equiv.) was added in one portion. The suspension was stirred for 1 hour. The reaction mixture was filtrated, concentrated *in vacuo* and purified by column chromatography on silica gel (hexane/EtOAc 3:7) to afford diol **225** as a clear oil. Yield 1.4 g (50%); $[\alpha]_D^{25}$ -0.80 (*c* = 1.78, $CHCl_3$), lit.[4] $[\alpha]_D^{25}$ -0.79 (*c* = 1.78, $CHCl_3$) ; ^{1}H NMR (400 MHz, $CDCl_3$) δ 3.74 – 3.68 (m, 1H), 3.68 – 3.61 (m, 4H), 3.43 (dd, *J* = 11.0, 7.6 Hz, 1H), 2.31 (t, *J* = 7.5 Hz, 2H), 2.09 (s, 2H), 1.64 (p, *J* = 7.4 Hz, 2H), 1.52 – 1.31 (m, 6H). ^{13}C NMR (101 MHz, $CDCl_3$) δ 174.4, 72.3, 66.9, 51.6, 34.1, 33.0, 29.2, 25.3, 24.9. HRESITOFMS: *m/z* 213.1098 $[M+Na]^+$ (calcd for $C_9H_{18}O_4Na$, 213.1097); TLC (hexane/EtOAc 3:7, CAM stain) R_f = 0.27.

8-Methoxy-8-oxooctane-1,2-diyl dibenzoate (246).

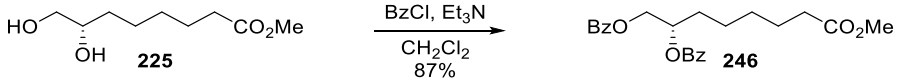

Diol **225** (25.0 mg, 132 µmol, 1.00 equiv.) in CH_2Cl_2 (0.65 mL) was added trimethylamine (55.2 µL, 396 µmol, 3.00 equiv) and benzoylchloride (47.5 µL, 409 µmol, 3.10 equiv.). After stirring overnight, the reaction mixture was quenched with sat. aq. $NaHCO_3$ (0.50 mL). The reaction mixture was extracted with CH_2Cl_2 (3 x 1.00 mL), dried (Na_2SO_4) and concentrated *in vacuo*. The crude product was purified by column chromatography on silica gel (hexane/EtOAc 85:15) to afford **246** as a clear oil. Yield 45.7 mg (87%); The enantiomeric excess was determined by HPLC analysis using a chiral column (AD-H, hexane/iPrOH 98:2, 1 mL/min): t_r (major) = 11.21 min and t_r (minor) = 12.22 min; $[\alpha]_D^{25}$ -15.2 (*c* = 0.24, MeOH); ^{1}H NMR (400 MHz,$CDCl_3$) δ 8.02 (dd, *J* = 18.5, 7.4 Hz, 4H), 7.55 (q, *J* = 7.3 Hz, 2H), 7.48 – 7.37 (m, 4H), 5.54 – 5.45 (m, 1H), 4.55 (dd, *J* = 11.9, 3.5 Hz, 1H), 4.46 (dd, *J* = 11.9, 6.6 Hz, 1H), 3.65 (s, 3H), 2.30 (t, *J* = 7.5 Hz, 2H), 1.92 – 1.74 (m, 2H), 1.64 (p, *J* = 7.5 Hz, 2H), 1.55 – 1.34 (m, 4H). ^{13}C NMR (101 MHz, $CDCl_3$) δ 174.2, 166.4, 166.2, 133.2, 133.2, 130.3, 129.9, 129.8 (4C), 128.5 (4C), 72.2, 65.8, 51.6, 34.0, 31.0, 29.1, 25.1, 24.9; HRESITOFMS: *m/z* 421.1621 $[M+Na]^+$ (calcd for $C_{23}H_{26}O_6Na$, 421.1622); TLC (hexane/EtOAc 9:1, CAM stain) R_f = 0.15.

Methyl (*S*)-7,8-bis((triethylsilyl)oxy)octanoate (226).

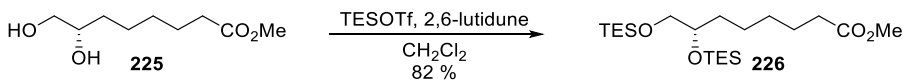

Diol **225** (650 mg, 3.42 mmol, 1.00 equiv.) was dissolved in CH_2Cl_2 (13.0 mL) and cooled to -78 °C. 2,6-lutidine (1.98 mL, 17.1 mmol, 5.00 equiv.) was added, followed by dropwise addition of TESOTf (1.93 mL, 8.55 mmol, 2.50 equiv.). After the reaction was deemed complete based on TLC-analysis (~1 hour), it was quenched with the addition of sat. aq. $NaHCO_3$ (15.0 mL). The reaction mixture was extracted with Et_2O (3 x 15.0 mL), dried (Na_2SO_4) and concentrated *in vacuo*. The crude product was purified by column chromatography on silica gel (hexane/EtOAc 95:5) to afford **226** as a clear oil. Yield 1.2 g (82%). $[\alpha]_D^{20}$ -11.1 (*c* = 0.80, MeOH); ^{1}H NMR (400 MHz, $CDCl_3$) δ 3.70 – 3.61 (m, 4H), 3.51 (dd, *J* = 9.9, 5.6 Hz, 1H), 3.39 (dd, *J* = 9.9, 6.3 Hz, 1H), 2.30 (t, *J* = 7.6 Hz, 2H), 1.71 – 1.45 (m, 4H), 1.41 – 1.27 (m, 4H), 0.95 (t, *J* = 8.0 Hz, 18H), 0.64 – 0.55 (m, 12H). ^{13}C NMR (101 MHz, $CDCl_3$) δ 174.4, 73.3, 67.3, 51.6, 34.4, 34.2, 29.6, 25.1, 25.0, 7.1 (3C), 6.9 (3C), 5.2 (3C), 4.5 (3C); HRESITOFMS: *m*/*z* 441.2826 $[M+Na]^+$ (calcd for $C_{21}H_{46}O_4Si_2Na$, 441.2827); TLC (hexane/EtOAc 9:1, CAM stain) R_f = 0.42.

Methyl (*S*)-8-oxo-7-((triethylsilyl)octanoate (205).

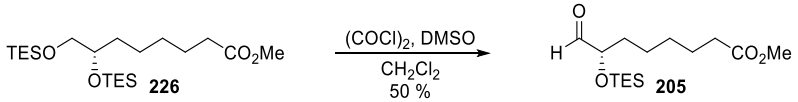

Oxalyl chloride (0.18 mL, 2.10 mmol, 4.40 equiv.) in CH_2Cl_2 (0.62 mL) was added dropwise to a solution of DMSO (0.30 mL, 4.20 mmol, 8.80 equiv.) in CH_2Cl_2 (0.94 mL) at -78 °C. The reaction mixture was stirred for 15 min. before the di-protected diol **226** (200 mg, 478 μmol, 1.00 equiv.) in CH_2Cl_2 (0.64 mL) was added dropwise and stirred for 20 min. at -78 °C before the temperature was raised to -40 °C. After 45 min, the temperature was lowered to -78 °C again, and Et_3N (1.00 mL) was added. The reaction mixture was allowed to warm up to room temperature before it was diluted with water (3.15 mL). The reaction mixture was extracted with CH_2Cl_2 (3 x 10.0 mL), dried (Na_2SO_4) and concentrated *in vacuo*. The crude product was purified by column chromatography on silica gel (hexane/EtOAc 9:1) to afford aldehyde **205** as a clear oil. Yield 72.5 mg (50%); $[\alpha]_D^{20}$ -10.7 (*c* = 0.31, MeOH); ^{1}H NMR (400 MHz, $CDCl_3$) δ 9.59 (d, *J* = 1.8 Hz, 1H), 3.95 (td, *J* = 6.3, 1.8 Hz, 1H), 3.67 (s, 3H), 2.30 (t, *J* = 7.5 Hz, 2H), 1.68 – 1.57 (m, 4H), 1.46 – 1.28 (m, 4H), 0.96 (t, *J* = 7.9 Hz, 9H), 0.62 (q, *J* = 8.0 Hz, 6H). ^{13}C NMR (101 MHz, $CDCl_3$) δ 204.5, 174.2, 77.4, 51.6, 34.1, 32.8, 29.2, 24.9, 24.4, 6.9 (3C), 4.9 (3C); HRESITOFMS: *m*/*z* 325.1806 $[M+Na]^+$ (calcd for $C_{15}H_{30}O_4SiNa$, 325.1806); TLC (hexane/EtOAc 9:1, CAM stain) R_f = 0.26.

(2*E*,4*E*)-5-Bromopenta-2,4-dienal (149).

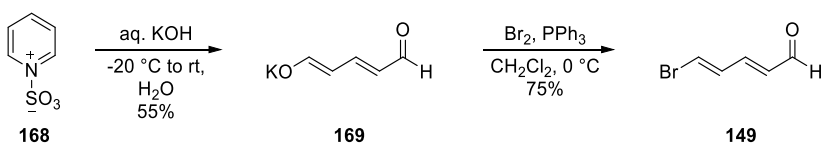

Vinylbromide **149** was prepared in two steps from commercially available pyridinium-1-sulfonate (**168**) in 41% (8.1 g) overall yield, as previously reported.[5,6] All spectroscopic and physical data were in agreement with those reported in literature.[6] ^{1}H NMR (300MHz, DMSO-d_6) δ 8.67 (d, J = 9.2 Hz, 2H), 7.04 (t, J = 12.9 Hz, 1H), 5.10 (dd, J =13.0, 9.1 Hz, 2H); ^{13}C NMR (75 MHz, DMSO-d_6) δ 184.4 (2C), 159.8, 106.2 (2C).

(*Z*)-Hex-3-en-1-yliodotriphenyl-λ^5-phosphane (210).

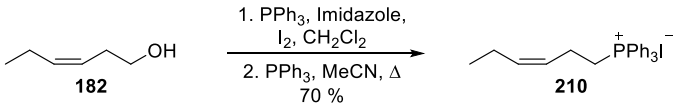

The Wittig salt **210** (6.00 g, 60.0 mmol) was prepared in two steps from commercially available (*Z*)-hex-3-en-1-ol (**182**) as previously reported,[7,8] in 70% (19.8 g) overall yield. All spectroscopic and physical data were in agreement with those reported in literature.[7] ^{1}H NMR (400 MHz, $CDCl_3$) δ 7.87 – 7.76 (m, 9H), 7.75 – 7.65 (m, 6H), 5.52 – 5.44 (m, 1H), 5.41–5.33 (m, 1H), 3.77 – 3.64 (m, 2H), 2.48– 2.38 (m, 2H), 1.80 (pd, J = 7.5, 1.5 Hz, 2H), 0.84 (t, J = 7.5 Hz, 3H). ^{13}C NMR (101 MHz, $CDCl_3$) δ 135.3 (d, 4'J_{CP} = 3.0 Hz, 3C), 134.5 (d, 4J_{CP} = 1.1 Hz), 133.8 (d, 3'J_{CP} = 10.1 Hz, 6C), 130.7 (d, 2'J_{CP} = 12.6 Hz, 6C), 125.2 (d, 3J_{CP} = 14.1 Hz), 118.2 (d, 1'J_{CP} = 85.8 Hz, 3C), 23.6 (d, 1J_{CP} = 48.5 Hz), 20.7, 20.4 (d, 2J_{CP} = 3.7 Hz), 14.1.

Trimethyl((3*Z*,6*Z*)-nona-3,6-dien-1-yn-1-yl)silane (211).

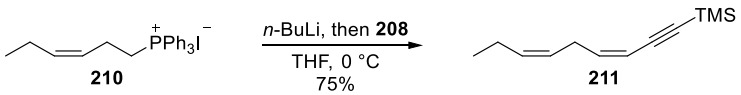

Wittig salt **210** (6.00 g, 12.7 mmol, 1.00 equiv.) was dissolved in THF (235 mL) and cooled to 0 °C. BuLi (5.08 mL, 12.7 mmol, 2.50 M) was added dropwise and the reaction mixture was stirred for 10 minutes. Next, aldehyde **208** (1.60 g, 12.7 mmol, 1.00 equiv.) dissolved in THF (15.0 mL) was added dropwise and the reaction was stirred at 0 °C for 1 hour and then quenched by the addition of phosphate buffer solution (35 mL, pH 7.00). The resulting biphasic mixture was extracted with Et_2O (3 x 50.0 mL), dried (Na_2SO_4) and concentrated *in vacuo* until a small amount of the reaction mixture in Et_2O was left. This solution was added to a short plug of silica gel and eluted with pentane. The filtrate was concentrated *in vacuo* and purified by flash column chromatography on silica gel (pentane) to afford **211** as a clear oil. Yield 1.83 g (75%); ^{1}H NMR (400 MHz, $CDCl_3$) δ 5.90 (dt, J = 10.7, 7.5 Hz, 1H), 5.52 – 5.41 (m, 2H), 5.39 – 5.30 (m, 1H), 3.08 (t, J = 7.5 Hz, 2H), 2.12 (p, J = 7.5 Hz, 2H), 0.98 (t, J = 7.5 Hz, 3H), 0.20 (s, 9H). ^{13}C NMR (101 MHz, $CDCl_3$) δ 143.4, 133.4, 125.3, 109.2, 102.0, 99.1, 29.0, 20.8, 14.4, 0.2; HRAPPIMS: *m*/*z* 192.1329 $[M]^+$ (calcd for $C_{12}H_{20}Si$, 192.1329); TLC (pentane, $KMnO_4$ stain) R_f = 0.37.

(3*Z*,6*Z*)-nona-3,6-dien-1-yne (206).

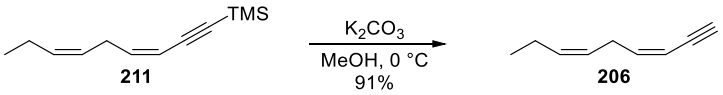

TMS-protected alkyne **211** (218 mg, 1.14 mmol, 1.00 equiv.) was dissolved in MeOH (17.0 mL) and cooled to 0 °C. Solid K_2CO_3 (472 mg, 3.42 mmol, 3.00 equiv.) was added in one portion and the reaction mixture was allowed to warm up to room temperature. It was stirred until deemed complete by TLC analysis (1.5 hours) and quenched with phosphate buffer (20 mL, pH = 7.00). Next, it was extracted with pentane (3 x 5.00 mL), dried (Na_2SO_4) and the suspension was passed through a short plug of silica gel, eluting with additional pentane. The filtrate was carefully concentrated *in vacuo* and the alkyne **206** was used directly without any further purification. Yield 124 mg (91%); ^{1}H NMR (400 MHz, $CDCl_3$) δ 5.95 (dt, *J* = 10.5, 7.4 Hz, 1H), 5.54 – 5.41 (m, 2H), 5.40 – 5.23 (m, 1H), 3.24 – 2.96 (m, 3H), 2.10 (p, *J* = 7.4 Hz, 2H), 0.98 (t, *J* = 7.5 Hz, 2H). ^{13}C NMR (101 MHz, $CDCl_3$) δ 144.1, 133.5, 125.2, 108.2, 81.8, 80.4, 28.8, 20.8, 14.4; TLC (heptane, $KMnO_4$ stain) R_f = 0.35.

(*S*,1*E*,3*E*,8*Z*,11*Z*)-1-bromotetradeca-1,3,8,11-tetraen-6-yn-5-ol (212).

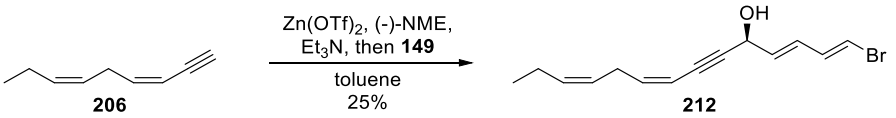

A flask was charged with dry $Zn(OTf)_2$ (1450 mg, 4.00 mmol, 3.00 equiv.) and (-)-NME (739 mg, 4.12 mmol, 3.10 equiv.) and purged with argon for 20 min. Next, dry, degassed toluene (8.70 mL) and Et_3N (575 µl, 4.12 mmol, 3.10 equiv.) was added and the reaction mixture was stirred for 2 hours at room temperature before the addition of alkyne **206** (492 mg, 4.11 mmol, 3.10 equiv.) in toluene (1.00 mL) in one portion. After stirring for 15 min, a solution of aldehyde **149** (213 mg, 1.33 mmol, 1.00 equiv.) in toluene (1.00 mL) was added in one portion. The reaction mixture was stirred for 3 hours before it was quenched by the addition of 4:2 NH_4Cl and $Na_2S_2O_3$ (8.50 mL), extracted with Et_2O (3 x 8.50 mL), dried (Na_2SO_4) and concentrated *in vacuo*. The crude product was purified by column chromatography on silica gel (hexane/EtOAc 85:15) to afford **212** as a clear oil. Yield 93.2 mg (25%); ^{1}H NMR (400 MHz, MeOD) δ 6.79 (dd, *J* = 13.4, 10.9 Hz, 1H), 6.54 (d, *J* = 13.5 Hz, 1H), 6.37 (dd, *J* = 15.1, 10.8 Hz, 1H), 5.97 – 5.75 (m, 2H), 5.52 (dq, *J* = 10.6, 1.6 Hz, 1H), 5.48 – 5.40 (m, 1H), 5.37 – 5.28 (m, 1H), 5.00 (d, *J* = 5.9 Hz, 1H), 3.06 (t, *J* = 7.4 Hz, 2H), 2.11 (p, *J* = 7.3 Hz, 2H), 0.97 (t, *J* = 7.5 Hz, 3H). ^{13}C NMR (101 MHz, MeOD) δ 143.4, 137.8, 134.8, 134.0, 129.5, 126.4, 110.9, 109.3, 93.7, 83.0, 63.2, 29.6, 21.6, 14.6; HRESITOFMS: *m*/*z* 303.0355 $[M+Na]^+$ (calcd for $C_{14}H_{17}BrONa$, 303.0355); TLC (hexane/Et_2O 7:3, $KMnO_4$ stain) R_f = 0.45.

(*R*,1*E*,3*E*,6*E*,8*Z*,11*Z*)-1-bromotetradeca-1,3,6,8,11-pentaen-5-ol (221).

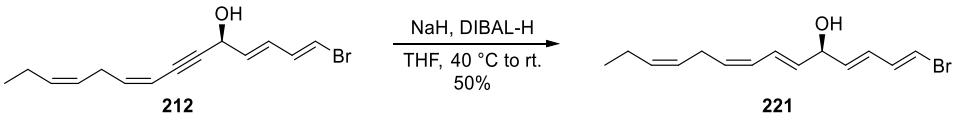

212 **221**

Vinyl bromide **212** (93.2 mg, 333 µmol, 1.00 equiv.) was dissolved in THF (2.93 mL) before NaH (14.6 mg, 366 µmol, 1.10 equiv.) was added. The temperature was raised to 40 °C and the reaction mixture was stirred for 30 min. Next, the temperature was lowered to room temperature and the DIBAL-H (1.0 M, 0.67 mL, 666 µmol, 2.00 equiv.) was added dropwise. After 2-3 hours, the reaction mixture was quenched with a 1:1 of Rochelle salt and phosphate buffer (2.00 mL), extracted with Et_2O (3 x 2.00 mL), dried (Na_2SO_4) and concentrated *in vacuo*. The crude product was purified by column chromatography on silica gel (hexane/Et_2O 85:15) to afford **221** as a clear oil. Yield 46.9 mg (50%); ^{1}H NMR (400 MHz, MeOD) δ 6.77 (dd, *J* = 13.4, 10.8 Hz, 1H), 6.57 (dd, *J* = 15.1, 11.1 Hz, 1H), 6.48 (d, *J* = 13.5 Hz, 1H), 6.22 (dd, *J* = 15.2, 10.6 Hz, 1H), 5.99 (t, *J* = 10.8 Hz, 1H), 5.78 (dd, *J* = 15.3, 6.2 Hz, 1H), 5.66 (dd, *J* = 15.2, 6.5 Hz, 1H), 5.48 – 5.26 (m, 3H), 4.64 (t, *J* = 6.3 Hz, 1H), 2.94 (t, *J* = 7.5 Hz, 2H), 2.10 (p, *J* = 7.3 Hz, 2H), 0.98 (t, *J* = 7.5 Hz, 2H). ^{13}C NMR (101 MHz, MeOD) δ 138.3, 137.2, 135.3, 133.2, 131.7, 129.0, 128.6, 127.7, 126.9, 109.8, 73.4, 26.9, 21.5, 14.6; HRESITOFMS: *m/z* 305.0513 $[M+Na]^+$ (calcd for $C_{14}H_{19}BrONa$, 305.0511); TLC (hexane/Et_2O 7:3, CAM stain) R_f = 0.32.

Mosher ester analysis of alcohol 221.

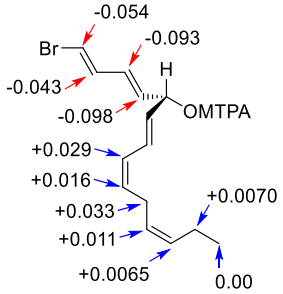

Figure 5.1 Resulting $\Delta\delta^{SR} = (\delta_S - \delta_R)$ values (in Hz) for each proton(s) identified.

General procedure for the preparation of Mosher esters.[9]

Alcohol **221** (100 µg, 0.355 µmol, 1.00 equiv.) was transferred to a flame dried 2.00 mL glass vial and dry pyridine (1.10 µL, 13.9 µmol, 39.0 equiv.) was added. The content was then dissolved in $CDCl_3$ (111 µL). The solvent was passed through a column of silica immediately before use. Next, *R*- or *S*-Morsher's acid chloride (1.10 µL, 5.68 µmol, 16.0 equiv.) was added to the mixture. Addition of *R*-(-)-MTPA-Cl generated the *S*-MTPA ester and vice versa. After the reaction was deemed complete by TLC-analysis (~1 hour), the reaction mixture was diluted with dry $CDCl_3$ (0.60 mL) and transferred to an NMR sample tube

before the ^{1}H NMR spectrum was recorded. The resulting $\Delta\delta^{SR}$ values are shown in the Figure 5.1. From the calculated $\Delta\delta^{SR}$ values, the configuration at C13 was deduced to be *R*. The *ee* value was calculated to be 90% from the ^{19}F NMR of the resulting Mosher esters (Figure 5.19 and Figure 5.20).

(((*R*,1*E*,3*E*,6*E*,8*Z*,11*Z*)-1-bromotetradeca-1,3,6,8,11-pentaen-5-yl)oxy)triethylsilane (204).

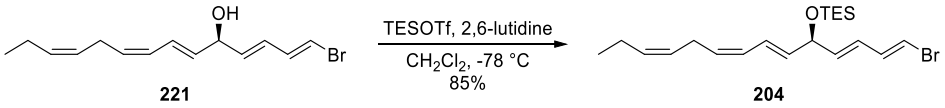

221 204

The secondary alcohol **221** (20.8 mg, 73.7 μmol, 1.00 equiv.) was dissolved in CH_2Cl_2 (1.00 mL) and cooled to -78 °C. 2,6-lutidine (25.7 μL, 221 μmol, 3.00 equiv.) was added, followed by dropwise addition of TESOTf (21.7 μL, 95.8 mmol, 1.30 equiv.). After the reaction was deemed complete based on TLC-analysis (~1 hour), it was quenched with the addition of sat. aq. $NaHCO_3$ (1.00 mL). The reaction mixture was extracted with Et_2O (3 x 3.00 mL), dried (Na_2SO_4) and concentrated *in vacuo*. The crude product was purified by column chromatography on silica gel (hexane/EtOAc 99:1) to afford **204** as a clear oil. Yield 24.8 mg (85%). $[\alpha]_D^{25}$ -17.3 (*c* = 0.53, toluene); ^{1}H NMR (400 MHz, C_6D_6) δ 6.69 (ddt, *J* = 15.1, 11.1, 1.1 Hz, 1H), 6.51 (dd, *J* = 13.5, 10.9 Hz, 1H), 6.14 – 5.79 (m, 4H), 5.61 (dd, *J* = 15.1, 6.0 Hz, 1H), 5.49 (dd, *J* = 15.2, 5.8 Hz, 1H), 5.45 – 5.36 (m, 2H), 4.59 (t, *J* = 5.9 Hz, 1H), 2.95 (t, *J* = 6.1 Hz, 2H), 2.00 (p, *J* = 7.6 Hz, 2H), 1.01 (t, *J* = 7.9 Hz, 9H), 0.90 (t, *J* = 7.5 Hz, 3H), 0.62 (q, *J* = 7.9 Hz, 6H). ^{13}C NMR (101 MHz, C_6D_6) δ 137.2, 136.9, 135.2, 132.6, 130.8, 127.9, 127.0, 126.7, 125.0, 109.0, 73.5, 26.5, 20.9, 14.4, 7.1 (3C), 5.4 (3C). HRESITOFMS: *m*/*z* 419.1375 $[M+Na]^+$ (calcd for $C_{20}H_{33}BrOSiNa$, 419.1376); TLC (hexane/EtOAc 99:1, CAM stain) R_f = 0.19.

(*E*)-1-(4-bromophenyl)hex-1-en-3-ol (223).

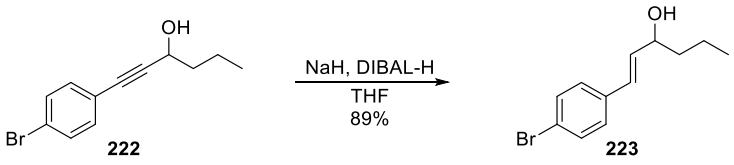

222 223

The propargylic alcohol **222** (100 mg, 395 μmol, 1.00 equiv.) was dissolved in THF (4.00 mL) and NaH (17.38 mg, 60% dispersion, 1.10 equiv.) was added. The resulting suspension was stirred until cessation of gas evolution, and cooled to 0 °C. DIBAL-H (1.0 M in THF, 0.79 mL, 790 μmol, 2.00 equiv.) was added dropwise and the reaction was stirred until deemed complete by TLC (30 min). The reaction was quenched with 10 mL solution of 1:1 phosphate buffer (pH = 7.00) and sat. aq. solution of Rochelle's salt, stirred vigorously, extracted with Et_2O (3 x 10 mL), dried (Na_2SO_4), filtrated and concentrated *in vacuo*. The

crude product was purified by column chromatography on silica gel (hexane/Et_2O 7:3) to afford **223** as a clear oil. Yield 90 mg (89%). All spectroscopic and physical data were in agreement with those reported in literature.[10] ^1H NMR (400 MHz, $CDCl_3$) δ 7.43 (d, *J* = 8.5 Hz, 2H), 7.23 (d, *J* = 8.4 Hz, 2H), 6.51 (d, *J* = 15.9 Hz, 1H), 6.21 (dd, *J* = 15.9, 6.6 Hz, 1H), 4.31 – 4.25 (m, 1H), 1.70 – 1.52 (m, 2H), 1.52 – 1.34 (m, 2H), 0.96 (t, *J* = 7.3 Hz, 3H). ^{13}C NMR (101 MHz, $CDCl_3$) δ 135.9, 133.6, 131.8, 129.0, 128.1, 121.5, 72.8, 39.6, 18.8, 14.1. TLC (hexane/Et_2O 7:3, $KMnO_4$ stain) R_f = 0.14.

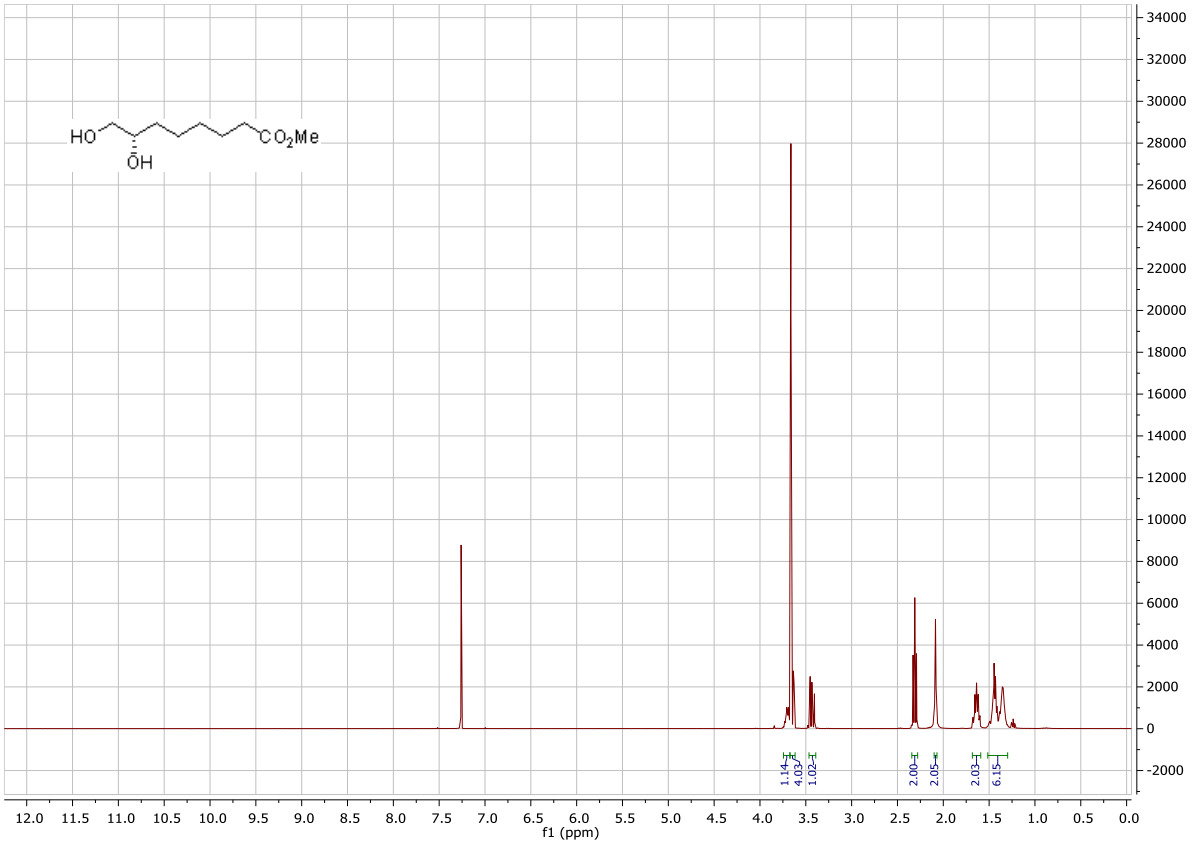

Figure 5.2 ^{1}H NMR spectrum of compound **225**.

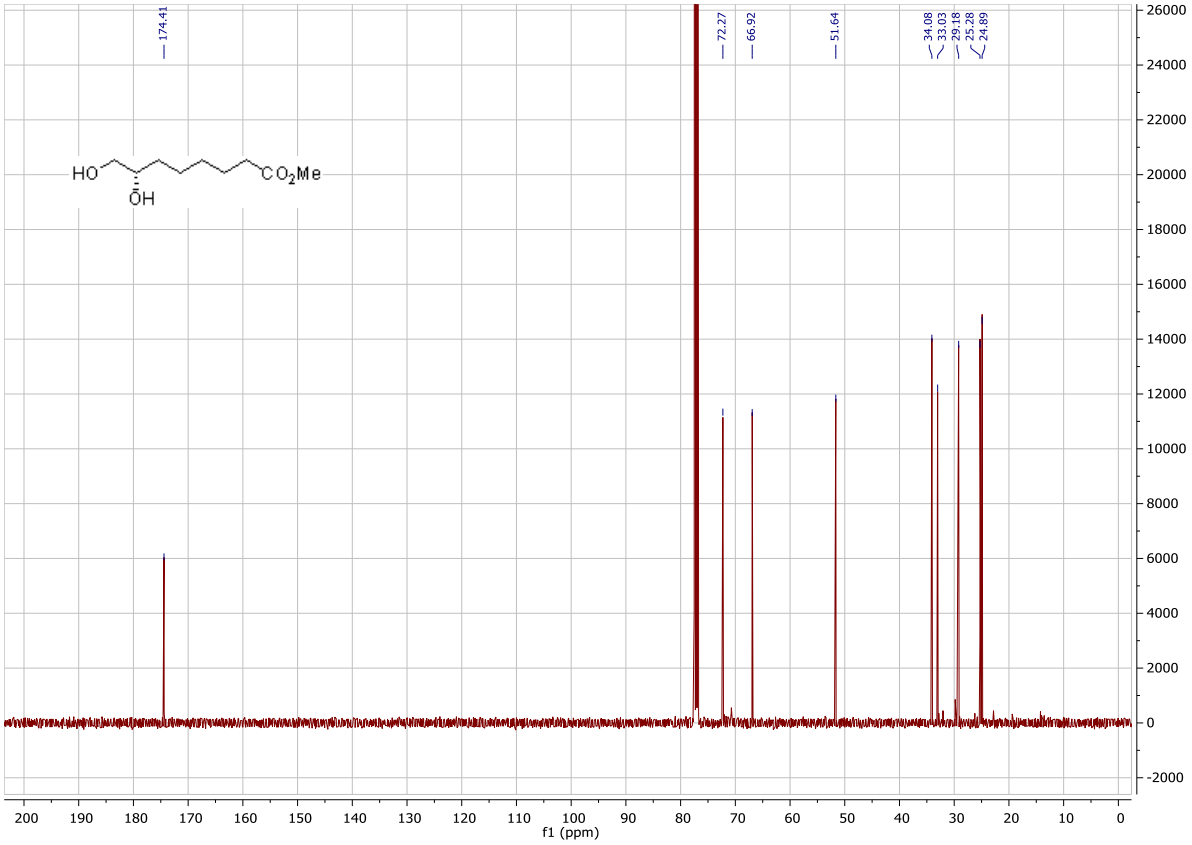

Figure 5.3 ^{13}C NMR spectrum of compound **225**.

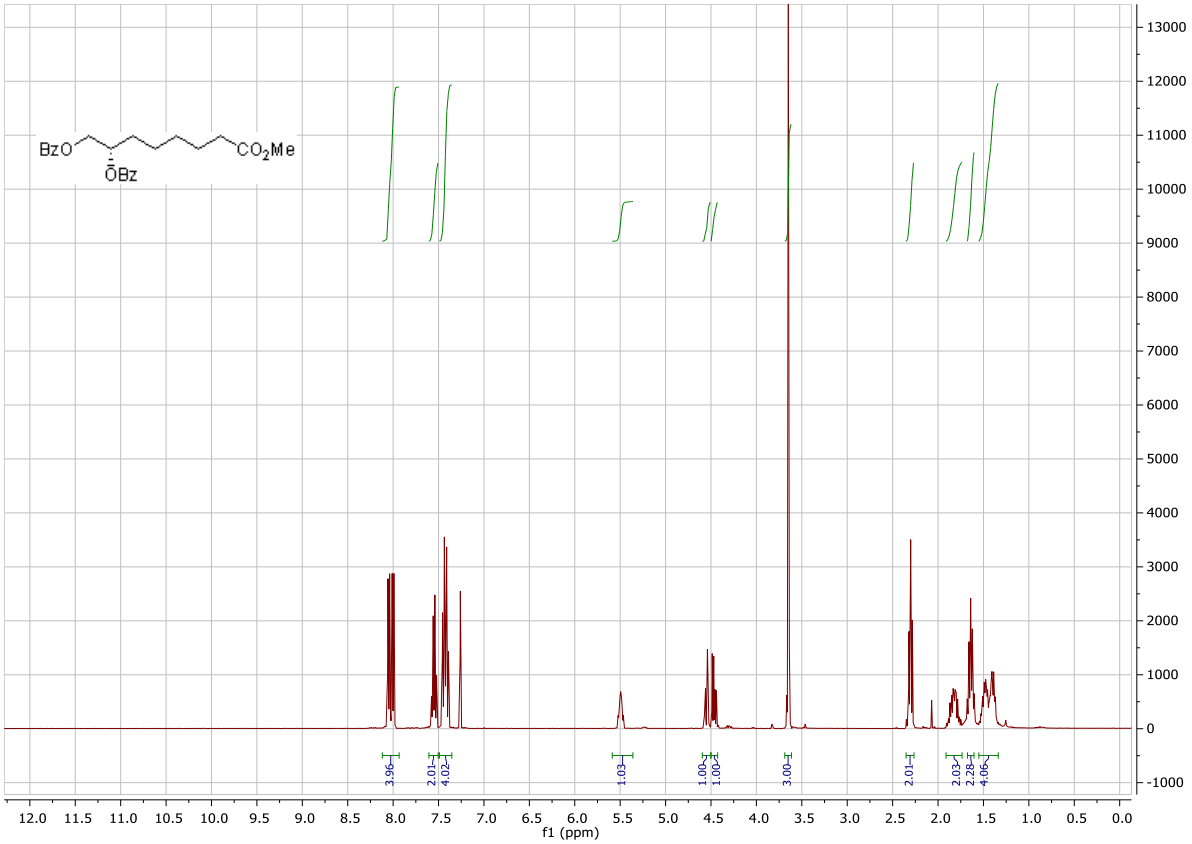

Figure 5.4 ^{1}H NMR spectrum of compound **246**.

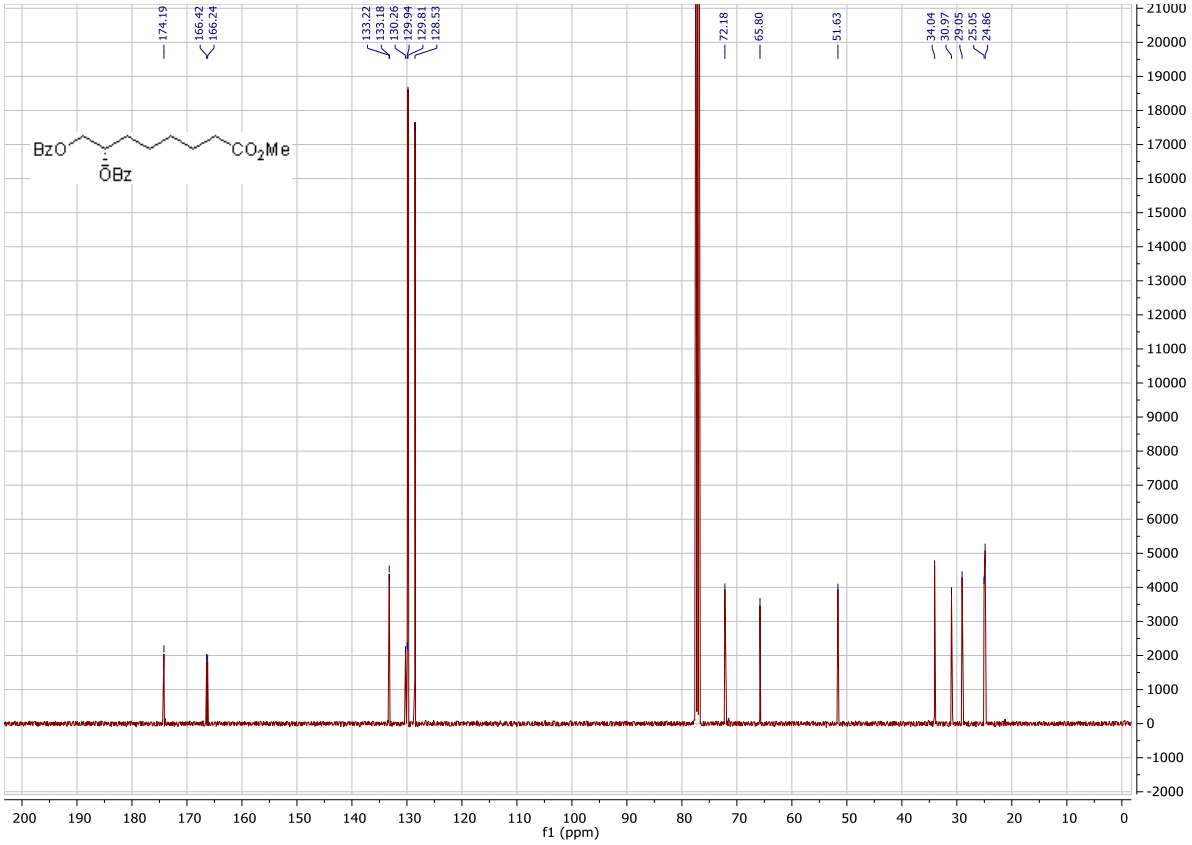

Figure 5.5 ^{13}C NMR spectrum of compound **246**.

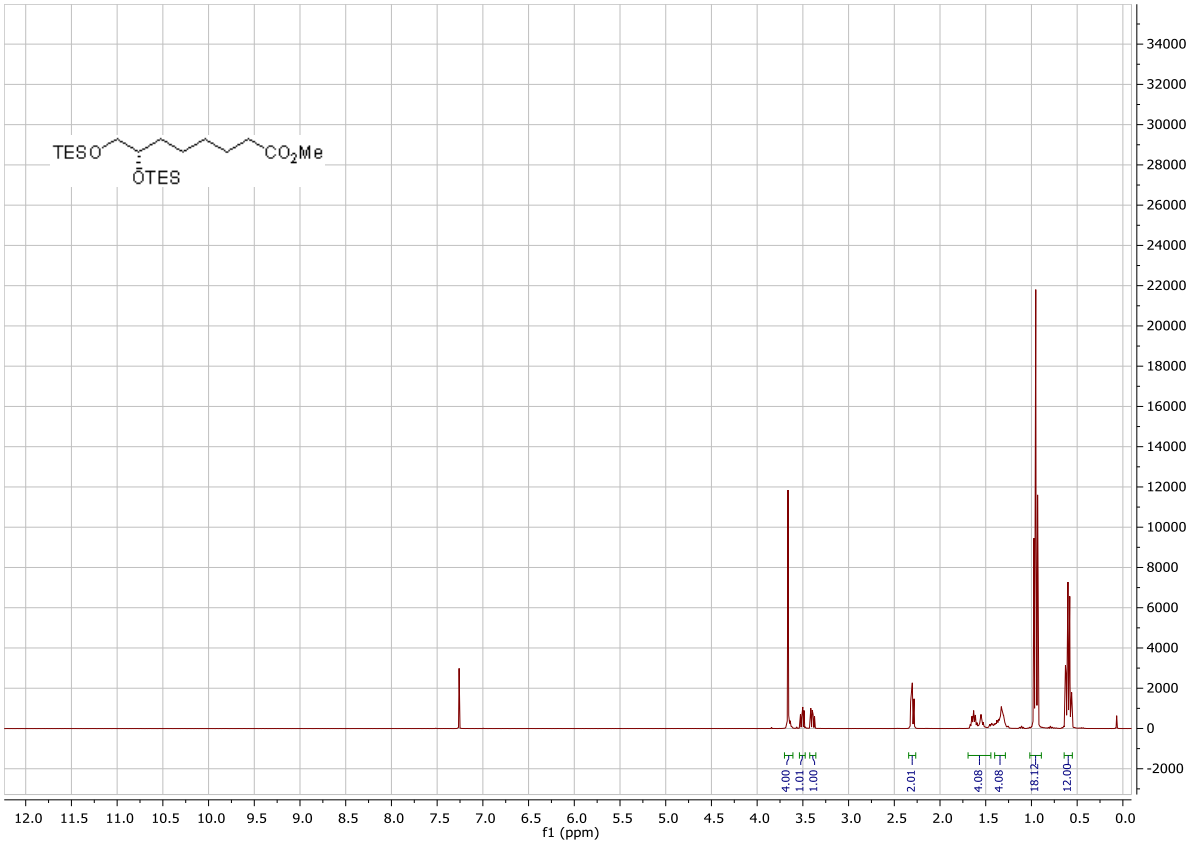

Figure 5.6 ^{1}H NMR spectrum of compound **226**.

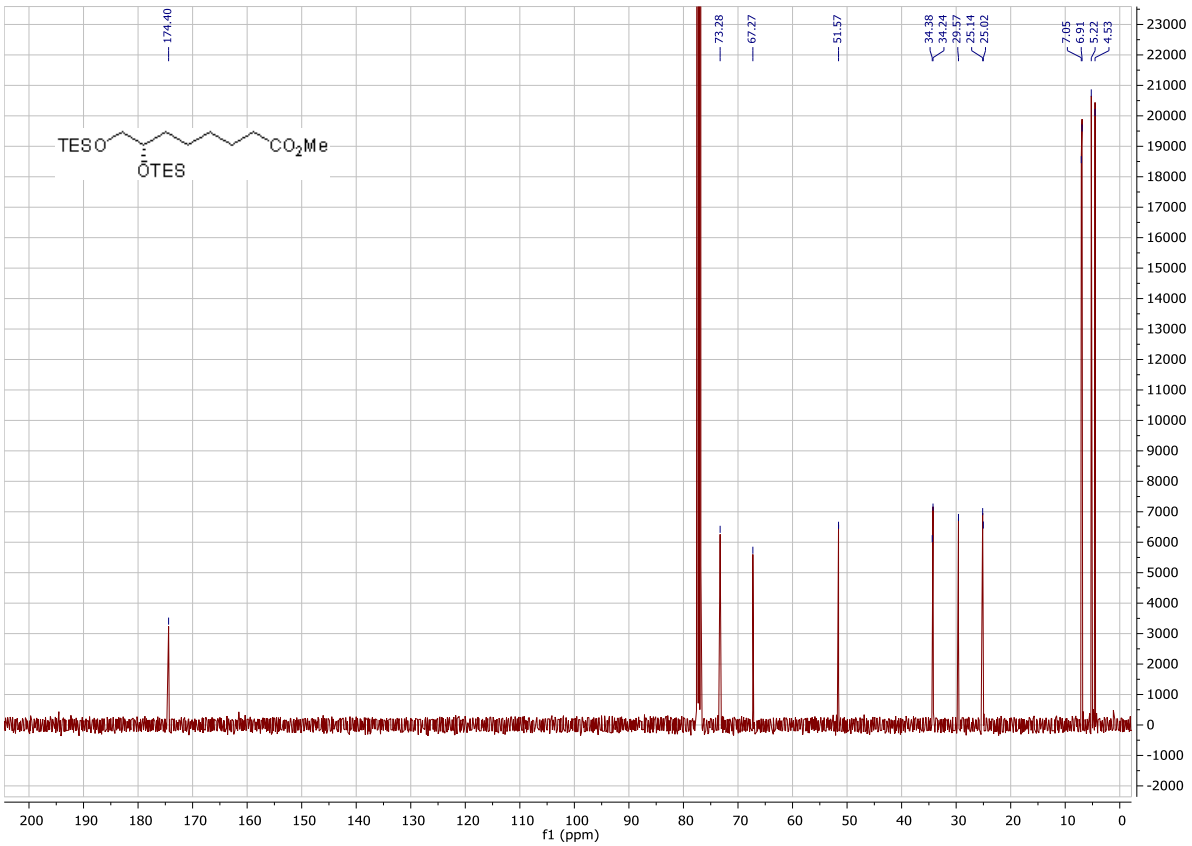

Figure 5.7 ^{13}C NMR spectrum of compound **226**.

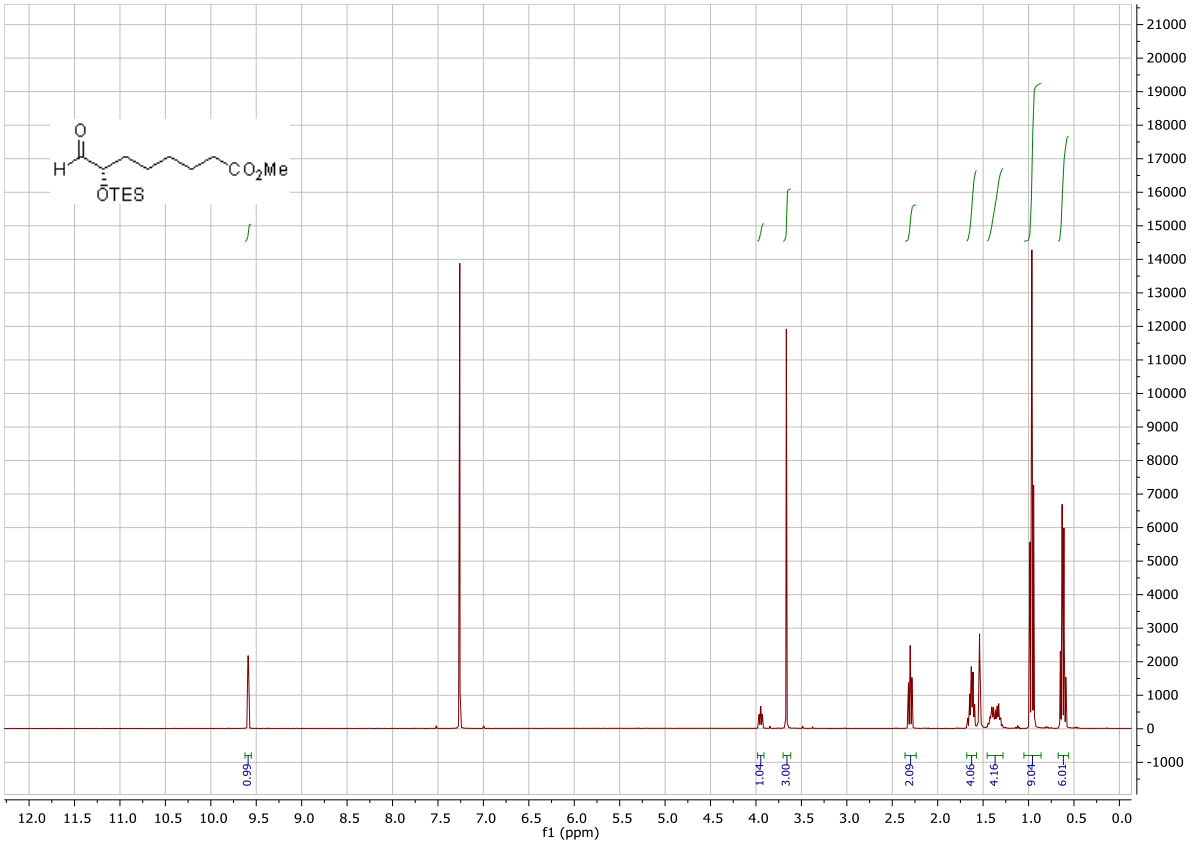

Figure 5.8 ^{1}H NMR spectrum of compound **205**.

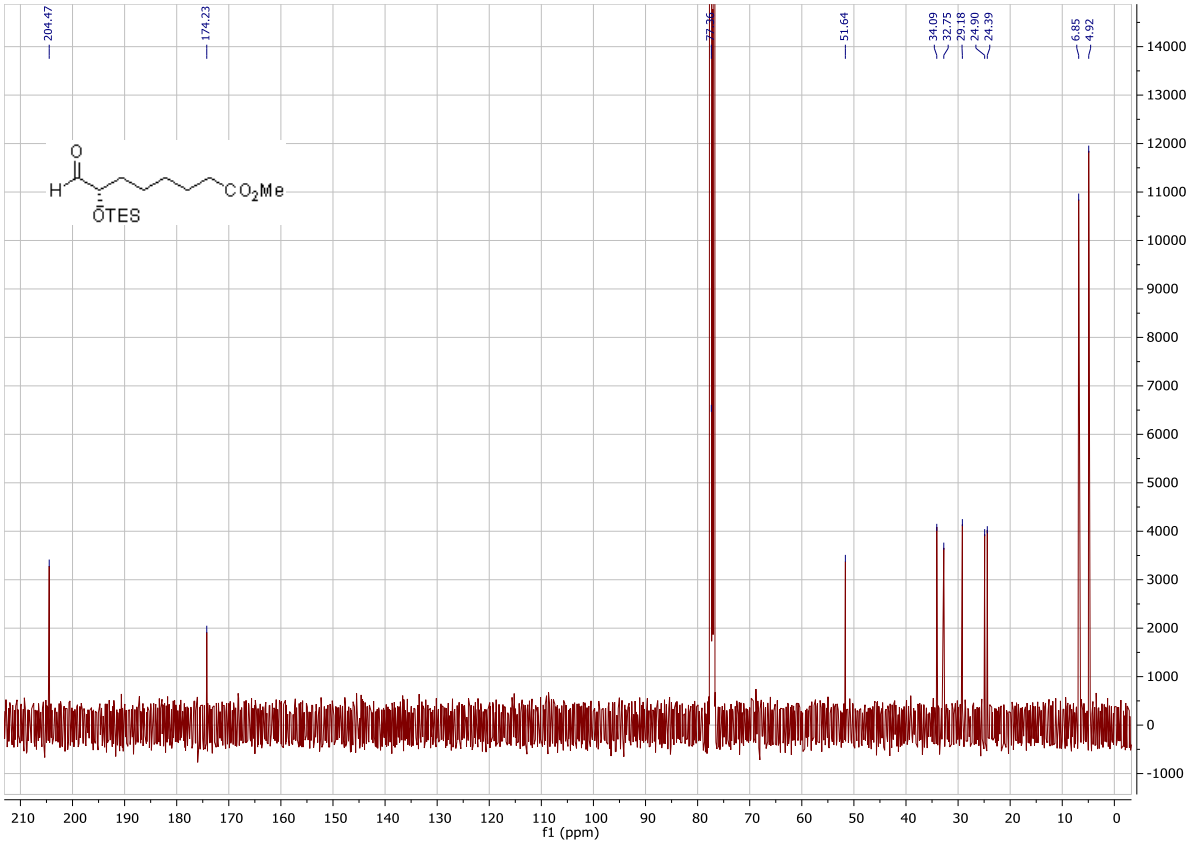

Figure 5.9 ^{13}C NMR spectrum of compound **205**.

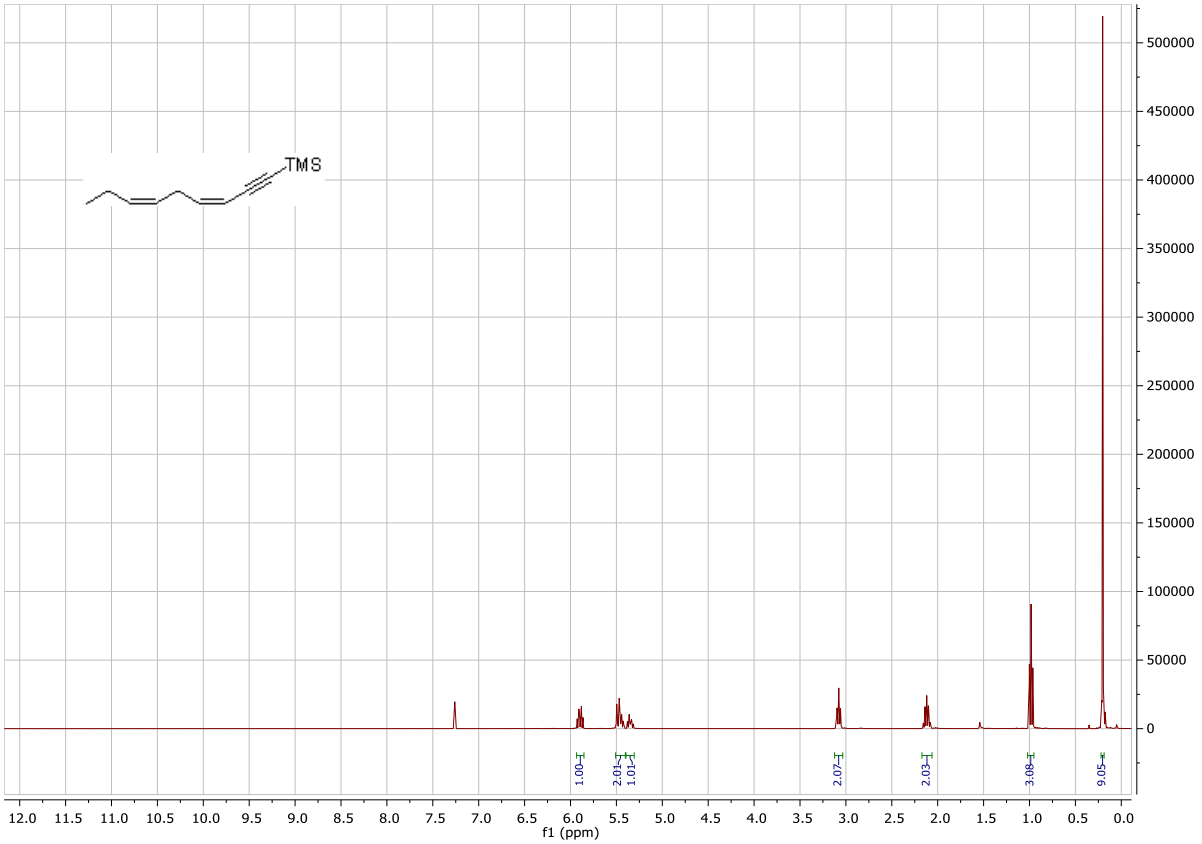

Figure 5.10 ^{1}H NMR spectrum of compound **211**.

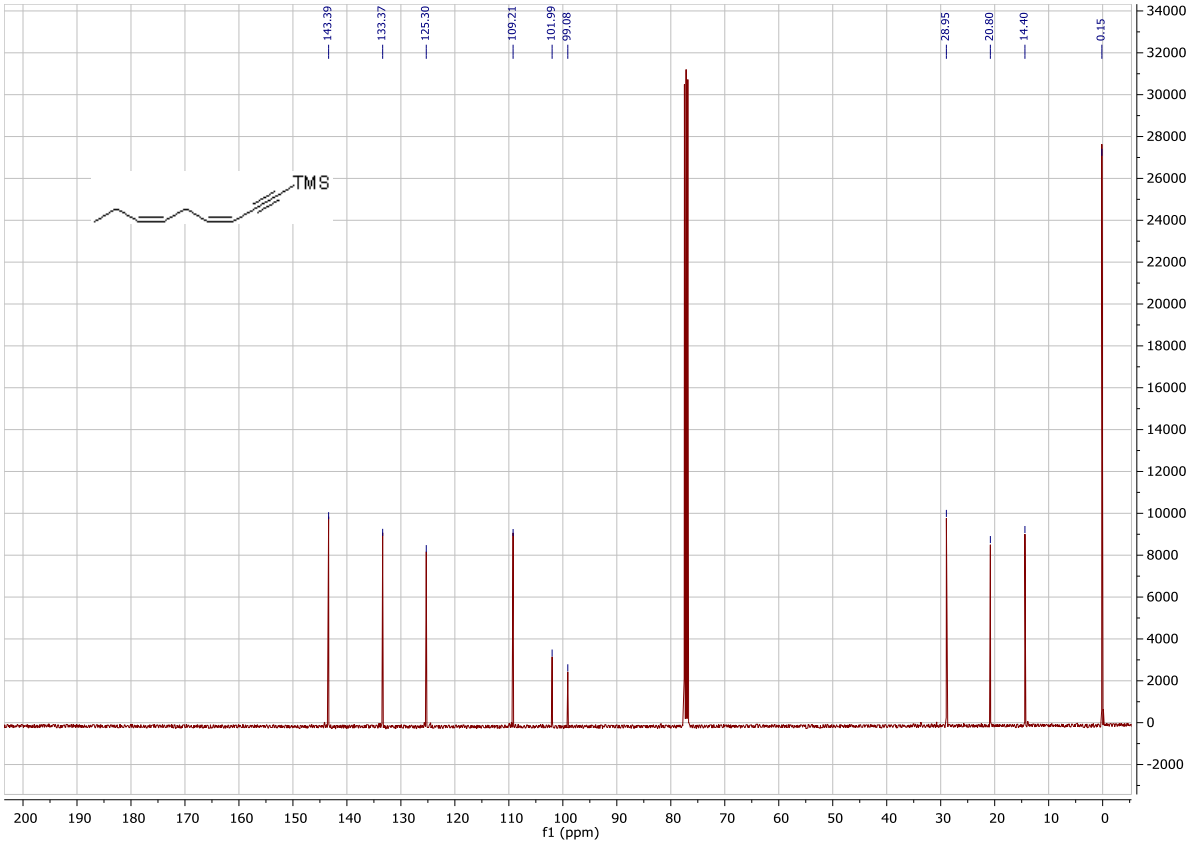

Figure 5.11 ^{13}C NMR spectrum of compound **211**.

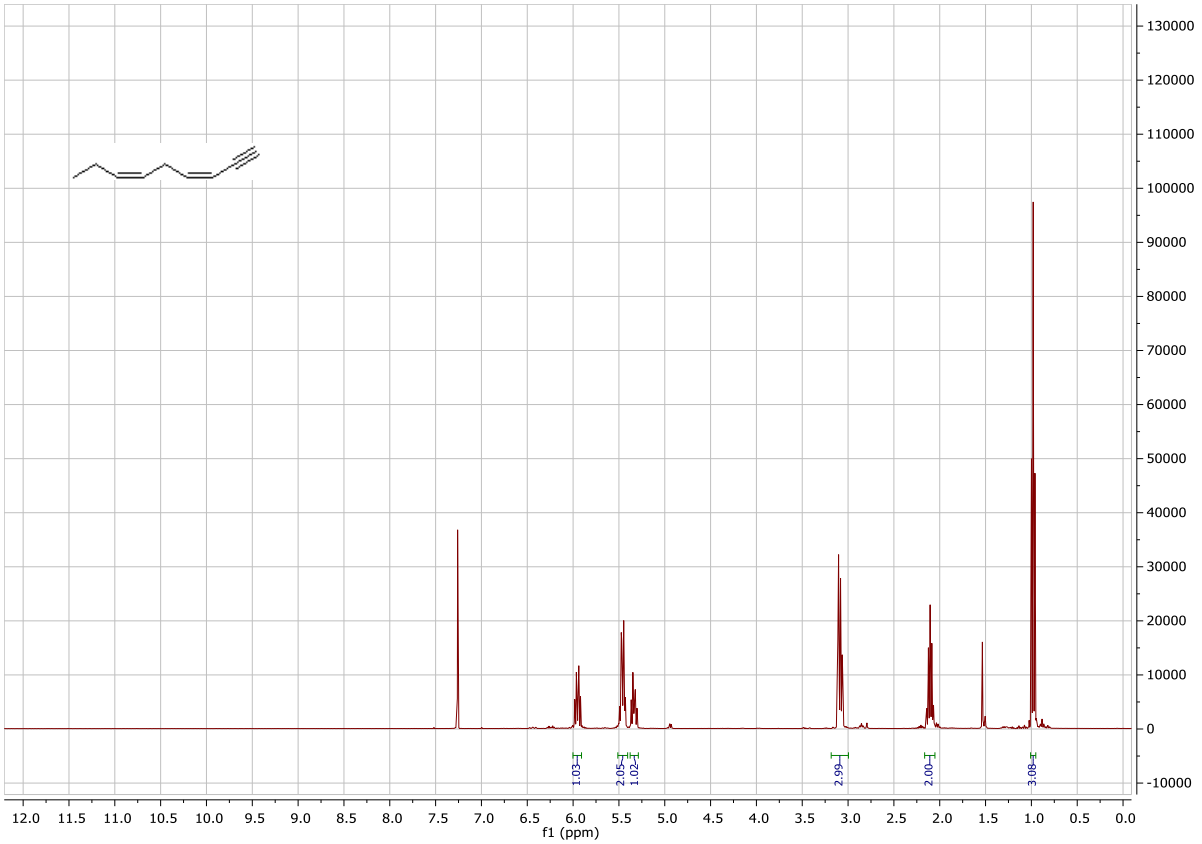

Figure 5.12 ^{1}H NMR spectrum of compound **206**.

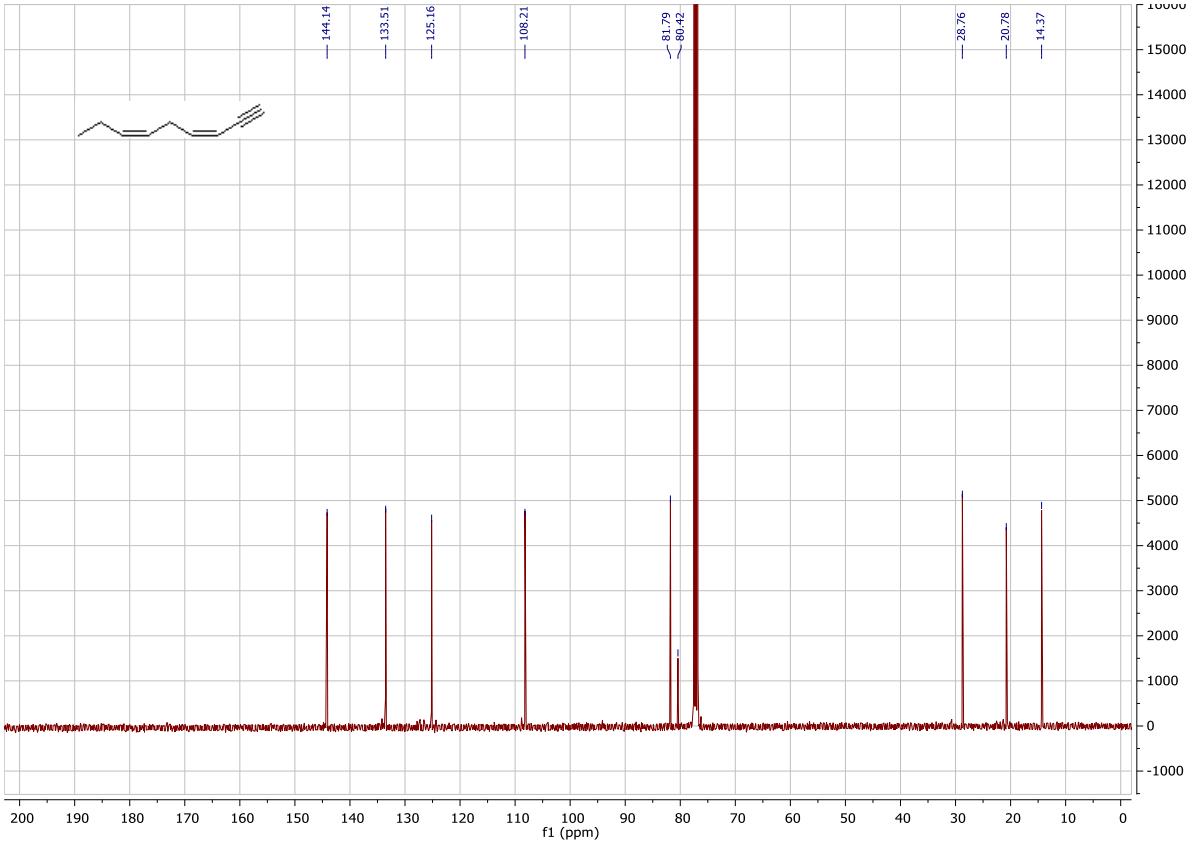

Figure 5.13 ^{13}C NMR spectrum of compound **206**.

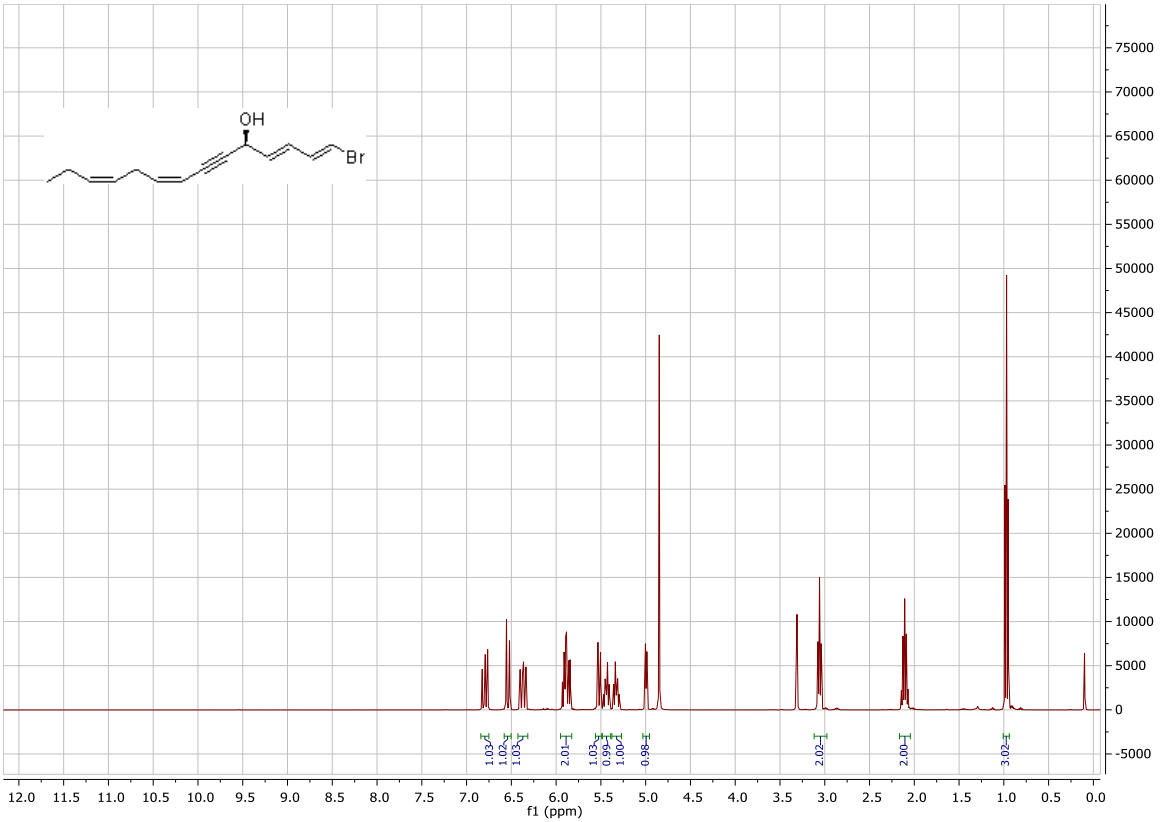

Figure 5.14 ^{1}H NMR spectrum of compound **212**.

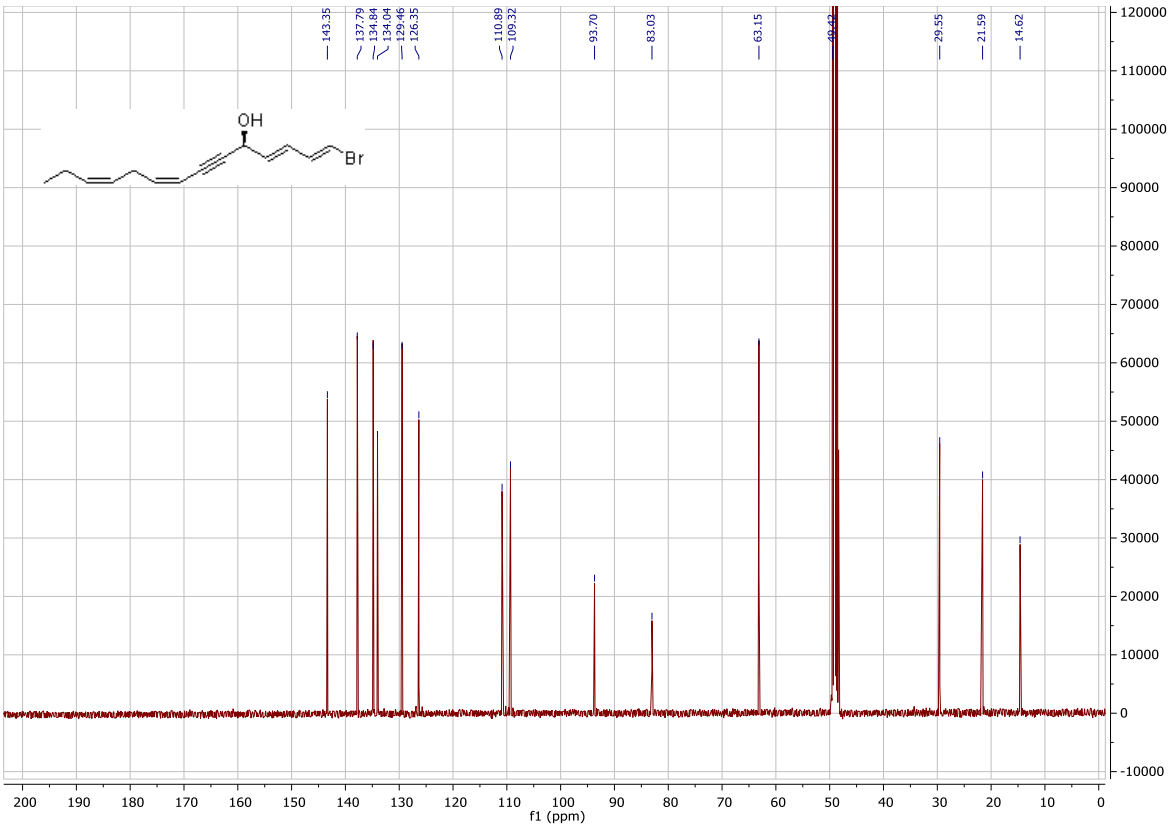

Figure 5.15 ^{13}C NMR spectrum of compound **212**.

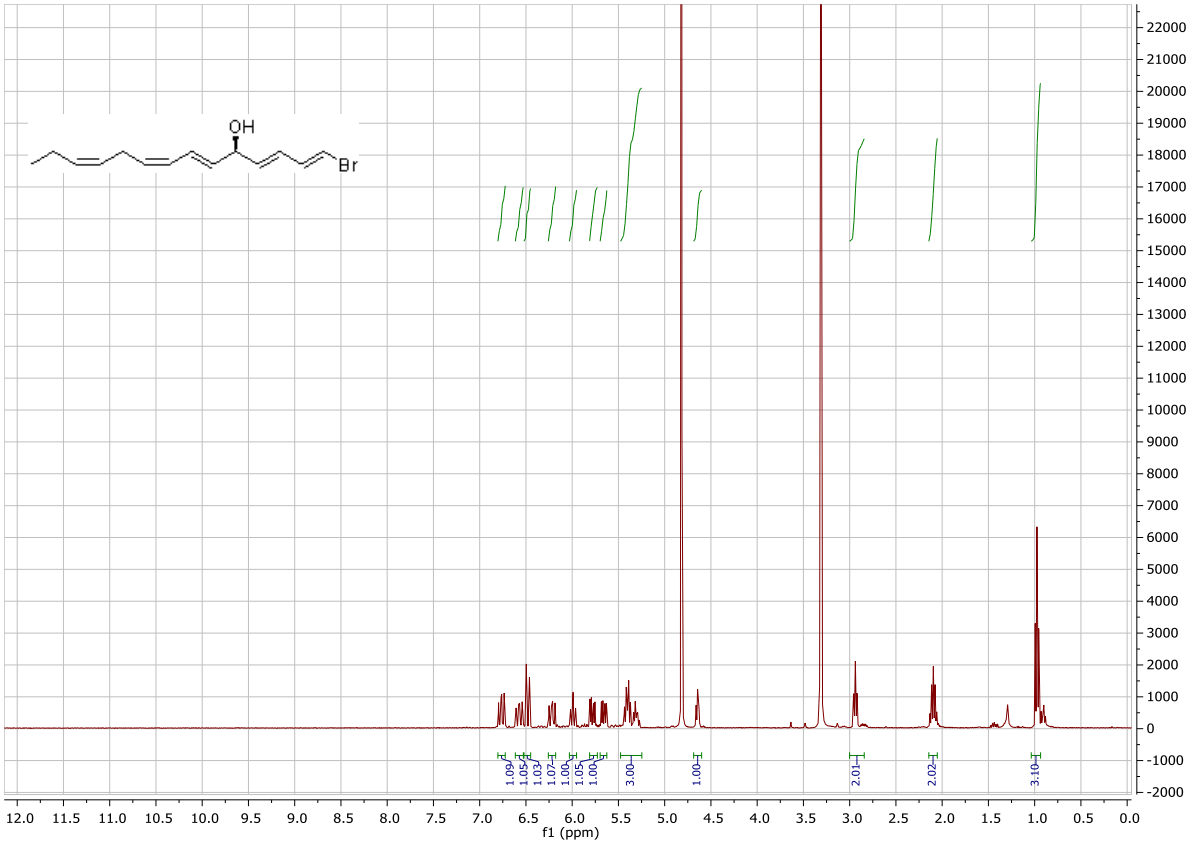

Figure 5.16 ^{1}H NMR spectrum of compound **221**.

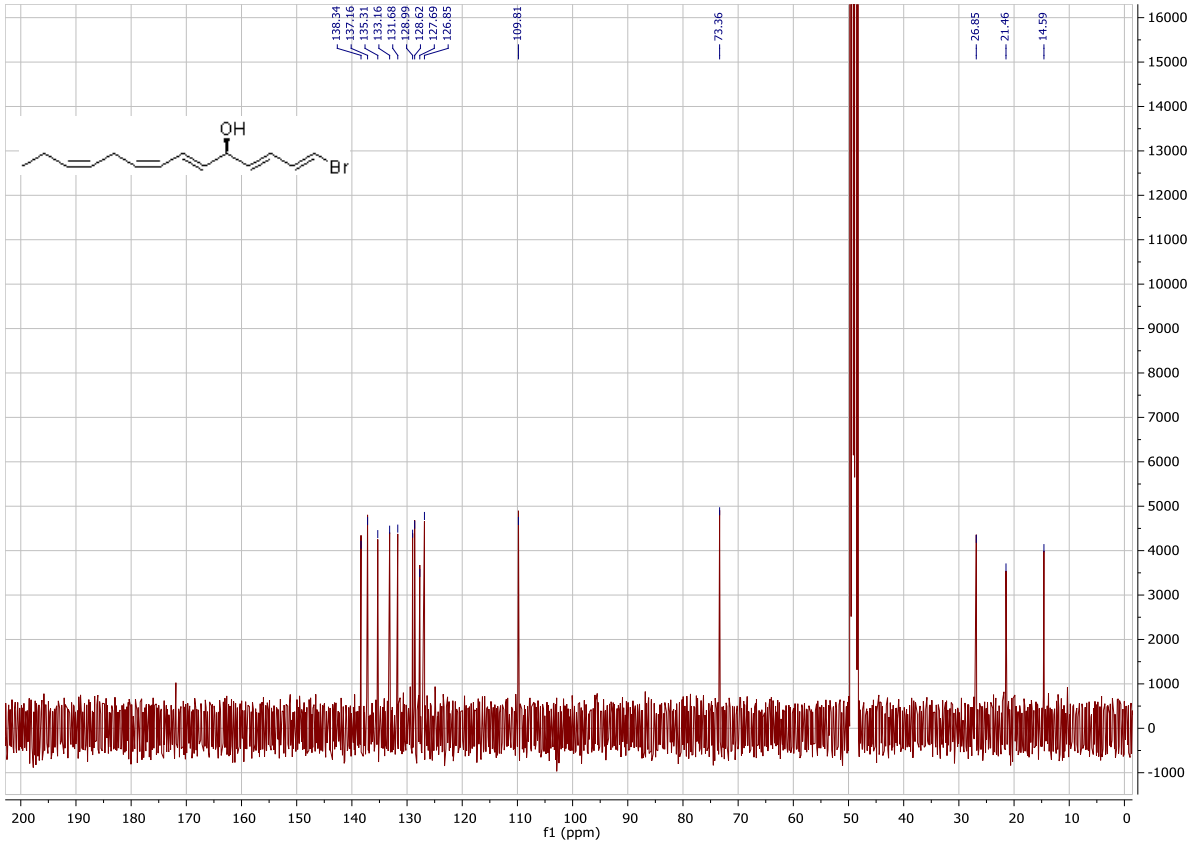

Figure 5.17 ^{13}C NMR spectrum of compound **221**.

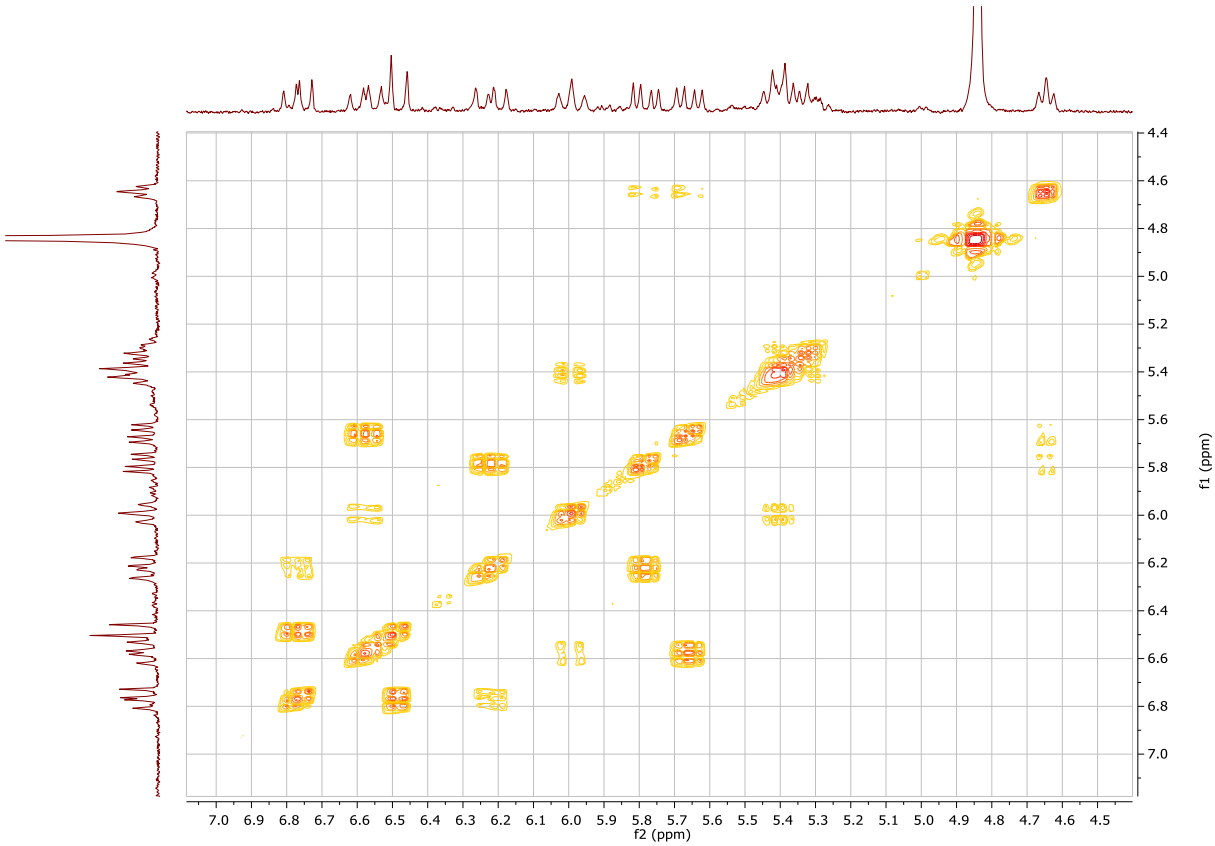

Figure 5.18 COSY spectrum of compound **221**.

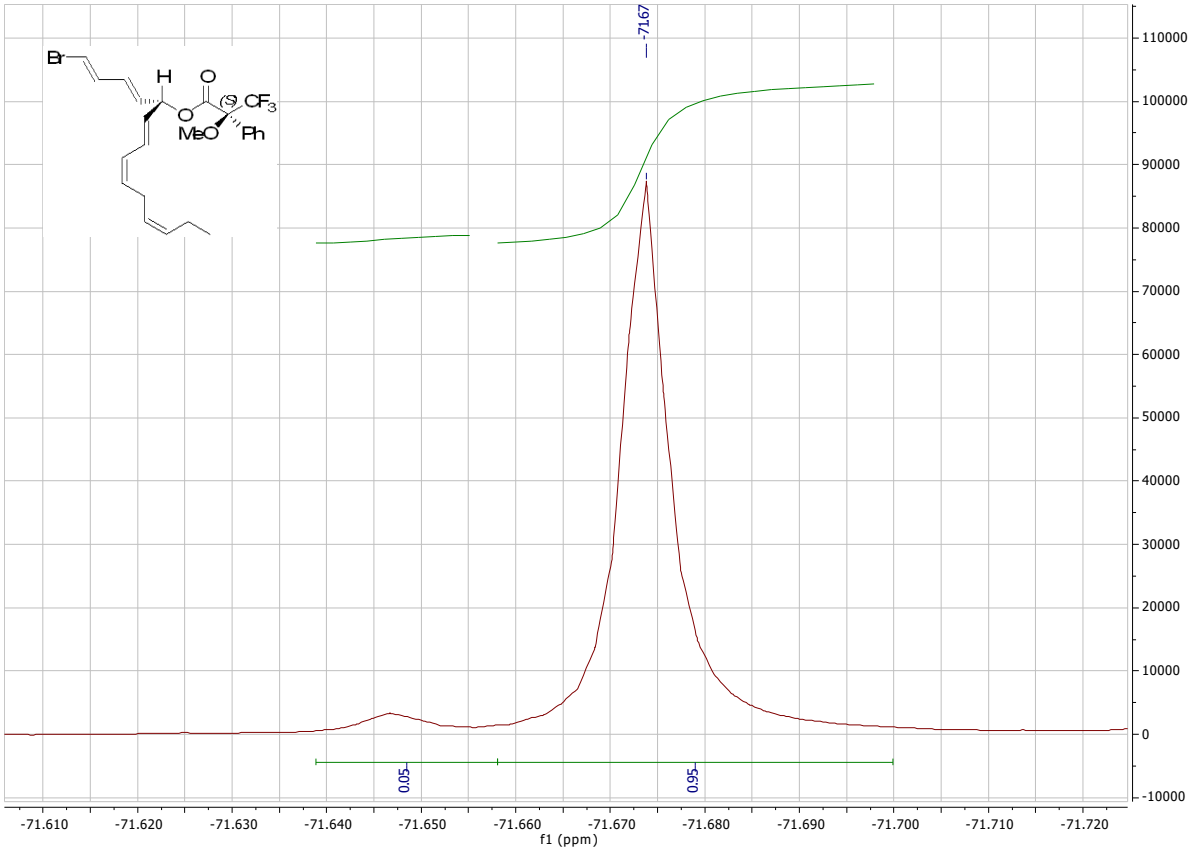

Figure 5.19 ^{19}F NMR spectrum of compound *S*-Mosher ester.

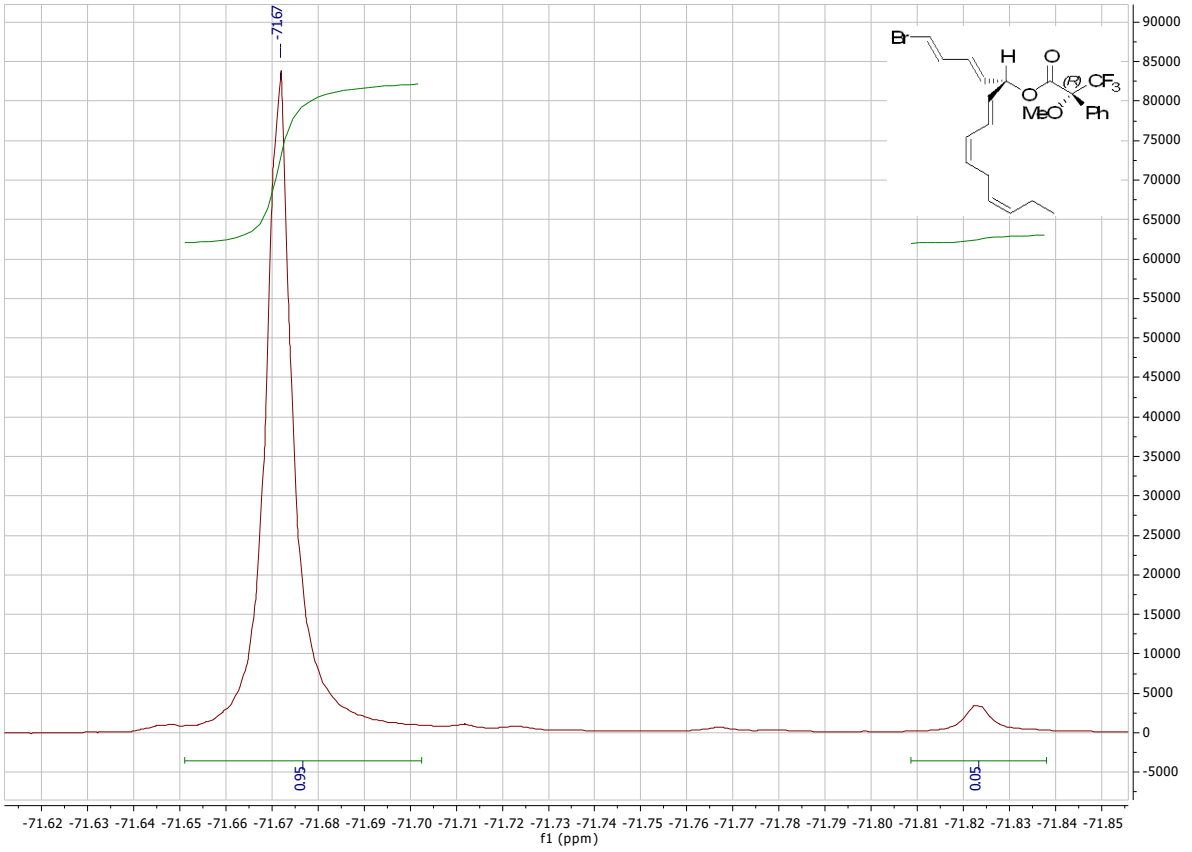

Figure 5.20 ^{19}F NMR spectrum of compound *R*-Mosher ester.

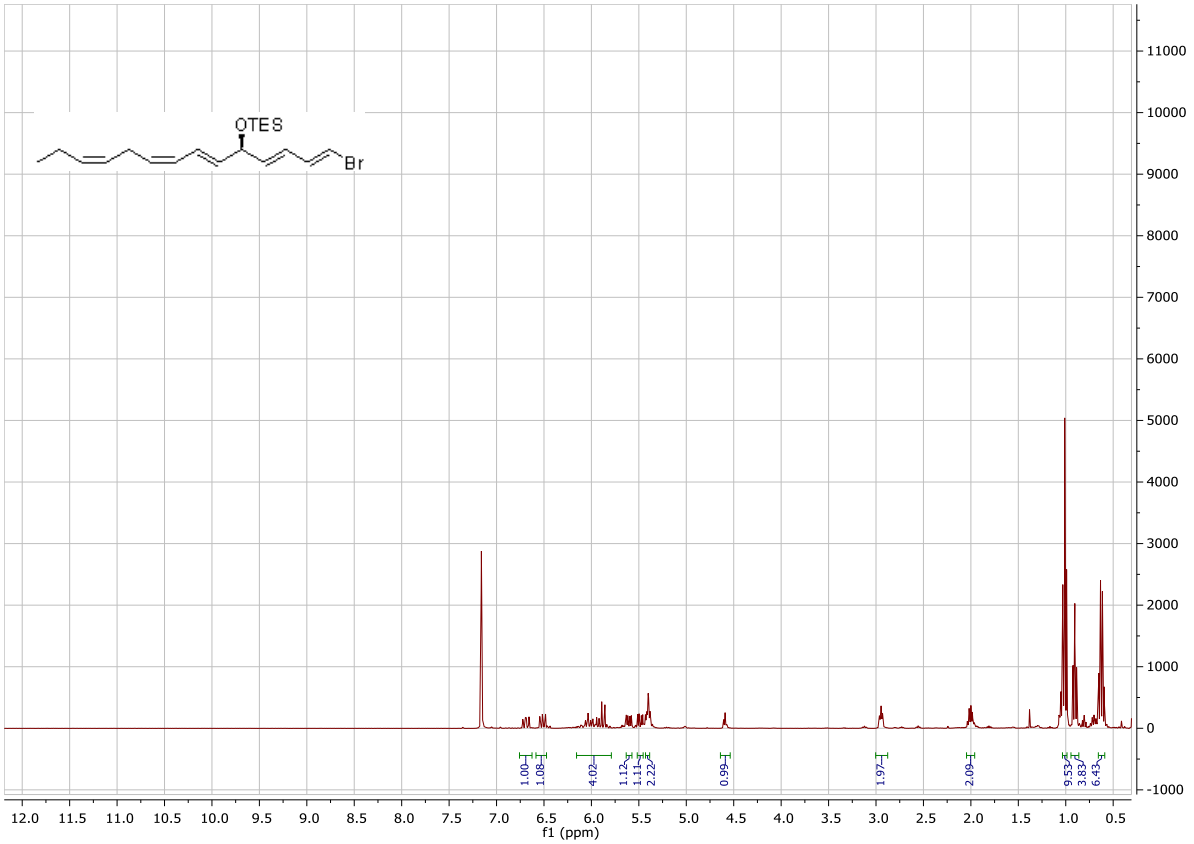

Figure 5.21 ^{1}H NMR spectrum of compound **204**.

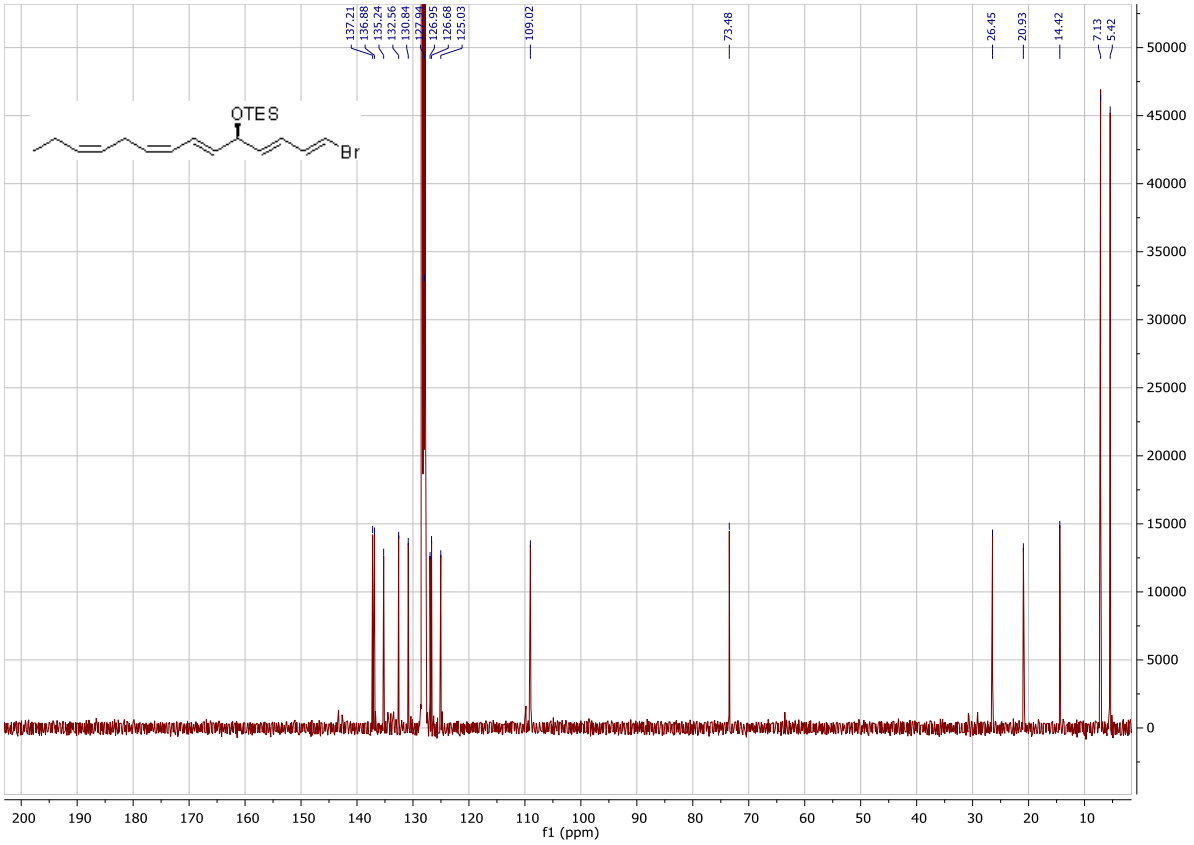

Figure 5.22 ^{13}C NMR spectrum of compound **204**.

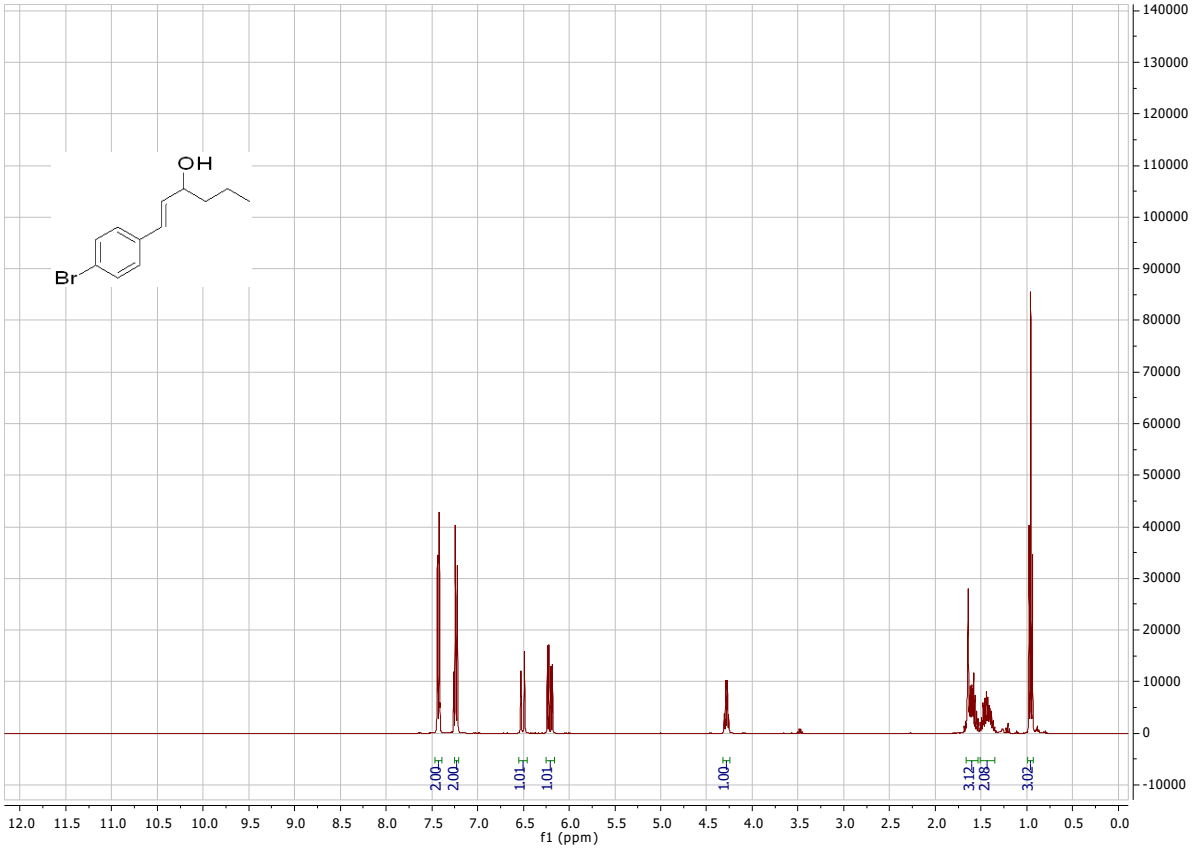

Figure 5.23 ^{1}H NMR spectrum of compound **223**.

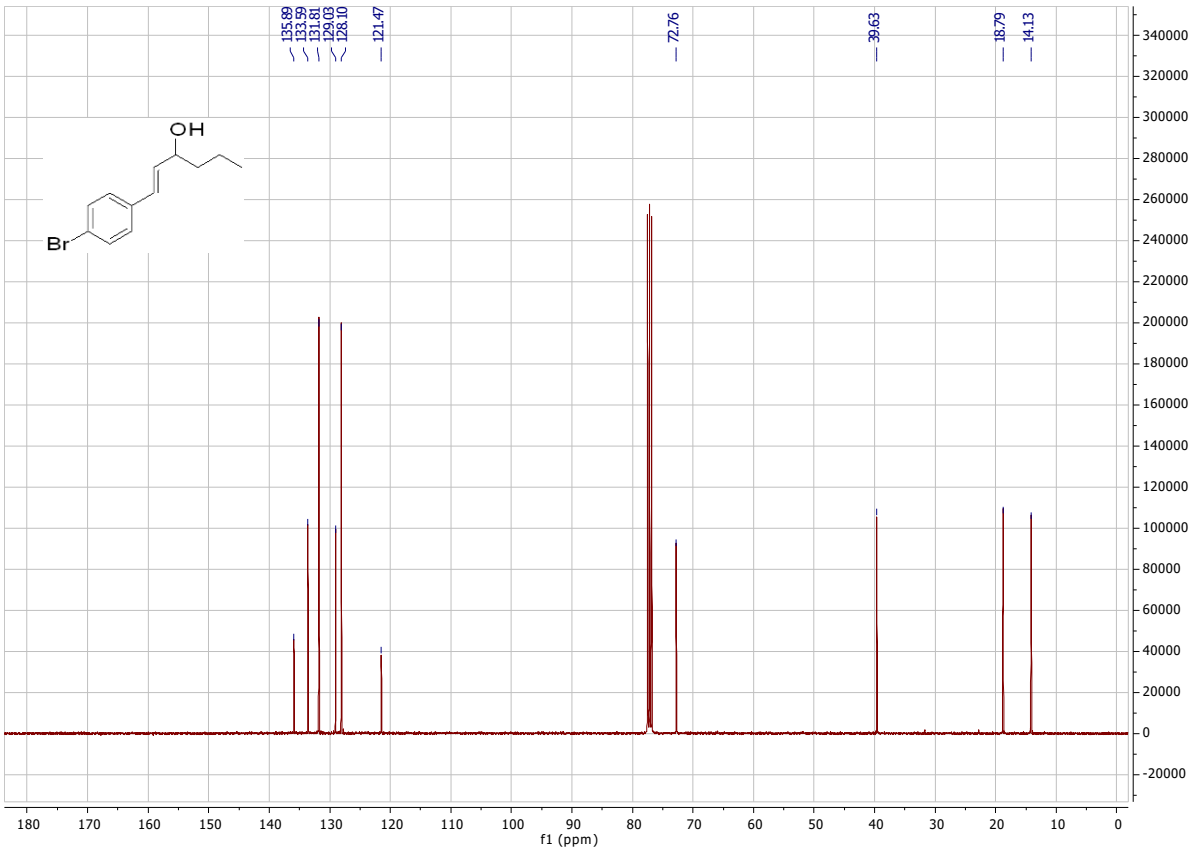

Figure 5.24 ^{13}C NMR spectrum of compound **223**.

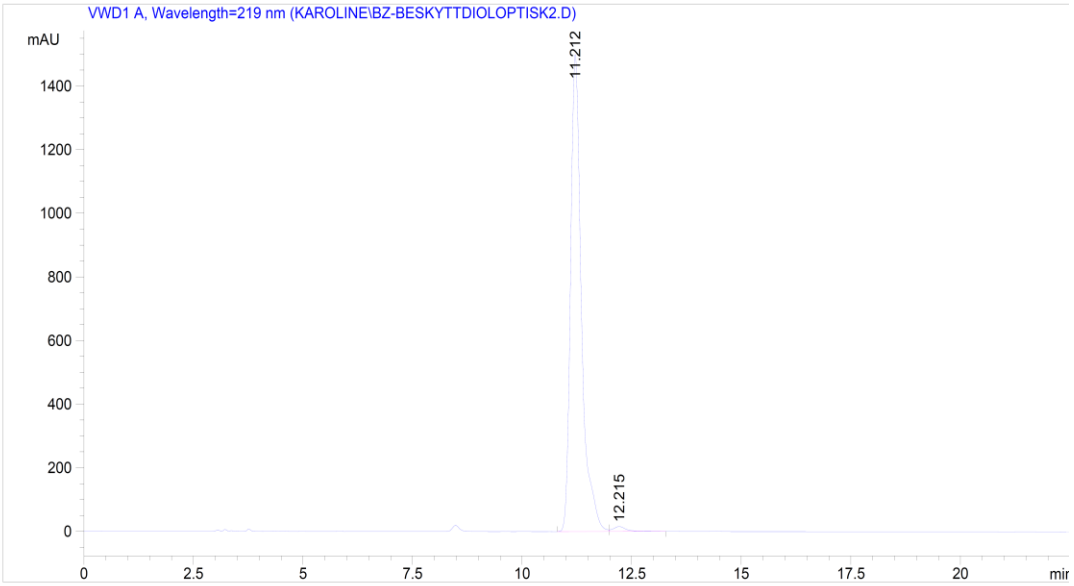


```
=====================================================================
                      Area Percent Report
=====================================================================

Sorted By             :      Signal
Multiplier            :      1.0000
Dilution              :      1.0000
Use Multiplier & Dilution Factor with ISTDs


Signal 1: VWD1 A, Wavelength=219 nm

Peak RetTime Type  Width     Area      Height     Area
  #   [min]        [min]  mAU   *s   [mAU   ]      %
----|-------|----|-------|----------|----------|--------|
   1  11.212 BV    0.2619 2.59915e4  1499.91150  98.7338
   2  12.215 VB    0.3148  333.31683   15.51127   1.2662

Totals :                  2.63248e4  1515.42277


=====================================================================
                      *** End of Report ***
```

Figure 5.25 HPLC chromatogram of optical **246**.

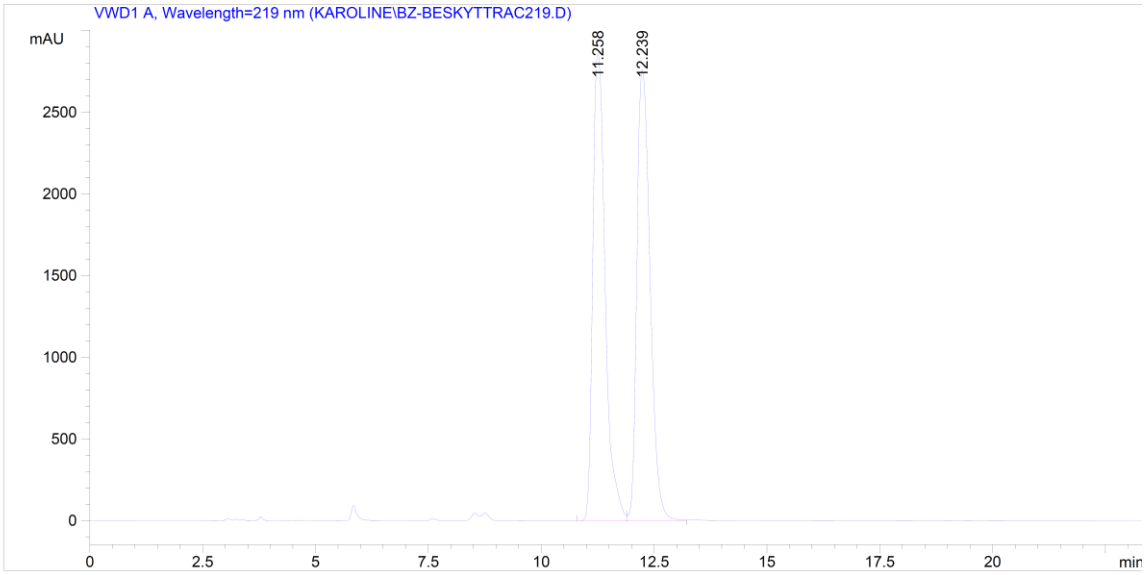


```
=====================================================================
                      Area Percent Report
=====================================================================

Sorted By             :      Signal
Multiplier            :      1.0000
Dilution              :      1.0000
Use Multiplier & Dilution Factor with ISTDs


Signal 1: VWD1 A, Wavelength=219 nm

Peak RetTime Type  Width     Area      Height     Area
  #   [min]        [min]  mAU   *s    [mAU   ]      %
----|-------|----|-------|----------|----------|--------|
   1  11.258 VV    0.2955 5.46120e4  2861.31934  49.2448
   2  12.239 VV    0.3195 5.62869e4  2759.36768  50.7552

Totals :                  1.10899e5  5620.68701


=====================================================================
                      *** End of Report ***
```

Figure 5.26 HPLC chromatogram of racemic **246**.

References

1. E. J. Corey.; S. W. Wright, *J. Org. Chem.*, 1990, **55**, 1670-1673.
2. G.-Y. Li.; C.-M. Che, *Org. Lett.*, 2004, **6**, 1621-1623.
3. M. J. Gorczynski.; J. Huang.; S. B. King, *Org. Lett.*, 2006, **8**, 2305-2308.
4. W. J. Lees.; G. M. Whitesides, *J. Org. Chem.*, 1993, **58**, 1887-1894.
5. J. Becher, *Org. Synth.*, 1979, **59**, 79-84.
6. D. Soullez.; G. Plé.; L. Duhamel, *J. Chem. Soc., Perkin Trans 1*, 1997, **11**, 1639-1646.
7. K. Kojima.; K. Koyama.; S. Amemiya, *Tetrahedron*, 1985, **41**, 4449-4462.
8. R. Detterbeck.; A. Guggisberg.; K. Popaj.; M. Hesse, *Helv. Chim. Acta*, 2002, **85**, 1742-1758.
9. T. R. Hoye.; C. S. Jeffrey.; F. Shao, *Nat. Protoc.*, 2007, **2**, 2451-2458.
10. M. Yus.; F. Foubelo, *Science of Synthesis*, 2010, **47b**, 1067-1094.

Appendix

Paper IV:

Synthesis of 13(R)-Hydroxy-7Z,10Z,13R,14E,16Z,19Z Docosapentaenoic Acid (13R-HDPA) and Its Biosynthetic Conversion to the 13-Series Resolvins

Karoline G. Primdahl, Marius Aursnes, Mary E. Walker, Roman A. Colas, Charles N. Serhan, Jesmond Dalli, Trond V. Hansen, Anders Vik.

Journal of Natural Products. **2016**, *79*, 2693-2702.

JOURNAL OF NATURAL PRODUCTS

Article

pubs.acs.org/jnp

Synthesis of 13(*R*)-Hydroxy-7*Z*,10*Z*,13*R*,14*E*,16*Z*,19*Z* Docosapentaenoic Acid (13*R*-HDPA) and Its Biosynthetic Conversion to the 13-Series Resolvins

Karoline G. Primdahl,[†,‡,§] Marius Aursnes,[†] Mary E. Walker,[‡] Romain A. Colas,[‡] Charles N. Serhan,[⊥] Jesmond Dalli,[*,‡] Trond V. Hansen,[*,†] and Anders Vik[*,†]

[†]School of Pharmacy, Department of Pharmaceutical Chemistry, University of Oslo, P.O. Box 1068 Blindern, N-0316 Oslo, Norway

[‡]William Harvey Research Institute, Barts and The London School of Medicine and Dentistry, Queen Mary University of London, Charterhouse Square, London, UK, EC1M 6BQ

[⊥]Center for Experimental Therapeutics and Reperfusion Injury, Department of Anesthesiology, Perioperative and Pain Medicine, Harvard Institutes of Medicine, Brigham and Women's Hospital and Harvard Medical School, Boston, Massachusetts 02115, United States

Supporting Information

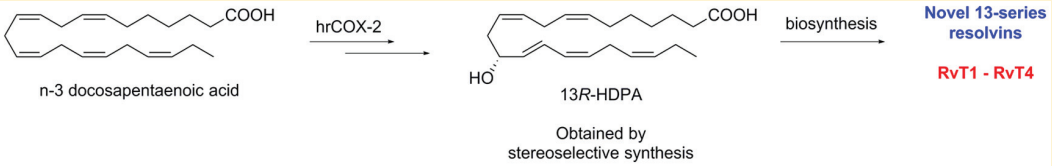

ABSTRACT: Specialized pro-resolving lipid mediators are biosynthesized during the resolution phase of acute inflammation from n-3 polyunsaturated fatty acids. Recently, the isolation and identification of the four novel mediators denoted 13-series resolvins, namely, RvT1 (**1**), RvT2 (**2**), RvT3 (**3**) and RvT4 (**4**), were reported, which showed potent bioactions characteristic for specialized pro-resolving lipid mediators. Herein, based on results from LC/MS-MS metabololipidomics and the stereoselective synthesis of 13(*R*)-hydroxy-7*Z*,10*Z*,13*R*,14*E*,16*Z*,19*Z* docosapentaenoic acid (13*R*-HDPA, **5**), we provide direct evidence that the four novel mediators **1**−**4** are all biosynthesized from the pivotal intermediate **5**. The UV and LC/MS-MS results from synthetic 13*R*-HDPA (**5**) matched those from endogenously and biosynthetically produced material obtained from *in vivo* infectious exudates, endothelial cells, and human recombinant COX-2 enzyme. Stereochemically pure **5** was obtained with the use of a chiral pool starting material that installed the configuration at the C-13 atom as *R*. Two stereoselective *Z*-Wittig reactions and two *Z*-selective reductions of internal alkynes afforded the geometrically pure alkene moieties in **5**. Incubation of **5** with isolated human neutrophils gave all four RvTs. The results presented herein provide new knowledge on the biosynthetic pathways and the enzymatic origin of RvTs **1**−**4**.

During the resolution of acute inflammation, a novel group of host-protective chemical mediators biosynthesized from the n-3 polyunsaturated fatty acids (PUFAs) eicosapentaenoic acid (EPA) and docosahexaenoic acid (DHA), termed specialized pro-resolving mediators (SPMs)[1] and their bioactive peptide-conjugates,[2] are resolution mediators and control tissue regeneration and promote the return to homeostasis.[3,4] The resolvins, protectins, and maresins constitute individual families of SPMs that are formed via distinct biosynthetic pathways.[4] During the resolution of acute inflammation, SPMs exhibit a wide range of potent pro-resolving actions, which include promoting the clearance of bacteria and apoptotic cells, counter-regulating the production and actions of pro-inflammatory mediators, and stimulating the resolution of inflammation.[5] The PUFA n-3 docosapentaenoic acid (n-3 DPA) is an intermediate in the biosynthesis of DHA from EPA and is also a precursor to novel bioactive mediators.[6−8] The isolation and structure elucidation of four new host-protective molecules was recently reported. These compounds were termed 13-series resolvins (RvTs), namely, RvT1 (**1**), RvT2 (**2**), RvT3 (**3**) and RvT4 (**4**), given that they share a hydroxy functionality at carbon 13.[8]

These four enzymatically oxygenated products are biosynthesized during neutrophil-endothelial cocultures and are present, after sterile inflammation as well as infection, in both human and mouse tissues. These four new natural products are biosynthesized from n-3 DPA during neutrophil-endothelial interactions where endothelial cyclooxygenase-2 (COX-2) converts n-3 docosapentaenoic acid to 13-hydro(peroxy)-7*Z*,10*Z*,13,14*E*,16*Z*,19*Z* docosapentaenoic acid that is then thought to react rapidly, via COX-2-mediated peroxidase activity, into 13(*R*)-hydroxy-7*Z*,10*Z*,13*R*,14*E*,16*Z*,19*Z* docosapentaenoic acid (Scheme 1).[8] The RvTs contain conjugated diene and triene moieties, as well as isolated *Z*-olefins, in

Received: July 8, 2016
Published: October 5, 2016

DOI: 10.1021/acs.jnatprod.6b00634
J. Nat. Prod. 2016, 79, 2693−2702

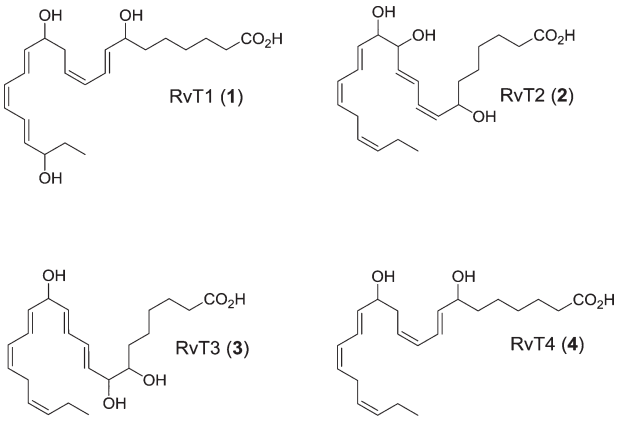

Scheme 1. Chemical Structure of 13*R*-HDPA (5) and Outline of Its Proposed Biosynthesis from n-3 DPA

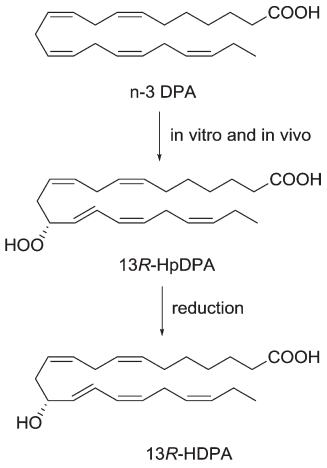

addition to the common hydroxy functionality at C-13. The RvT family of mediators demonstrated potent protective actions increasing mice survival during *Escherichia coli* (*E. coli*) infections, and regulate human and mouse phagocyte responses that result in increased bacterial phagocytosis and regulation of inflammasome components.[8]

The presence of a secondary alcohol functionality at C-13 in all four RvTs caught our attention as a common and important chemical feature that most likely is involved early in the biosynthesis of all four RvTs. LC/MS-MS-based experiments using lipid mediator metabololipidomics with materials obtained from human neutrophil-endothelial cell interactions allowed for the identification of a 13-hydroxylated C22-compound biosynthesized in human endothelial cell assays. Incubations of n-3 DPA with human recombinant cyclooxygenase-2 (hrCOX-2), together with UV experiments and chiral-phase LC-MS/MS analyses, provided evidence for the involvement of the hydroperoxide of a 13(*R*)-hydroxydocosapentaenoic acid intermediate (13*R*-HpDPA) in the biosynthesis of the 13 series resolvins.[8] Given the potency of these molecules (pM−nM) and the fact that they are produced in small amounts (pg−ng) within biological systems, it was not possible to determine the exact configurations of the double bonds or the absolute configurations of the secondary alcohols in RvTs **1**−**4**. Based on biosynthetic considerations,[4,5,9] we tentatively assigned the configurations of the double bonds as depicted.

As bacterial infections in humans remain a serious health concern due to the rise in antibiotic resistance toward existing antibacterial therapeutics, an imminent need for new treatment strategies exists.[10] Of interest toward this aim, the RvTs **1**−**4** exert anti-inflammatory and potent pro-resolving activities by regulating key innate protective responses during *E. coli* infections in mice.[8] Due to the interesting and potent biological activities of the RvTs **1**−**4**, it is of considerable interest to further investigate their biosynthetic pathways. Herein, we present direct evidence for the configurational assignment of the key biosynthetic intermediate in the RvT pathway, namely, 13*R*-HDPA (**5**), by matching material obtained from total synthesis with that isolated from (a) human endothelial cells, (b) mouse infectious exudates, and (c) human recombinant COX-2. We also demonstrate that 13*R*-HDPA is converted by human neutrophils to all four RvTs, thereby confirming the role of 13*R*-HDPA as a key biosynthetic intermediate in RvT formation.

RESULTS AND DISCUSSION

To establish evidence of the existence of 13*R*-HDPA (**5**) as a pivotal intermediate and its role in the biosynthesis of the novel 13-series resolvins (RvT **1**−**4**), stereochemically pure **5** was obtained by total synthesis. First, a synthesis of the terminal alkyne **10** from commercially available 2-pentyn-1-ol (**6**), Scheme 2, was needed. The preparation of diyne **8** was

Scheme 2. Synthesis of (*Z*)-Hept-4-en-1-yne (10)

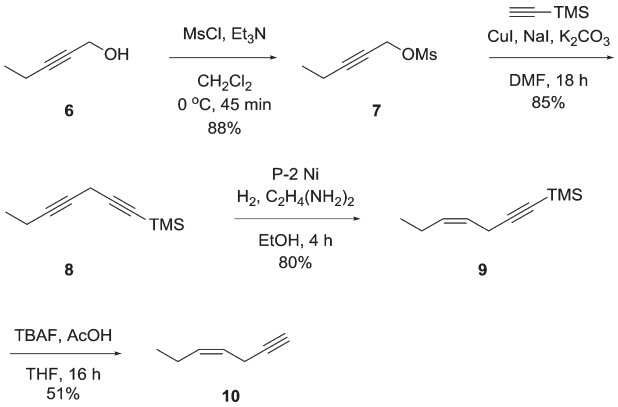

performed as previously reported.[11] Unfortunately, attempted Lindlar reduction of the internal alkyne in **8** gave no conversion to wanted **9**. However, the stereoselective *Z*-reduction of the internal alkyne was successfully achieved with P-2 nickel boride (P-2 Ni),[12,13] which provided **9** in 80% yield. Removal of the TMS-protecting group was achieved using TBAF buffered with acetic acid. Addition of acetic acid was absolutely necessary to suppress the formation of the *E*-isomer of **10**. The modest overall yield of **10** by this sequence is attributed to the high volatility of **10**.

Next, vinyl iodide **13** was prepared from commercially available (*R*)-α-hydroxy-γ-butyrolactone (**11**), via known alcohol **12**.[14] An alkyne hydrozirconation of **12**, followed by treatment with iodine, furnished the vinyl iodide **13** in fair yield (Scheme 3).

The Wittig salt **19** was prepared from cycloheptanone (**14**) in eight steps. Phosphonium salt **15** was obtained as previously reported[7] in a sequence involving a Baeyer−Villager oxidation of **14**, subsequent methanolysis of the resulting lactone,

DOI: 10.1021/acs.jnatprod.6b00634
J. Nat. Prod. 2016, 79, 2693−2702

Scheme 3. Synthesis of Vinyl Iodide 13

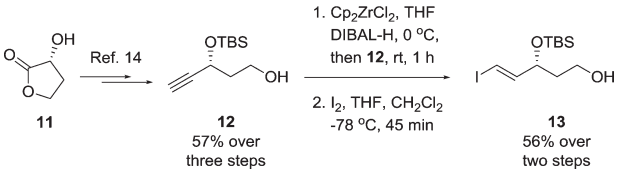

11 **12** 57% over three steps **13** 56% over two steps

conversion of the formed primary alcohol to its iodide that was reacted with triphenylphospine to give **15**. A Wittig reaction of **15** with TBS-protected 3-hydroxypropanal (**16**) and subsequent removal of the silyl group[15] afforded the alcohol **17**. This was then converted into the corresponding iodide **18** via an Appel reaction, followed by treatment with triphenylphospine in refluxing acetonitrile that afforded the desired Wittig salt **19** in 81% yield over the two steps (Scheme 4).

Scheme 4. Synthesis of Wittig Salt 19

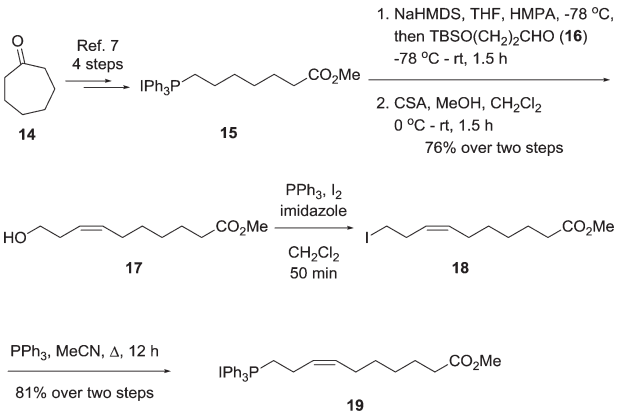

14 **15** **17** **18** **19**

Then terminal alkyne **10** and vinyl iodide **13** were assembled in a Sonogashira cross-coupling reaction, which produced the conjugated enyne **20** in 86% yield. Oxidation of the alcohol in **20** gave aldehyde **21**, which was immediately reacted in a *Z*-selective Wittig reaction with the ylide of Wittig salt **19**; the latter was generated at −78 °C after treatment with NaHMDS. This afforded the ester **22** in 77% yield. Finally, after removal of the silyl group with in situ-generated HCl from AcCl in MeOH, the internal alkyne in **23** was stereoselectively reduced using the Boland protocol,[16] furnishing the conjugated *E,Z*-diene **24** in 67% yield (Scheme 5). The chemical purity of ester **24** was >98%. Saponification with LiOH[17] afforded chemically (>98%) and stereochemically pure 13*R*-HDPA (**5**) (>99% ee) according to LC-MS/MS analyses using a chiral-phase column (Figure 1).

We next tested whether synthetic **5** matched authentic 13*R*-HDPA (**5**). We first isolated material from human umbilical endothelial cells[8] that in RP-HPLC-MS-MS metabololipidomics[18] gave a sharp peak with retention time (R_T) of 17.5 min (Figure 1A). 13-HDPA from infectious exudates and from hrCOX-2 also eluted with R_T 17.5 min (Figure 1B,C). The same retention time was observed (R_T = 17.5 min) for synthetic 13*R*-HDPA (**5**), Figure 1D. Moreover, coinjection of biological 13-HPDA with synthetic material of **5** gave a single sharp peak with R_T 17.5 min (Figure 1E).

Then we sought evidence for the absolute configuration at C-13 and that synthetic material of **5** eluted with biological 13*R*-HDPA in a chiral environment. In all biological systems tested,

Scheme 5. Synthesis of 13*R*-HDPA (5)

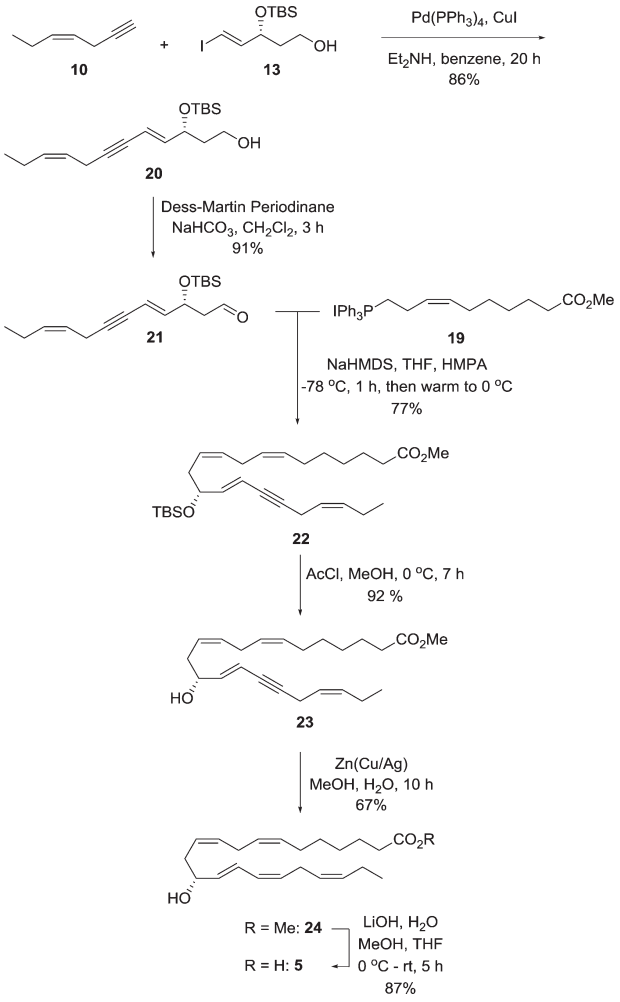

13*R*-HDPA was the main product giving a sharp peak at R_T 5.1 min in a chiral-phase chromatography-tandem mass spectrometry system (Figures 2A−C). Synthetic 13*R*-HDPA (**5**) also gave R_T 5.1 min (Figure 2D), and when this material was coinjected with biological material, a sharp peak only at R_T 5.1 min was observed (Figure 2E). Of note, in the endothelial cell and recombinant enzyme incubations, we also identified the *S*-isomer of 13-HDPA that was found to be the minor product in both incubations forming ∼10% of the overall 13-HDPA levels in the HUVEC incubations (Figure 2A) and <5% in the recombinant enzyme incubations (Figure 2C). This is in accordance with published findings that COX-2 stereoselectively converts n-3 DPA to the *R*-configured stereoisomer with a small proportion of the substrate being converted to the *S*-stereoisomer.[8] This is also observed for other enzymes that lipoxygenate their substrate.[19] Altogether, these efforts established that the synthetic material of **5** eluted together with biologically produced 13-HDPA and that the absolute configuration at C-13 is *R* for biogenic 13-HDPA (**5**).

To obtain further evidence for matching physical properties of authentic and synthetic material of **5**, MS-MS spectra for 13*R*-HDPA from HUVEC incubations, infectious exudates and synthetic material of **5** were recorded, that gave essentially identical MS-MS spectra including fragments at *m/z* 327, 301, 283, 223, 205, and 195 (Figure 3A−C).

DOI: 10.1021/acs.jnatprod.6b00634
J. Nat. Prod. 2016, 79, 2693−2702

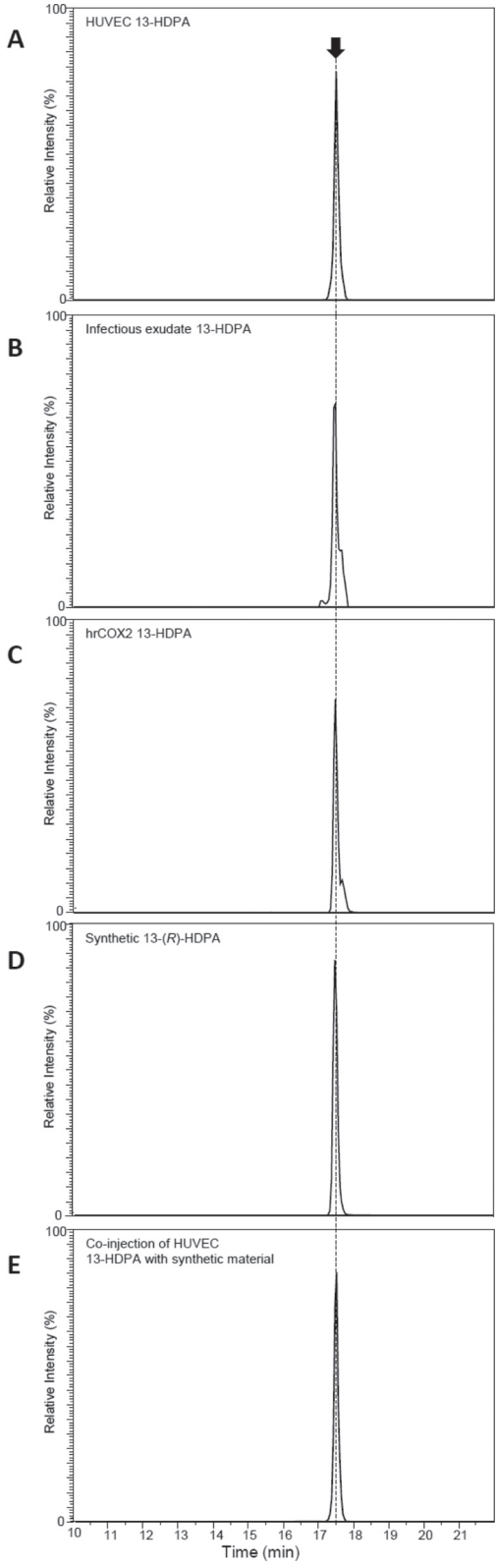

Figure 1. 13-HDPA MRM chromatograms from (A) endothelial cells, (B) infectious exudates, (C) hrCOX-2, and (D) synthetic material of **5**. (E) Coinjection of endothelial and synthetic **5**.

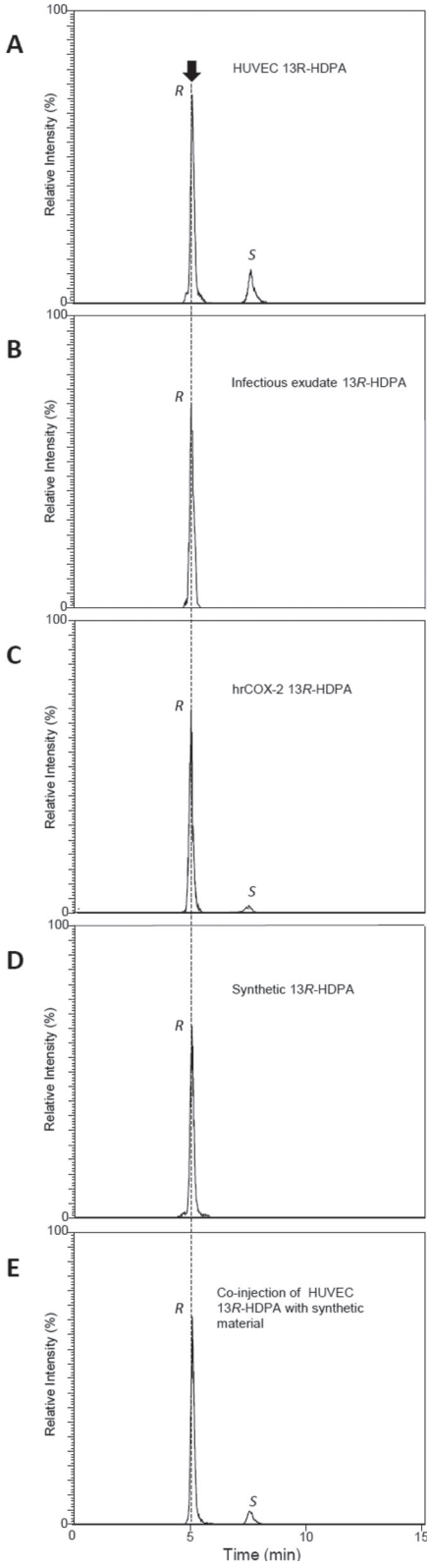

Figure 2. 13-HDPA chiral LC-MS-MS derived from (A) endothelial cells, (B) infectious exudates, (C) hrCOX-2, and (D) synthetic material. (E) Coinjection of endothelial and synthetic 13*R*-HDPA.

DOI: 10.1021/acs.jnatprod.6b00634
J. Nat. Prod. 2016, 79, 2693−2702

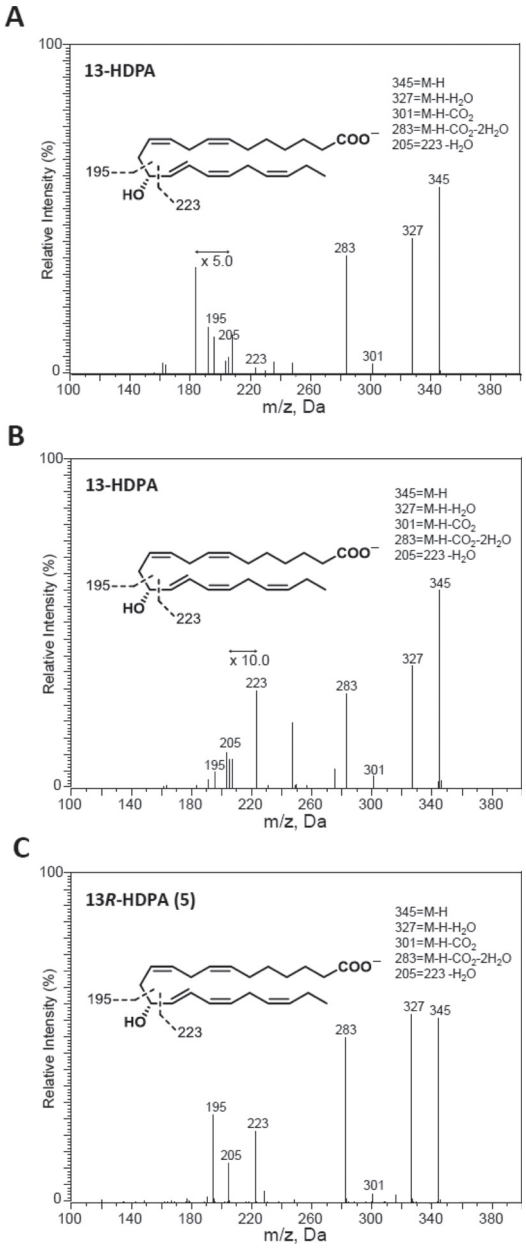

Figure 3. MS-MS spectra employed in the identification of 13-HDPA from (A) endothelial cells, (B) infectious exudates, and (C) synthetic material. n = 3 endothelial cell donors, n = 3 mouse exudates, and n = 3 for synthetic material.

Assessment of the UV chromophore of biogenic 13*R*-HDPA from hrCOX-2 and that of the synthetic material of **5**, both gave λ_{max}^{MeOH} of 237 nm (Figure 4A,B), adding additional confidence in our structural assignment.

We next tested whether the synthetic material **5** was a substrate for the conversion to any of the four RvTs by human neutrophils. Incubation of synthetic 13*R*-HDPA (**5**) with human neutrophils gave RvT1 (**1**), RvT2 (**2**), RvT3 (**3**), and RvT4 (**4**), as determined using both retention time (Figure 5A) and MS-MS spectra (Figure 5B). Of note in incubations with neutrophils without 13*R*-HDPA (**5**), levels of RvT1 (**1**), RvT2 (**2**), RvT3 (**3**), and RvT4 (**4**), were >75% lower than those found in incubations with the synthetic material. These results are in accordance with published findings[8] and indicate that while PMN may utilize endogenous 13*R*-HDPA, which may be esterified and released upon cellular activation as observed for other SPM biosynthetic intermediates,[20] these cells rely on other cell types to donate this key biosynthetic intermediate for RvT biosynthesis. Together these results establish the exact structural assignment of 13*R*-HDPA as 13(*R*)-hydroxy-7*Z*,10*Z*,13*R*,14*E*,16*Z*,19*Z* docosapentaenoic acid (**5**), as well as its key role in the RvT biosynthetic pathway.

CONCLUSIONS

The biosynthesis of SPMs in human physiological systems affords the E- and D-series resolvins with either a *E*,*E*,*Z*,*E*-tetraene or a *E*,*E*,*Z*-triene moiety.[2,4] On the other hand, the 13*R*-series-resolvins display diene and triene moieties, isolated *Z*-olefins, and a hydroxy functionality at C-13. These features distinguish the 13*R*-series-resolvins from the established families of SPMs (i.e., the resolvins, protectins, and maresins), as well as other oxygenated natural products of nonhuman origin.[21] Herein, we have demonstrated that the COX-2 enzyme is involved in the first step in the biosynthetic pathways of the 13*R*-series-resolvins. Most likely, as for the other SPM families,[5] the first step involves the formation of a hydroperoxide intermediate that undergoes distinct enzymatic multistep sequences to the individual natural products **1**−**4**. Because all families of SPMs,[22] as well as other oxygenated PUFA-derivatives,[21,23] exhibit potent and interesting pharmacological actions, these natural products are of interest as lead compounds toward the clinical development of different treatments for human diseases, via a novel mechanism as resolution agonists. Such efforts will be more expedient with knowledge of the complete structural assignment and biosynthetic pathways of SPMs such as the 13*R*-series resolvins.

EXPERIMENTAL SECTION

General Experimental Procedures. Optical rotations were measured using a 0.7 mL cell with a 1.0 dm path length on an Anton Paar MCP 100 polarimeter. The UV−vis spectra from 190 to 900 nm were recorded on a Shimadzu UV-1800 spectrophotometer using quartz cuvettes. NMR spectra were recorded on a Bruker AVII400 spectrometer at 400 MHz or a Bruker AVII600 spectrometer at 600 MHz for ^{1}H NMR, and at 100 or 150 MHz for ^{13}C NMR. Spectra are referenced relative to the central residual protium solvent resonance in ^{1}H NMR ($CDCl_3$ δ_H = 7.27, and MeOH-d_4 δ_H = 3.31) and the central carbon solvent resonance in ^{13}C NMR ($CDCl_3$ δ_C = 77.00 ppm, and MeOH-d_4 = δ_C = 49.00). High-resolution mass spectra were recorded on a Waters Prospec Q spectrometer using ES as the method of ionization. Thin-layer chromatography was performed on silica gel 60 F254 aluminum-backed plates fabricated by Merck. Flash column chromatography was performed on silica gel 60 (40−63 μm) produced by Merck. HPLC analyses for chemical purities were performed on an Agilent Technologies 1200 Series instrument with diode array detector set at 254 nm and equipped with a C18 stationary phase (Eclipse XDB-C18 5 μm 4.6 × 150 mm), applying the conditions stated. GLC-analyses were performed on an Agilent Technologies 7820A GC instrument with split injection, FID detector and equipped with an Agilent J&W HP-5 GC column (30 m × 0.32 mm, 0.25 μm) applying the conditions stated. Unless stated otherwise, all commercially available reagents and solvents were used in the form they were supplied without any further purification. All reactions were performed under an argon atmosphere, unless otherwise stated. The stated yields are based on isolated material. Liquid chromatography (LC)-grade solvents were purchased from Fisher Scientific. The Eclipse Plus C18 column (100 × 4.6 mm × 1.8 μm) was obtained from Agilent and C18 SPE columns were from Waters. Commercially available lipid mediators were obtained from Cayman Chemical.

DOI: 10.1021/acs.jnatprod.6b00634
J. Nat. Prod. 2016, 79, 2693−2702

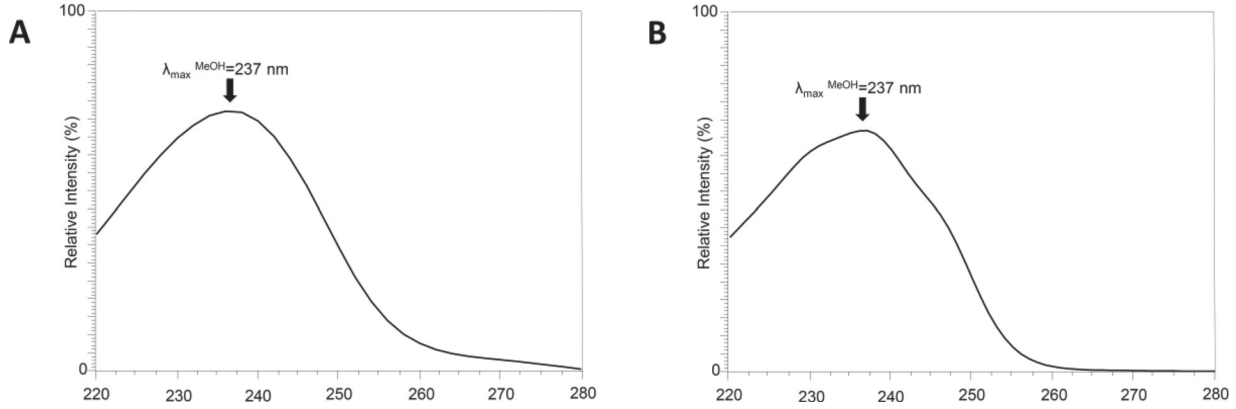

Figure 4. UV spectra for (A) hrCOX-2 13-HDPA and (B) synthetic 13*R*-HDPA (**5**).

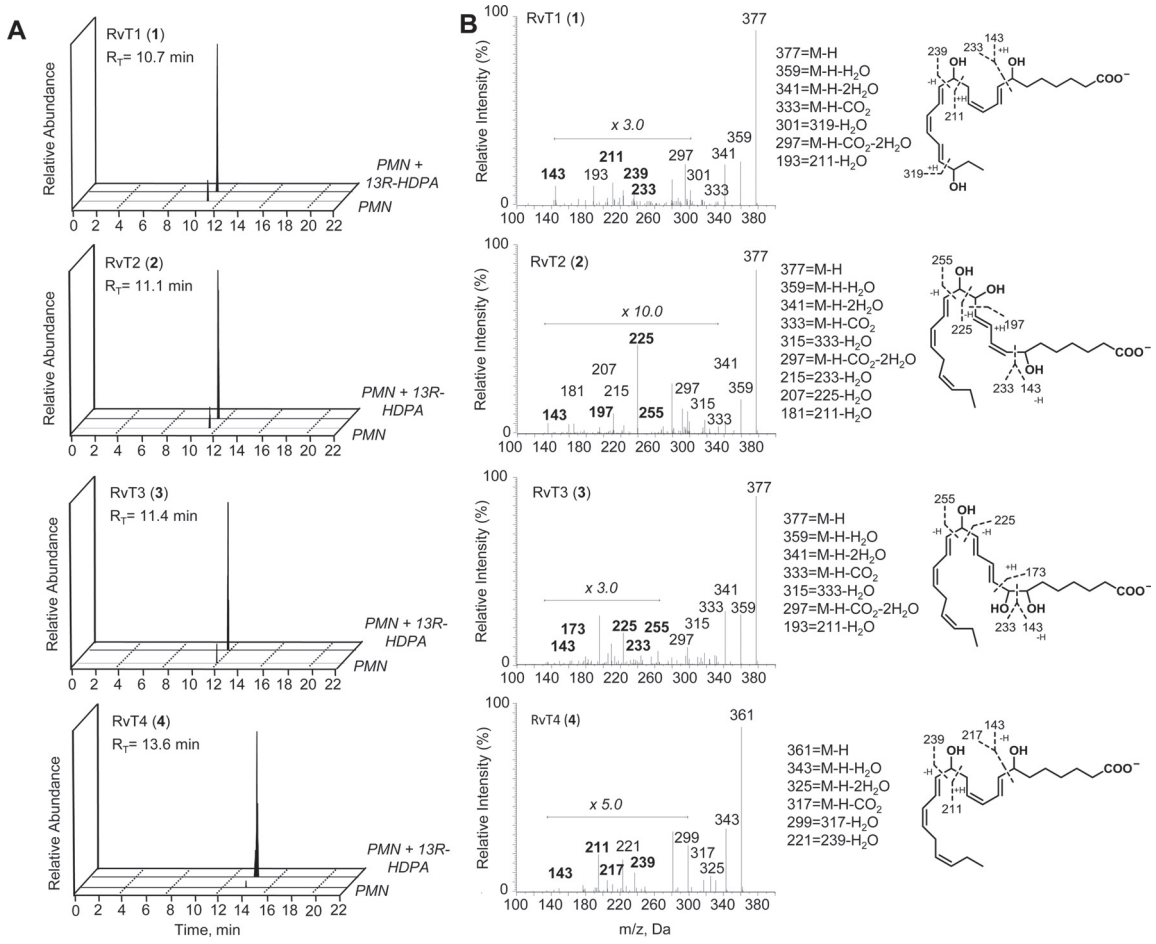

Figure 5. Human neutrophils convert 13*R*-HDPA (**5**) to RvT1−4 (**1**−**4**). Human neutrophils were isolated from peripheral blood of healthy donors and incubated (2×10^7 cells/mL) with or without 13*R*-HDPA (**5**) (45 min, 37 °C, 2 μM A23187, PBS, pH = 7.45). Incubations were quenched with two volumes of ice cold MeOH and products extracted and profiled using lipid mediator metabololipidomics. (A) MRM chromatograms for each of the RvT1−4 with relative abundances to their levels in each of the incubations. (B) MS-MS spectra employed in the identification of RvT1 (**1**), RvT2 (**2**), RvT3 (**3**) and RvT4 (**4**). Results are representative of n = 3 healthy volunteers.

*(Z)-Hept-4-en-1-yn-1-yltrimethylsilane (**9**).* A suspension of sodium borohydride (32.9 mg, 0.87 mmol) in EtOH (1.3 mL) was added dropwise to a flask containing nickel acetate tetrahydrate (217 mg, 0.87 mmol, 14 mol%) in EtOH (13.0 mL) at 0 °C under stirring. The reaction mixture turned black. After stirring for 15 min at room temperature, ethylenediamine (116 μL, 105 mg, 1.74 mmol) was added, and the stirring was continued for 10 min. The flask was evacuated and refilled with hydrogen gas before the skipped diyne **8**[11] was added (1.00 g, 6.09 mmol, 1.00 equiv). The reaction mixture was stirred at room temperature under hydrogen atmosphere until completion (~4 h), then filtered through a short plug of silica gel that was washed with pentane (10 mL). The filtrate was transferred to a separatory funnel and washed with H_2O (3 × 5.0 mL). The organic layer was dried ($MgSO_4$), and the solvent was removed *in vacuo*.

DOI: 10.1021/acs.jnatprod.6b00634
J. Nat. Prod. 2016, 79, 2693−2702

Purification by flash chromatography on silica gel (pentane) afforded the desired product **9** as a colorless oil. Yield: 810 mg (80%); ^{1}H NMR (400 MHz, $CDCl_3$) δ_H 5.51−5.42 (m, 1H), 5.42−5.35 (m, 1H), 2.98 (m, 2H), 2.06 (p, J = 7.5 Hz, 2H), 0.98 (t, J = 7.5 Hz, 3H), 0.15 (s, 9H). ^{13}C NMR (101 MHz, $CDCl_3$) δ_C 133.7, 123.4, 105.7, 84.2, 20.7, 18.4, 14.1, 0.3. TLC (hexane, $KMnO_4$ stain) R_f = 0.12. The spectroscopic data were in agreement with those previously reported for this compound.[24]

*(Z)-Hept-4-en-1-yne (**10**).* (*Z*)-Hept-4-en-1-yn-1-yltrimethylsilane (**9**) (700 mg, 4.21 mmol, 1.00 equiv) was added to a solution of TBAF (1.0 M in THF, 6.74 mL, 6.74 mmol, 1.60 equiv) and acetic acid (0.40 mL, 6.95 mmol). The reaction was stirred at room temperature for 16 h and quenched with H_2O (6.0 mL). Pentane (40 mL) was added, and the organic layer was washed with saturated aq $NaHCO_3$ (7.0 mL), water (10 × 7.0 mL) to remove the remaining THF, and then dried ($MgSO_4$). Pentane was removed by distillation. After distillation, the product still contained traces of solvents, but that was accounted for in the next step. Yield: 189 mg (47%); ^{1}H NMR (400 MHz, $CDCl_3$) δ_H 5.53−5.45 (m, 1H), 5.44−5.36 (m, 1H), 2.94 (m, 2H), 2.13−2.00 (m, 2H), 1.97 (t, J = 2.7 Hz, 1H), 0.99 (t, J = 7.5 Hz, 3H); ^{13}C NMR (101 MHz, $CDCl_3$) δ_C 134.0, 123.1, 83.2, 68.1, 20.6, 16.9, 14.0. The spectroscopic data were in agreement with those previously reported for this compound.[25]

*(R,E)-3-((tert-Butyldimethylsilyl)oxy)-5-iodopent-4-en-1-ol (**13**).* Compound **12** was prepared as previously reported.[14] The Schwartz's reagent was prepared *in situ* following the procedure by Huang and Negishi.[26] Cp_2ZrCl_2 (1.24 g, 4.23 mmol, 2.10 equiv) in THF (5.00 mL) was cooled to 0 °C and stirred under argon. A solution of DIBAL-H (1.0 M in THF, 4.23 mL, 4.23 mmol) was added dropwise. The resultant suspension was stirred for 30 min at 0 °C and protected from light with aluminum foil, before the terminal alkyne **12** (431 mg, 2.02 mmol, 1.00 equiv) in THF (1.00 mL) was added. The cooling bath was removed, and the reaction mixture stirred at room temperature until a homogeneous solution was observed (ca. 1 h) and then cooled to −78 °C. A solution of I_2 (665 mg, 5.24 mmol, 1.24 equiv) in THF/CH_2Cl_2 (3.00 mL, 1:1) was added. The reaction mixture was stirred 45 min before it was filtered through a plug of silica gel that was successively washed with 20% EtOAc in heptane. The solvent was removed under reduced pressure, and the crude product was purified by column chromatography on silica gel (heptane/EtOAc 8:2) to afford the vinyl iodine **13** as a pale yellow oil. Yield: 385 mg (56%); $[\alpha]_D^{20}$ + 58 (c = 0.29, MeOH); ^{1}H NMR (400 MHz, $CDCl_3$) δ_H 6.56 (dd, J = 14.4, 6.0 Hz, 1H), 6.29 (dd, J = 14.4, 1.2 Hz, 1H), 4.37 (m, 1H), 3.79 (ddd, J = 10.9, 7.9, 4.3 Hz, 1H), 3.70 (m, 1H), 2.02 (s, 1H), 1.81 (m, 1H), 1.72 (m, 1H), 0.90 (s, 9H), 0.09 (s, 3H), 0.06 (s, 3H); ^{13}C NMR (101 MHz, $CDCl_3$) δ_C 148.4, 76.5, 74.3, 59.7, 39.1, 25.9 (3C), 18.3, −4.4, −4.9;. HRESITOFMS: m/z 365.0403 [M + Na]$^+$ (calcd for $C_{11}H_{23}IO_2SiNa$, 365.0410); TLC (hexane/EtOAc 7:3, $KMnO_4$ stain) R_f = 0.37.

*Methyl (Z)-10-hydroxydec-7-enoate (**17**).* The ester **17** was prepared according to a literature procedure.[2c] The known Wittig salt **15**[7] (1.70 g, 3.19 mmol, 1.00 equiv) was dissolved in THF (42.0 mL) and HMPA (4.20 mL) and cooled to −78 °C. NaHMDS (0.60 M in toluene, 5.30 mL, 3.18 mmol, 1.00 equiv) was added dropwise, and the reaction mixture was stirred for 30−45 min. Aldehyde **6** (631 mg, 3.35 mmol, 1.05 equiv) in THF (4.20 mL) was then added dropwise, and stirring was continued for 1.5 h at −78 °C. The flask was allowed to slowly warm up to 0 °C, and the reaction was quenched with phosphate buffer (21.1 mL, pH = 7.2). The aq phase was extracted with Et_2O (2 × 20.0 mL), and the combined organic layers were dried (Na_2SO_4) and concentrated *in vacuo*. The crude material was passed through a short plug of silica that was washed with 5% EtOAc in heptane (R_f = 0.26). The crude product (868 mg, 2.76 mmol, 1.00 equiv) was dissolved in CH_2Cl_2/MeOH (1:2, 34.0 mL) and cooled to 0 °C. Camphor-10-sulfonic acid (642 mg, 2.76 mmol, 1.00 equiv) was added in one portion, and the reaction mixture was stirred for 30 min at 0 °C before it was allowed to slowly warm up to room temperature and stirred for 1 h. The reaction was quenched with saturated aq $NaHCO_3$ (33.3 mL), extracted with CH_2Cl_2 (2 × 15.0 mL), dried (Na_2SO_4), and concentrated *in vacuo*. The crude product was purified by column chromatography on silica gel (heptane/EtOAc 7:3) to afford hydroxyl methyl ester **17** as a clear oil. The chemical purity (>99%) was determined by GLC analysis: Initial temperature 100 °C, rate: 5 °C/min, final temperature 200 °C, t_r (minor) = 8.90 min, t_r (major) = 9.22 min. Yield: 483 mg (76%); ^{1}H NMR (400 MHz, MeOH-d_4) δ_H 7.08−6.90 (m, 2H), 5.21 (s, 3H), 5.09 (t, J = 7.0 Hz, 2H), 3.92−3.77 (m, 4H), 3.64 (q, J = 6.7 Hz, 2H), 3.18 (q, J = 7.3 Hz, 2H), 2.93 (m, 4H). ^{13}C NMR (101 MHz, MeOH-d_4) δ_C 176.0, 132.7, 126.9, 62.8, 51.9, 34.8, 31.8, 30.4, 29.8, 28.1, 25.9. HRMS (TOF ES$^+$): m/z 223.1305 [M + Na]$^+$ (calcd for $C_{11}H_{20}O_3Na$, 223.1310). TLC (Heptane/EtOAc 7:3, $KMnO_4$ stain): R_f = 0.23.

*Methyl (Z)-10-(iodotriphenyl-λ5-phosphanyl)dec-7-enoate (**19**).* Iodide **18** was prepared from hydroxy ester **17** (483 mg, 2.42 mmol, 1.00 equiv) according to a procedure reported by Mioskowski and co-workers[27] and used directly in the next reaction. Iodide **18** (638 g, 2.06 mmol, 1.00 equiv) was dissolved in dry MeCN (20.0 mL). Triphenylphosphine (1.08 g, 4.12 mmol, 2.00 equiv) was added, and the reaction mixture was heated to reflux for 12 h. The reaction mixture was concentrated *in vacuo*. The crude product was purified by column chromatography on silica gel (CH_2Cl_2/MeOH 95:5) to afford the Wittig salt **19** as a clear oil. Yield: 1.12 g (81%); ^{1}H NMR (400 MHz, MeOH-d_4) δ 8.00−7.64 (m, 15H), 5.56−5.42 (m, 2H), 3.63 (s, 3H), 3.57−3.45 (m, 2H), 2.49−2.38 (m, 2H), 2.28 (t, J = 7.3 Hz, 2H), 1.90 (q, J = 6.8 Hz, 2H), 1.52 (p, J = 7.4 Hz, 2H), 1.36−1.19 (m, 4H). ^{13}C NMR (101 MHz, MeOH-d_4) δ_C 175.8, 136.3 (d, $4'J_{CP}$ = 3.0 Hz, 3C), 134.9 (d, $3'J_{CP}$ = 10.0 Hz, 6C), 133.5, 131.6 (d, $2'J_{CP}$ = 12.6 Hz, 6C), 127.4 (d, $3'J_{CP}$ = 16.1 Hz), 119.8 (d, $1'J_{CP}$ = 86.2 Hz, 3C), 52.0, 34.6, 29.9, 29.6, 27.9, 25. 7, 23.0 (d, $1'J_{CP}$ = 49.2 Hz), 21.3 (d, $2'J_{CP}$ = 3.3 Hz). HRESITOFMS: m/z 445.2287 [M]$^+$ (calcd for $C_{29}H_{34}O_2P$, 445.2296); TLC (CH_2Cl_2/MeOH 95:5) R_f = 0.47.

*(R,4E,9Z)-3-((tert-Butyldimethylsilyl)oxy)dodeca-4,9-diene-6-yn-1-ol (**20**).* To a solution of vinyl iodide **13** (385 mg, 1.13 mmol, 1.00 equiv) in Et_2NH (2.50 mL) and benzene (2.20 mL) was added $Pd(PPh_3)_4$ (39.2 mg, 33.9 μmol, 3.00 mol%). The reaction mixture was stirred for 45 min in the dark before CuI (11.2 mg, 58.8 μmol, 5.00 mol%) in a minimum amount of Et_2NH was added followed by dropwise addition of alkyne **10** (213 mg) in Et_2NH (2.20 mL). After stirring for 20 h at room temperature, the reaction was quenched with a saturated aq solution of NH_4Cl (23 mL). The aq phase was extracted with Et_2O (3 × 3.0 mL) before the combined organic layers were dried (Na_2SO_4) and concentrated *in vacuo*. The crude product was purified by column chromatography on silica gel (heptane/EtOAc 8:2) to afford compound **20** as an orange oil. Yield: 299 mg (86%); $[\alpha]_D^{20}$ + 32 (c 0.40, MeOH); ^{1}H NMR (400 MHz, $CDCl_3$) δ_H 6.04 (dd, J = 15.8, 5.7 Hz, 1H), 5.65 (dq, J = 15.8, 2.1 Hz, 1H), 5.51−5.43 (m, 1H), 5.43−5.34 (m, 1H), 4.43 (q, J = 4.9 Hz, 1H), 3.78 (m, 1H), 3.68 (m, 1H), 3.05 (d, J = 6.6 Hz, 2H), 2.27 (s, 1H), 2.12−1.99 (m, 2H), 1.83 (m, 1H), 1.69 (m, 1H), 0.98 (t, J = 7.5 Hz, 3H), 0.90 (s, 9H), 0.08 (s, 3H), 0.05 (s, 3H); ^{13}C NMR (101 MHz, $CDCl_3$) δ_C 144.1, 133.7, 123.4, 110.1, 89.4, 78.2, 72.0, 59.9, 39.4, 25.9, 20.6, 18.2, 17.9, 14.1, −4.3, −4.9; HRESITOFMS: m/z 331.2063 [M + Na]$^+$ (calcd for $C_{18}H_{32}O_2SiNa$, 331.2064); TLC (hexane/EtOAc 7:3, $KMnO_4$ stain) R_f = 0.37.

*(R,4E,9Z)-3-((tert-Butyldimethylsilyl)oxy)dodeca-4,9-dien-6ynal (**21**).* Alcohol **20** (240 mg, 77.9 μmol, 1.00 equiv) was dissolved in CH_2Cl_2 (23.0 mL) before $NaHCO_3$ (375 mg, 4.46 mmol, 5.70 equiv) and Dess−Martin periodinane (406 mg, 95.7 μmol, 1.23 equiv) were added. The reaction mixture was stirred at room temperature for 3 h before saturated aq $Na_2S_2O_3$ (5.0 mL) was added to quench the reaction. The aq phase was extracted with CH_2Cl_2 (2 × 7.0 mL), and the combined organic layers were dried and concentrated *in vacuo*. The crude product was purified by column chromatography on silica gel (heptane/EtOAc 8:2) to afford aldehyde **21** as a pale yellow oil. Yield: 219 mg (91%); $[\alpha]_D^{20}$ + 19 (c 0.41, MeOH); ^{1}H NMR (400 MHz, $CDCl_3$) δ_H 9.75 (t, J = 2.3 Hz, 1H), 6.07 (dd, J = 15.8, 5.6 Hz, 1H), 5.72 (dq, J = 15.8, 2.1 Hz, 1H), 5.55−5.34 (m, 2H), 4.68 (m, 1H), 3.11−3.02 (m, 2H), 2.61 (ddd, J = 16.0, 6.7, 2.5 Hz, 1H), 2.52 (ddd, J = 16.0, 5.1, 2.1 Hz, 1H), 2.07 (p, J = 7.3 Hz, 2H), 0.98 (t, J = 7.5 Hz, 3H), 0.87 (s, 9H), 0.06 (s, 3H), 0.05 (s, 3H). ^{13}C NMR (101 MHz, $CDCl_3$) δ_C 201.1, 143.1, 133.8, 123.3, 110.7, 90.1, 77.9, 68.6,

DOI: 10.1021/acs.jnatprod.6b00634
J. Nat. Prod. 2016, 79, 2693−2702

51.3, 25.9, 20.7, 18.2, 17.9, 14.1, −4.3, −4.9. HRESITOFMS: m/z 329.1907 $[M + Na]^+$ (calcd for $C_{18}H_{30}O_2SiNa$, 329.1913); TLC (hexane/EtOAc 85:15, $KMnO_4$ stain) R_f = 0.38.

*Methyl-(R,7Z,10Z,14E,19Z)-13-((tert-butyldimethylsilyl)oxy)-docosa-7,10,14,19-tetraen-16-ynoate (**22**).* Wittig salt **19** (374 mg, 65.4 μmol, 1.00 equiv) was dissolved in THF (8.80 mL) and HMPA (0.88 mL), cooled to −78 °C and added NaHMDS (0.6 M in toluene, 1.09 mL, 65.4 μmol, 1.00 equiv). The reaction mixture was stirred for 45 min before aldehyde **21** (200 mg, 65.5 μmol, 1.00 equiv) in THF (0.88 mL) was added dropwise. The reaction was stirred for 1 h at −78 °C and then the reaction mixture was allowed to slowly warm to 0 °C. Phosphate buffer (4.7 mL, pH = 7.2) was added to quench the reaction and the aq. phase was extracted with Et_2O (2 × 4.0 mL). The combined organic layers were dried (Na_2SO_4) and concentrated *in vacuo*. The crude product was purified by column chromatography on silica gel (heptane/EtOAc 95:5, $KMnO_4$ stain) to afford compound **22** as a pale yellow oil. Yield: 239 mg (77%); $[\alpha]_D^{20}$ + 2.1 (*c* 0.39, $CHCl_3$); ^{1}H NMR (400 MHz, MeOH-d_4) δ_H 5.98 (dd, *J* = 15.8, 5.8 Hz, 1H), 5.62 (dq, *J* = 15.8, 2.0 Hz, 1H), 5.51−5.29 (m, 6H), 4.22 (q, *J* = 5.6 Hz, 1H), 3.65 (s, 3H), 3.05 (d, *J* = 6.7 Hz, 2H), 2.78 (q, *J* = 5.9 Hz, 2H), 2.32 (t, *J* = 7.4 Hz, 2H), 2.27 (q, *J* = 6.9 Hz, 2H), 2.08 (q, *J* = 7.0 Hz, 4H), 1.62 (p, *J* = 7.5 Hz, 2H), 1.45−1.28 (m, 4H), 0.99 (t, *J* = 7.5 Hz, 3H), 0.91 (s, 9H), 0.07 (s, 3H), 0.05 (s, 3H) ; ^{13}C NMR (101 MHz, MeOH-d_4) δ_C 175.9, 145.6, 134.2, 131.3, 130.9, 129.0, 126.2, 124.8, 110.8, 89.7, 79.1, 74.0, 52.0, 37.1, 34.8, 30.4, 29.8, 28.1, 26.8, 26.40 (3C), 25.9, 21.4, 19.1, 18.2, 14.4, −4.3, −4.5; HRESITOFMS: m/z 495.3265 $[M + Na]^+$ (calcd for $C_{29}H_{48}O_3SiNa$, 495.3270); TLC (hexane/EtOAc 85:15, $KMnO_4$ stain) R_f = 0.47.

*Methyl-(R,7Z,10Z,14E,19Z)-13-hydroxydocosa-7,10,14,19-tetraen-16-ynoate (**23**).* The TBS-protected intermediate **22** (64.1 mg, 0.136 mmol, 1.00 equiv) was twice azeotroped with 2-Me-THF and then stirred under argon at 0 °C before a solution of AcCl in dry MeOH (1.00 mL, 20.4 μmol, 15.0 mol%) was added. The solution of AcCl in MeOH was prepared just prior to use by adding AcCl (3.0 μL) to dry MeOH (2.0 mL) under argon. The reaction mixture was stirred for 7 h at 0 °C. Then CH_2Cl_2 (2.7 mL) was added, and the reaction was neutralized with a 10% aq solution of $NaHCO_3$ (140 μL) and washed with H_2O (1.4 mL). The combined organic layers were dried (Na_2SO_4), and the solvent was removed *in vacuo*, before the crude product was purified by column chromatography on silica gel (heptane/EtOAc 85:15) to afford the alcohol **23** as a clear oil. Yield: 44.7 mg (92%); $[\alpha]_D^{20}$ = −9.0 (*c* = 0.27, MeOH); UV(MeOH) λ_{max} 229, (log ε 3.97); ^{1}H NMR (400 MHz, MeOH-d_4) δ_H 6.01 (dd, *J* = 15.9, 6.1 Hz, 1H), 5.66 (dq, *J* = 15.9, 2.2 Hz, 2H), 5.52−5.32 (m, 6H), 4.11 (dq, J= 6.4, 1.0 Hz, 1H), 3.67 (s, 3H), 3.06 (d, *J* = 6.8 Hz, 2H), 2.81 (m, 2H), 2.38−2.27 (m, 4H), 2.15−2.05 (m, 4H), 1.64 (p, *J* = 7.4 Hz, 2H), 1.47−1.29 (m, 4H), 1.00 (t, *J* = 7.5 Hz, 3H). ^{13}C NMR (101 MHz, MeOH-d_4) δ_C 176.0, 145.2, 134.2, 131.4, 131.0, 128.9, 126.0, 124.8, 111.2, 89.6, 79.1, 72.7, 52.0, 36.1, 34.8, 30.4, 29.8, 28.0, 26.8, 25.9, 21.4, 18.2, 14.3; HRESITOFMS: m/z 381.2400 $[M+Na]^+$ (calcd for $C_{23}H_{34}O_3Na$, 381.2406); TLC (hexane/EtOAc 80:20, $KMnO_4$ stain) R_f = 0.36. The chemical purity (>98%) was determined by HPLC analysis (Eclipse XDB-C18, MeOH/H_2O 85:15, 1.0 mL/min): t_r (major) = 12.94 min and t_r (minor) = 15.74 min.

*Methyl (R,7Z,10Z,14E,16Z,19Z)-13-hydroxydocosa-7,10,14,16,19-pentaenoate (**24**).* The activated Zn was prepared according to the literature.[16] A suspension of Zn dust (2.04 g) in distilled H_2O (12.3 mL) was stirred under argon for 15 min. $Cu(OAc)_2{\cdot}H_2O$ (204 mg, 1.02 mmol) was added, the flask was sealed immediately, and the mixture stirred vigorously for 15 min. Then $AgNO_3$ (204 mg, 1.2 mmol) was added (exothermic reaction), and the reaction mixture was stirred for an additional 30 min. The activated Zn was filtered under argon atmosphere and washed successively with H_2O, MeOH, acetone, and Et_2O to give a wet material (the activated Zn was not dried completely). Alkyne **23** (30 mg, 83.7 μmol) was dissolved in MeOH/H_2O (2:1) (6.00 mL), and then the wet activated Zn was added quickly under a blanket of argon. The reaction was stirred for 10 h in the dark. After completion, the mixture was filtered through Celite with Et_2O, and the aq phase was extracted with EtOAc (3 × 3.0 mL). The organic layers were dried (Na_2SO_4) and the solvent removed *in vacuo*, before the crude product was purified by column chromatography on silica gel (heptane/EtOAc 90:10) to afford the methyl ester **24** as a clear oil. Yield 20.2 mg (67%): $[\alpha]_D^{20}$ − 0.5 (*c* = 0.74, MeOH); UV(MeOH) λ_{max} 237, (log ε = 4.41); ^{1}H NMR (400 MHz, MeOH-d_4) δ_H 6.55 (ddt, *J* = 15.1, 11.0, 1.1 Hz, 1H), 5.97 (t, *J* = 10.9 Hz, 1H), 5.68 (dd, *J* = 15.2, 6.5 Hz, 1H), 5.50−5.26 (m, 7H), 4.15 (q, *J* = 6.5 Hz, 1H), 3.65 (s, 3H), 2.94 (t, *J* = 7.2 Hz, 2H), 2.80 (t, *J* = 5.5 Hz, 2H), 2.43−2.21 (m, 4H), 2.18−2.02 (m, 4H), 1.61 (p, *J* = 7.4 Hz, 2H), 1.46−1.26 (m, 4H), 0.98 (t, *J* = 7.5 Hz, 3H); ^{13}C NMR (101 MHz, MeOH-d_4) δ_C 176.0, 137.2, 133.1, 131.2, 131.0, 130.9, 129.2, 129.0, 127.8, 126.4, 126.4, 73.1, 52.0, 36.4, 34.8, 30.4, 29.8, 28.0, 26.9, 26.8, 25.9, 21.5, 14.6; HRESITOFMS: m/z 383.2555 $[M + Na]^+$ (calcd for $C_{23}H_{36}O_3Na$, 383.2562); TLC (hexane/EtOAc 75:25, $KMnO_4$ stain) R_f = 0.33. The chemical purity (>98%) was determined by HPLC analysis (Eclipse XDB-C18, MeOH/H_2O 85:15, 1.0 mL/min): t_r (minor) = 13.72 and 17.53 min, and t_r (major) = 16.53 min.

*(R,7Z,10Z,14E,16Z,19Z)-13-Hydroxydocosa-7,10,14,16,19-pentaenoic Acid, 13R-HDPA (**5**).* Methyl ester **24** (12.0 mg, 33.3 μmol, 1.00 equiv) was dissolved in THF/MeOH/H_2O (2:2:1, 3.90 mL) and cooled to 0 °C. LiOH (24 mg, mmol, 30.0 equiv) was added in one portion. The reaction mixture was stirred for 3 h at 0 °C before it was allowed to warm up to room temperature and stirred until completion, as monitored by TLC (∼2 h). Saturated aq NaH_2PO_4 (6.0 mL) was added. The aq phase was extracted (2 × 3.0 mL), dried (Na_2SO_4), and the solvent was removed *in vacuo*. The crude product was purified by column chromatography on silica gel (heptane/EtOAc 50:50, $KMnO_4$ stain) to afford the hydroxy acid **5** as colorless oil. Yield: 10.0 mg (87%); $[\alpha]_D^{25}$ - 0.64 (*c* = 0.47, MeOH); UV(MeOH) λ_{max} 236, (log ε = 4.39); ^{1}H NMR (400 MHz, MeOH-d_4) δ_H 6.55 (ddt, *J* = 15.2, 11.1, 1.2 Hz, 1H), 5.97 (t, *J* = 10.9 Hz, 1H), 5.68 (dd, *J* = 15.2, 6.5 Hz, 1H), 5.49−5.26 (m, 7H), 4.15 (q, *J* = 6.5 Hz, 1H), 2.94 (t, *J* = 7.2 Hz, 2H), 2.80 (t, *J* = 5.8 Hz, 2H), 2.40−2.22 (m, 4H), 2.09 (q, *J* = 7.6, 6.9 Hz, 4H), 1.61 (p, *J* = 7.4 Hz, 2H), 1.38 (m, 4H), 0.98 (t, *J* = 7.5 Hz, 3H); ^{13}C NMR (101 MHz, MeOH-*d*4) δ_C 177.7, 137.1, 133.1, 131.2, 131.1, 130.9, 129.2, 129.0, 127.8, 126.4, 126.4, 73.1, 36.4, 35.0, 30.4, 29.9, 28.1, 26.9, 26.8, 26.0, 21.5, 14.6; HRESITOFMS: m/z 369.2400 $[M + Na]^+$ (calcd for $C_{22}H_{34}O_3Na$, 369.2406); TLC (hexane/EtOAc 50:50, $KMnO_4$ stain) R_f = 0.27.

Biogenic 13R-HDPA. Human umbilical vein endothelial cells (HUVEC; 8.5 × 10^5 cells/9.6 cm^2) were incubated with IL-1β (10 ng/mL) and TNF-α (10 ng/mL; 16 h, 37 °C, 5% CO_2). Incubations were quenched using 2 volumes of MeOH containing deuterium labeled d_8-5*S*-HETE.[8]

In separate experiments n-3 DPA (Cayman Chemical Company) was incubated with human recombinant COX-2 (Cayman Chemicals; in 0.1 M Tris-HCl, pH 8.0, 20 μM porcine hematin, 0.67 mM phenol) for 30 min at room temperature. Incubations were stopped with two volumes of MeOH and products extracted using diethyl ether.[8] 13-HDPA was isolated using RP-HPLC (1260 Series; Agilent Technologies) and an Agilent C18 Poroshell column (3.5 μm × 4.6 mm × 150 mm) with a mobile phase consisting of MeOH/H_2O (60:40, vol/vol) at 0.5 mL/min that was ramped up to 98:2 (v/v) for 20 min.

Infectious exudates were collected from mice (6−8 week old, male, FvB, Charles River, UK) 12h after administration of *E. coli* (10^5 CFU).[28] Exudates were collected in 4 mL of PBS (containing calcium and magnesium) and placed in 2 volumes of ice-cold MeOH containing d_8-5*S*-HETE and commercially available lipid mediators. In these experiments, male FvB mice (6−8 weeks of age) were used. These animals were maintained on a standard chow pellet diet and had access to water ad libitum, with a 12-h light−dark cycle. All animal experiments were approved and performed under the guidelines of the Ethical Committee for the Use of Animals, Barts and The London School of Medicine, and in accordance with the U.K. Home Office regulations (Guidance on the Operation of Animals, Scientific Procedures Act, 1986).

RvT Biosynthesis. Human peripheral blood was collected according to a protocol approved by Barts and the London Research Ethics Committee, London, United Kingdom (QMREC 2014:61). Written informed consent was received from participants prior to inclusion in

DOI: 10.1021/acs.jnatprod.6b00634
J. Nat. Prod. 2016, 79, 2693−2702

the study according to the Declaration of Helsinki. Neutrophils were prepared following density separation by layering on Ficoll-Histopaque 1077−1. The cells were then centrifuged at 300*g* (30 min, 4 °C), and contaminating red blood cells were lysed by hypotonic lyses as in ref 8. Neutrophils 20 × 10^6 cells/mL ($PBS^{+/+}$, pH = 7.45) were then incubated with synthetic 13*R*-HDPA (**5**) (10 μM) for 45 min (37 °C). Incubations were stopped with 2 volumes of ice-cold MeOH. $NaBH_4$ was then added to reduce the hydroperoxides produced by the neutrophil lipoxygenases (1.0 mg/mL; Sigma-Aldrich), and products were isolated using C18 solid phase extraction as detailed below.

Lipid Mediator Profiling. MeOH (two volumes) was added to cell incubations, plasma (mouse and human), and infectious exudates, and samples were stored at −20 °C until extraction. Prior to extraction, samples were then centrifuged (1200*g*, 4 °C, 10 min). Supernatants were then collected and brought to less than 1.0 mL of MeOH content using a gentle stream of nitrogen gas using a TurboVap LV system (Biotage). The RvT1−4 and 13-HDPA products were extracted using an ExtraHera (Biotage) automated extraction system as follows. Solid-phase C18 cartridges were equilibrated with 3.0 mL of MeOH and 6.0 mL of H_2O. Nine milliliters of aq HCl solution (pH = 3.5) was then added to the samples, and the acidified solutions were rapidly loaded onto the conditioned C18 columns that were washed with 4.0 mL of H_2O. Next, 5.0 mL of hexane was added, and the products were eluted with 4.0 mL of methyl formate. Products were brought to dryness using the automated evaporation system (TurboVap LV, Biotage) and immediately suspended in MeOH−H_20 (50:50 vol/vol) for LC-MS-MS automated injections as previously reported.[8]

Extracted samples were analyzed by an LC-MS-MS system, Qtrap 5500 (AB Sciex) equipped with a Shimadzu SIL-20AC autoinjector and LC-20AD binary pump (Shimadzu Corp.). A Poroshell C18 column (100 mm × 4.6 mm × 2.7 μm) was used with a gradient of MeOH/H_2O/AcOH of 55:45:0.01 (v/v/v) that was ramped to 85:15:0.01 (v/v/v) over 10 min and then to 98:2:0.01 (v/v/v) for the next 8 min. This was subsequently maintained at 98:2:0.01 (v/v/v) for 2 min. The flow rate was maintained at 0.4 mL per minute.

To monitor and quantify the levels of lipid mediators, a multiple reaction monitoring (MRM) method was developed with signature ion fragments (m/z) for each molecule monitoring the parent ion (Q1) and a characteristic daughter ion (Q3). Identification was conducted using published criteria where a minimum of 6 diagnostic ions were employed, see ref 18 for details. Detection limit was ∼0.1 pg.

For chiral-phase lipidomic analysis, a Chiralpak AD-RH column (150 mm × 2.1 mm × 5 μm) was used with isocratic MeOH/H_2O/AcOH 95:5:0.01 (v/v/v) at 0.15 mL/min. To monitor isobaric monohydroxy docosapentaenoic acid levels, a multiple reaction monitoring (MRM) method was developed using signature ion fragments 345 > 195 described.[8]

■ ASSOCIATED CONTENT

Supporting Information

The Supporting Information is available free of charge on the ACS Publications website at DOI: 10.1021/acs.jnatprod.6b00634.

^{1}H, ^{13}C spectral data, HRMS and UV−vis spectra, as well as chromatograms from HPLC analyses of synthetic intermediates and 13*R*-HDPA (**5**) (PDF)

■ AUTHOR INFORMATION

Corresponding Authors

*E-mail: j.dalli@qmul.ac.uk.
*E-mail: t.v.hansen@farmasi.uio.no.
*E-mail: anders.vik@farmasi.uio.no.

Author Contributions

The manuscript was written through contributions of all authors. All authors have given approval to the final version of the manuscript.

Notes

The authors declare the following competing financial interest(s): J. D. and C. N. S. have filed patents on RvT1 (**1**), RvT2 (**2**), RvT3 (**3**), RvT4 (**4**), 13*R*-HDPA (**5**) and related compounds. C. N. S.s interests are reviewed and are managed by BWH and Partners HealthCare in accordance with their conflict of interest policies.

[§](K.G.P.) On leave from the School of Pharmacy, Department of Pharmaceutical Chemistry, University of Oslo.

■ ACKNOWLEDGMENTS

The Norwegian Research Council is gratefully acknowledged for funding to T.V.H and a postdoctoral fellowship to M.A. (FRIPRO-FRINATEK 230470). We are thankful to the School of Pharmacy, University of Oslo, for a Ph.D. scholarship to K.G.P. and for the generous support from the Norwegian Ph.D. School of Pharmacy (Nasjonal forskerskole i farmasi, NFIF) for a travel grant. J.D. is supported by a Sir Henry Dale Fellowship jointly funded by the Wellcome Trust and the Royal Society (Grant number 107613/Z/15/Z). C.N.S. is supported by the National Institutes of Health GM Grant PO1GM095467.

■ REFERENCES

(1) Serhan, C. N.; Dalli, J.; Colas, R. A.; Winkler, J. W.; Chiang, N. *Biochim. Biophys. Acta, Mol. Cell Biol. Lipids* **2015**, *1851*, 397−413.
(2) (a) Dalli, J.; Chiang, N.; Serhan, C. N. *Proc. Natl. Acad. Sci. U. S. A.* **2014**, *111*, E4753−E4761. (b) Dalli, J.; Ramon, S.; Norris, P. C.; Colas, R. A.; Serhan, C. N. *FASEB J.* **2015**, *29*, 2120−2136. (c) Ramon, S.; Dalli, J.; Sanger, J. M.; Winkler, J. W.; Aursnes, M.; Tungen, J. E.; Hansen, T. V.; Serhan, C. N. *Am. J. Pathol.* **2016**, *186*, 962−973.
(3) Sugimoto, M. A.; Sousa, L. P.; Pinho, V.; Perretti, M.; Teixeira, M. M. *Front. Immunol.* **2016**, *7*, 160.
(4) Tabas, I.; Glass, C. K. *Science* **2013**, *339*, 166−172.
(5) Serhan, C. N.; Petasis, N. A. *Chem. Rev.* **2011**, *111*, 5922−5943 and references cited therein.
(6) Dalli, J.; Colas, R. A.; Serhan, C. N. *Sci. Rep.* **2013**, *3*, 1940.
(7) Aursnes, M.; Tungen, J. E.; Vik, A.; Colas, R.; Cheng, C.-Y.; Dalli, J.; Serhan, C. N.; Hansen, T. V. *J. Nat. Prod.* **2014**, *77*, 910−916.
(8) Dalli, J.; Chiang, N.; Serhan, C. N. *Nat. Med.* **2015**, *21*, 1071−1075.
(9) Serhan, C. N. *Biochim. Biophys. Acta, Lipids Lipid Metab.* **1994**, *1212*, 1−25.
(10) (a) Neu, H. C. *Science* **1992**, *257*, 1064−1073. (b) Ward, P. A. *EMBO Mol. Med.* **2012**, *4*, 1234−1243.
(11) Mowat, J.; Senior, J.; Kang, B.; Britton, R. *Can. J. Chem.* **2013**, *91*, 235−239.
(12) Brown, C. A.; Ahuja, V. K. *J. Chem. Soc., Chem. Commun.* **1973**, 553−554.
(13) Hansen, T. V.; Stenstrøm, Y. *Tetrahedron: Asymmetry* **2001**, *12*, 1407−1409.
(14) Tungen, J. E.; Aursnes, M.; Dalli, J.; Arnardottir, H.; Serhan, C. N.; Hansen, T. V. *Chem. - Eur. J.* **2014**, *20*, 14575−14578.
(15) Khan, A. T.; Mondal, E. *Synlett* **2003**, 694−698.
(16) Boland, W.; Schroer, N. C.; Sieler, C. M.; Feigel, M. *Helv. Chim. Acta* **1987**, *70*, 1025−1040.
(17) Aursnes, M.; Tungen, J. T.; Vik, A.; Dalli, J.; Hansen, T. V. *Org. Biomol. Chem.* **2014**, *12*, 432−437.
(18) Colas, R. A.; Shinohara, M.; Dalli, J.; Chiang, N.; Serhan, C. N. *Am. J. Physiol. Cell. Physiol.* **2014**, *307*, C39−54.
(19) Haeggström, J. Z.; Funk, C. C. *Chem. Rev.* **2011**, *111*, 5866−5898.
(20) Brezinski, M. E.; Serhan, C. N. *Proc. Natl. Acad. Sci. U. S. A.* **1990**, *87*, 6248−6252.
(21) Gerwick, W. H. *Chem. Rev.* **1993**, *93*, 1807−1823.
(22) Serhan, C. N. *Nature* **2014**, *510*, 92−101.

DOI: 10.1021/acs.jnatprod.6b00634
J. Nat. Prod. 2016, 79, 2693−2702

(23) (a) Samuelsson, B. *J. Biol. Chem.* **2012**, *287*, 10070−10080. (b) Barbosa, M.; Valentão; Andrade, P. B. *Mar. Drugs* **2016**, *14*, 23. (c) Basil, M. C.; Levy, B. D. *Nat. Rev. Immunol.* **2016**, *16*, 51−67.
(24) Trost, B. M.; Pinkerton, A. B. *J. Org. Chem.* **2001**, *66*, 7714−7722.
(25) Billington, D. C.; Bladon, P.; Helps, M.; Pauson, P. L.; Thomson, W.; Willison, D. *J. Chem. Res., Synop.* **1988**, 2601−2609.
(26) Huang, Z.; Negishi, E.-I. *Org. Lett.* **2006**, *8*, 3675−3678.
(27) Lucet, D.; Heyse, P.; Gissot, A.; Le Gall, T.; Mioskowski, C. *Eur. J. Org. Chem.* **2000**, *2000* (21), 3575−3579.
(28) Chiang, N.; Fredman, G.; Backhed, F.; Oh, S. F.; Vickery, T.; Schmidt, B. A.; Serhan, C. N. *Nature* **2012**, *484*, 524−529.

DOI: 10.1021/acs.jnatprod.6b00634
J. Nat. Prod. 2016, 79, 2693−2702

Supporting information for

Synthesis of 13(*R*)-Hydroxy-7*Z*,10*Z*,13R,14,*E*,16*Z*,19*Z* docosapentaenoic acid (13*R*-HDPA) and its Biosynthetic Conversion to the 13-Series Resolvins

Karoline G. Primdahl,[†,‡,§] Marius Aursnes,[†] Mary E. Walker,[‡] Romain A. Colas,[‡] Charles N. Serhan,[⊥] Jesmond Dalli,[*,‡] Trond V. Hansen[*,†] and Anders Vik[*,†]

[†]*School of Pharmacy, Department of Pharmaceutical Chemistry, University of Oslo, PO Box 1068 Blindern, N-0316 Oslo, Norway.*
[‡]*William Harvey Research Institute, Barts and The London School of Medicine and Dentistry, Queen Mary University of London, Charterhouse Square, London, UK, EC1M 6BQ.*
[§]*Center for Experimental Therapeutics and Reperfusion Injury, Department of Anesthesiology, Perioperative and Pain Medicine, Harvard Institutes of Medicine, Brigham and Women's Hospital and Harvard Medical School, Boston, Massachusetts, 02115.*

[§]*On leave from the School of Pharmacy, Department of Pharmaceutical Chemistry, University of Oslo.*

Table of Contents:

General Information

Unless stated otherwise, all commercially available reagents and solvents were used in the form they were supplied without any further purification. The stated yields are based on isolated material. All reactions were performed under an argon atmosphere using Schlenk techniques. Reaction flasks were covered with aluminium foil during reactions and storage to minimize exposure to light. Thin layer chromatography was performed on silica gel 60 F_{254} aluminum-backed plates fabricated by Merck. Flash column chromatography was performed on silica gel 60 (40-63 μm) produced by Merck. NMR spectra were recorded on a Bruker AVI600, Bruker AVII400 or a Bruker DPX300 spectrometer at 600 MHz, 400 MHz or 300 MHz respectively for ^{1}H NMR and at 150 MHz, 100 MHz or 75 MHz respectively for ^{13}C NMR. Coupling constants (*J*) are reported in hertz and chemical shifts are reported in parts per million (δ) relative to the central residual protium solvent resonance in ^{1}H NMR ($CDCl_3$ =

δ 7.26, DMSO-d_6 = δ 2.50 and MeOH-d_4 = δ 3.31) and the central carbon solvent resonance in ^{13}C NMR ($CDCl_3$ = δ 77.00 ppm, DMSO-d_6 = δ 39.43 and MeOH-d_4 = δ 49.00). High resolution mass spectra were recorded on Waters Prospec Q spectrometer using ES as the method of ionization. Optical rotations were measured using a 0.7 mL cell with a 1.0 dm path length on a Anton Paar MCP 100 polarimeter. GLC-analyses were performed on an Agilent Technologies 7820A GC instrument with split injection, FID detector and equipped with an Agilent J&W HP-5 GC column (30 m × 0.32 mm, 0.25 μm) applying the conditions stated. HPLC analyses were performed on an Agilent Technologies 1200 Series instrument with diode array detector set at 229-254 nm and equipped with a C_{18} stationary phase (Eclipse XDB-C18 5μm 4.6 × 250 mm), applying the conditions stated. The UV/Vis spectra from 190-900 nm were recorded using a Biochrom Libra S32PC spectrometer using quartz cuvettes.

Pent-2-ynyl methanesulfonate (7)

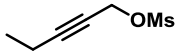

7

Mesylate **7** was prepared according to literature procedure by Mowat et al.[1] Pent-2-yn-1-ol (**6**) (2.52 g, 29.8 mmol, 1.00 equiv.) and Et_3N (6.20 mL) in CH_2Cl_2 (42.0 mL) was stirred at 0 °C. Methanesulfonyl chloride (3.00 mL, 38.8 mmol, 1.30 equiv.) was added dropwise. The reaction mixture was stirred for 45 min at 0 °C and then filtered. The filtrate was washed with H_2O (17.0 mL), a 1.0 M aq. solution of HCl (17.0 mL), brine (17.0 mL) and then dried ($MgSO_4$) and concentrated *in vacuo* to give crude mesylate **7**, that was used without further purification. The spectroscopic data were in agreement with those reported in the literature.[2] Yield: 4.25 g (88%); ^{1}H NMR (200 MHz, $CDCl_3$) δ_H 4.84 (t, J = 2.2 Hz, 2H), 3.11 (s, 3H), 2.26 (qt, J = 7.5, 2.2 Hz, 2H), 1.16 (t, J = 7.5 Hz, 3H).

Hepta-1,4-diynyltrimethylsilane (8)

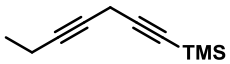

8

Compound **8** was prepared as reported by Mowat and co-workers,[1] K_2CO_3 (5.60 g, 40.6 mmol, 2.00 equiv.), CuI (3.90 g, 20.3 mmol, 1.00 equiv.) and NaI (6.10 g, 20.3 mmol, 2.00 equiv.) were added to a flask. The flask was evacuated and backfilled with argon three times before DMF (35.5 mL) was added. A solution of mesylate **7** (3.29 g, 20.3 mmol, 1.00 equiv.) in DMF (11.0 mL) was added followed by TMS-acetylene (5.73 mL, 40.6 mmol, 2.00 equiv.). The reaction mixture was stirred for 18 h and then filtered. The filtrate was diluted with Et_2O (50.0 mL), washed with H_2O (25.0 mL), brine (7 × 25.0 mL) and dried ($MgSO_4$). The solvent was removed *in vacuo* affording the title compound **8**. Yield: 2.83 g (85%); ^{1}H NMR (200 MHz, $CDCl_3$) δ_H 3.19 (t, J = 2.4 Hz, 2H), 2.18 (qt, J = 7.4, 2.4 Hz, 2H), 1.12 (t, J = 7.5 Hz, 3H), 0.16 (s, 9H), ^{13}C NMR (101 MHz, $CDCl_3$) δ_C 100.9, 84.8, 82.5, 72.8, 14.0, 12.6, 11.0, 0.08. TLC (hexane, $KMnO_4$ stain): R_f = 0.40.

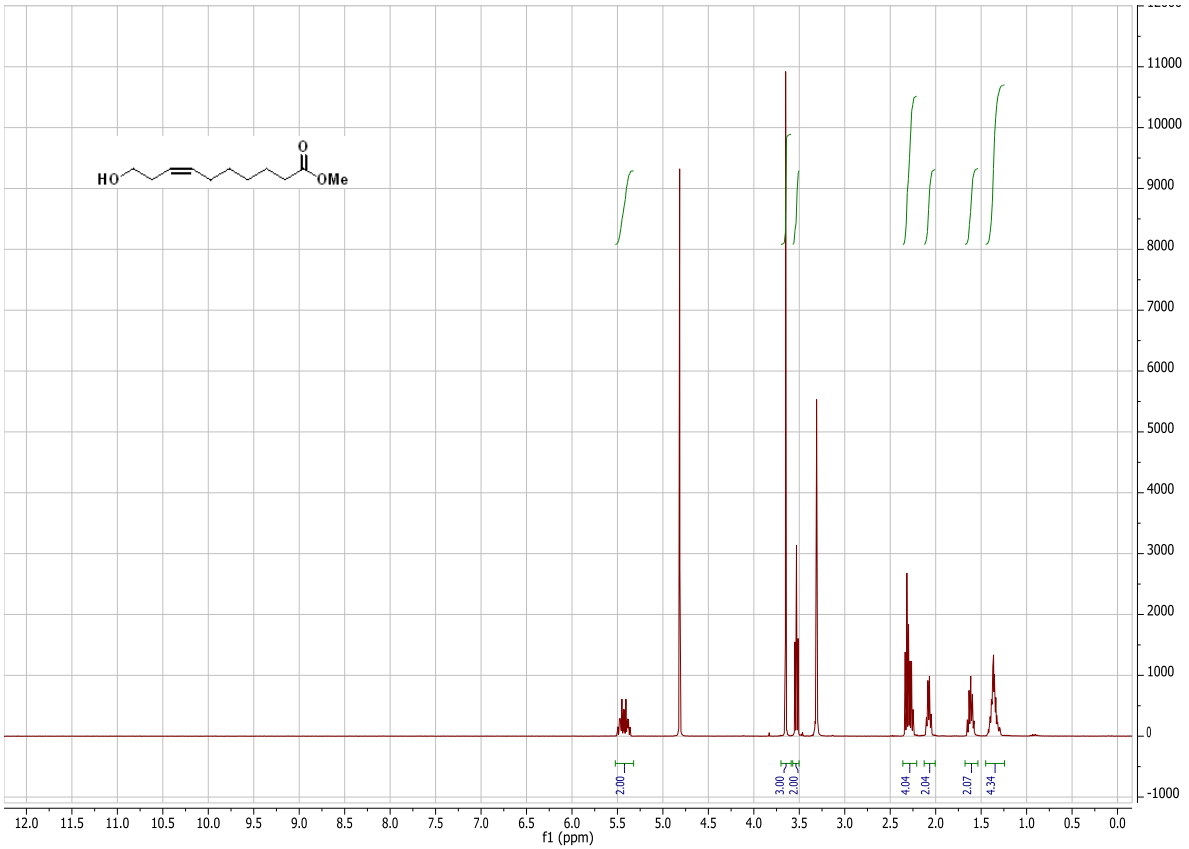

Figure S-1 ^{1}H-NMR spectrum of compound **17**.

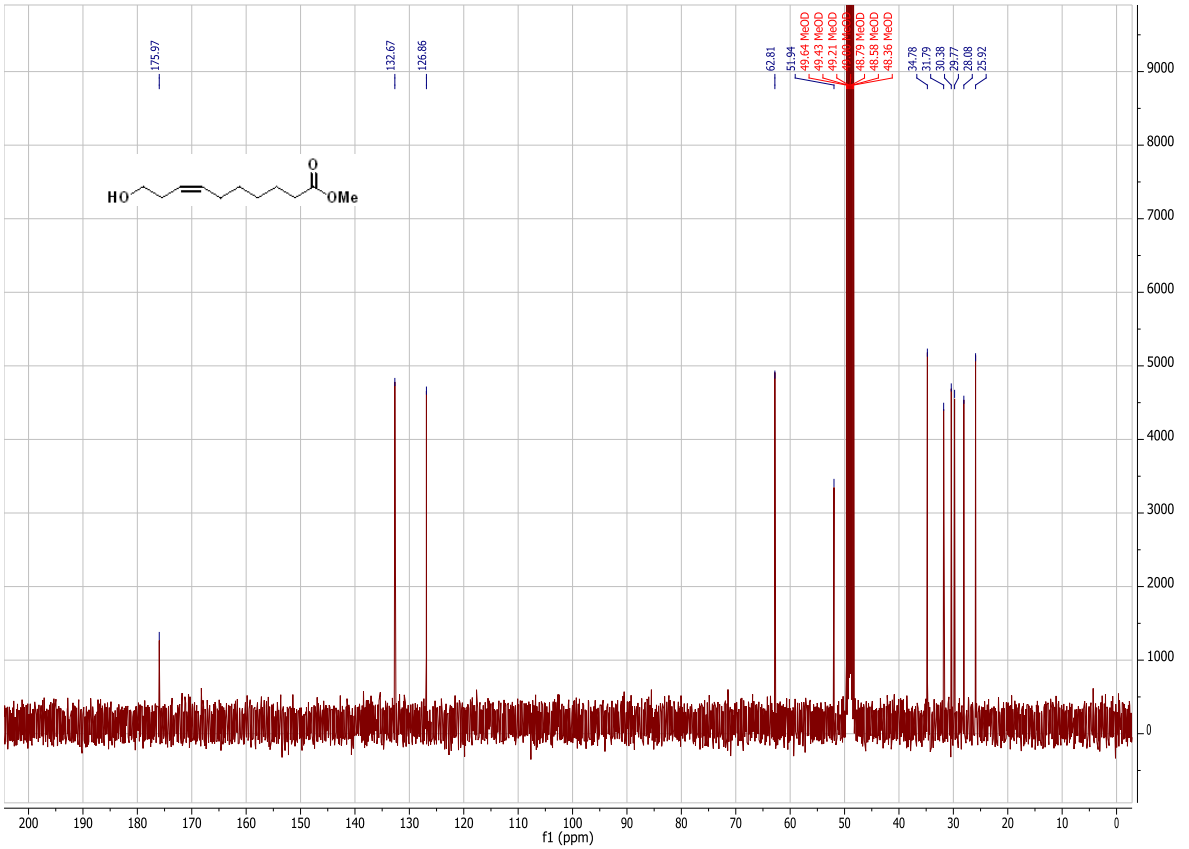

Figure S-2 ^{13}C-NMR spectrum of compound **17**.

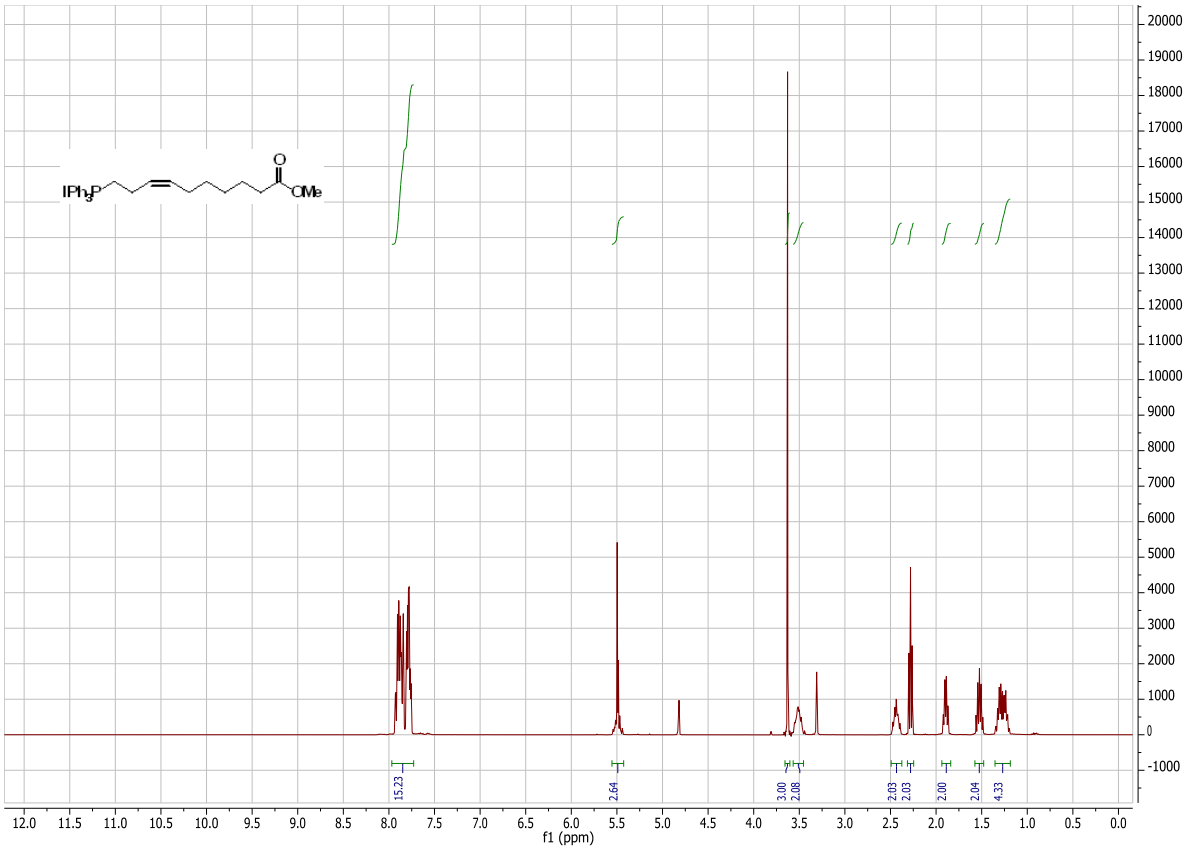

Figure S-3 ^{1}H-NMR spectrum of compound **19**.

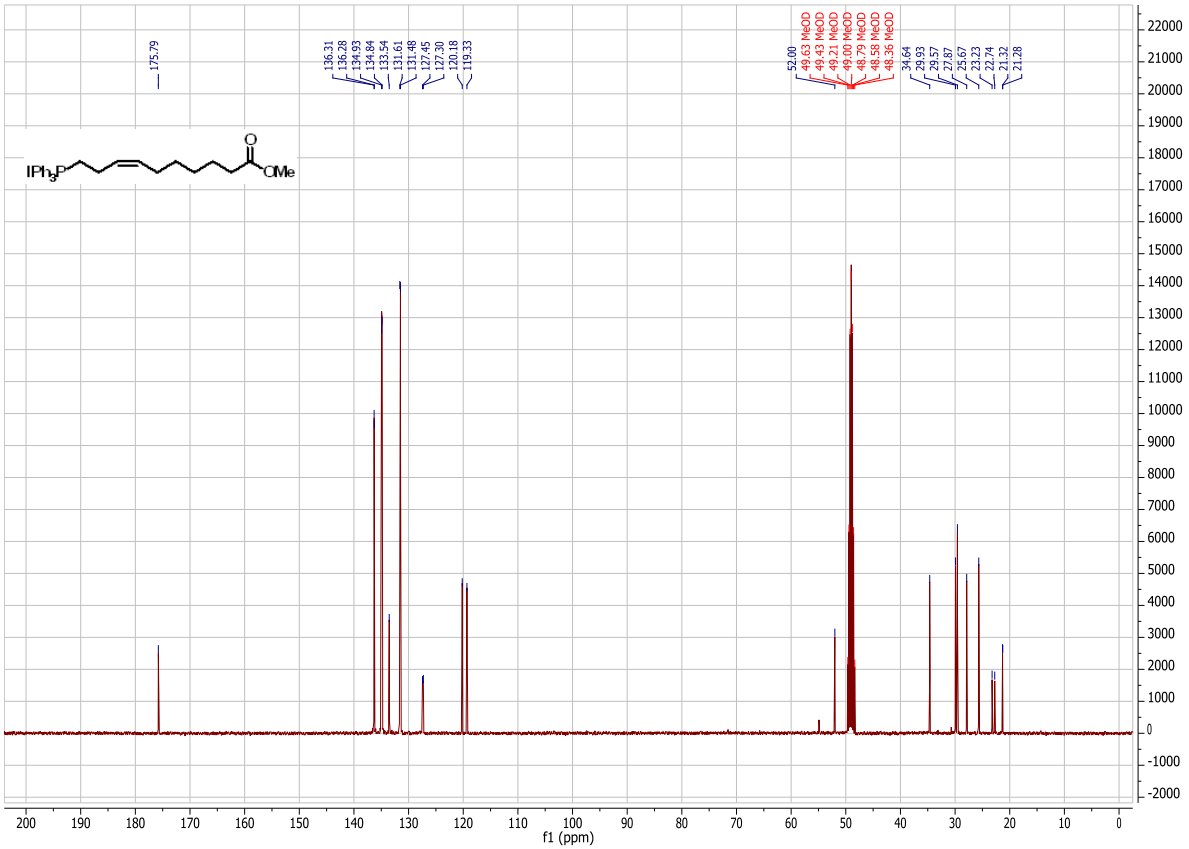

Figure S-4 ^{13}C-NMR spectrum of compound **19**.

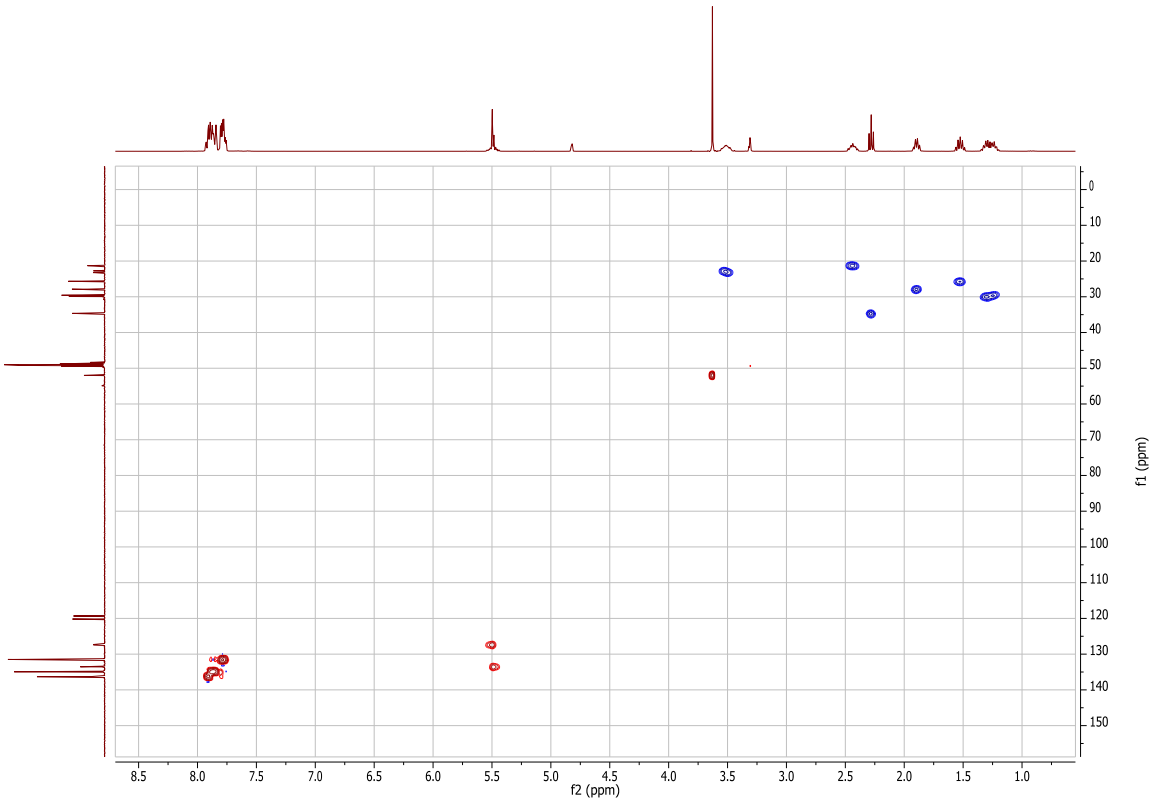

Figure S-5 HSQC-NMR spectrum of compound **19**.

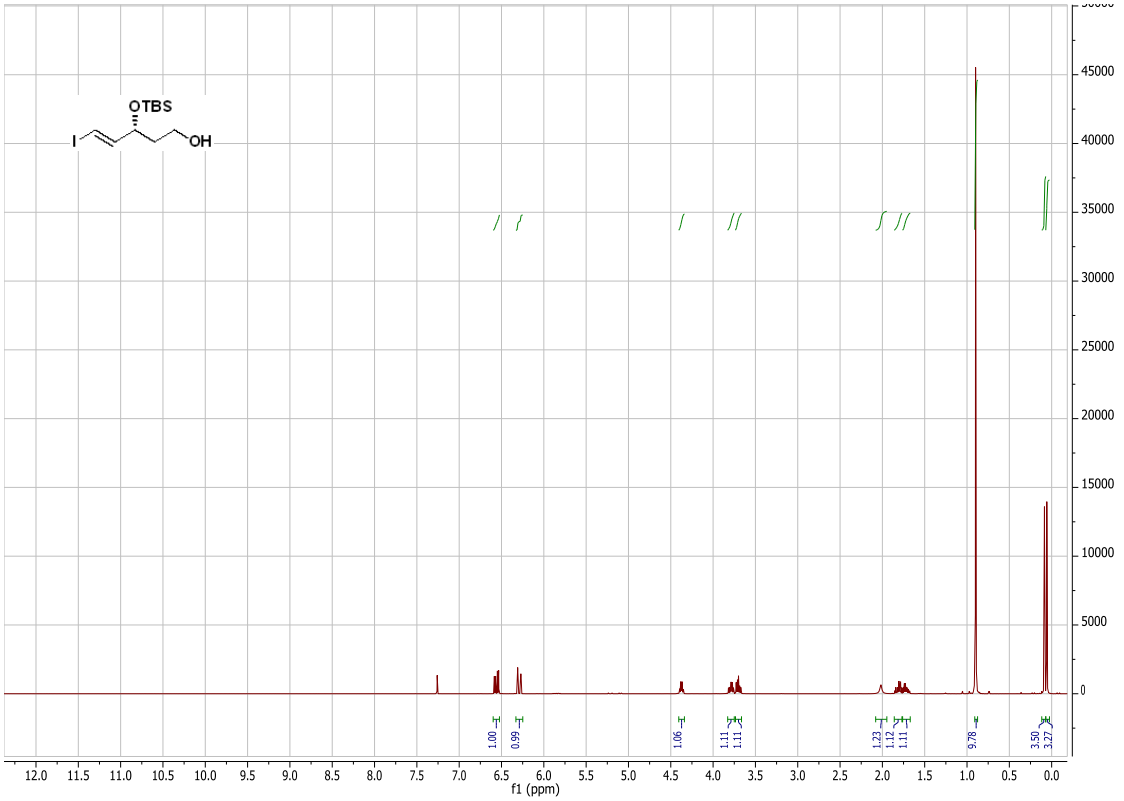

Figure S-6 ^{1}H-NMR spectrum of compound **13**.

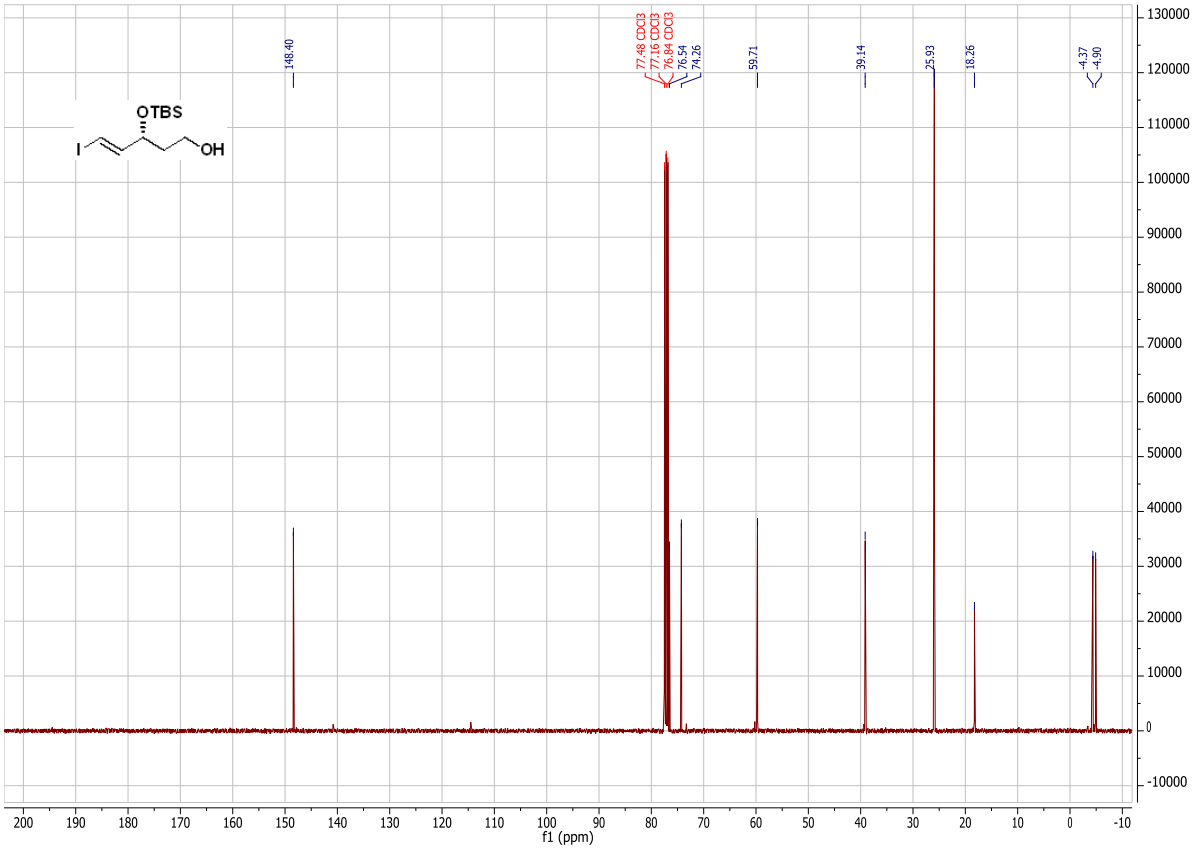

Figure S-7 ^{13}CNMR spectrum of compound **13**.

Figure S-8 ^{1}H-NMR spectrum of compound **20**.

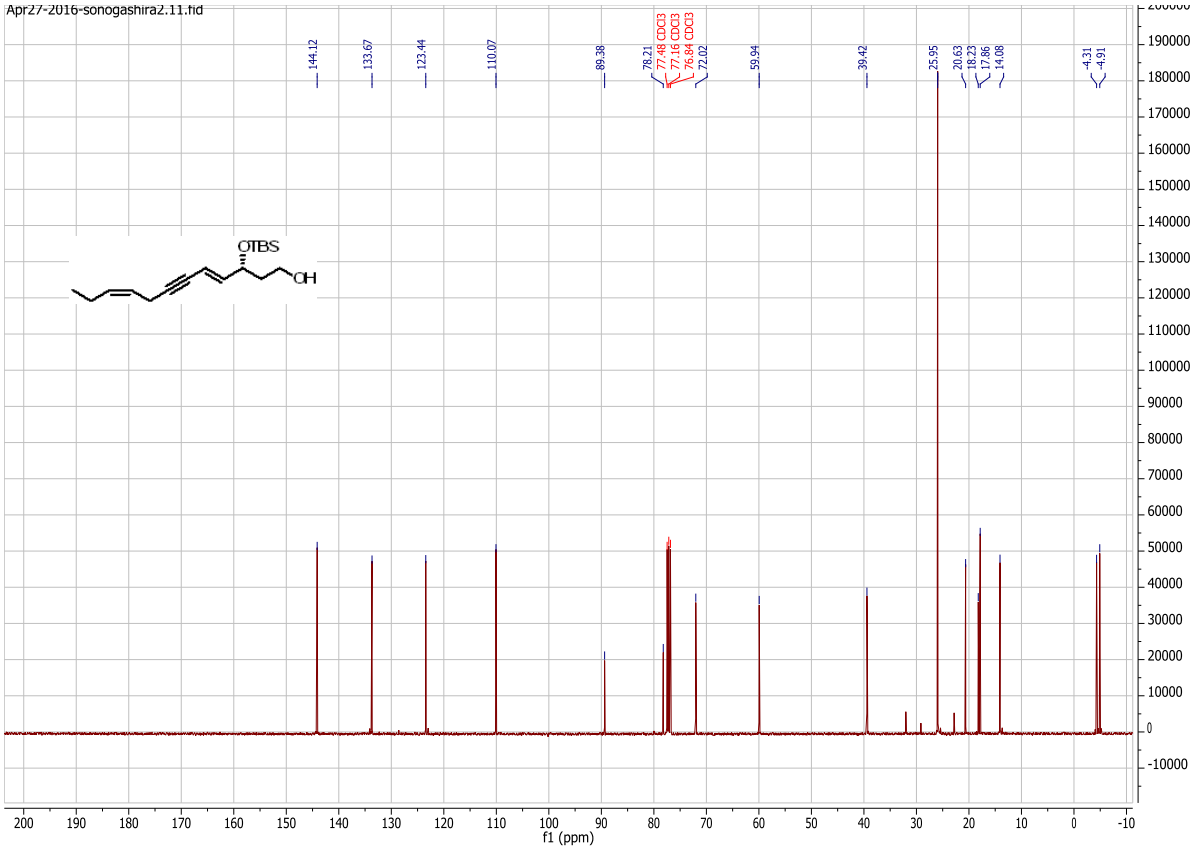

Figure S-9 ^{13}C-NMR spectrum of compound **20**.

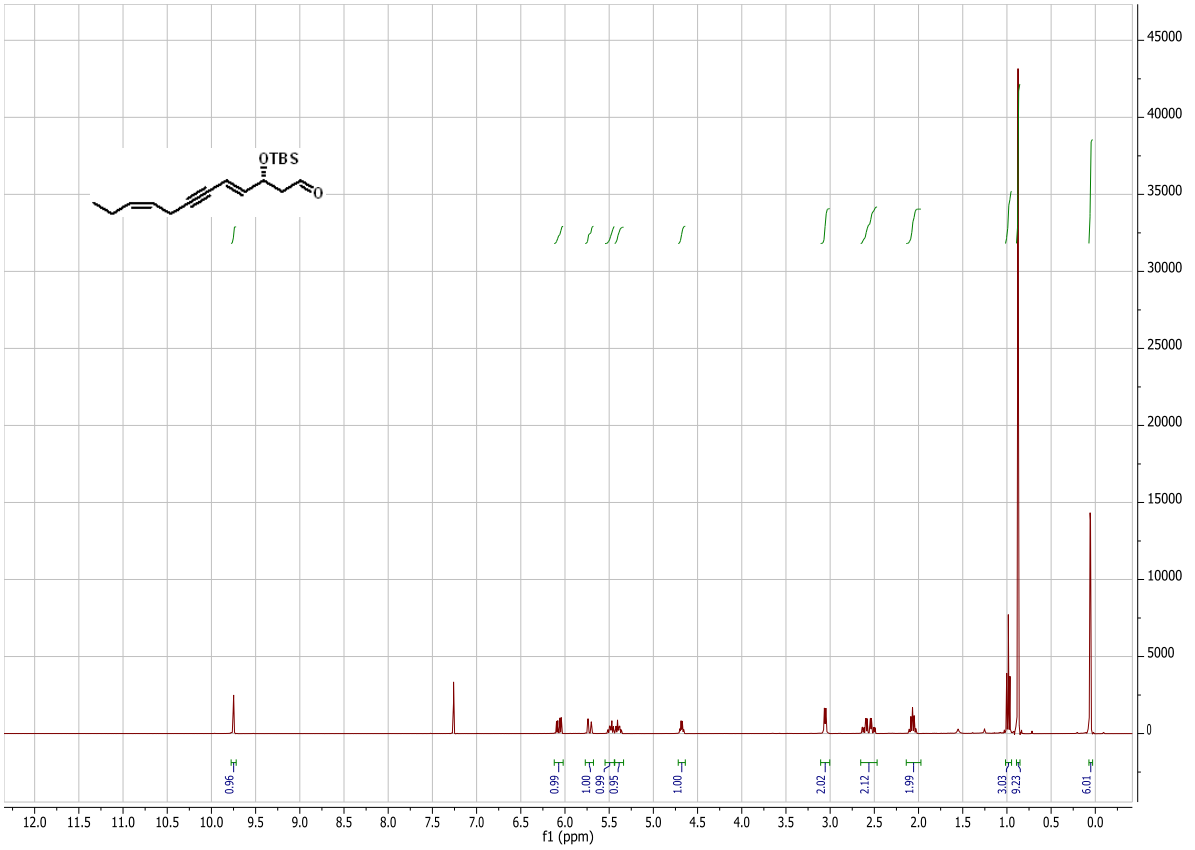

Figure S-10 ^{1}H-NMR spectrum of compound **21**.

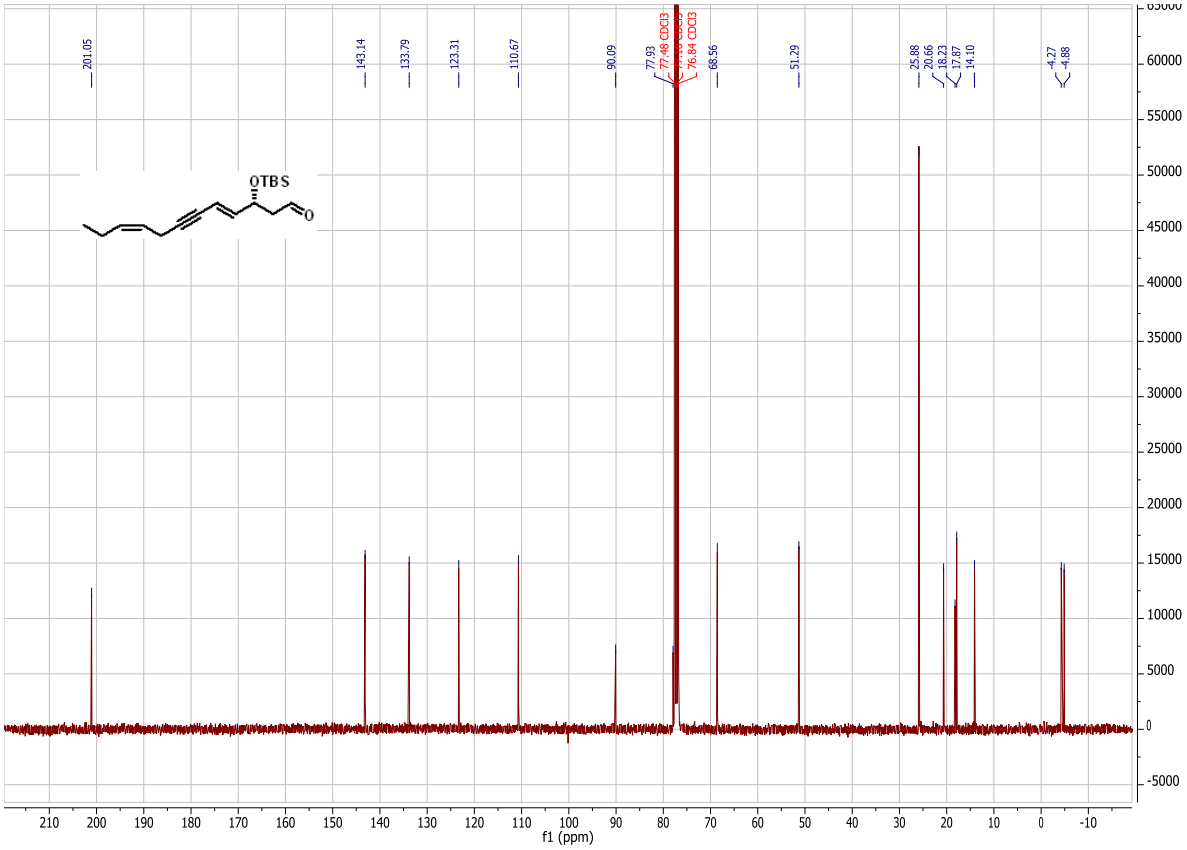

Figure S-11 ^{13}C-NMR spectrum of compound **21**.

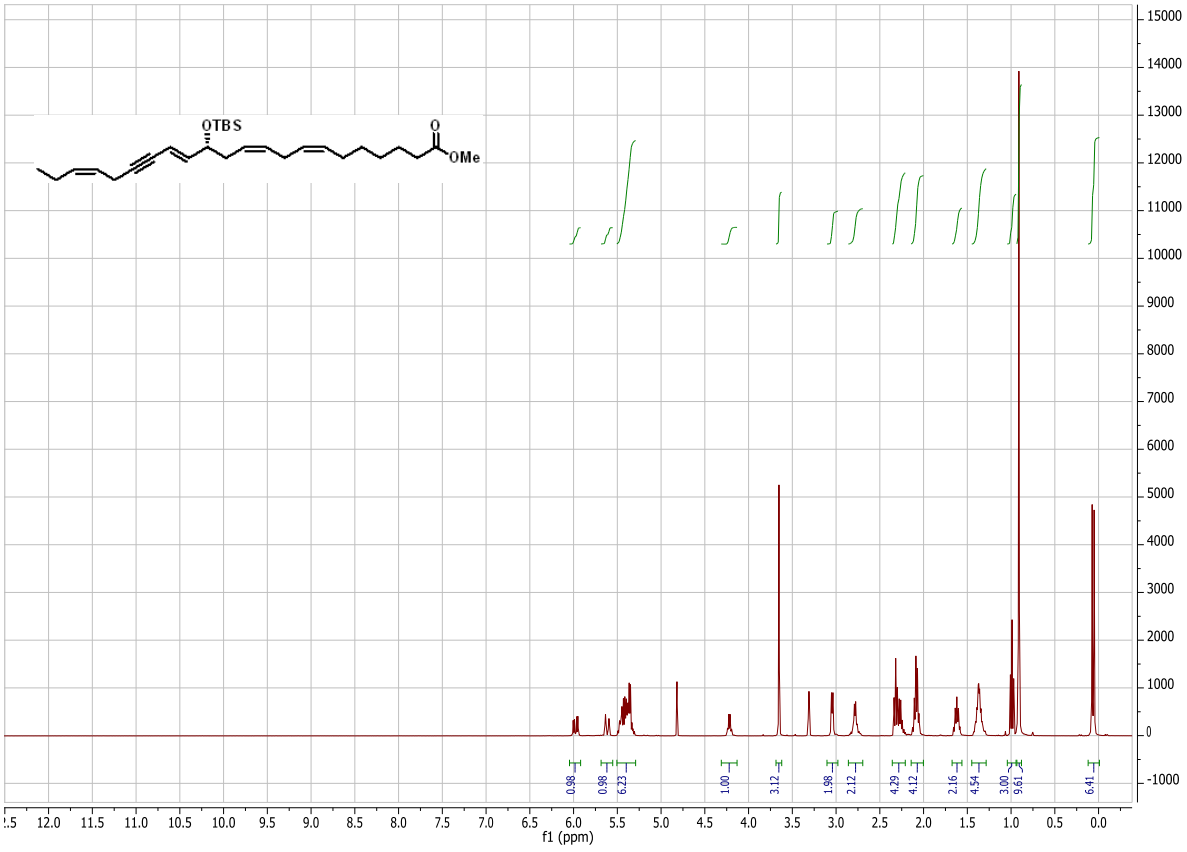

Figure S-12 ^{1}H-NMR spectrum of compound **22**.

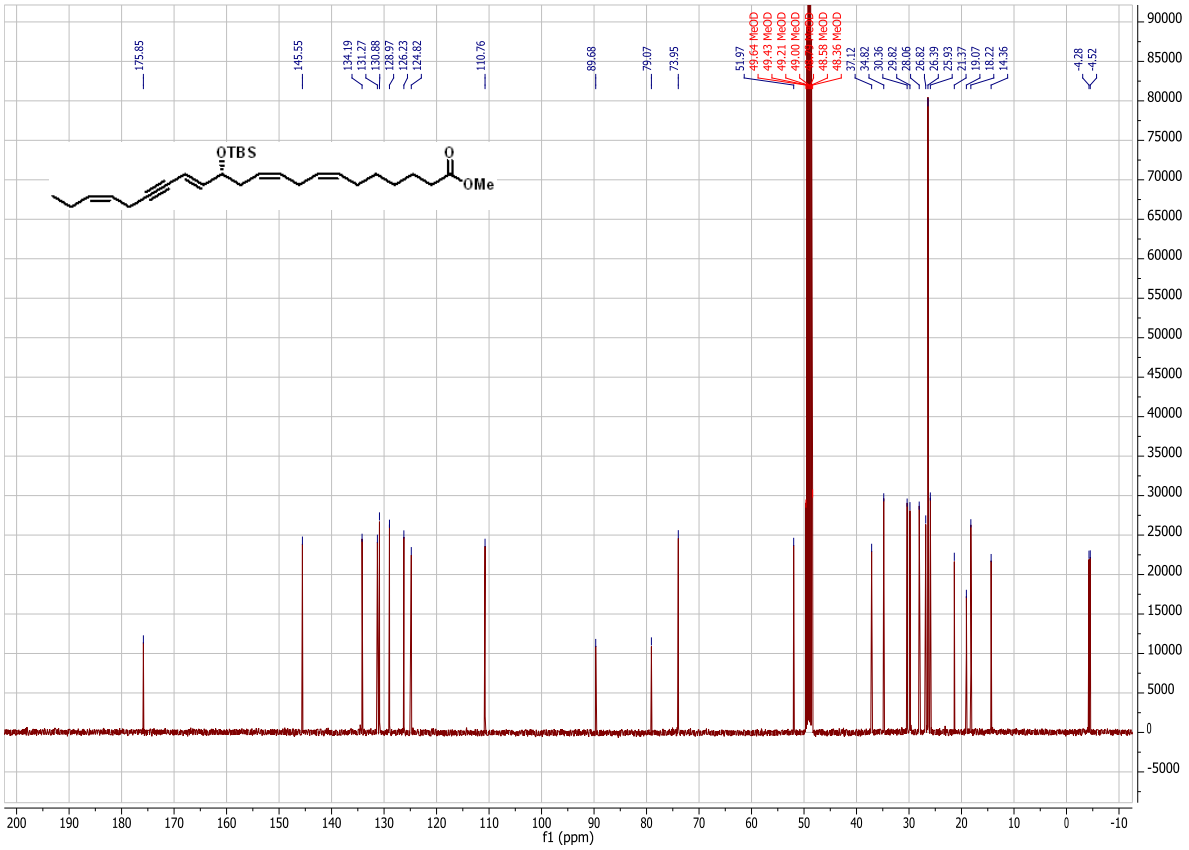

Figure S-13 ^{13}C-NMR spectrum of compound **22**.

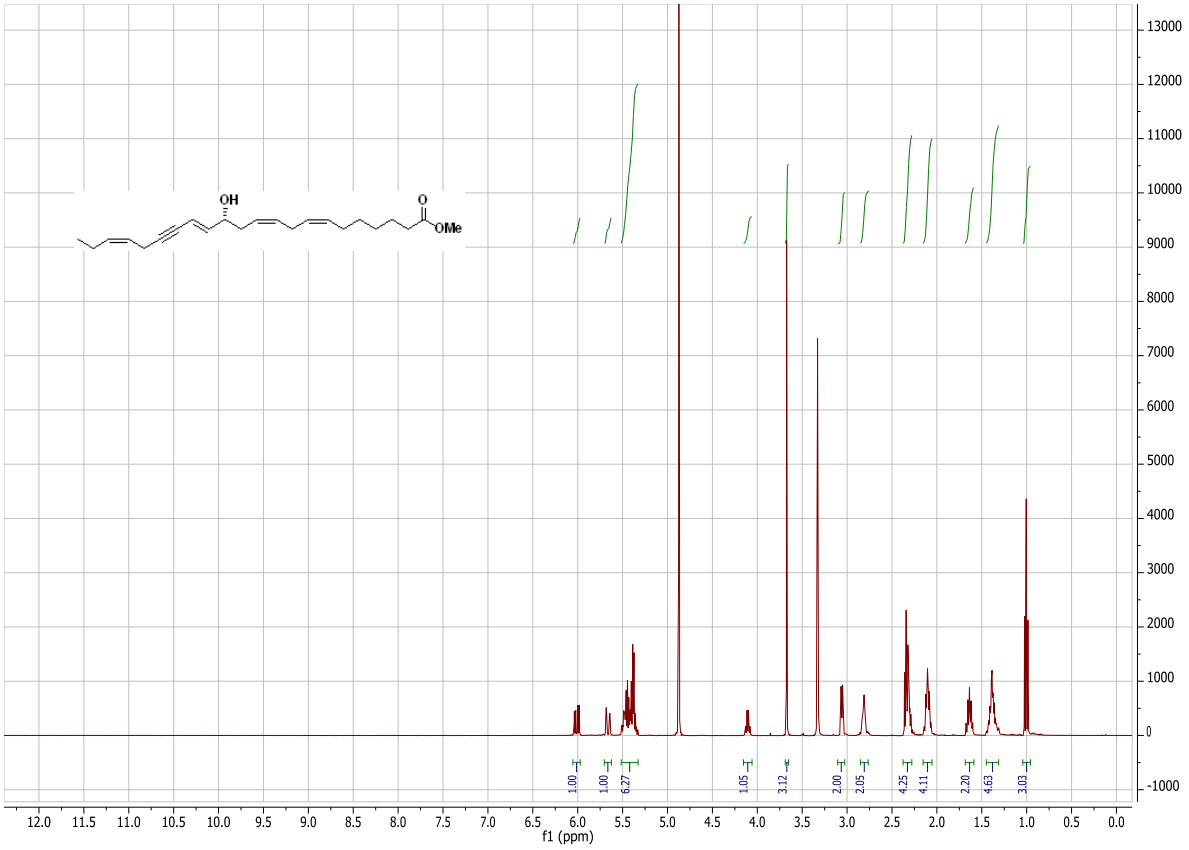

Figure S-14 ^{1}H-NMR spectrum of compound **23**.

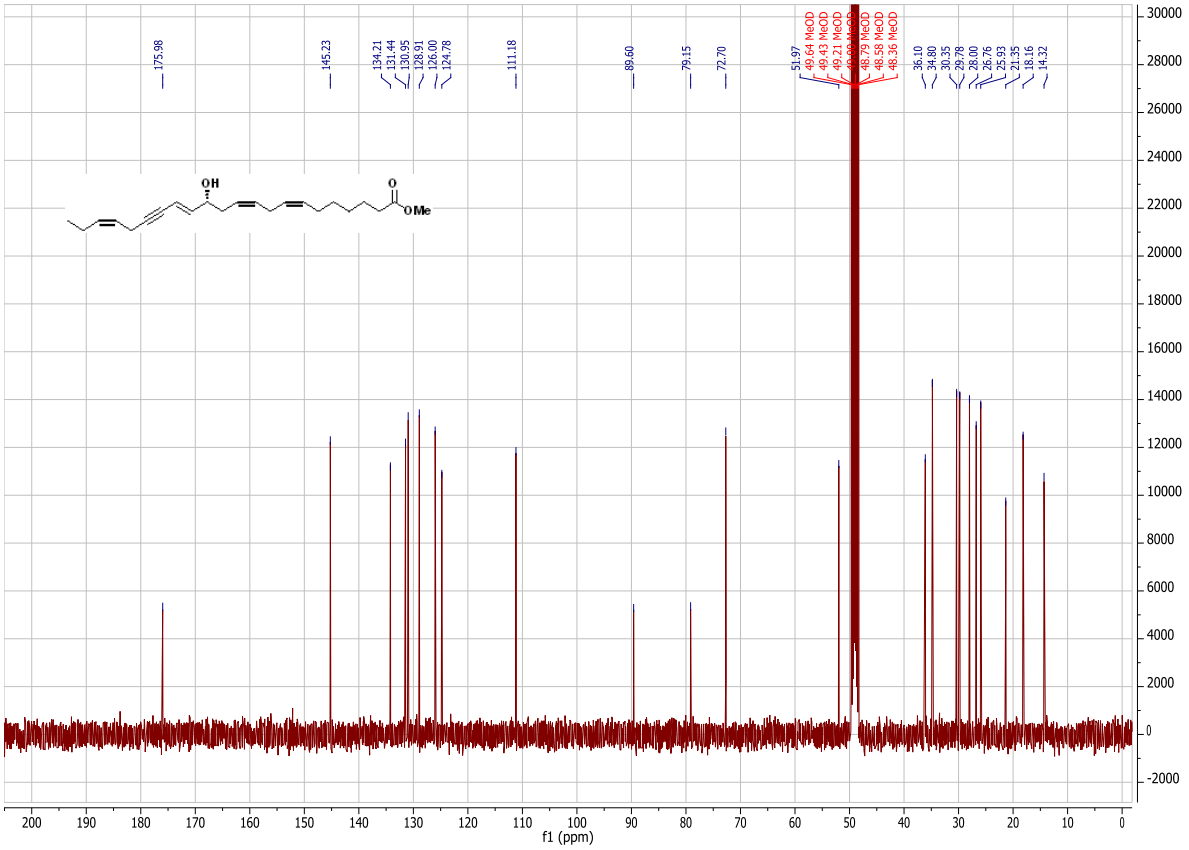

Figure S-15 ^{13}C-NMR spectrum of compound **23**.

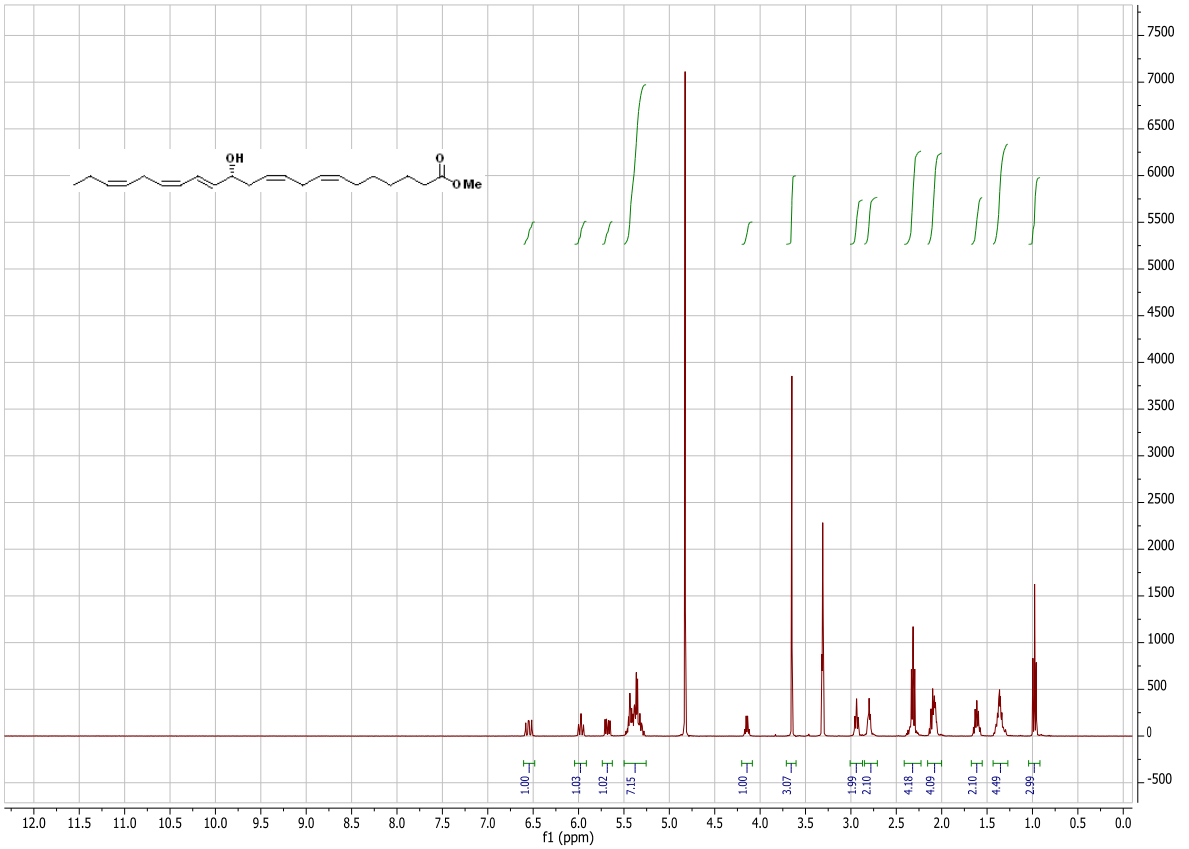

Figure S-16 ^{1}H-NMR spectrum of compound **24**.

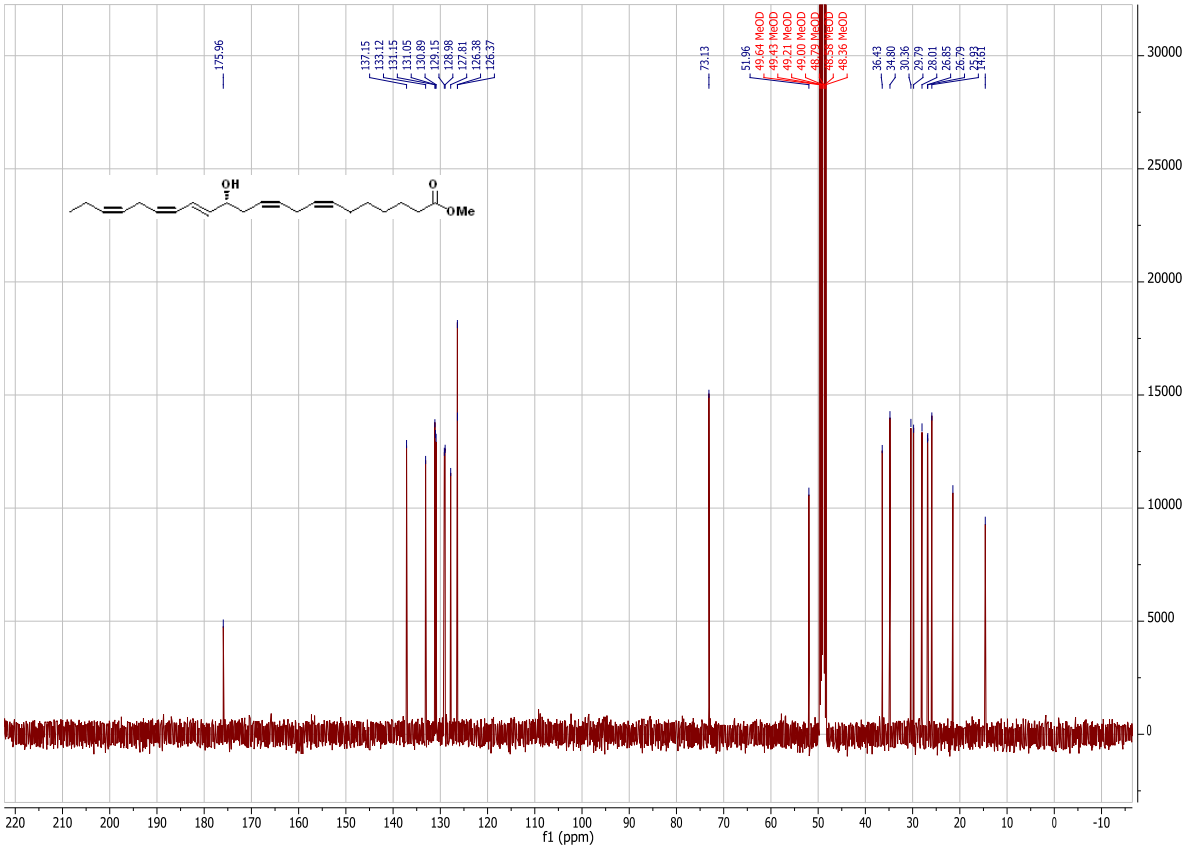

Figure S-17 ^{13}C-NMR spectrum of compound **24**.

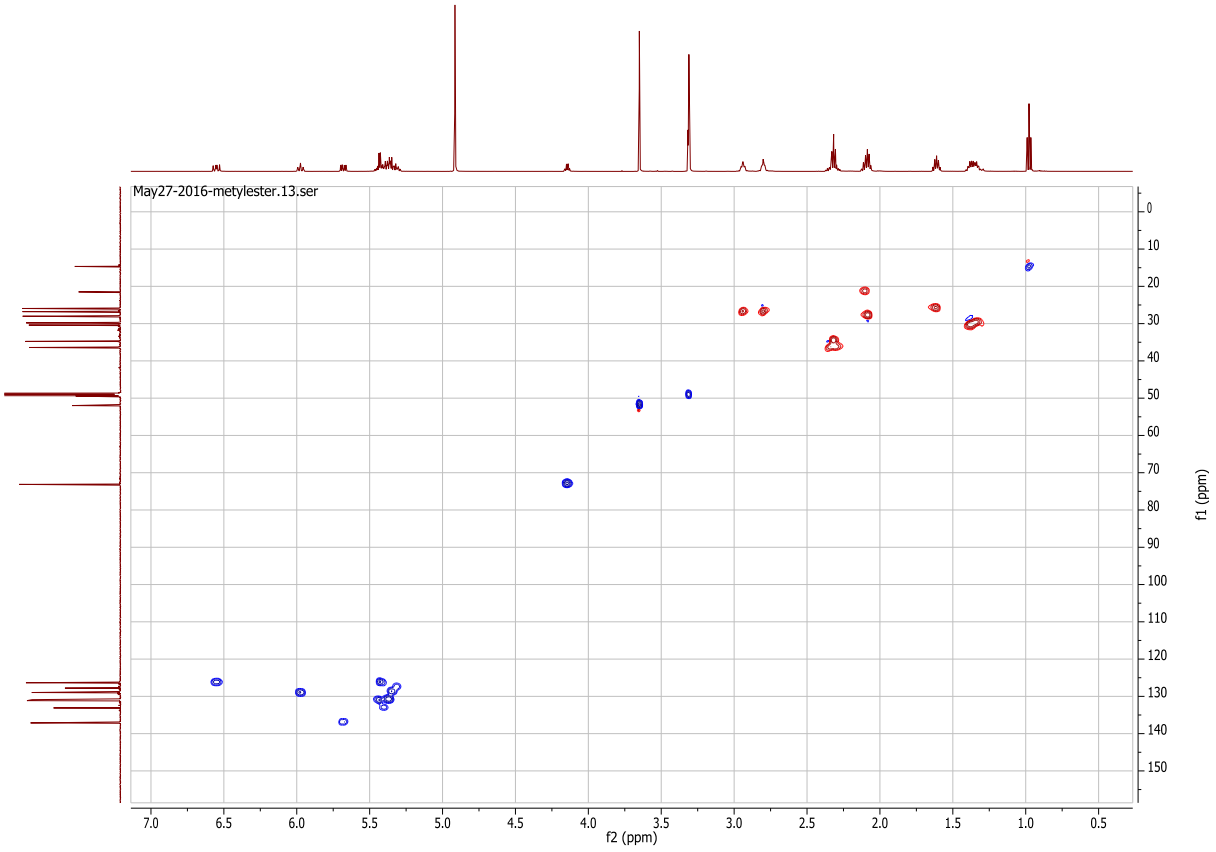

Figure S-18 HSQC-NMR spectrum of compound **24**.

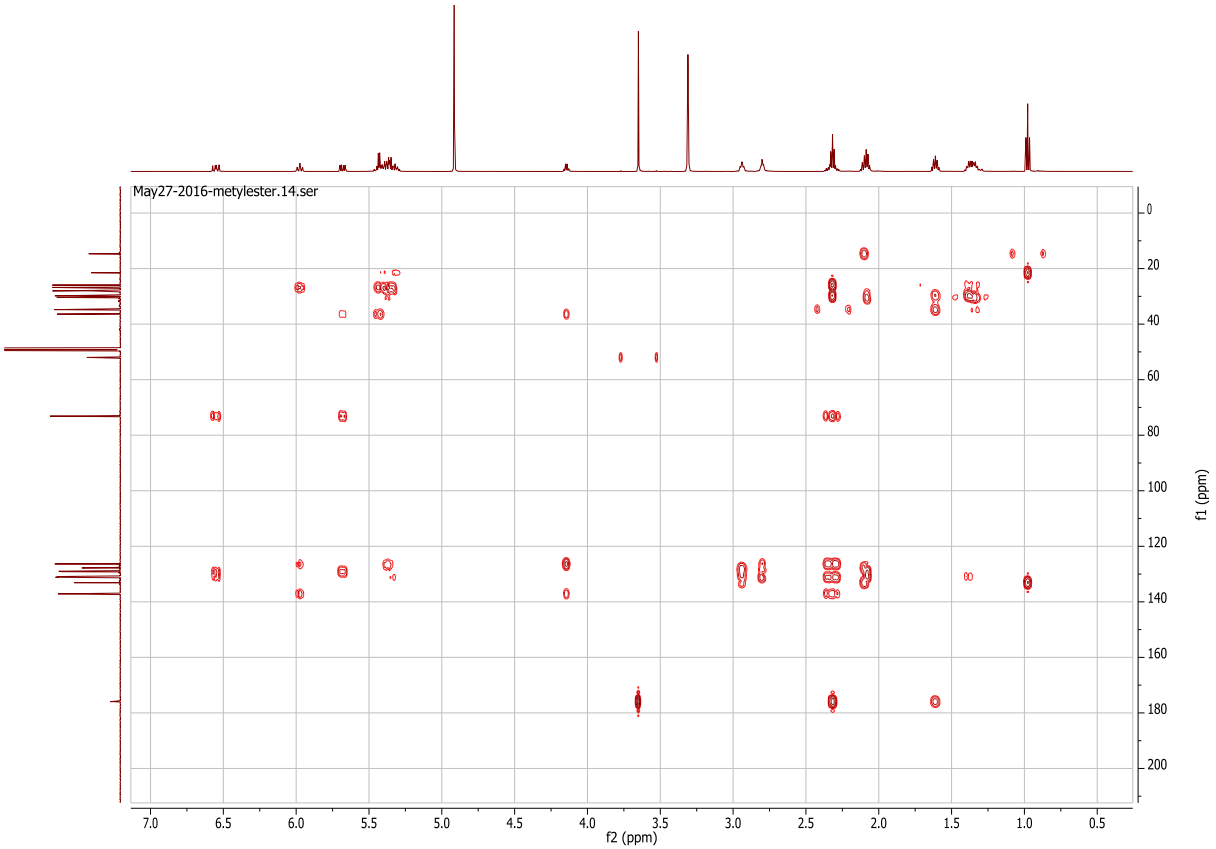

Figure S-19 HMBC-NMR spectrum of compound **24**.

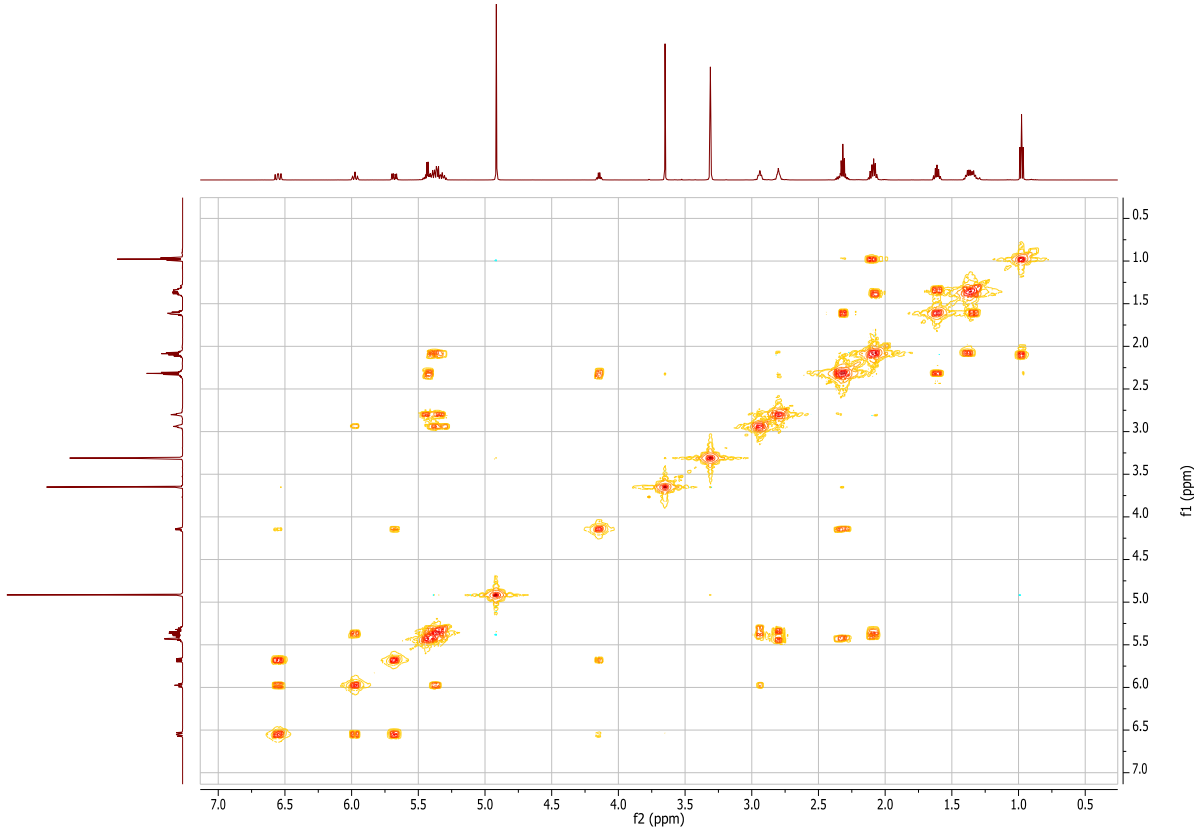

Figure S-20 COSY-NMR spectrum of compound **24**.

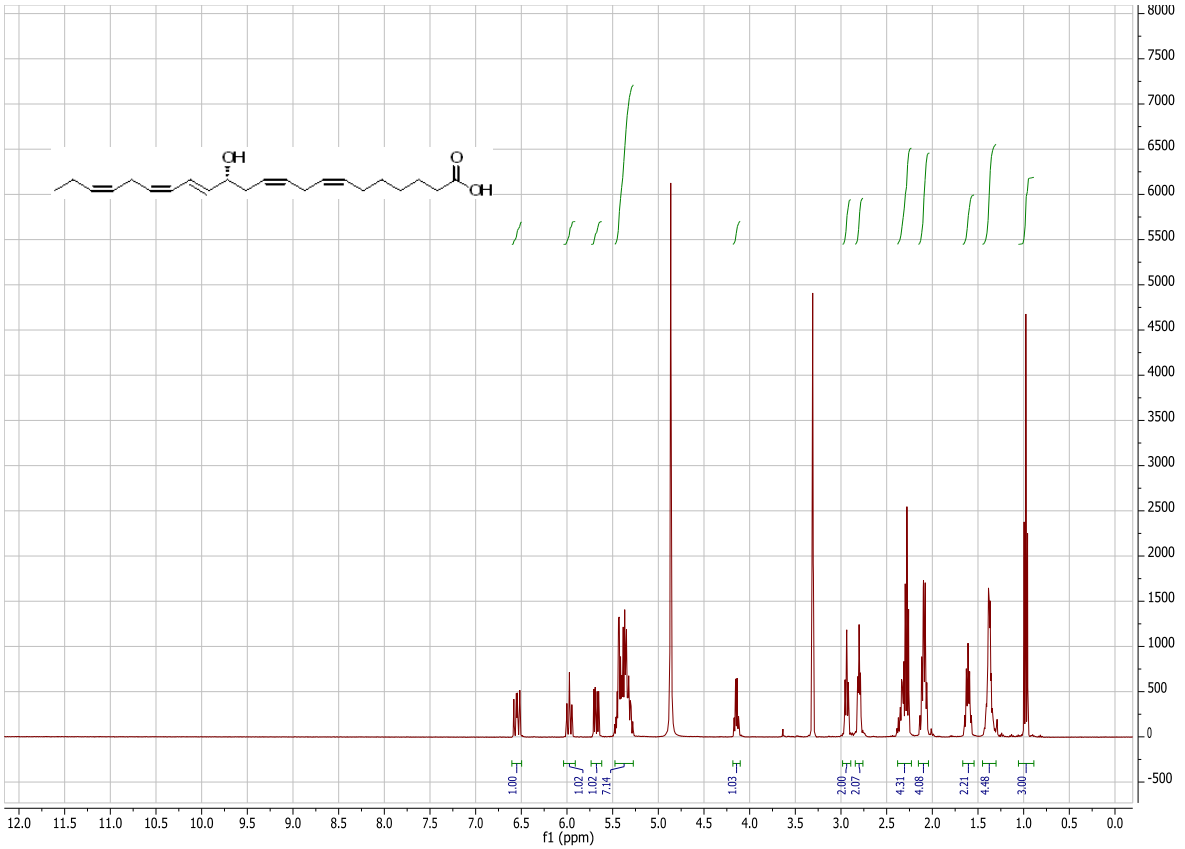

Figure S-21 ^{1}H-NMR spectrum of 13*R*-HDPA **5**.

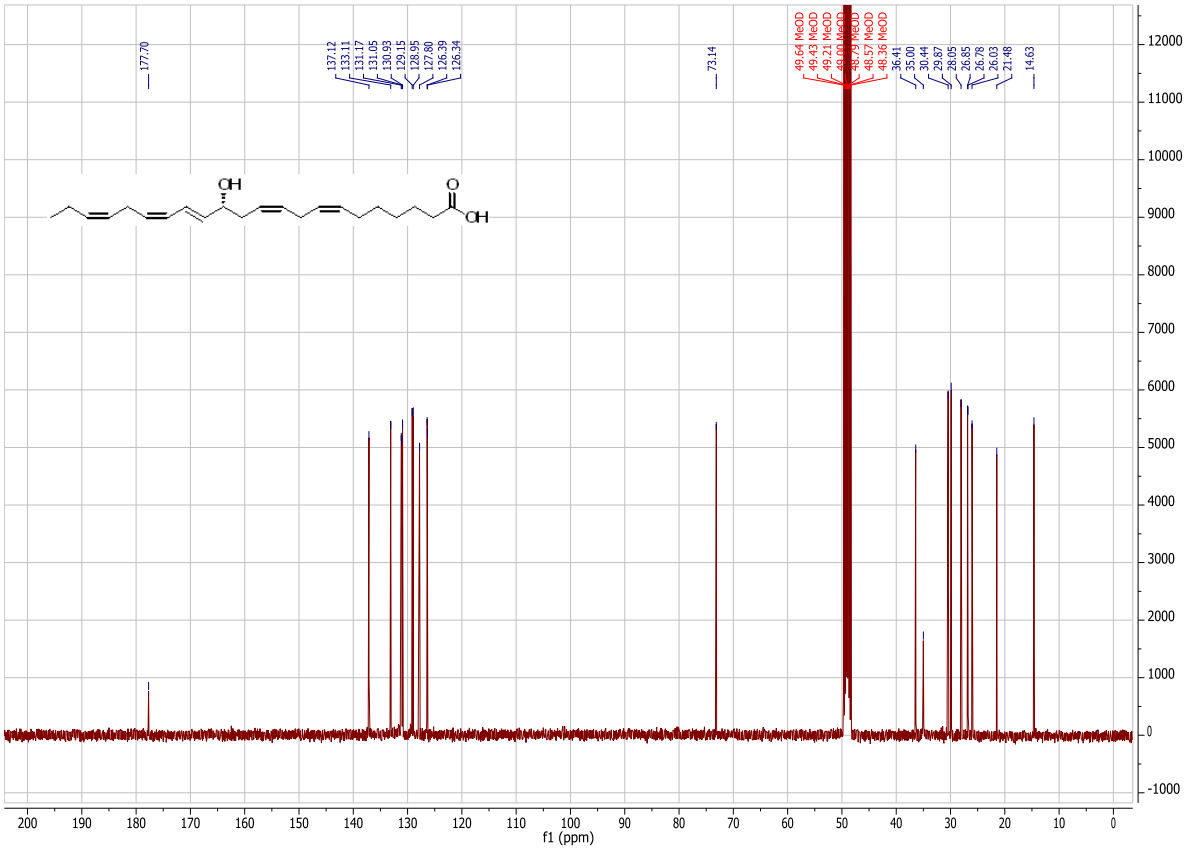

Figure S-22 ^{13}C-NMR spectrum 13*R*-HDPA **5**.

Data File C:\CHEM32\1\DATA\KAROLINE\AVBESKYTTALKYN13HDPA4.D
Sample Name: avbeskyttalkyn13HDPA4

```
Acq. Operator   : Karoline
Acq. Instrument : Instrument 1                    Location : Vial 1
Injection Date  : 24.05.2016 14:57:59
                                                  Inj Volume : 5 µl
Acq. Method     : C:\CHEM32\1\DATA\JORN\AD-H ISOKRATISK.M
Last changed    : 24.05.2016 14:52:54  by Karoline
                  (modified after loading)
Analysis Method : C:\CHEM32\1\DATA\JORN\AD-H ISOKRATISK.M
Last changed    : 24.05.2016 15:21:38  by Karoline
                  (modified after loading)
Sample Info     : Siste wittig 13R-HDPA etter avbeskyttelse med AcCl. H2O
                  /MeOH 15/85, 1.0 ml/min, C-18
```

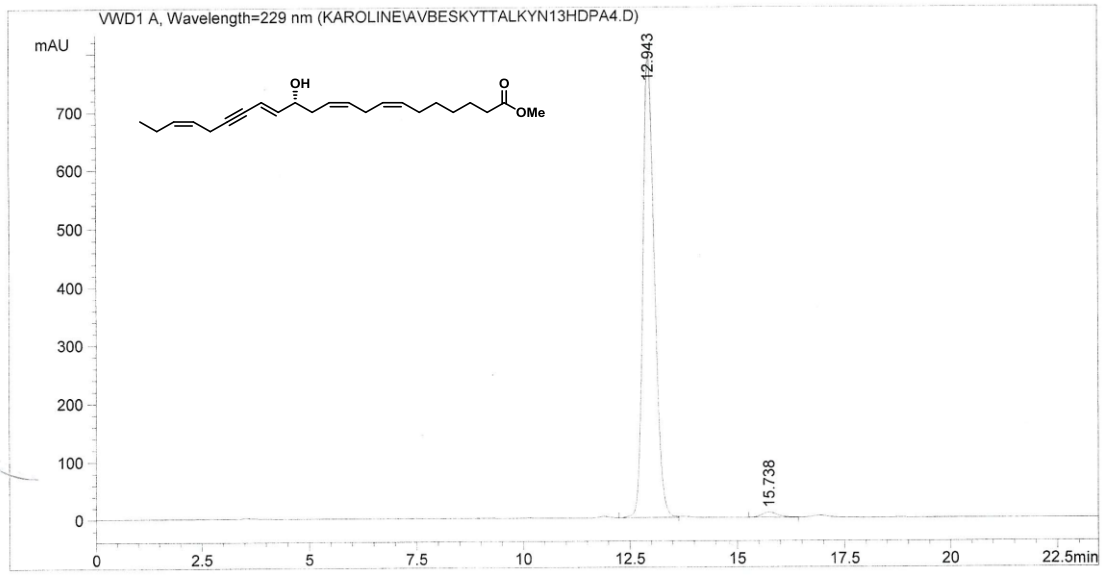


```
                          Area Percent Report

Sorted By             :      Signal
Multiplier            :      1.0000
Dilution              :      1.0000
Use Multiplier & Dilution Factor with ISTDs


Signal 1: VWD1 A, Wavelength=229 nm

Peak RetTime Type  Width     Area      Height     Area
  #   [min]        [min]  mAU   *s   [mAU   ]      %
----|-------|----|-------|----------|----------|--------|
   1  12.943 VV    0.2887 1.48500e4   791.95667  98.5446
   2  15.738 BB    0.3906  219.31461    8.73133   1.4554

Totals :                  1.50694e4   800.68799


                          *** End of Report ***

Instrument 1 24.05.2016 15:22:03  Karoline                    Page   1 of 1
```

Figure S-23 HPLC chromatogram of alkyne **23**.

```
Data File C:\CHEM32\1\DATA\KAROLINE\BOLANDMETYLESTER.D
 Sample Name: Bolandmetylester.D

    ======================================================================
    Acq. Operator   : Karoline
    Acq. Instrument : Instrument 1                    Location : Vial 1
    Injection Date  : 31.05.2016 12:48:06
                                                     Inj Volume : 5 µl
    Method          : C:\CHEM32\1\DATA\JORN\AD-H ISOKRATISK.M
    Last changed    : 31.05.2016 12:32:54  by RENATE
                      (modified after loading)
    Sample Info     : Boland prod, reneste frak, 85 % MeOH i H2O, 1 mL/min, 5
                       mikroliter injeksjonsvolum, C-18 kolonne
```

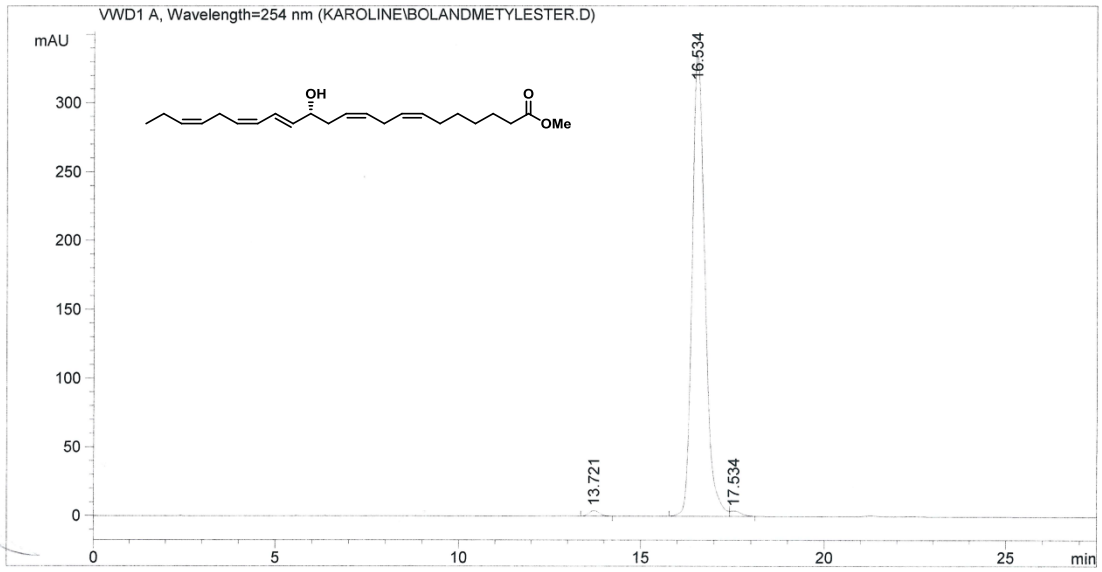


```
    ======================================================================
                              Area Percent Report
    ======================================================================

    Sorted By             :      Signal
    Multiplier            :      1.0000
    Dilution              :      1.0000
    Use Multiplier & Dilution Factor with ISTDs


    Signal 1: VWD1 A, Wavelength=254 nm

    Peak RetTime Type  Width     Area      Height     Area
      #   [min]        [min]  mAU   *s   [mAU   ]      %
    ----|-------|----|-------|----------|----------|--------|
       1  13.721 BB    0.2999   80.18535    4.14527   0.9625
       2  16.534 BV    0.3759 8169.00635  335.38226  98.0581
       3  17.534 VB    0.3088   81.59078    3.93708   0.9794

    Totals :                  8330.78248  343.46462

    ======================================================================
                              *** End of Report ***
```

Figure S-24 HPLC chromatogram of methyl ester **24**.

```
Data File C:\CHEM32\1\DATA\TEST\STD TEST217.D
Sample Name:

    ======================================================================
    Acq. Operator   : SYSTEM
    Sample Operator : SYSTEM
    Acq. Instrument : 7820 GC                       Location : Vial 1
    Injection Date  : 1/15/2016 13:36:24
                                                   Inj Volume : Manually
    Method          : C:\CHEM32\1\METHODS\ANDERS METODER\MARIUS WITTIG.M
    Last changed    : 1/15/2016 13:35:35 by SYSTEM
                      (modified after loading)
    Additional Info : Peak(s) manually integrated
```

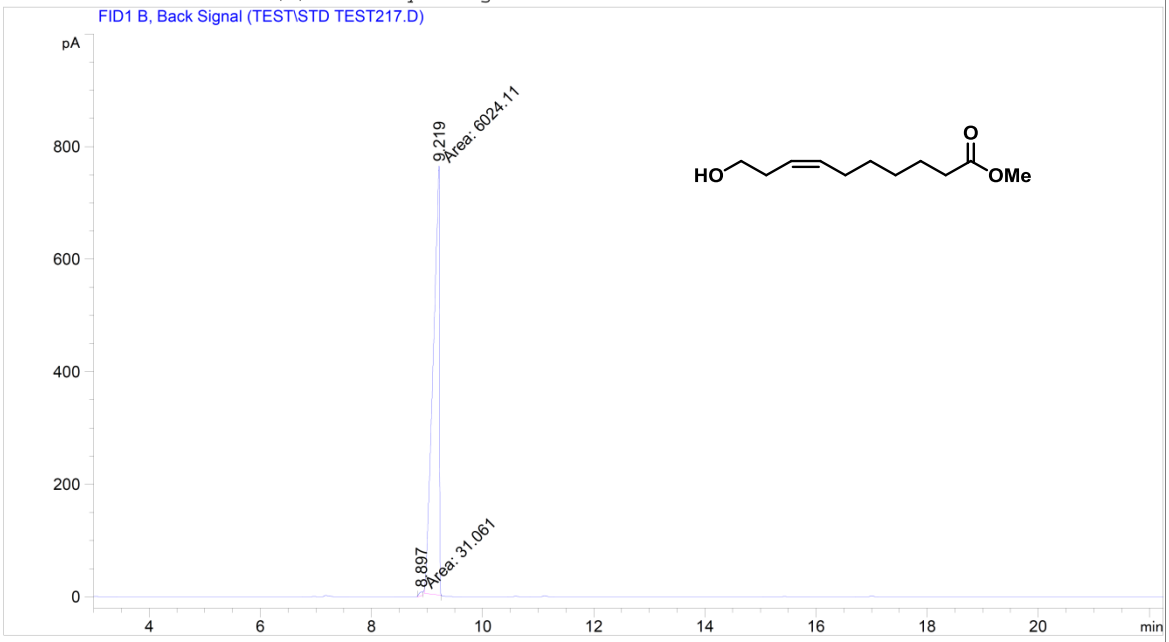


```
    ======================================================================
                          External Standard Report
    ======================================================================

    Signal 1: FID1 B, Back Signal

    Peak RetTime Type  Width     Area      Height     Area
      #   [min]        [min]   [pA*s]      [pA]        %
    ----|-------|----|-------|----------|----------|--------|
       1   8.897 MM    0.0758   31.06104    6.82525  0.51297
       2   9.219 MM    0.1317 6024.11377  762.55573 99.48703

    Totals :                   6055.17481  769.38097

    ======================================================================
                             *** End of Report ***
```

Figure S-25 GC chromatogram of ester **17**.

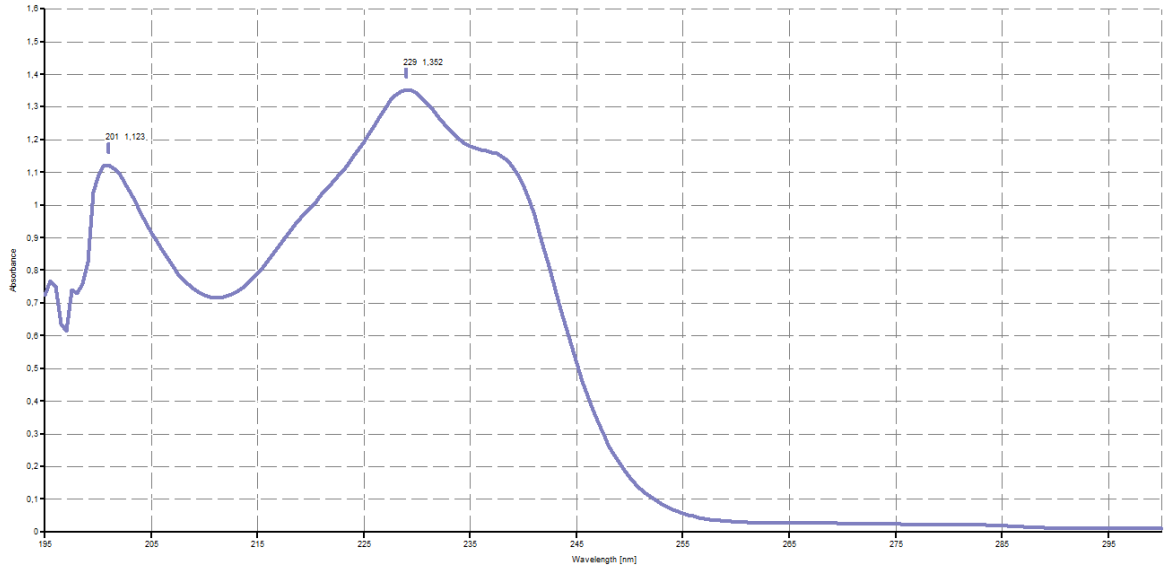

Figure S-26 UV-Vis chromatogram of the alkyne **23**.

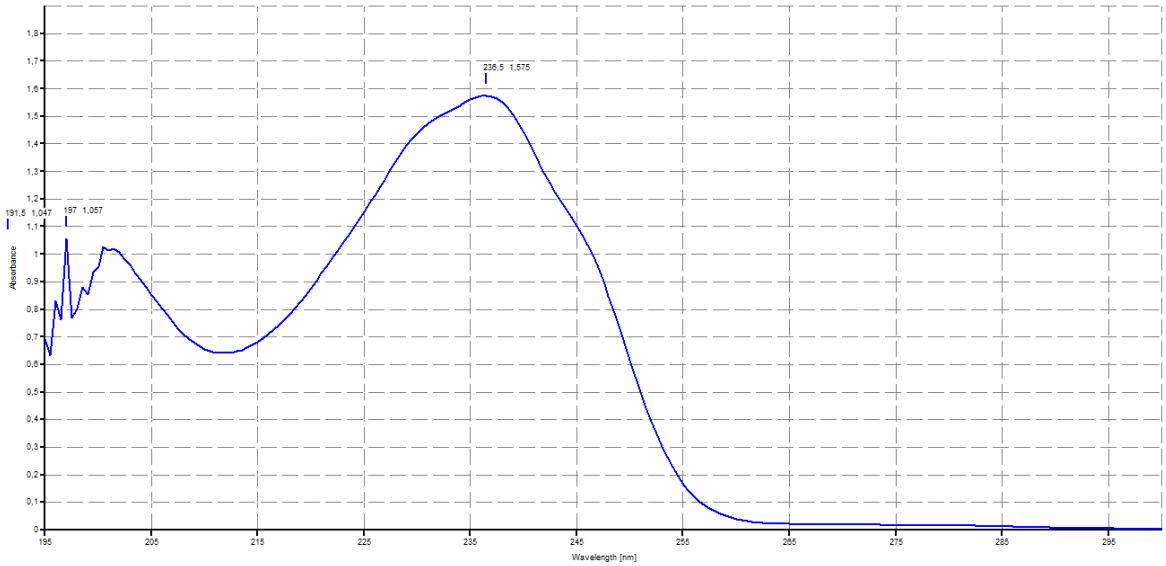

Figure S-27 UV-Vis chromatogram of the methyl ester **24**.

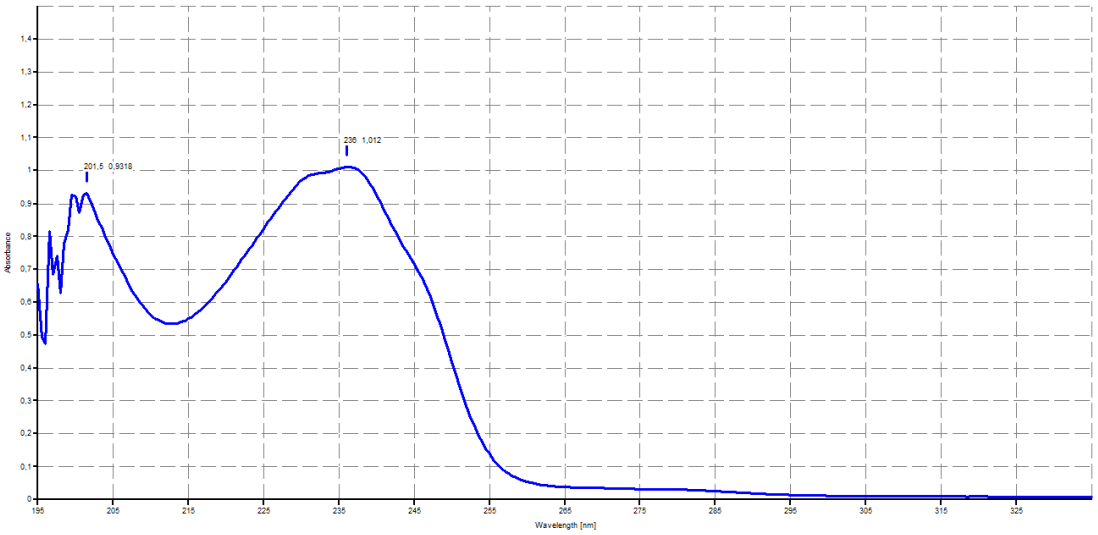

Figure S-28 UV-Vis chromatogram of synthetic 13*R*-HDPA (**5**).

References

1. Mowat, J.; Senior, J.; Kang, B.; Britton, R. *Can. J. Chem*. **2013**, *91*, 235.

2. White, W. L.; Anzeveno, P. B. *J. Org. Chem*. **1982**, *47*, 2379.